



THE UNIVERSITY OF
WAIKATO
Te Whare Wānanga o Waikato

Research Commons

<http://waikato.researchgateway.ac.nz/>

Research Commons at the University of Waikato

Copyright Statement:

The digital copy of this thesis is protected by the Copyright Act 1994 (New Zealand).

The thesis may be consulted by you, provided you comply with the provisions of the Act and the following conditions of use:

- Any use you make of these documents or images must be for research or private study purposes only, and you may not make them available to any other person.
- Authors control the copyright of their thesis. You will recognise the author's right to be identified as the author of the thesis, and due acknowledgement will be made to the author where appropriate.
- You will obtain the author's permission before publishing any material from the thesis.

The Chemistry of Cycloaurated Complexes



THE UNIVERSITY OF
WAIKATO
Te Whare Wānanga o Waikato

A thesis submitted in partial fulfillment of
the requirements for the degree of

Doctor of Philosophy in Chemistry

at

The University of Waikato

by

Kelly J. Kilpin

February 2009

ABSTRACT

New cycloaurated complexes have been synthesised and characterised. The biological and catalytic activity (in the addition of 2-methylfuran to methyl vinyl ketone) of selected complexes was evaluated. New complexes reported in this thesis were fully characterised by NMR (^1H , ^{13}C and ^{31}P when appropriate) and IR spectroscopy, ESI-mass spectrometry and elemental analysis.

The simple cycloaurated iminophosphoranes $(2\text{-AuCl}_2\text{C}_6\text{H}_4)\text{Ph}_2\text{P}=\text{N-R}$ ($\text{R} = (R,S)\text{-CHMePh}$, $(S)\text{-CHMePh}$, $p\text{-C}_6\text{H}_4\text{F}$ or Bu^t) were synthesised by the reaction of the appropriate *ortho*-mercurated compound with $[\text{Me}_4\text{N}][\text{AuCl}_4]$ and $[\text{Me}_4\text{N}]\text{Cl}$ in acetonitrile; the complex $(2\text{-AuCl}_2\text{C}_6\text{H}_4)\text{Ph}_2\text{P}=\text{N-(S)-CHMePh}$ was structurally characterised. The *cis* chloride ligands on the complexes were replaced by chelating dianionic ligands such as thiosalicylate and catecholate – the resulting bis-metallacyclic complexes have a better anti-tumour activity (against P388 murine leukemia cells) than the parent dichlorides. The nitrogen-gold coordinate bond is relatively robust and is not cleaved by cyanide or dithiocarbamate ligands. The reaction of $(2\text{-AuCl}_2\text{C}_6\text{H}_4)\text{Ph}_2\text{P}=\text{N-Ph}$ with PPh_3 results in substitution of the chloride ligand *trans* to the nitrogen (shown by an X-ray crystal structure). Both the *endo* ($(2\text{-AuCl}_2\text{C}_6\text{H}_4)\text{Ph}_2\text{P}=\text{NC(O)Ph}$) and *exo* ($(2\text{-AuCl}_2\text{C}_6\text{H}_4)\text{C(O)N=PPh}_3$) cycloaurated isomers of the stabilised iminophosphorane $\text{Ph}_3\text{P}=\text{NC(O)Ph}$ were synthesised and structurally characterised.

Cycloaurated $\text{Ph}_3\text{P}=\text{S}$ and $\text{Ph}_3\text{P}=\text{Se}$ were synthesised by a transmetallation reaction from $2\text{-Hg}[(\text{C}_6\text{H}_4)\text{P(E)Ph}_2]_2$ ($\text{E} = \text{S}$ or Se). The synthesis of cycloaurated $\text{Ph}_3\text{P}=\text{O}$ by an analogous method was unsuccessful. $\text{PhP(S)(NEt}_2)_2$ was also cycloaurated *via* a transmetallation reaction. X-ray crystallography confirmed the sulfur (not the nitrogen) was coordinated to the gold centre. The complexes show a similar stability and reactivity to the *C,N* cycloaurated species – the *cis* chloride ligands can be replaced by the chelating thiosalicylate ligand. Again the bis-metallacyclic species showed better biological activity than the parent dichloride.

The direct reaction of the 2-pyridyl sulfonamide ligands 2-(C₅H₅N)CH₂NHSO₂R (R = *p*-tolyl, Ph or Me), 2-(C₅H₅N)CH₂CH₂NHSO₂R (R = *p*-tolyl or Ph) or 8-(*p*-tosylamino)quinoline with refluxing aqueous H[AuCl₄] gave *N,N'* coordinated complexes containing a five- or six-membered cycloaurated ring. The cycloaurated complexes derived from the ligands 2-(C₅H₅N)CH₂NHSO₂Me and 8-(*p*-tosylamino)quinoline were structurally characterised. The cycloaurated *N,N'* systems were not as stable as the *C,N* systems – reaction with reducing agents led to reduction of Au(III) to Au(I) and elemental gold.

The 2-pyridine thiocarboxamide ligands 2-(C₅H₅N)C(S)NHR (R= *p*-tolyl, CH₂Ph, Me, *p*-C₆H₅OMe) also underwent direct cycloauration upon reaction with H[AuCl₄]. Coordination *via* the pyridyl nitrogen and sulfur atom was confirmed by an X-ray crystal structure of cycloaurated 2-(C₅H₅N)C(S)NHCH₂Ph. The *N,S* cycloaurated systems show poor stability in solution and decompose relatively quickly so applications are limited. The ligand with a 2-pyridyl substituent reacted with H[AuCl₄] in a different manner. Instead of cycloauration, the ligand was oxidised and an internal cyclisation occurred to give a 1,2,4-thiadiazolo[2,3-*a*]pyridinium heterocyclic ring.

The reaction of the cycloaurated dichloride complexes (2-benzylpyridine)AuCl₂ and (2-AuCl₂C₆H₄)Ph₂P=N-Ph with the tripodal Kläui ligands (Na[(C₅H₅)Co{P(O)R₂}₃], R = OMe or OEt) and Tl[BF₄] resulted in the formation of cationic gold(III) salts. In the solid state the Kläui ligand is strongly coordinated through two of the three oxygen atoms, and weakly by the third, giving the gold a distorted square pyramidal geometry. In solution there is rapid interchange between the coordinated and non-coordinated oxygen atoms.

ACKNOWLEDGEMENTS

Firstly I would like to extend my gratitude towards my supervisors Professors Bill Henderson and Brian Nicholson for their extensive help and guidance over the last three years. Without their enthusiasm and dedication this work would not have been possible.

I also wish to acknowledge the following people: Wendy Jackson and Pat Gread (electrospray mass spectrometry), Prof. Alistair Wilkins (NMR), Assoc. Prof Lyndsay Main (organic chemistry), Dr Tania Groutso (University of Auckland) and Dr Jan Wikaira (University of Canterbury) for collection of X-ray crystallography data sets and Gill Ellis (University of Canterbury) for biological assays. Special thanks must go to my lab colleagues, especially Bevan Jarman who has been a good friend since we were both weedy little first years.

Lastly, financial support from the Tertiary Education Commission (Top Achievers Doctoral Scholarship) and the New Zealand Federation of Graduate Women (Merit Award for Doctoral Study) has been greatly appreciated.

TABLE OF CONTENTS

Abstract	iii
Acknowledgements	v
Table of Contents	vi
List of Figures	xi
List of Tables	xiv
List of Abbreviations	xvi

CHAPTER ONE – Metallacyclic Gold(III) Complexes formed from Bidentate Monoanionic Ligands

1.1 Introduction to Gold(III) Chemistry	1
1.2 Metallacyclic Gold(III) Complexes formed from Bidentate Monoanionic Ligands	3
1.2.1 Complexes formed from <i>C,N</i> donor ligands	3
1.2.2 Complexes formed from <i>C,P</i> donor ligands	15
1.2.3 Complexes formed from <i>N,N'</i> donor ligands	17
1.2.4 Complexes formed from <i>N,O'</i> donor ligands	20
1.2.5 Complexes formed from <i>O,O'</i> donor ligands	23
1.2.6 Complexes formed from <i>S,S'</i> donor ligands	24
1.3 Scope of this Thesis	26
1.4 References	26

CHAPTER TWO – The Cycloauration of Iminophosphorane Ligands

2.1 Introduction	31
2.1.1 Synthesis of iminophosphorane ligands	31
2.1.2 Stability of iminophosphorane ligands	33
2.1.3 Cyclometallated iminophosphoranes	34
2.1.4 Scope of this work	46
2.2 Results and Discussion	46
2.2.1 Synthesis of simple <i>ortho</i> -mercurated and cycloaurated iminophosphorane complexes	46
2.2.2 X-ray crystal structure of $(2\text{-AuCl}_2\text{C}_6\text{H}_4)\text{Ph}_2\text{P}=\text{N}-(S)\text{CHMePh}$, 2.29c	48
2.2.3 Spectroscopic and mass spectrometric characterisation of simple <i>ortho</i> -mercurated and cycloaurated iminophosphoranes	50

2.2.4	Reactivity of simple cycloaurated iminophosphorane complexes with dianionic ligands	52
2.2.5	Reactivity of simple cycloaurated iminophosphoranes with phosphines	56
2.2.6	Attempted displacement of the <i>N</i> -donor ligand in simple cycloaurated iminophosphoranes	58
2.2.7	Synthesis of stabilised <i>ortho</i> -mercurated and cycloaurated iminophosphoranes	59
2.2.8	X-ray crystal structures of (2-HgClC ₆ H ₄)C(O)N=PPh ₃ 2.42 , (2-AuCl ₂ C ₆ H ₄)C(O)N=PPh ₃ 2.43 and (2-AuCl ₂ C ₆ H ₄)Ph ₂ P=NC(O)Ph 2.46	64
2.2.9	Spectroscopic and mass spectrometric characterisation of <i>ortho</i> -mercurated and cycloaurated stabilised iminophosphoranes	70
2.2.10	Biological activity	74
2.3	Conclusions	75
2.4	Experimental	75
2.4.1	General	75
2.4.2	Syntheses of simple <i>ortho</i> -metallated iminophosphoranes and the reactions they undergo	76
2.4.3	Syntheses of <i>ortho</i> -metallated stabilised iminophosphoranes	84
2.4.4	X-ray crystal structure determinations	88
2.5	References	90

CHAPTER THREE – The Cycloauration of Phosphine Chalcogenides

3.1	Introduction	93
3.1.1	Metal complexes of phosphine chalcogenides	93
3.1.2	Scope of this work	95
3.2	Results and Discussion	95
3.2.1	Synthesis and properties of <i>ortho</i> -mercurated phosphine chalcogenides complexes	95
3.2.2	Synthesis of cycloaurated gold(III) phosphine chalcogenides	100
3.2.3	X-ray crystal structures of (2-AuCl ₂ C ₆ H ₄)P(S)Ph ₂ 3.16b , (2-AuCl ₂ C ₆ H ₄)P(Se)PPh ₃ 3.16c , and (2-AuCl ₂ C ₆ H ₄)P(S)(NEt ₂) ₂ 3.17	102
3.2.4	Spectroscopic and mass spectrometric characterisation of cycloaurated triphenylphosphine chalcogenides	107
3.2.5	Reaction of (2-AuCl ₂ C ₆ H ₄)P(S)(NEt ₂) ₂ 3.17 with thiosalicylic acid	109
3.2.6	Biological activity	109
3.3	Conclusions	110

3.4	Experimental	110
3.4.1	General	110
3.4.2	Syntheses.....	110
3.4.3	X-ray crystal structure determinations of 3.13 , 3.16b , 3.16c and 3.17	117
3.5	References	120

CHAPTER FOUR – The Cycloauration of Pyridyl Sulfonamides

4.1	Introduction.....	123
4.1.1	2-Pyridyl derived sulfonamides as bidentate ligands.....	123
4.1.2	Examples of complexes of bidentate sulfonamide ligands	123
4.1.3	Scope of this work.....	124
4.2	Results and Discussion.....	125
4.2.1	Syntheses.....	125
4.2.2	X-ray crystal structures of 4.8c and 4.10 · CH ₂ Cl ₂	128
4.2.3	NMR and IR spectroscopic characterisation.....	131
4.2.4	ESI mass spectrometric characterisation.....	133
4.2.5	Biological activity	134
4.2.6	Reactivity	135
4.3	Conclusions.....	135
4.4	Experimental	136
4.4.1	General	136
4.4.2	Syntheses.....	136
4.4.3	X-ray crystal structure determinations of 4.8c and 4.10 · CH ₂ Cl ₂	142
4.5	References	144

CHAPTER FIVE – The Cycloauration of Pyridine-2-Thiocarboxamide Ligands

5.1	Introduction.....	147
5.1.1	<i>N</i> -Substituted pyridine-2-thiocarboxamides as bidentate ligands.....	147
5.1.2	Coordination complexes of <i>N</i> -substituted pyridine-2-thiocarboxamides with heavy transition metals	148
5.1.3	Scope of this work.....	150

5.2	Results and Discussion	150
5.2.1	Reaction of <i>N</i> -substituted pyridine-2-thiocarboxamides ligands 5.12a-d with H[AuCl ₄].....	150
5.2.2	X-ray crystal structure of 5.13b	151
5.2.3	Spectroscopic characterisation of complexes 5.13a – 5.13d	154
5.2.4	Mass spectrometric characterisation of complexes 5.13a – 5.13d	156
5.2.5	Reaction of <i>N</i> -(2-pyridyl)pyridine-2-thiocarboxamide (5.15) with H[AuCl ₄]	156
5.3	Conclusions.....	160
5.4	Experimental.....	160
5.4.1	General.....	160
5.4.2	Syntheses.....	160
5.4.3	X-ray crystal structure determinations of 5.13b and 5.16	165
5.5	References.....	167

CHAPTER SIX – Gold(III) Complexes formed with Kläui Ligands

6.1	Introduction.....	169
6.1.1	Synthesis and properties of the Kläui ligand	169
6.1.2	Scope of this work	170
6.2	Results and Discussion	171
6.2.1	Syntheses.....	171
6.2.2	X-ray crystal structure of 6.5b	172
6.2.3	NMR spectroscopic analysis.....	176
6.3	Conclusions.....	182
6.4	Experimental.....	182
6.4.1	General.....	182
6.4.2	Syntheses.....	183
6.4.3	X-ray crystal structure determination of 6.5b	185
6.5	References.....	186

CHAPTER SEVEN – A Preliminary Study of the Catalytic Activity of Gold(III) Complexes

7.1	Introduction.....	189
7.1.1	Gold(III) homogeneous catalysis.....	189
7.1.2	Catalytic addition of 2-methylfuran to methyl vinyl ketone.....	190

7.1.3	Scope of this work.....	196
7.2	Results and Discussion.....	197
7.2.1	Development of method.....	197
7.2.2	Catalytic activity of <i>C,N</i> cycloaurated complexes	198
7.2.3	Catalytic activity of <i>C,E</i> (E=S, Se) cycloaurated complexes.....	201
7.2.4	Catalytic activity of <i>N,N'</i> cycloaurated complexes.....	202
7.3	Conclusions.....	204
7.4	Experimental.....	204
7.4.1	General.....	204
7.4.2	Catalysis conditions	205
7.4.3	GC-MS conditions	205
7.5	References.....	205

APPENDIX ONE - General Experimental Procedures, Instrumental Techniques and Preparation of Starting Materials

I.1	General Experimental Procedures.....	207
I.2	Instrumental Techniques and Analysis	208
I.2.1	Infrared Spectroscopy	208
I.2.2	Nuclear Magnetic Resonance Spectroscopy.....	208
I.2.3	Mass Spectrometry.....	212
I.2.4	X-ray Crystallography.....	212
I.2.5	Microelemental Analysis	212
I.2.6	Biological Assays.....	213
I.3	Preparation of Inorganic and Organometallic Precursors.....	213
I.4	References.....	215

LIST OF FIGURES

2.1	Molecular diagram of (2-Cl ₂ AuC ₆ H ₄)Ph ₂ P=N-(<i>S</i>)-CHMePh 2.29c , showing the atom numbering scheme	49
2.2	³¹ P{ ¹ H} NMR spectra for the series of simple iminophosphanes with a Bu ^t substituent	51
2.3	Molecular diagram of 2.36f , showing the atom numbering scheme.....	55
2.4	Molecular diagram of 2.36f , showing the fold angle of the thiosalicylate ligand and puckering of the iminophosphorane ring	55
2.5	Molecular diagram of [(2-AuCl(PPh ₃)C ₆ H ₄)Ph ₂ P=NPh] ⁺	57
2.6	Molecular structure of (2-Mn(CO) ₄ C ₆ H ₄)C(O)N=PPh ₃ , 2.41	62
2.7	Molecular structure of (2-HgClC ₆ H ₄)C(O)N=PPh ₃ , 2.42 , showing the atom numbering scheme	65
2.8	Molecular structure of (2-AuCl ₂ C ₆ H ₄)C(O)N=PPh ₃ , 2.43 showing the atom numbering scheme	67
2.9	Molecular structure of (2-AuCl ₂ Cl ₂ C ₆ H ₄)C(O)N=PPh ₃ , 2.46 , showing the atom numbering scheme	69
2.10	³¹ P{ ¹ H} NMR spectra of the series of <i>exo</i> cyclometallated complexes	71
2.11	³¹ P{ ¹ H} NMR spectra of the series of <i>endo</i> cyclometallated complexes	72
3.1	Structure of the complex (2-HgClC ₆ H ₄)P(S)Ph ₂ 3.13 showing the atom numbering scheme.....	99
3.2	Molecular diagram of (2-AuCl ₂ C ₆ H ₄)P(S)Ph ₂ 3.16b showing the atom labelling scheme.....	103
3.3	Molecular diagram of (2-AuCl ₂ C ₆ H ₄)P(Se)Ph ₂ 3.16c indicating the atom numbering scheme	103
3.4	Molecular structure of (2-AuCl ₂ C ₆ H ₄)P(S)(NEt ₂) ₂ 3.17 showing one of the unique molecules in the asymmetric unit	106

4.1	Molecular structure of 4.8c showing one of the unique molecules in the asymmetric unit, and the atom numbering scheme.....	128
4.2	Molecular structure of 4.10 · CH ₂ Cl ₂ , showing the atom numbering scheme	129
4.3	(a) Structure of 4.8c (molecule 1) showing the envelope conformation of the cycloaurated ring with N(2) sitting above the plane of the ring; (b) structure of 4.10 · CH ₂ Cl ₂ , showing the planarity of the quinoline group, with Au(1) sitting below the plane.	131
4.4	¹ H NMR spectra of (a) 4.5a and (b) 4.8a , showing changes in the spectra upon coordination of the ligand to gold.....	132
4.5	Positive ion ESI mass spectra of 4.8b showing the observed ions under different ionisation conditions: (a) neat solution; (b) with addition of NaCl; (c) with addition of pyridine (py).	134
5.1	Molecular diagram of 5.13b showing one of the unique molecules present in the asymmetric unit, and the atom numbering scheme.....	152
5.2	Diagram showing the gold-sulfur interactions between the two molecules in the asymmetric unit of 5.13b . The different orientations of the phenyl rings can clearly be seen.....	153
5.3	¹ H NMR spectra of (a) 5.12a and (b) 5.13a showing the changes in the spectra upon coordination of the ligand to gold.	155
5.4	Molecular diagram of 5.16 showing the atom labelling scheme.	158
6.1	Molecular diagram of the cationic moiety of 6.5b	172
6.2	Molecular structure of the palladium Kläui complex 6.6	173
6.3	Molecular structure of the palladium Kläui complex 6.7	174
6.4	Variable temperature ³¹ P{ ¹ H} NMR spectra of 6.3b	178
6.5	Variable temperature ³¹ P{ ¹ H} NMR spectra of 6.5b	179
6.6	Variable temperature ¹ H NMR spectra of a) 6.3a at 303K, b) 6.3a at 223K, c) 6.3b at 303K and d) 6.3b at 223 K.....	181
7.1	Response factor curve (determined by the area under the peaks) for 7.3 relative to <i>o</i> -xylene at different molar concentrations of 7.3 and <i>o</i> -xylene	198

A.1	^1H - ^1H COSY spectrum of 4.8c	209
A.2	1D-SELTOCSY NMR spectra of 4.8c with mixing times of a) 15 ms, b) 30 ms and c) 50 ms. The spectrum shown in d) is a standard ^1H NMR spectrum of 4.8c	210
A.3	a) 1D-SELNOESY spectrum of 4.8c , with the signal at 4.96 ppm irradiated and showing a through space interaction to the proton at 8.05 ppm; b) standard ^1H NMR spectrum of 4.8c	211

LIST OF TABLES

2.1	Selected structural parameters for (2-Cl ₂ AuC ₆ H ₄)Ph ₂ P=N-(<i>S</i>)-CHMePh, 2.29c	50
2.2	Selected structural parameters for 2.36f	56
2.3	Selected bond parameters for [(2-AuCl(PPh ₃)C ₆ H ₄)Ph ₂ P=NPh]PF ₆ ·0.5Et ₂ O 2.39	58
2.4	Selected bond lengths (Å) and angles (°) for the complex 2.42	66
2.5	Selected bond lengths (Å) and angles (°) for the complex 2.43	68
2.6	Selected bond lengths (Å) and angles (°) for the complex 2.46	70
2.7	Selected IR absorbances (KBr disk) for the metallated iminophosphorane Ph ₃ P=NC(O)Ph, including <i>endo</i> and <i>exo</i> isomers.....	73
2.8	Anti-tumour (P388 murine leukaemia) activities for selected gold(III) iminophosphoranes and related systems.	74
2.9	Crystallographic data for the complexes 2.29c , 2.35f , 2.39 , 2.42 , 2.43 and 2.46	89
3.1	Selected structural parameters for the complex 2-HgCl(C ₆ H ₄)P(S)Ph ₂ 3.13	99
3.2	Selected structural parameters for the complexes 3.16b and 3.16c	104
3.3	Results of a search of the Cambridge Crystallographic Database for η ¹ coordinated Ph ₃ P=E ligands.....	105
3.4	Selected structural parameters for the complex (2-AuCl ₂ C ₆ H ₄)P(S)(NEt ₂) ₂ 3.17	107
3.5	³¹ P{ ¹ H} NMR chemical shifts (ppm) of the metallated phosphine chalcogenide ligands used in this study	108
3.6	Crystal and refinement data for the complexes 3.13 , 3.16b , 3.16c and 3.17	119
4.1	A comparison of selected bond lengths (Å) for the crystal structures of 4.8c (two independent molecules) and 4.10 · CH ₂ Cl ₂	129
4.2	A comparison of selected bond angles (°) for the crystal structures of 4.8c (including the two independent molecules) and 4.10 · CH ₂ Cl ₂	130
4.3	Crystal and refinement data for the complexes 4.8c and 4.10 · CH ₂ Cl ₂	143
5.1	Selected structural parameters for 5.13b (both molecules).....	154

5.2	Selected structural parameters for 5.16	158
5.3	Unit cell and crystallographic refinement data for the complexes 5.13b and 5.16	166
6.1	Selected bond lengths (Å) and angles (°) for the complex 6.5b	173
6.2	¹ H and ³¹ P{ ¹ H} NMR chemical shifts (ppm) for the Kläui ligands 6.2a and 6.2b (as the sodium salts) and the gold(III) complexes	177
6.3	Crystal and refinement data for the complex 6.5b	186
7.1	Performance of cyclometallated complexes in the addition of 2-methylfuran to MVK	194
7.2	Performance of <i>C,N</i> cyclometallated iminophosphoranes as catalysts in the addition of 2-methylfuran to MVK.....	199
7.3	Performance of cycloaurated triphenylphosphine sulfide and selenide as catalysts in the addition of 2-methylfuran to MVK.....	201
7.4	Performance of <i>N,N'</i> cycloaurated 2-pyridylsulfonamides as catalysts in the addition of 2-methylfuran to MVK.....	203

LIST OF ABBREVIATIONS

Ac	-	acetyl
acac	-	acetylacetonato
asym	-	asymmetric (IR)
bipy	-	2,2'-bipyridyl
br	-	broad
Bu	-	butyl
Bu ^t	-	tertiary butyl
Cp	-	cyclopentadienyl (η^5 -C ₅ H ₅)
cy	-	cyclohexyl
d	-	doublet
DMF	-	dimethyl formamide
DMSO	-	dimethyl sulfoxide
Et	-	ethyl
ESI-MS	-	electrospray mass spectrometry
IR	-	infrared
<i>J</i>	-	coupling constant in Hz (NMR)
m	-	medium (IR) or multiplet (NMR)
Me	-	methyl
MVK	-	methyl vinyl ketone
<i>m/z</i>	-	mass to charge ratio (ESI-MS)
NMR	-	nuclear magnetic resonance
Ph	-	phenyl
py	-	pyridine
q	-	quartet (NMR)
s	-	strong (IR) or singlet (NMR)
sym	-	symmetric (IR)
t	-	triplet (NMR)
Tf	-	triflate (trifluoromethanesulfonate)
THF	-	tetrahydrofuran
vs	-	very strong (IR)
vq	-	virtual quartet (NMR)
w	-	weak (IR)
ν	-	stretching frequency (IR)
δ	-	chemical shift (NMR)

CHAPTER ONE

Metallacyclic Gold(III) Complexes formed from Bidentate Monoanionic Ligands

1.1 Introduction to Gold(III) Chemistry

Gold and man have had a long and interesting association with each other. The earliest civilisations treasured gold - it was seen as a symbol of light and beauty. The chemical symbol for gold, Au, is derived from the Latin *aurum* which translates to 'shining dawn'. The ancient Egyptian, Aztec and Inca cultures all linked gold to the gods and Aurora, the Roman goddess of dawn was named for the element. Since prehistoric times gold has also been recognised as a symbol of wealth. The Chinese were the first to legalise gold as a monetary unit as early as 1091 BC (little squares of the metal were traded) and later the Lydians (*ca.* 640 – 630 BC) introduced gold coins into circulation.⁽¹⁾ Although gold is no longer issued as an official currency it is still seen as a safe investment.

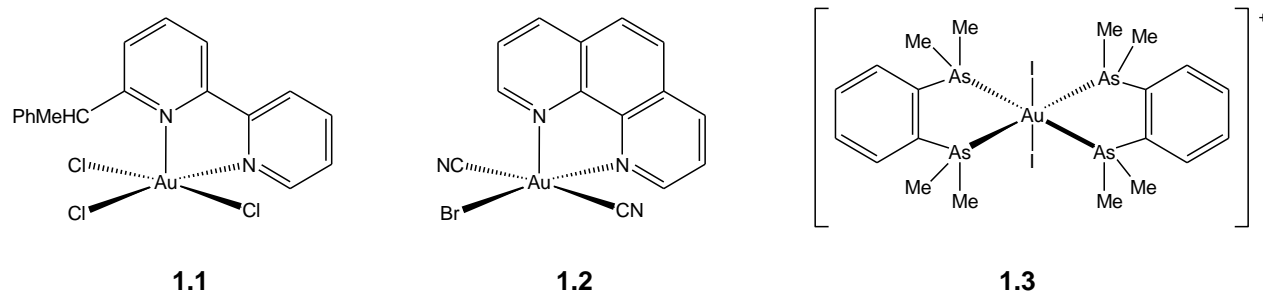
The quest for gold has led man on many interesting journeys. The earliest was perhaps the infamous King Midas who had the desire that everything he touched turned to gold. Alchemists - the earliest inorganic chemists - had the common goal of transmutating base metals into gold. In the late 19th and early 20th centuries the value of gold sparked many to join the gold rushes of California, Colorado, Australia and New Zealand.

In nature gold occurs in the metallic form, often as an alloy with silver. It is a soft yellow metal whose beauty has led to its use in jewellery and other decorative purposes. Gold has the highest malleability and ductility of any element and the high thermal and electrical conductivity means gold has found many uses in electronics. It is the most noble of all metals and is not attacked by either oxygen or sulfur and only readily dissolves in aqua regia. The two predominant oxidation states of gold are +I and +III, although compounds containing

gold(II) are also well known. AuF_5 and the complex ion $[\text{AuF}_6]^-$ are the sole examples of gold in the +V oxidation state and both compounds are highly oxidising.⁽²⁾

Gold(I) has ten d -electrons (the full electron configuration is $[\text{Xe}]4f^{14}5d^{10}$) therefore compounds containing the metal in this oxidation state are diamagnetic and adopt a linear, two coordinate geometry. Being a soft acid (a Class b metal) gold(I) tends to prefer coordination to soft donor ligands.

Gold(III) has a d^8 electron configuration ($[\text{Xe}]4f^{14}5d^8$) and typically forms diamagnetic four coordinate $16e^-$ species with predominantly square-planar geometry. Five coordinate gold(III) complexes are rare, but rigid bidentate nitrogen ligands (see Scheme 1.1 for recent examples containing bipyridine⁽³⁾ **1.1** or phenanthroline⁽⁴⁾ **1.2** backbones) form a distorted square pyramidal arrangement around the gold and it is assumed that intermediates in ligand substitution reactions have trigonal bi-pyramidal geometry. Octahedral geometry has been demonstrated crystallographically for the six coordinate species $[\text{Au}(\text{diars})_2\text{I}_2]^+$ **1.3**,⁽⁵⁾ Scheme 1.1. Being in a higher oxidation state, gold(III) is not as soft as gold(I) but still prefers to form complexes with soft ligands. For example, NCO^- bonds to the gold *via* the nitrogen donor, NCS^- *via* the sulfur.⁽⁶⁾



Scheme 1.1 Recent examples of unusual five- and six-coordinate gold(III) compounds.

Gold(III) is isoelectronic and isosteric with platinum(II), however the gold centre is much more oxidising and labile than the platinum centre. Compared with the chemistry of

platinum(II) [and palladium(II)], the chemistry of gold(III) (especially the organometallic aspects) has been relatively unexplored.

1.2 Metallacyclic Gold(III) Complexes formed from Bidentate Monoanionic Ligands

Consider the 14 electron gold(III) species AuR_3 . This will be electron deficient, unstable and therefore highly reactive. However, the coordination of a neutral two electron donor (X:) will form a stable species $\text{X:}\rightarrow\text{AuR}_3$. If one of the sigma bound ligands (R) has a pendant arm with a neutral two electron donor then there is the possibility of forming a cyclometallated complex.

As already stated, the chemistry of cyclometallated gold(III) complexes has historically been neglected relative to the other platinum group metals. However over the last twenty years this trend seems to be changing. Since the discovery of the anticancer activity of *cisplatin* (and other platinum(II) complexes) many gold(III) cyclometallated complexes (which show a structural similarity to *cisplatin*) have been synthesised with the aim of discovering biologically active complexes. In addition, the popularity of homogenous catalysis has spurred much research in the area.

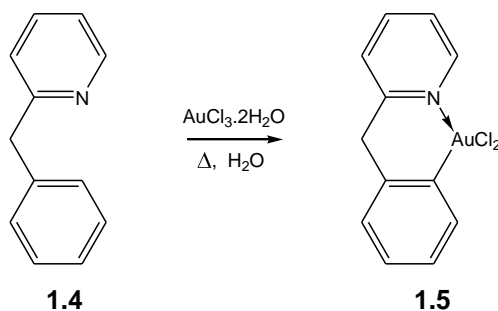
The following review attempts to give an overview of metallacyclic gold(III) compounds formed from the coordination of mono-anionic bidentate ligands, with more attention given to systems directly related to this work. It is limited to the formation of neutral species with an emphasis on the synthesis, reactivity and applications of such compounds.

1.2.1 Complexes formed from C,N donor ligands

Cycloaurated complexes containing C,N donor ligands are by far the most extensively studied systems and because they form the basis of a recent review⁽⁷⁾ the following discussion will only be a brief overview of the synthesis and reactivity of such compounds.

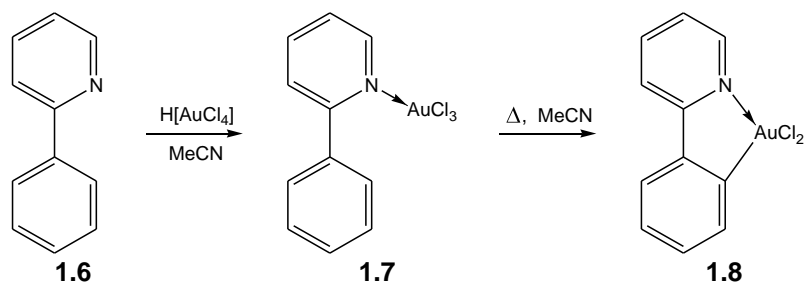
Synthesis by direct C-H bond activation

There are two main synthetic routes to cycloaurated *C,N* complexes - the most simple procedure involves the direct activation of a C-H bond in the ligand by a gold(III) source, typically $\text{H}[\text{AuCl}_4]$, $\text{Na}[\text{AuCl}_4]$ or $\text{AuCl}_3 \cdot x\text{H}_2\text{O}$. The reaction is typically carried out in refluxing polar solvents such as water, ethanol or acetonitrile. The insolubility of the cyclometallated gold complex in such solvents allows the product to be isolated easily in good yields. Scheme 1.2 shows the synthesis of cycloaurated 2-benzylpyridine **1.5** by the direct reaction of the ligand **1.4** with AuCl_3 .⁽⁸⁾ Other ligands which undergo analogous C-H bond activations to give cycloaurated six-membered ring systems containing pyridyl donor atoms include substituted 2-anilino-,^(9,10) 2-phenoxy-⁽¹⁰⁾ and 2-(phenylsulfanyl)-pyridine.⁽¹⁰⁾



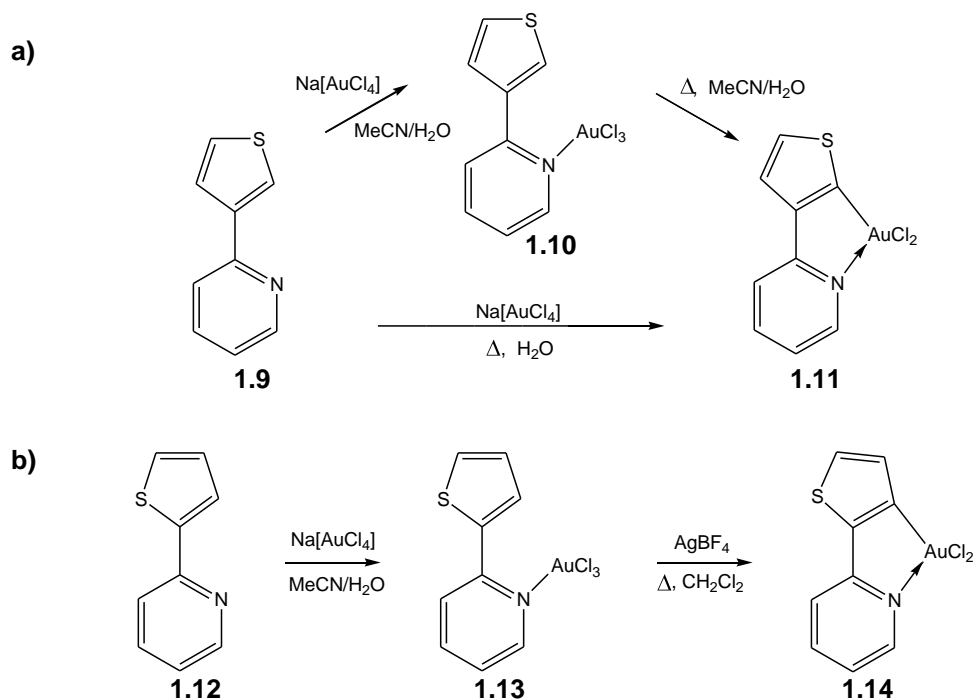
Scheme 1.2 Synthesis of cycloaurated 2-benzylpyridine **1.5** by direct C-H bond activation.

In some cases the direct reaction of the ligand with the gold(III) source does not immediately result in C-H bond activation and the formation of a cycloaurated complex – instead the simple nitrogen coordinated adduct $\text{L} \rightarrow \text{AuCl}_3$ is obtained. It is possible that this type of species is an intermediate in the direct cycloauration reaction as further heating of such complexes can lead to a metallacyclic product. As an example the cycloauration of 2-phenylpyridine **1.6** is shown in Scheme 1.3. The simple *N*-coordinated adduct **1.7** is obtained (in near quantitative yields as a yellow solid) when 2-phenylpyridine is added to an acetonitrile solution of $\text{H}[\text{AuCl}_4]$ at room temperature. Refluxing **1.7** in aqueous acetonitrile yields the (white) cyclometallated complex **1.8** in 80% yield.⁽¹¹⁾ Other ligands such as 2-(*p*-tolyl)pyridine⁽¹²⁾ and substituted 2-phenoxy pyridine derivatives⁽¹³⁾ also undergo cyclometallation reactions where the *N*-coordinated adduct is first obtained.



Scheme 1.3 Synthesis of cycloaurated 2-phenylpyridine **1.8** via the *N*-coordinated complex.

The cyclometallated complexes described so far refer to C-H bond activation of phenyl rings. Fuchita *et al.* reported that activation of a C-H bond in thiophene rings is also possible, thus the cycloauration of 2-(3-thienyl)pyridine **1.9** occurs directly upon reaction with Na[AuCl₄] in a refluxing acetonitrile/water solution. Alternatively, **1.11** can be obtained via the *N*-coordinated adduct **1.10**.

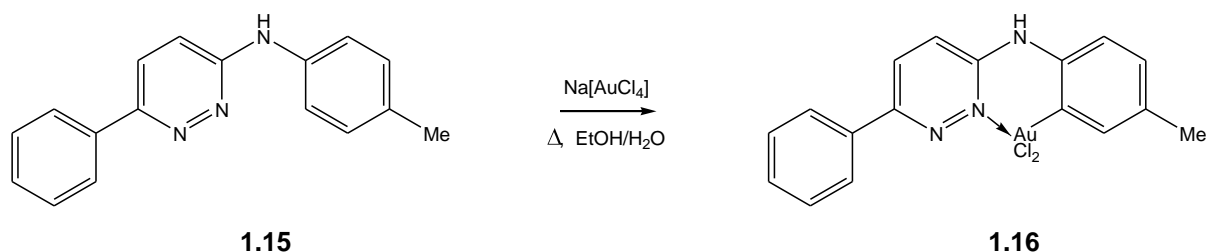


Scheme 1.4 Different reactivity of the 2-(thienyl)pyridine isomers a) 2-(3-thienyl)pyridine **1.9** and b) 2-(2-thienyl)pyridine **1.12** towards [AuCl₄]⁻.

The isomer containing a 2-thienyl substituent (**1.12**) does not react in the same way. Direct cycloauration does not occur, however the *N*-coordinated complex **1.13** is obtained when **1.12** is reacted directly with Na[AuCl₄]. In this case heating the adduct **1.13** does not induce C-H bond activation. Instead, the addition of Ag[BF₄] to a refluxing solution of **1.13** promotes cycloauration to yield **1.14**, possibly by the formation of a vacant coordination site on the gold *via* abstraction of a chloride ligand.⁽¹⁴⁾ The presence of silver(I) salts is also required for the cyclometallation of 2-benzoylpyridine.⁽¹⁵⁾

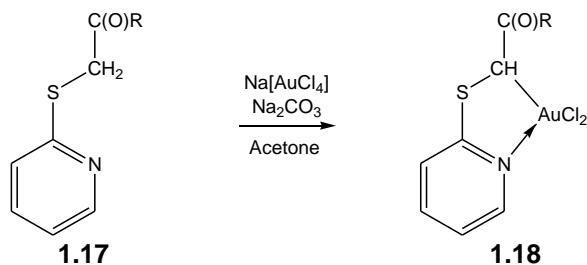
In the examples presented so far, the neutral nitrogen atom is from a pyridyl group, however this does not always have to be the case. Indeed the imidazole group can also provide a neutral nitrogen donor. Therefore, the reaction of 1-ethyl-2-phenylimidazole with H[AuCl₄] in ethanol gives the *N*-coordinated adduct. This can be converted to the cycloaurated complex (albeit in low yields) by refluxing in dichloromethane with the aid of Ag[BF₄].⁽¹⁶⁾ Using an analogous reaction scheme, 2-phenylthiazole undergoes a cycloauration reaction. In this case the nitrogen donor originates from a thiazole ring.⁽¹⁷⁾

It can be inferred from the preceding discussion that both five- and six-membered cycloaurated rings are common. 3-Phenyl-6-*p*-toluidinopyridazine **1.15** is an interesting ligand as it has two different sites for metallation, which can result in either the formation of a five- or six-membered metallacyclic ring. Interestingly, though the reasons are not clear, the reaction of the ligand **1.15** with Na[AuCl₄] is regioselective and the six-membered auracyclic compound **1.16** is formed.⁽¹⁸⁾



Scheme 1.5 Regioselective cycloauration of 3-phenyl-6-*p*-toluidinopyridazine **1.15** to give the six-membered auracycle **1.16**.

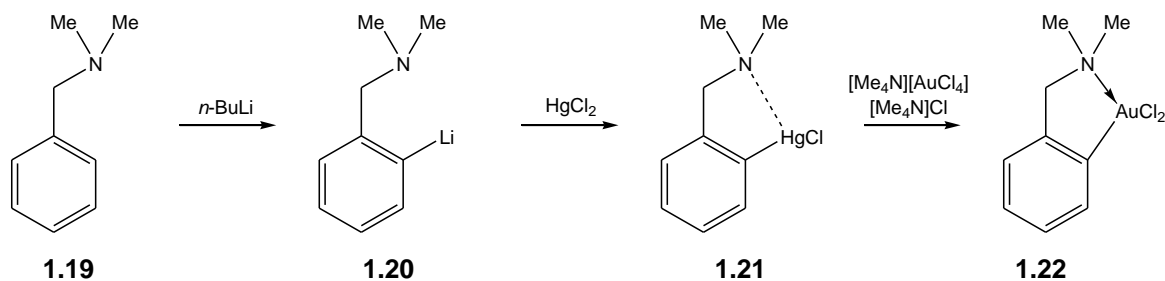
Although much less common than sp^2 C-H bond activation, direct sp^3 C-H bond activation by gold(III) is also possible. Vicente *et al.* demonstrated this nicely – the reaction of the 2-(alkylthio)pyridine ligands **1.17** with $\text{Na}[\text{AuCl}_4]$ and Na_2CO_3 in acetone at room temperature (2:2:1 mole ratio) gave the cycloaurated complexes **1.18** in moderate yields (Scheme 1.6). It was proposed that the reaction is in equilibrium; the presence of Na_2CO_3 removes HCl from the system thus increasing the yield of the cyclometallated product.⁽¹⁹⁾



Scheme 1.6 Auration of the alkyl C-H bond of 2-(alkylthio)pyridine ligands **1.17** (R = Ph, Me or OMe) by $[\text{AuCl}_4]$.

Synthesis by transmetallation reactions

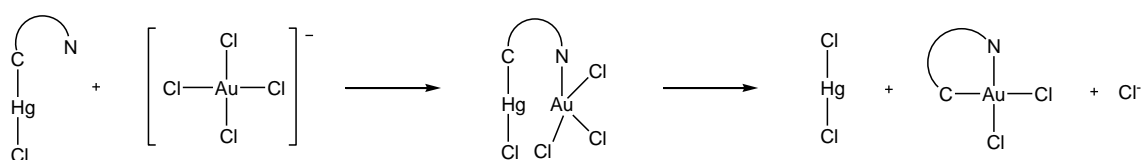
If direct cycloauration of a ligand is not successful, transmetallation from an *ortho*-mercurated complex is a method often employed to obtain the desired cycloaurated complex. Such is the case for the 2-(*N,N*-dimethylaminomethyl)phenyl (damp) ligand **1.19**. Scheme 1.7 shows the synthesis of the cycloaurated complex (damp) AuCl_2 , **1.22**. The *ortho*-mercurated complex **1.21** is synthesised by the reaction of an organolithium intermediate **1.20** with mercury(II) chloride. A subsequent reaction between the organomercury compound **1.21** and a gold precursor then transfers the organic group from the mercury to the gold.⁽²⁰⁾



Scheme 1.7 Scheme for the synthesis of (damp) AuCl_2 **1.22** by a transmetallation reaction from an organomercury precursor.

A range of other cycloaurated compounds is able to be synthesised by a transmetallation reaction from the corresponding *ortho*-mercurated compounds. These include substituted damp and oxazoline complexes,⁽²¹⁾ azobenzene, imines,⁽²²⁾ phosphorimines,^(23, 24) 2-phenylpyridines and 2-phenyl-4-(methylcarboxylato)quinoline.⁽²⁵⁾

Parish *et al.* proposed that the transmetallation reaction occurs as in Scheme 1.8, for a general *C,N* coordinated ligand. Initially the amine (which only weakly interacts with the mercury) coordinates to the gold giving a bimetallic intermediate. The aryl group is then transferred from the mercury to the gold, with the elimination of HgCl₂, to give the cycloaurated complex. [Me₄N]Cl is often used in the synthesis as it promotes the precipitation of mercury as insoluble [Me₄N]₂[Hg₂Cl₆], thus forcing the formation of the cycloaurated complex.⁽²¹⁾

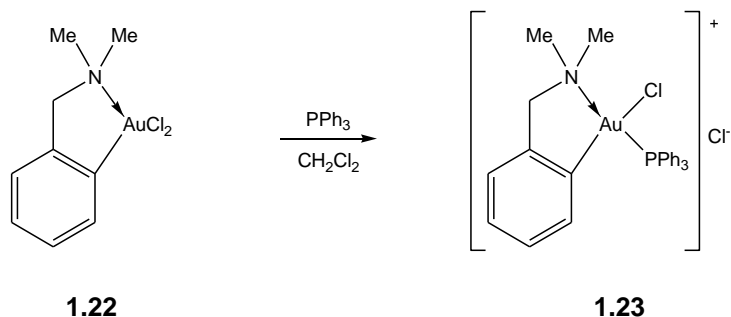


Scheme 1.8 Proposed mechanism for the transfer of an organic group from mercury to gold.

Chloride substitution reactions with phosphines

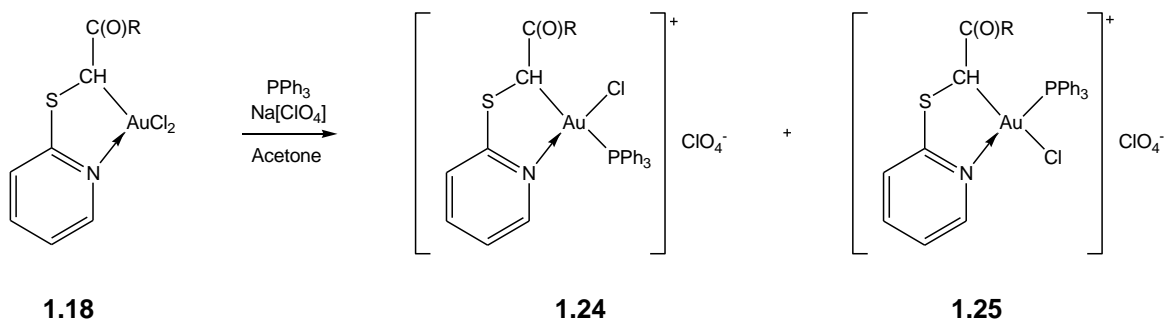
The strength of the interaction of the nitrogen donor with the gold greatly affects the chemistry of the cycloaurated complexes. Such an interaction has been evaluated by the reaction of cycloaurated complexes with tertiary phosphines.

The complex (damp)AuCl₂ **1.22** (Scheme 1.7) has a relatively strong nitrogen-gold bond – when reacted with a molar equivalent of triphenylphosphine the nitrogen-gold bond (and hence the metallacyclic ring) remains intact and a chloride ligand is replaced to give the cationic gold complex **1.23** (Scheme 1.9).⁽²⁰⁾ Other cycloaurated systems which show a similar behaviour are those containing 2-thienyl-,⁽¹⁴⁾ (Scheme 1.4), 2-anilino-^(9, 10) and 2-benzylpyridine derivatives⁽⁸⁾ or 1-ethyl-2-phenylimidazole⁽¹⁶⁾ ligands.



Scheme 1.9 Reaction of (damp)AuCl₂ **1.22** with PPh₃ which results in replacement of a chloride ligand to give complex **1.23**.

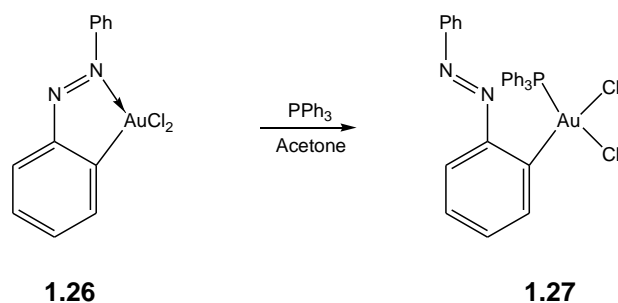
In the above cases, X-ray crystallography has shown the phosphine is coordinated *trans* to the nitrogen donor atom. Presumably the phosphine initially replaces the chloride ligand *trans* to the carbon because of the greater *trans* effect of the aryl carbon over the nitrogen. An isomerisation step (by an unknown mechanism) would then follow to give the most (thermodynamically) stable isomer with the carbon and the phosphine *cis* to each other.⁽²⁶⁾ Interestingly, the reaction of cycloaurated 2-(alkylthio)pyridine complexes **1.18** (Scheme 1.6) with PPh₃ and Na[ClO₄] results in both isomers **1.24** and **1.25** being formed (Scheme 1.10). However, upon refluxing in chloroform they convert to **1.25**, the most thermodynamically stable isomer.⁽¹⁹⁾



Scheme 1.10 Reaction of (2-(alkylthio)pyridyl)AuCl₂ **1.18** (R = Ph or Me) with PPh₃ which results in replacement of a chloride ligand to give the isomers **1.24** and **1.25**, which are converted to **1.25** upon refluxing in chloroform.

Alternatively, if the nitrogen-gold bond is relatively weak then a tertiary phosphine will displace the nitrogen donor to give a neutral complex which no longer contains a metallacyclic

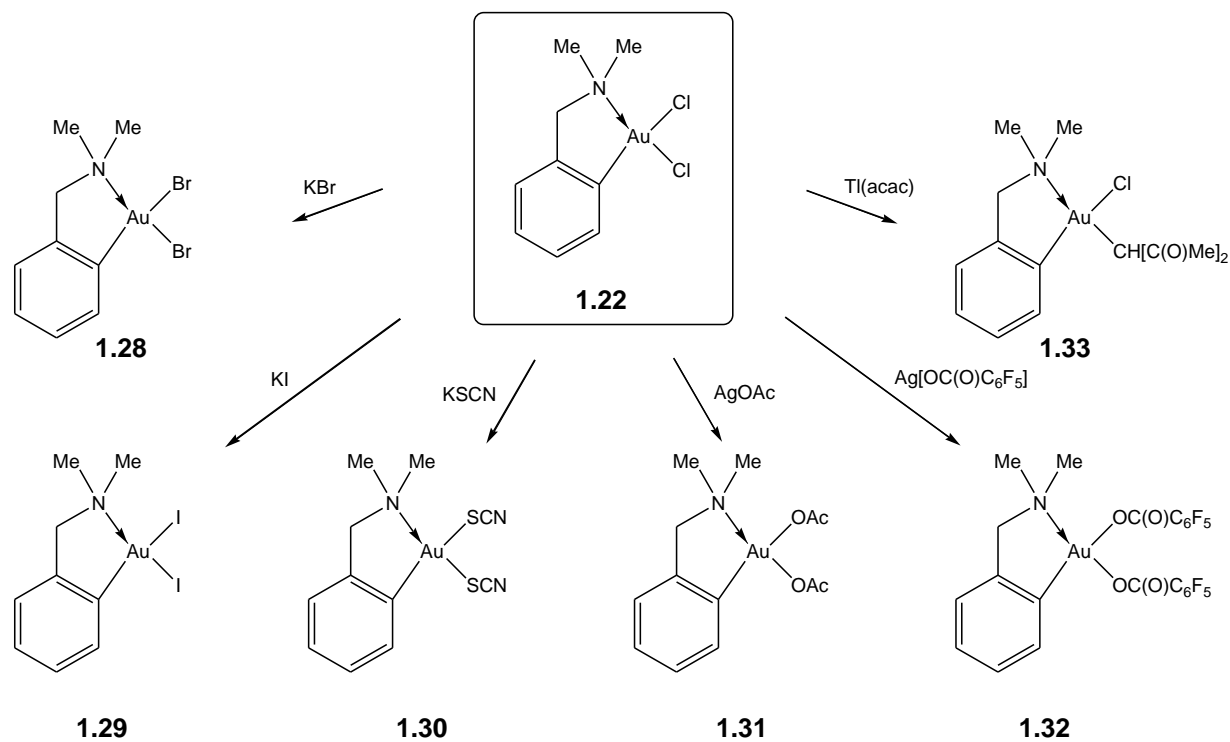
ring. This was observed for cycloaurated azobenzene⁽²⁷⁾ **1.26** (shown in Scheme 1.11), 2-phenoxy- and 2-(phenylsulfanyl)-pyridine⁽¹⁰⁾ and 2-benzoyl pyridine.⁽¹⁵⁾



Scheme 1.11 Reaction of (azobenzene) AuCl_2 **1.26** with PPh_3 which results in displacement of the neutral nitrogen donor atom.

Chloride substitution reactions with monoanionic ligands

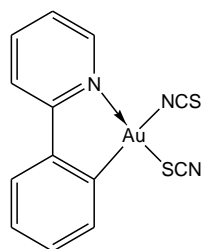
The *cis* chloride ligands on the cycloaurated complexes can readily be replaced by other monoanionic ligands.



Scheme 1.12 Chloride substitution reactions of (damp) AuCl_2 **1.22** with monoanionic ligands.

The reactions shown in Scheme 1.12 are not exclusive to the damp complex **1.22**, however this cycloaurated system has been the most extensively studied and chosen to give a general overview of the substitution reactions that are possible. The review by Henderson includes details of the analogous reactions other cycloaurated systems undergo.⁽⁷⁾ A simple metathesis reaction with KBr or KI gives the dibromo **1.28** or diiodo **1.29** complexes respectively, however the diiodo complex is unstable in solution.⁽²⁰⁾ A similar metathesis reaction with KSCN gives the dithiocyanato complex **1.30**.⁽²⁸⁾ The carboxylate derivatives **1.31** and **1.32** are best obtained by reaction of **1.22** with AgOAc⁽²⁰⁾ or Ag[O₂CC₆F₅] respectively. The acetate derivative **1.31** shows better solubility than the parent dichloride **1.22** and also shows promising anti-tumour activity.⁽²⁹⁾ Reaction of **1.22** with Tl(acac) gives the C-bonded acetylacetonato complex **1.33**.⁽³⁰⁾

It is worthy to note that in complex **1.30** the ambidentate thiocyanate ligands have been assigned to be *S*-bound to the gold centre, on the basis of IR spectroscopy. Because gold(III) is a soft metal this is not surprising. However a crystal structure of complex **1.34** shows that one thiocyanate ligand is *S*-bound (the one *trans* to the nitrogen) and the other is *N*-bound.⁽³¹⁾



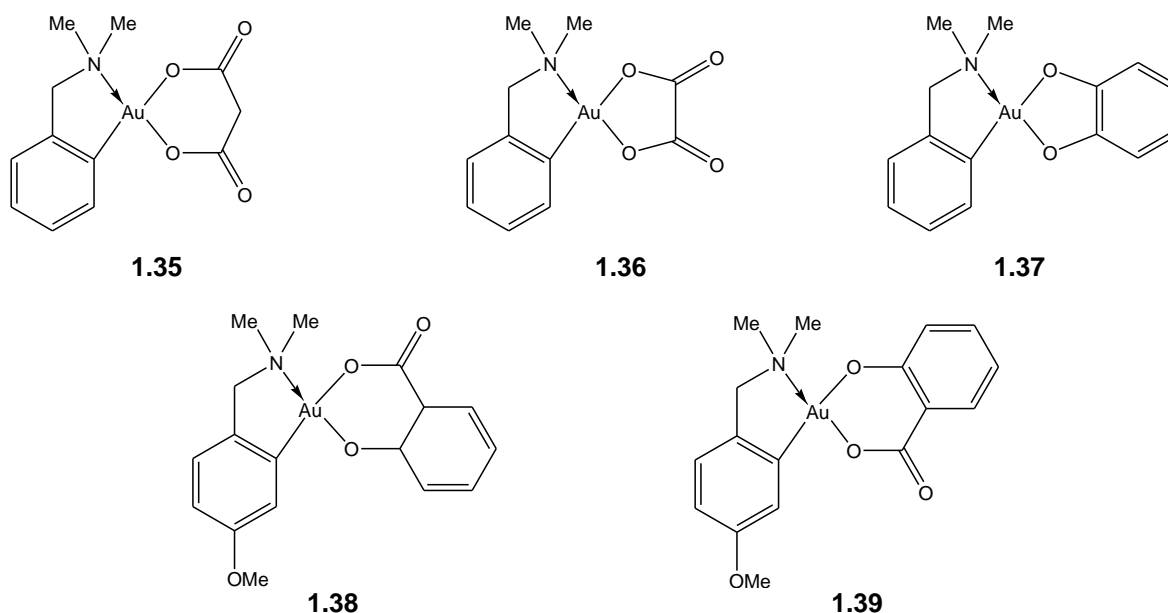
1.34

Scheme 1.13 The di-thiocyanate derivative of cycloaurated 2-phenylpyridine **1.8**. X-ray crystallography has shown that the one thiocyanate ligand is *S*-bonded, the other *N*-bonded.

Chloride substitution reactions with dianionic bidentate ligands

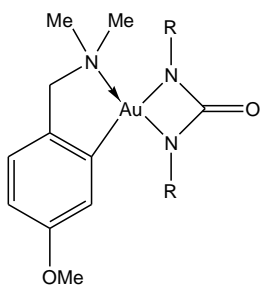
The chloride ligands are also able to be replaced by dianionic chelating ligands forming complexes with two metallacyclic rings. Again, the reactions presented are not exclusive to the damp system but instead give a general overview of the chemistry that can occur.

The reaction of (damp)AuCl₂ **1.22** with either silver malonate or silver nitrate/oxalic acid gave the *O,O'* bonded bis-carboxylate compounds **1.35** and **1.36** respectively.⁽²⁹⁾ The *O,O'* bonded catecholate complex **1.37** was formed when the parent dichloride was reacted with catechol in hot methanol, using trimethylamine as a base.⁽³²⁾ The salicylate complexes **1.38** and **1.39** were synthesised by reaction of the 4-methoxy-substituted damp complex with salicylic acid – this time silver(I) oxide was employed as the base. Initially two isomers **1.38** and **1.39** were formed but converted to **1.39** upon standing.⁽³³⁾

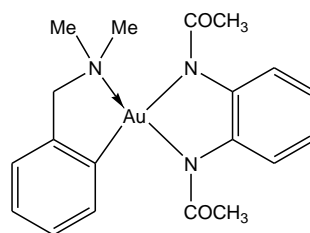


Scheme 1.14 Bicyclic gold(III) complexes formed when the two *cis* chloride ligands of the parent gold(III) dichloride complexes are replaced by *O,O'*-bidentate ligands.

The complexes **1.40** and **1.41** (Scheme 1.15), which contain *N,N'* bidentate ligands were synthesised by the reaction of the parent dichloride with either a urea⁽³⁴⁾ or a bis-amide⁽³⁵⁾ ligand. In both cases the reactions were carried out in refluxing dichloromethane using silver(I) oxide as the base.



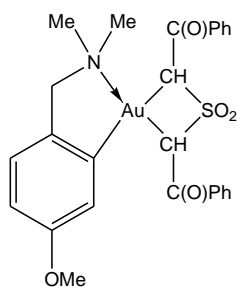
1.40



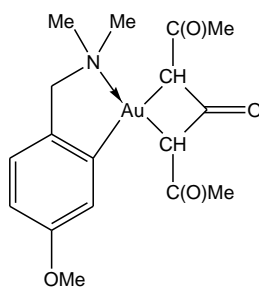
1.41

Scheme 1.15 Ureylene **1.40** ($R = \text{Ph}$ or COCH_3) and bis-amidate **1.41** complexes formed when the two *cis* chloride ligands of the parent dichlorides are replaced by *N,N'*-bidentate ligands.

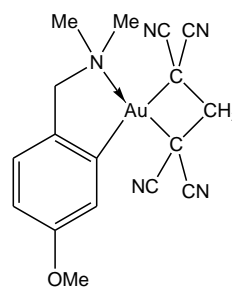
The aurathietane-3,3-dioxide⁽³⁶⁾ **1.42**, auracyclobutan-3-one⁽³⁶⁾ **1.43** and auracyclobutane⁽³⁷⁾ **1.44** complexes all contain four-membered cycloaurated rings, formed by the coordination of *C,C'* bidentate anionic ligands. As with the *N,N'* cycloaurated complexes the reactions were carried out in refluxing dichloromethane with silver(I) oxide as a base. The auralactam complex **1.45**, synthesised by an analogous method, also contains a four-membered cycloaurated ring which is coordinated to the gold *via* carbon and a nitrogen atoms.⁽³⁸⁾ Crystallography has shown in the cases of **1.44** and **1.45** the four-membered rings are slightly puckered.



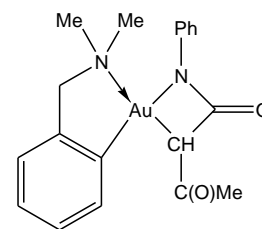
1.42



1.43



1.44

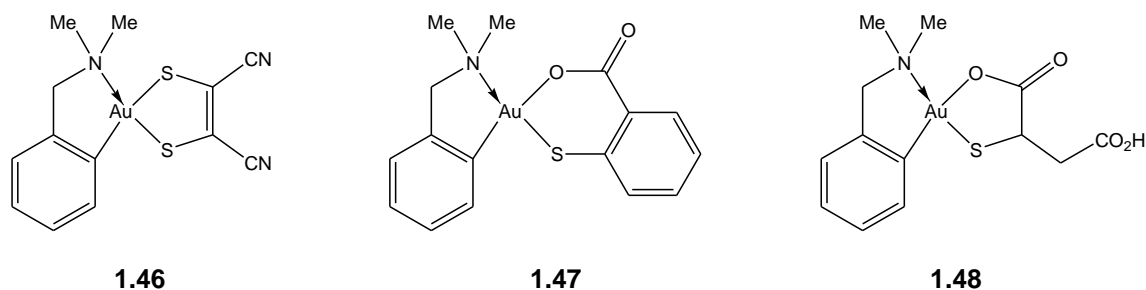


1.45

Scheme 1.16 Four-membered metallacycles formed by the reaction of gold(III) dichloride complexes with *C,C'* and *C,N* bidentate ligands.

The reaction of (damp) AuCl_2 **1.22** (Scheme 1.7) with $\text{Na}_2[\text{S}_2\text{C}_2(\text{CN})_2]$ in aqueous acetonitrile gave the maleonitriledithiolate complex **1.46** (Scheme 1.17), which contains a bidentate *S,S'*

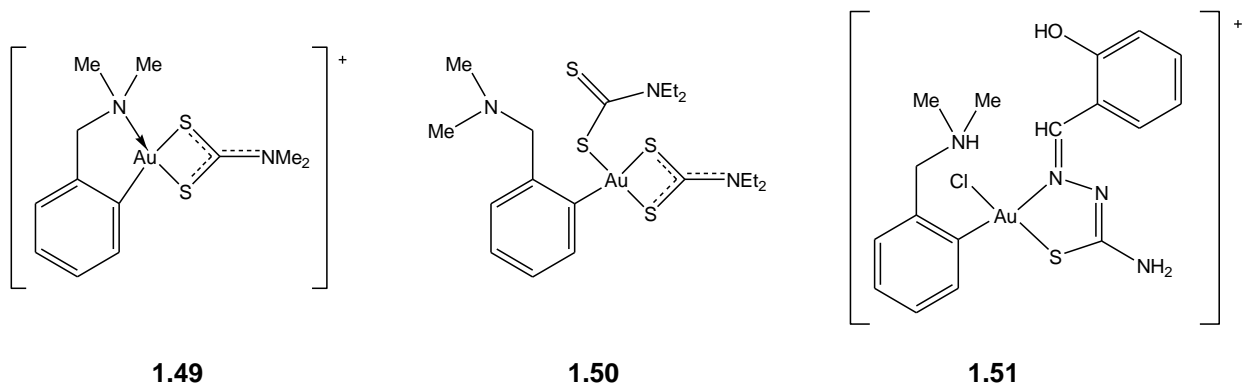
coordinated ligand.⁽³⁹⁾ Complexes with *S,O* bidentate ligands (**1.47** and **1.48**) were formed by the reaction of the parent dichloride complexes with ligands such as thiosalicylic acid (with the aid of Ag₂O)⁽³³⁾ or mercaptosuccinic acid (as the silver salt).⁽²⁸⁾



Scheme 1.17 Complexes formed when (damp)AuCl₂ **1.22** is reacted with sodium maleonitriledithiolate **1.46**, thiosalicylic acid **1.47** and silver mercaptosuccinate **1.48**.

Displacement of the nitrogen donor ligand

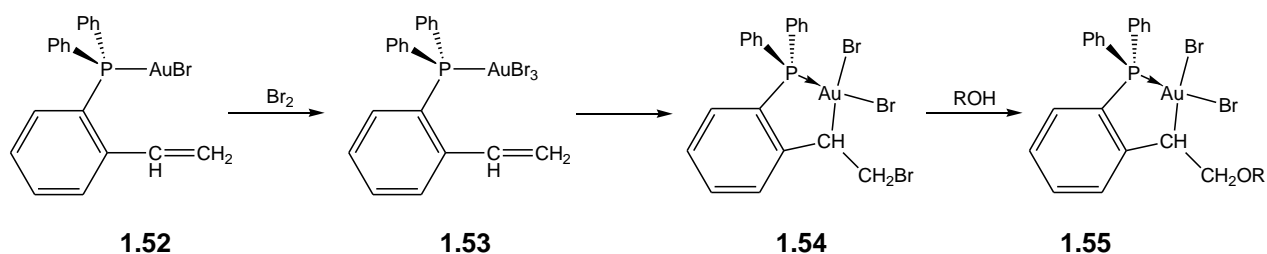
In the majority of the reactions discussed so far the original metallacyclic ring remains intact – the exception is the displacement of the neutral nitrogen donor by phosphine ligands, shown in Scheme 1.11. However, reaction of the parent dichloride complexes with ligands that are more strongly binding than the chloride anions can result in displacement of the nitrogen and cleavage of the metallacyclic ring. For example, when (damp)AuCl₂ **1.22** was reacted with excess KCN the NMe₂ group was displaced and the anionic complex [(damp)Au(CN)₃]⁻ was obtained (as the potassium salt).⁽²⁸⁾ Dithiocarbamates can also displace the NMe₂ group, but the reaction is dependent on the mole ratios employed. One equivalent of dithiocarbamate resulted in the cationic complex **1.49**, which contains the original metallacyclic ring and a chelating dithiocarbamate ligand.⁽²⁸⁾ Two equivalents of dithiocarbamate led to displacement of the NMe₂ group and complex **1.50**, which is fluxional in solution but has also been characterised crystallographically.⁽²⁸⁾ Semicarbazones also displace the nitrogen donor, and in addition protonate the NMe₂ group. This has been shown for a range of semicarbazones; **1.51** is an example of such a compound that has been structurally characterised.⁽⁴⁰⁾



Scheme 1.18 Products of the reaction of (damp)AuCl₂ **1.22** with sodium dialkyldithiocarbamates (**1.49** and **1.50**) and salicylaldehyde thiosemicarbazone **1.51**.

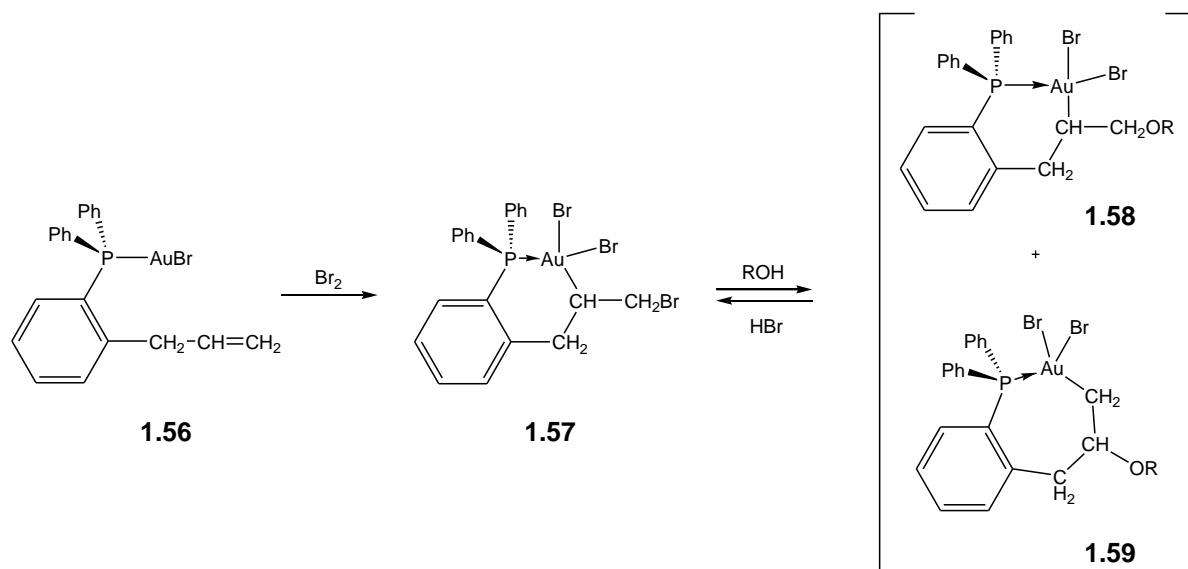
1.2.2 Complexes formed from *C,P* donor ligands

Examples of cycloaurated complexes containing a carbon-gold sigma bond and phosphorus-gold coordinate bond are limited to the systems developed by Bennett. The oxidation of the gold(I) *o*-styryldiphenylphosphine **1.52** with bromine (in benzene, at room temperature) gave yellow crystals which had microelemental data that were consistent with the formulation LAuBr₃. It was proposed that the gold(III) tribromide **1.53** was formed initially but then one Au-Br bond adds across the C=C bond of the styrene moiety forming the metallacycle **1.54**, the structure of which was confirmed by X-ray crystallography.⁽⁴¹⁾ The bromine attached to the methyl group could be replaced by OMe, OEt or OH groups when **1.54** was refluxed in methanol, ethanol or aqueous acetone respectively. The dichloride analogue of **1.54** could be synthesised by the oxidation of the gold(I) chloride (analogous to **1.52**) with chlorine.⁽⁴²⁾



Scheme 1.19 Proposed reaction scheme for the formation of five-membered *C,P* cycloaurated complexes.

The *o*-allyl-phenyl derivative **1.56** underwent a similar reaction with bromine and the six-membered auracycle **1.57** was obtained. When **1.57** was heated in either methanol or ethanol two alkoxy-derivatives were obtained in a 1:1 ratio. Separation by chromatography and fractional crystallisation revealed the presence of a six-membered (**1.58**) and unusually, a seven-membered auracycle **1.59** (Scheme 1.20).⁽⁴³⁾



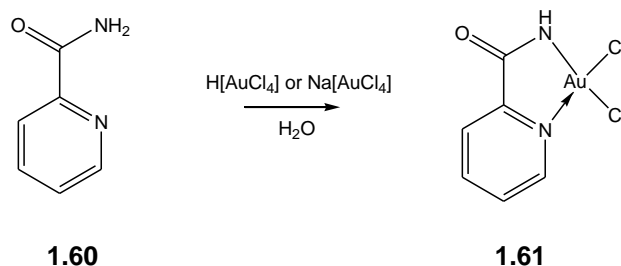
Scheme 1.20 Proposed reaction scheme for the formation of six- and seven-membered *C,P* cycloaurated complexes.

Parish *et al.* investigated the substitution reactions of the bromide ligands of **1.54** and **1.55** (and the chloride ligands of the analogous derivatives) and found in some ways they mirror the results seen with the analogous *C,N* cyclometallated complexes. Thus, a metathesis reaction with silver acetate gave a light-sensitive compound that was characterised as the diacetate complex on the basis of NMR spectrometry. With one equivalent of potassium thiocyanate the chloride ligand *trans* to the phosphorus was replaced. In the reaction with two equivalents of AgCN both the chloride ligands were replaced by cyanide ligands, however if NaCN or KCN were used in place of AgCN the reaction was more complex and reduction to gold(I) was observed. With one equivalent of diethyldithiocarbamate the cation analogous to **1.49** (Scheme 1.18) was obtained.⁽⁴²⁾

1.2.3 Complexes formed from *N,N'* donor ligands

Compared with the vast amount of research that has been accomplished using the *C,N* systems described above, little work investigating the analogous *N,N'* cycloaurated systems has been carried out. This is surprising as a N-H bond is somewhat weaker than a C-H bond hence the direct deprotonation and the formation of a Au-N bond would appear to be more facile.

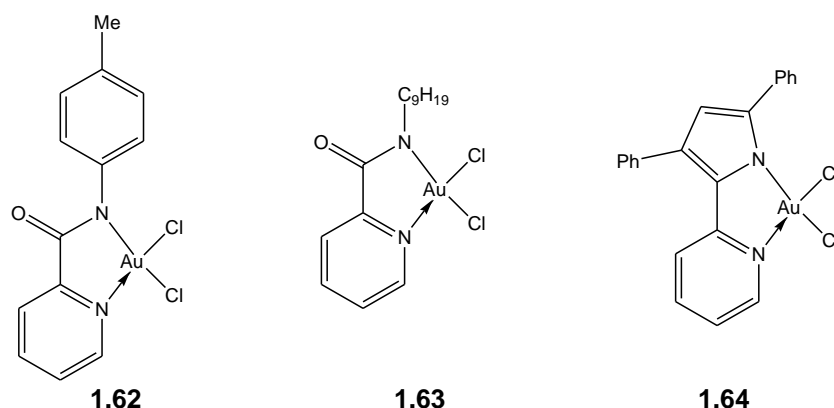
The majority of bidentate *N,N'* coordinated gold(III) complexes contain either picolinamide (2-pyridinecarboxamide) **1.60** or *N*-substituted picolinamide ligands. Two groups have independently described the reaction of picolinamide **1.60** with either H[AuCl₄] or Na[AuCl₄] in water to form the five-membered metallacycle **1.61** in good yields (Scheme 1.21).^(44, 45) The amide functionality has been deprotonated and forms a coordinate bond to the gold, the neutral donor is provided by the pyridyl nitrogen. *In vitro* cytotoxicity assays of **1.61** with MOLT-4 (a human tumour cell line) and C2C12 (a mouse tumour cell line) indicate that **1.61** has a cytotoxicity similar to that of *cisplatin*.⁽⁴⁵⁾



Scheme 1.21 Direct N-H bond activation of picolinamide **1.60** by [AuCl₄] to form the five-membered metallacycle **1.61**.

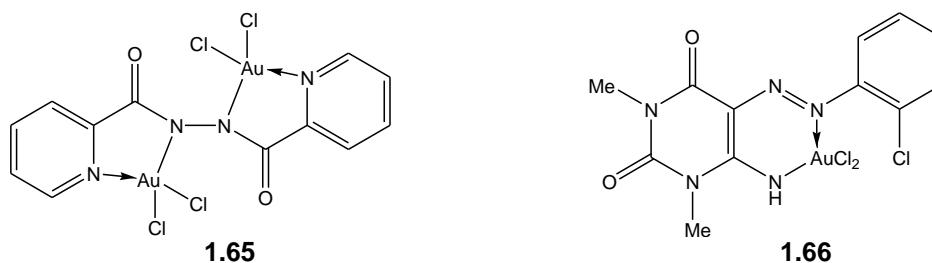
The *N*-(*p*-tolyl) derivative also undergoes cycloauration to yield **1.62** which has been structurally characterised. In addition, this complex has been shown to react with biological molecules. ESI-MS studies have indicated that the compound reacts with GMP (guanosine 5'-monophosphate) to give the bis-GMP adduct [LAu(5-GMP)₂].⁽⁴⁶⁾ In a separate report, the *N*-alkyl (-C₉H₁₉) substituted complex **1.63**, which has been structurally characterised, was shown to be an effective catalyst in dihydroindole formation from substituted furans and tetrahydroquinolines.⁽⁴⁷⁾

The related ligand 2-(3,5-diphenyl-1H-pyrrol-2-yl)pyridine also undergoes a cyclometallation reaction with Na[AuCl₄]. Again a five-membered auracycle **1.64** was obtained in good yields. The metallacycle appears relatively stable – the *cis* chloride ligands could be replaced in a transmetallation reaction with SnMe₄ to give the *cis* methyl derivative in good yields.⁽⁴⁸⁾



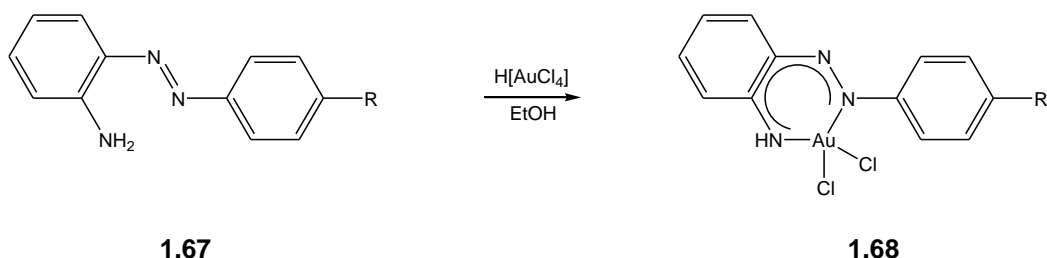
Scheme 1.22 Complexes formed by direct N-H bond activation of 2-pyridine substituted ligands to form five-membered metallacycles.

The di-nuclear gold(III) complex **1.65** can be formed when the ligand *N,N'*-bis(α -picolinoyl)hydrazine is reacted with K[AuCl₄] in water. X-ray crystallography has indicated uninterrupted π -conjugation of the system.⁽⁴⁹⁾ In addition, the ligand 6-amino-1,3-dimethyl-5-(2-chlorophenylazo)uracil also reacted with H[AuCl₄] in refluxing ethanol and gave the six-membered auracycle **1.66** as a red solid. The uncoordinated ligand possesses antineoplastic activity; disappointingly there was no report on the biological activity of the gold complex **1.66**.⁽⁵⁰⁾



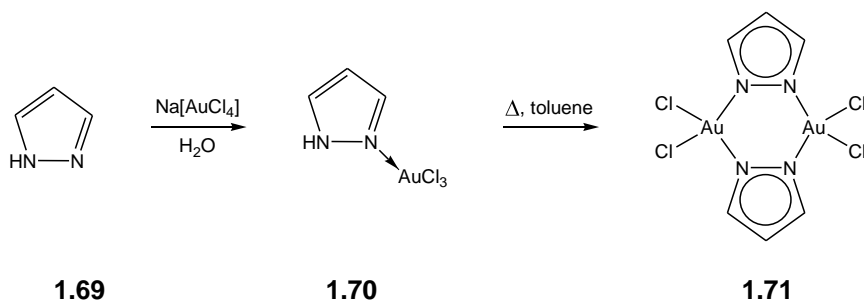
Scheme 1.23 Cycloaurated complexes formed by direct N-H bond activation of *N,N'*-bis(α -picolinoyl)hydrazine (**1.65**) and 6-amino-1,3-dimethyl-5-(2-chlorophenylazo)uracil (**1.66**).

The reaction of a series of β -diazoketiminates **1.67** with $\text{H}[\text{AuCl}_4]$ in ethanol efficiently yielded the gold complexes **1.68**. The six-membered chelate ring that formed showed a high degree of delocalisation, which was indicated by an X-ray crystal structure analysis of the phenyl substituted derivative.⁽⁵¹⁾



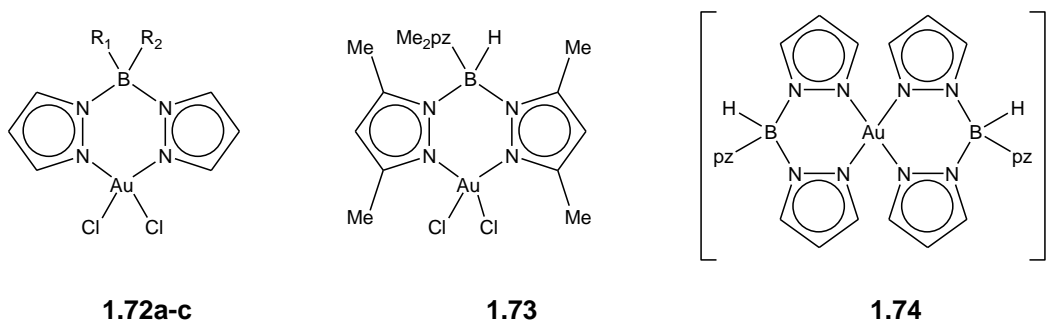
Scheme 1.24 Synthesis of β -diazoketimate complexes of gold(III) (R = H, CH_3 or Cl).

The reactivity of gold(III) towards pyrazole (Hpz) has also been investigated. That is, when pyrazole **1.69** was reacted with aqueous $\text{Na}[\text{AuCl}_4]$ (1:1 mole ratio) the adduct $[\text{Au}(\text{Hpz})\text{Cl}_3]$ **1.70**, where the neutral pyrazole ligand was coordinated through the non-protonated nitrogen, formed immediately. Refluxing **1.70** in toluene resulted in N-H bond activation and formation of the cycloaurated species **1.71**, where two pyrazolide ions bridge two gold centres. When 3-methylpyrazole was used in place of pyrazole the reaction proceeded directly to the cycloaurated species but in this case two geometric isomers were obtained. The gold complexes showed cytotoxicity against MOLT-4 and C2C12 cell lines that was comparable to that of *cisplatin*.⁽⁴⁵⁾



Scheme 1.25 Synthesis of dinuclear gold(III) complexes containing bridging pyrazolide ions.

A series of poly(pyrazole)borate anions ($[\text{HB}(\text{pz})_3]^-$, $[\text{HB}(\text{Me}_2\text{pz})_3]^-$, $[\text{B}(\text{pz})_4]^-$ and $[\text{Ph}_2\text{B}(\text{pz})_2]^-$) were reacted with $\text{H}[\text{AuCl}_4]^-$ in ethanol to give neutral Au(III) compounds **1.72** and **1.73** in acceptable yields. To maintain the square planar geometry required with gold(III) only two of the three pyrazolyl groups can be coordinated to the metal at any one time. However, at room temperature the ^1H NMR spectrum showed three equivalent pyrazolyl rings. Variable temperature NMR studies of **1.72c** found that at -60°C three sets of signals occur indicating that above this temperature rapid interchange between the free and coordinated pyrazolyl rings is occurring which results in the equivalence of the three rings. Similar behaviour was seen for the other complexes. In an analogous reaction with $[\text{H}_2\text{B}(\text{pz})_2]^-$ no product could be isolated probably because of the high reducing power of the borate anion that still contains two hydrogen atoms.⁽⁵²⁾ Vicente *et al.* reinvestigated the reaction of $[\text{HB}(\text{pz})_3]^-$ with $[\text{AuCl}_4]^-$ and found that carrying out the reaction in water led to almost quantitative yields of **1.72c**. In addition, a 2:1 ratio of $[\text{HB}(\text{pz})_3]^-$ to $[\text{AuCl}_4]^-$ gave the homoleptic cation **1.74**. Unlike the *C,N* cyclometallated complexes, substitution of the chloride ligands was more difficult and the reaction of **1.72c** with PPh_3 led to unidentified gold(I) compounds.⁽⁵³⁾

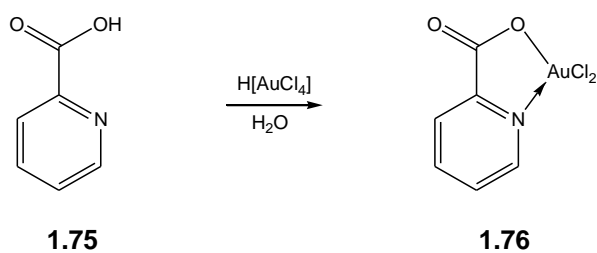


Scheme 1.26 Poly(pyrazolyl)borate gold(III) complexes. (**1.72a** $\text{R}_1 = \text{R}_2 = \text{Ph}$; **1.72b** $\text{R}_1 = \text{R}_2 = \text{pz}$; **1.72c** $\text{R}_1 = \text{H}$, $\text{R}_2 = \text{pz}$).

1.2.4 Complexes formed from *N,O'* donor ligands

The *N,O* donor ligands that form complexes with gold(III) contain an anionic oxygen atom (which forms a sigma bond to the gold) and neutral nitrogen, arising from either a pyridyl or imine (Schiff base) group. To the best of our knowledge there are no examples of gold(III) complexes which contain ligands with a nitrogen-gold sigma bond and a neutral oxygen donor.

The cycloauration of a variety of 2-substituted pyridine compounds has been investigated. The reaction of pyridine-2-carboxylic acid **1.75** with $\text{H}[\text{AuCl}_4]$ in water yielded the cycloaurated *N,O* coordinated complex **1.76**, which contains a five-membered metallacyclic ring (Scheme 1.27).⁽⁵⁴⁾ Pyridine-2-methanol⁽⁵⁵⁾ and 8-quinolinol⁽⁵⁶⁾ also reacted in an analogous manner to give five-membered metallacycles. The decomposition pathway of these complexes has been investigated and it appears that for the carboxylate derivative **1.76** the first step is displacement of the nitrogen donor followed by cleavage of the gold-oxygen bond.⁽⁵⁴⁾

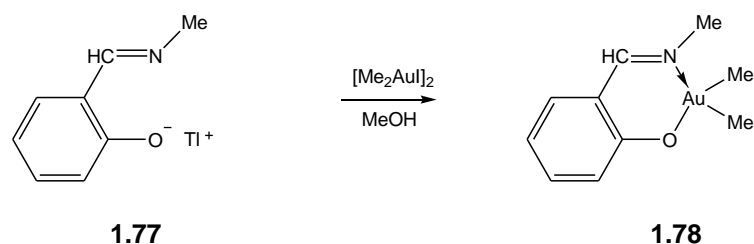


Scheme 1.27 The reaction of pyridine-2-carboxylic acid **1.75** with $\text{H}[\text{AuCl}_4]$ to give the five-membered metallacycle **1.76**.

The biological activity of cycloaurated pyridine-2-methanol has been investigated. The compound was stable under physiological conditions (pH 7.4, 50 μM phosphate buffer, 0.1 M NaOH) – although the metallacycle remained intact, the chloride ligands underwent hydrolysis in water. The complex reacts with the proteins albumin and transferrin and in the case of albumin the gold(III) is reduced to gold(I), possibly by the cysteine residues – no reduction is seen with transferrin. In addition the compound also binds DNA and shows good cytotoxicity.⁽⁵⁷⁾ The carboxylic acid derivative **1.76** has been shown to be catalytically active in numerous organic reactions.^(47, 58-66)

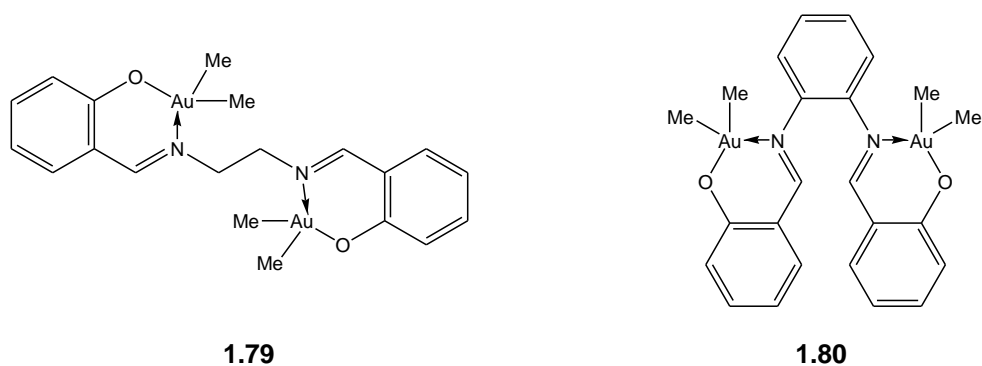
Gold(III) complexes of Schiff bases were first described in 1973. The reaction of the thallium(I) salt of the Schiff base salicylaldehyde **1.77** with $[\text{Me}_2\text{AuI}]_2$ in methanol afforded the six-membered cycloaurated complex **1.78**, which contains *cis* methyl ligands, in good yields (Scheme 1.28).⁽⁶⁷⁾ The ‘in situ’ deprotonation of the phenol group of salicylaldehyde by NaHCO_3 , followed by the reaction with $[\text{Me}_2\text{AuI}]_2$, also gave the *cis* methyl compounds but

excluded the use of toxic thallium salts.⁽⁶⁸⁾ *N*-Isopropyl and cyclohexyl derivatives of salicylaldimine also undergo an analogous reaction - the resulting complexes are readily soluble in methanol and most other organic solvents. In addition, the cycloaurated complexes have volatility characteristics which make them ideal for metal-organic chemical vapour deposition (MOCVD) applications.⁽⁶⁸⁾



Scheme 1.28 Synthesis of cycloaurated complexes containing a deprotonated salicylaldimine ligand.

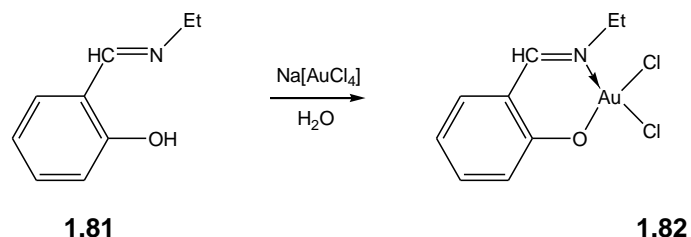
Reactions of the bis-bidentate imine ligands (as the thallium salts) $Tl_2(\text{salen})$ ($\text{salenH}_2=N,N'$ -ethylenebis(salicylaldimine)) and $Tl_2(\text{salphen})$ ($\text{salphenH}_2=N,N'$ -*o*-phenylenebis(salicylaldimine)) with $[Me_2AuI]_2$ gave the bis-cycloaurated complexes **1.79** and **1.80** respectively, which are expected to have a bridged binuclear structure (Scheme 1.29).⁽⁶⁷⁾



Scheme 1.29 Proposed structures of bis-cycloaurated complexes containing bidentate *N,O* ligands.

The direct reaction of the *N*-ethylsalicylaldimine **1.81** with aqueous $Na[AuCl_4]$ gave the *cis* dichloride complex **1.82** which is blue-green in colour (Scheme 1.30).^(69, 70) The biological

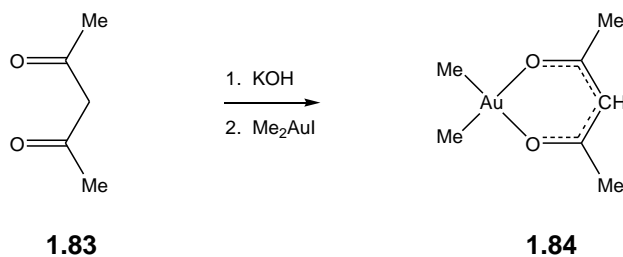
activity of **1.82** was explored, and it showed good binding properties towards DNA. The binding is tight but reversible and it results in modest stabilisation of the double helix. Therefore, binding to DNA may be the mechanism by which the compounds are cytotoxic, however **1.82** has limited pharmaceutical applications because of poor stability in physiological media.⁽⁶⁹⁾



Scheme 1.30 Synthesis of cycloaurated *N*-ethylsalicylaldimine **1.82**.

1.2.5 Complexes formed from *O,O'* donor ligands

Examples of *O,O'* mononegative bidentate ligands which coordinate to the gold(III) centre are limited to β -diketones, mainly acetylacetonate (Hacac) **1.83**, although other examples (*e.g.* dipivaloylmethane and dibenzoylmethane) are also known. The synthesis typically involves the addition of $[\text{Me}_2\text{AuI}]_2$ to the potassium salt of the β -diketone at room temperature, in a solvent such as ethanol (Scheme 1.31). The complexes are volatile (see later) so can be purified by sublimation onto a cold finger.^(71, 72) Alternatively, reaction of the solvated cations $[\text{Au}(\text{C}_6\text{F}_5)_2\text{Z}_2]^+$ (Z = acetone, diethyl ether) with acac gave the complex $[\text{Au}(\text{C}_6\text{F}_5)_2(\text{acac})]$.⁽⁷³⁾



Scheme 1.31 Synthesis of β -ketonate gold(III) complexes.

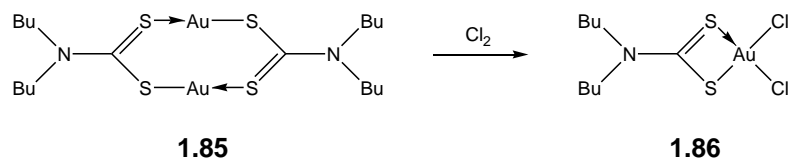
The resulting chelates tend to be white crystalline solids with low melting points and a sharp odour. They are unstable towards light and require storage at sub-zero temperatures.⁽⁷¹⁾ It has

been proposed that the first step in the thermal decomposition of these complexes takes place by the opening of the chelate ring.⁽⁷⁴⁾

As mentioned above, the gold(III) *O,O'* coordinated β -diketonate complexes are volatile and have been used for chemical vapour deposition (CVD), particularly **1.84** which is available commercially.⁽⁷⁵⁻⁷⁷⁾ The decomposition of the compounds allows a convenient method to deposit gold species (cations and nanoparticles) onto surfaces for use in heterogeneous catalysis.⁽⁷⁸⁾

1.2.6 Complexes formed from *S,S'* donor ligands

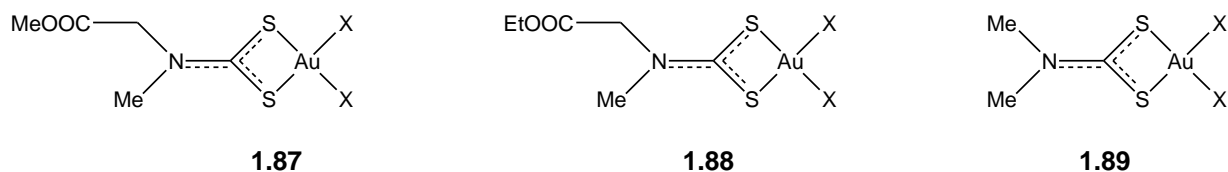
Gold(III) complexes which contain monoanionic *S,S'* bidentate ligands are mainly restricted to examples of dithiocarbamate compounds. The initial work on dithiocarbamate compounds came from the laboratory of van der Kerk where a range of different synthetic methods were employed to synthesise the cycloaurated complexes. The dihalide gold(III) complexes were synthesised by the reaction of a dimeric gold(I) *N,N*-bis-dialkyldithiocarbamate with a molar equivalent of either chlorine gas, thionyl chloride (to give the dichlorides), bromine, *N*-bromosuccinimide or *N*-bromophthalimide (to give the dibromides). For example, Scheme 1.32 depicts the reaction of the gold(I) *N,N*-bis-dibutyldithiocarbamate **1.85** with chlorine to yield dichloro gold(III) *N,N*-bis-dibutyldithiocarbamate **1.86**. Alternatively, the reaction of $\text{AuCl}_3 \cdot \text{py}$ with $\text{NaS}_2\text{CNMe}_2$ in DMF produces the dichloro gold(III) *N,N*-bis-dimethyldithiocarbamate in 68% yield.⁽⁷⁹⁾



Scheme 1.32 Synthesis of dichloro gold(III) *N,N*-bis-dibutyldithiocarbamate **1.86** by the reaction of gold(I) *N,N*-bis-dibutyldithiocarbamate with chlorine.

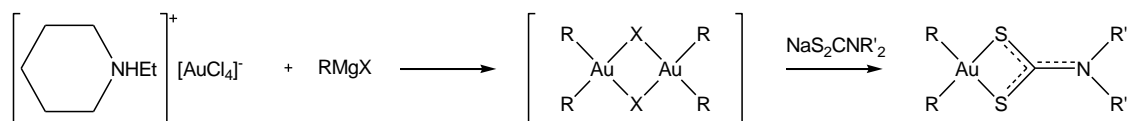
The biological activity of dihalo-gold(III) dialkyldithiocarbamates has received a notable amount of attention lately, mainly because of the noted similarities of the complexes with

cisplatin. The methylsarcosine derivative **1.87** has an activity that is significantly higher, or at least comparable to *cisplatin* against human tumours (HL60 or HeLa cell lines).⁽⁸⁰⁾ In addition, complexes **1.88** and **1.89** are much more cytotoxic *in vitro* than *cisplatin* towards human tumour cell lines.⁽⁸¹⁾



Scheme 1.33 Gold(III) dithiocarbamate complexes that are biologically active (X=Cl or Br).

Synthesis of dialkyl gold(III) *N,N*-bis-dialkyldithiocarbamates was also investigated by van der Kerk. These can be synthesised by the reaction depicted in Scheme 1.34. In addition, the reaction of dihalo gold(III) dialkyldithiocarbamates (*e.g.* **1.86**) with either an alkyl magnesium halide or dialkyl cadmium reagent also gave dialkyl gold(III) dialkyldithiocarbamates. The resulting gold(III) complexes were insoluble in water but soluble in most organic solvents. They show appreciable stability towards dilute acids and bases and mild reducing agents.⁽⁷⁹⁾ It was later shown that the reaction of $[\text{Me}_2\text{AuI}]_2$ with sodium salts of dialkyldithiocarbamates is also a convenient synthetic method, the related xanthate complexes can also be synthesised by this method.⁽⁸²⁾ Such compounds may have applications in CVD.⁽⁸³⁾ Diaryl gold(III) dialkyldithiocarbamates, containing pentafluorophenyl groups were synthesised either by the reaction of the gold(III) dimer $[\text{Au}(\mu\text{-Cl})(\text{C}_6\text{F}_5)_2]_2$ with two equivalents of the sodium dialkyldithiocarbamate or by oxidising the dimeric gold(I) complex $[\text{Au}(\text{S}_2\text{CNEt}_2)]_2$ with $\text{Ti}(\text{C}_6\text{F}_5)_2\text{Cl}$.⁽⁸⁴⁾



Scheme 1.34 Synthesis of dialkyl gold(III) *N,N*-bis-dialkyldithiocarbamate complexes.

1.3 Scope of this Thesis

As mentioned above, there is still a large scope for the development of new cycloaurated complexes. Therefore, this thesis explores the synthesis, characterisation and properties of a range of new cycloaurated complexes. The cycloaurated iminophosphorane complexes described in Chapter Two contain the traditional *C,N* donor ligands. Chapter Three details the synthesis and properties of cycloaurated phosphine chalcogenide ligands which retain the carbon-gold sigma bond but also introduce either a sulfur or selenium as the neutral donor atom. Chapters Four and Five move away from carbon bonded organometallic compounds to nitrogen and sulfur based ligands respectively – as can be seen in the discussion above, little work has been done looking at the reactivity and properties of cycloaurated complexes with ligands other than *C,N* donor atoms. In Chapter Six the chemistry of the cationic complexes formed with the Kläui ligand are discussed. Finally, Chapter Seven evaluates the use of these new compounds as catalysts in the addition of methyl vinyl ketone (MVK) to 2-methylfuran.

1.4 References

1. H. Schmidbaur, *Gold Progress in Chemistry, Biochemistry and Technology*. Chichester: John Wiley & Sons Ltd; **1999**.
2. R. J. Puddephatt; *The Chemistry of Gold*, Elsevier Scientific Publishing Company, Amsterdam, **1978**
3. M. A. Cinellu, A. Zucca, S. Stoccoro, G. Minghetti, M. Manassero and M. Sansoni; *J. Chem. Soc., Dalton Trans.*, **1996**, 4217.
4. G. Marangoni, B. Pitteri, V. Bertolasi, G. Gilli and V. Ferretti; *J. Chem. Soc., Dalton Trans.*, **1986**, 1941.
5. V. F. Duckworth, C. M. Harris and N. C. Stephenson; *Inorg. Nucl. Chem. Lett.*, **1968**, 4, 419.
6. N. J. DeStefano and J. L. Burmeister; *Inorg. Chem.*, **1971**, 10, 998.
7. W. Henderson; *Adv. Organomet. Chem.*, **2006**, 54, 207.
8. M. A. Cinellu, A. Zucca, S. Stoccoro, G. Minghetti, M. Manassero and M. Sansoni; *J. Chem. Soc., Dalton Trans.*, **1995**, 2865.
9. M. Nonoyama, K. Nakajima and K. Nonoyama; *Polyhedron*, **1997**, 16, 4039.
10. Y. Fuchita, H. Ieda, A. Kayama, J. Kinoshita-Nagaoka, H. Kawano, S. Kameda and M. Mikuriya; *J. Chem. Soc., Dalton Trans.*, **1998**, 4095.

11. E. C. Constable and T. A. Leese; *J. Organomet. Chem.*, **1989**, 363, 419.
12. W. Henderson, B. K. Nicholson, S. J. Faville, D. Fan and J. D. Ranford; *J. Organomet. Chem.*, **2001**, 631, 41.
13. Y. Zhu, B. R. Cameron and R. T. Skerlj; *J. Organomet. Chem.*, **2003**, 677, 57.
14. Y. Fuchita, H. Ieda, S. Wada, S. Kameda and M. Mikuriya; *J. Chem. Soc., Dalton Trans.*, **1999**, 4431.
15. Y. Fuchita, H. Ieda, Y. Tsunemune, J. Kinoshita-Nagaoka and H. Kawano; *J. Chem. Soc., Dalton Trans.*, **1998**, 791.
16. Y. Fuchita, H. Ieda and M. Yasutake; *J. Chem. Soc., Dalton Trans.*, **2000**, 271.
17. H. Ieda, H. Fujiwara and Y. Fuchita; *Inorg. Chim. Acta*, **2001**, 319, 203.
18. M. Nonoyama, K. Nakajima and K. Nonoyama; *Polyhedron*, **2001**, 20, 3019.
19. J. Vicente, M. T. Chicote, M. I. Lozano and S. Huertas; *Organometallics*, **1999**, 18, 753.
20. J. Vicente, M. T. Chicote and M. D. Bermúdez; *J. Organomet. Chem.*, **1984**, 268, 191.
21. P. A. Bonnardel, R. V. Parish and R. G. Pritchard; *J. Chem. Soc., Dalton Trans.*, **1996**, 3185.
22. J. Vicente, M. D. Bermúdez, F.-J. Carrión and P. G. Jones; *Chem. Ber.*, **1996**, 129, 1301.
23. S. D. J. Brown, W. Henderson, K. J. Kilpin and B. K. Nicholson; *Inorg. Chim. Acta*, **2007**, 360, 1310.
24. D. Aguilar, M. Contel, R. Navarro and E. P. Urriolabeitia; *Organometallics*, **2007**, 26, 4604.
25. R. V. Parish, J. P. Wright and R. G. Pritchard; *J. Organomet. Chem.*, **2000**, 596, 165.
26. R. V. Parish; *Gold Bull.*, **1997**, 30, 55.
27. J. Vicente, M. T. Chicote and M. D. Bermúdez; *Inorg. Chim. Acta*, **1982**, 63, 35.
28. R. V. Parish, B. P. Howe, J. P. Wright, J. Mack, R. G. Pritchard, R. G. Buckley, A. M. Elsome and S. P. Fricker; *Inorg. Chem.*, **1996**, 35, 1659.
29. R. G. Buckley, A. M. Elsome, S. P. Fricker, G. R. Henderson, B. R. C. Theobald, R. V. Parish, B. P. Howe and L. R. Kelland; *J. Med. Chem.*, **1996**, 39, 5208.
30. J. Vicente, M. D. Bermúdez, M. T. Chicote and M.-J. Sánchez-Santano; *J. Chem. Soc., Dalton Trans.*, **1990**, 1945.
31. D. Fan, C.-T. Yang, J. D. Ranford, J. J. Vittal and P. F. Lee; *Dalton Trans.*, **2003**, 3376.
32. C. H. A. Goss, W. Henderson, A. L. Wilkins and C. Evans; *J. Organomet. Chem.*, **2003**, 679, 194.
33. M. B. Dinger and W. Henderson; *J. Organomet. Chem.*, **1998**, 560, 233.
34. M. B. Dinger and W. Henderson; *J. Organomet. Chem.*, **1998**, 557, 231.
35. K. J. Kilpin, W. Henderson and B. K. Nicholson; *Polyhedron*, **2007**, 26, 434.
36. M. B. Dinger and W. Henderson; *J. Organomet. Chem.*, **1997**, 547, 243.

37. M. B. Dinger and W. Henderson; *J. Organomet. Chem.*, **1999**, 577, 219.
38. W. Henderson, B. K. Nicholson and A. G. Oliver; *J. Organomet. Chem.*, **2001**, 620, 182.
39. J. Mack, K. Ortner, U. Abram and R. V. Parish; *Z. Anorg. Allg. Chem.*, **1997**, 623, 873.
40. U. Abram, K. Ortner, R. Gust and K. Sommer; *J. Chem. Soc., Dalton Trans.*, **2000**, 735.
41. M. A. Bennett, K. Hoskins, W. R. Kneen, R. S. Nyholm, P. B. Hitchcock, R. Mason, G. B. Robertson and A. D. C. Towl; *J. Am. Chem. Soc.*, **1971**, 93, 4591.
42. R. V. Parish, P. Boyer, A. Fowler, T. A. Kahn, W. I. Cross and R. G. Pritchard; *J. Chem. Soc., Dalton Trans.*, **2000**, 2287.
43. M. A. Bennett; *J. Organomet. Chem.*, **1986**, 300, 7.
44. D. T. Hill, K. Burns, D. D. Titus, G. R. Girard, W. M. Reiff and L. M. Mascavage; *Inorg. Chim. Acta*, **2003**, 346, 1.
45. D. Fan, C.-T. Yang, J. D. Ranford and J. J. Vittal; *Dalton Trans.*, **2003**, 4749.
46. T. Yang, J.-Y. Zhang, C. Tu, J. Lin, Q. Liu and Z.-J. Guo; *Wuji Huaxue Xuebao (Chin. J. Inorg. Chem.)*, **2003**, 19, 45.
47. A. S. K. Hashmi, M. Rudolph, J. W. Bats, W. Frey, F. Rominger and T. Oeser; *Chem-Eur. J.*, **2008**, 14, 6672.
48. S. Schouteeten, O. R. Allen, A. D. Haley, G. L. Ong, G. D. Jones and D. A. Vicic; *J. Organomet. Chem.*, **2006**, 691, 4975.
49. A. Dogan, B. Schwederski, T. Schleid, F. Lissner, J. Fiedler and W. Kaim; *Inorg. Chem. Comm.*, **2004**, 7, 220.
50. E. Colacio Rodríguez, J. Ruiz Sánchez, J. D. López-González, J. M. Salas Peregrín, M. J. Olivier, M. Quirós and A. L. Beauchamp; *Inorg. Chim. Acta*, **1990**, 171, 151.
51. N. Maiti, B. K. Dirghangi and S. Chattopadhyay; *Polyhedron*, **2003**, 22, 3109.
52. N. F. Borkett, M. I. Bruce and J. D. Walsh; *Aust. J. Chem.*, **1980**, 33, 949.
53. J. Vicente, M. T. Chicote, R. Guerrero and U. Herber; *Inorg. Chem.*, **2002**, 41, 1870.
54. G. Annibale, L. Canovese, L. Cattalini, G. Marangoni, G. Michelon and M. L. Tobe; *J. Chem. Soc., Dalton Trans.*, **1984**, 1641.
55. L. Canovese, L. Cattalini, G. Marangoni and M. L. Tobe; *J. Chem. Soc., Dalton Trans.*, **1985**, 731.
56. E. Rivarola, G. C. Stocco, B. Lessandro Pepe and R. Barbieri; *J. Organomet. Chem.*, **1968**, 14, 467.
57. P. Calamai, S. Carotti, A. Guerri, L. Messori, E. Mini, P. Orioli and G. P. Speroni; *J. Inorg. Biochem.*, **1997**, 66, 103.
58. A. S. K. Hashmi, J. P. Weyrauch, M. Rudolph and E. Kurpejović; *Angew. Chem. Int. Ed.*, **2004**, 43, 6545.
59. A. S. K. Hashmi, M. Rudolph, J. P. Weyrauch, M. Wöelfle, W. Frey and J. W. Bats; *Angew. Chem. Int. Ed.*, **2005**, 44, 2798.

60. S. Wang and L. Zhang; *J. Am. Chem. Soc.*, **2006**, 128, 8414.
61. S. Wang and L. Zhang; *J. Am. Chem. Soc.*, **2006**, 128, 14274.
62. A. S. K. Hashmi, M. Wöelfle, F. Ata, M. Hamzic, R. Salathé and W. Frey; *Adv. Synth. Catal.*, **2006**, 348, 2501.
63. C. Ferrer, C. H. M. Amijs and A. M. Echavarren; *Chem-Eur. J.*, **2007**, 13, 1358.
64. X. Huang and L. Zhang; *J. Am. Chem. Soc.*, **2007**, 129, 6398.
65. G. Li and L. Zhang; *Angew. Chem. Int. Ed.*, **2007**, 46, 5156.
66. N. D. Shapiro and F. D. Toste; *J. Am. Chem. Soc.*, **2008**, 130, 9244.
67. K. S. Murray, B. E. Reichert and B. O. West; *J. Organomet. Chem.*, **1973**, 61, 451.
68. A. A. Bessonov, N. B. Morozova, N. V. Gelfond, P. P. Semyannikov, I. A. Baidina, S. V. Trubin, Y. V. Shevtsov and I. K. Igumenov; *J. Organomet. Chem.*, **2008**, 693, 2572.
69. P. Calamai, A. Guerri, L. Messori, P. Orioli and G. P. Speroni; *Inorg. Chim. Acta*, **1999**, 285, 309.
70. A. Dar, K. Moss, S. M. Cottrill, R. V. Parish, C. A. McAuliffe, R. G. Pritchard, B. Beagley and J. Sandbank; *J. Chem. Soc., Dalton Trans.*, **1992**, 1907.
71. G. I. Zharkova, I. A. Baidina and I. K. Igumenov; *J. Struct. Chem.*, **2006**, 47, 1117.
72. G. I. Zharkova, M. N. Tyukalevskaya, K. I. Igumenov and S. V. Zemskov; *Koordinats. Khim.*, **1988**, 14, 1362.
73. R. Usón, A. Laguna and M. L. Arrese; *Syn. React. Inorg. Met.*, **1984**, 14, 557.
74. P. P. Semyannikov, G. I. Zharkova, V. M. Grankin, N. M. Tyukalevskaya and I. K. Igumenov; *Metalloorg. Khim.*, **1988**, 1, 1105.
75. M. Mihaylov, B. C. Gates, J. C. Fierro-Gonzalez, K. Hadjiivanov and H. Knözinger; *J. Phys. Chem. C*, **2007**, 111, 2548.
76. T. Ishida, M. Nagaoka, T. Akita and M. Haruta; *Chem-Eur. J.*, **2008**, 14, 8456.
77. P. P. Semyannikov, B. L. Moroz, S. V. Trubin, G. I. Zharkova, P. A. Pyryaev, M. Y. Smirnov and V. I. Bukhtiyarov; *J. Struct. Chem.*, **2006**, 47, 458.
78. V. Aguilar-Guerrero and B. C. Gates; *Chem. Comm.*, **2007**, 3210.
79. H. J. A. Blaauw, R. J. F. Nivard and G. J. M. van der Kerk; *J. Organomet. Chem.*, **1964**, 2, 236.
80. L. Giovagnini, L. Ronconi, D. Aldinucci, D. Lorenzon, S. Sitran and D. Fregona; *J. Med. Chem.*, **2005**, 48, 1588.
81. L. Ronconi, L. Giovagnini, C. Marzano, F. Bettio, R. Graziani, G. Pilloni and D. Fregona; *Inorg. Chem.*, **2005**, 44, 1867.
82. C. Papparizos and J. P. Fackler Jnr; *Inorg. Chem.*, **1980**, 19, 2886.
83. G. I. Zharkova, I. A. Baidina and I. K. Igumenov; *J. Struct. Chem.*, **2007**, 48, 108.

84. R. Usón, A. Laguna, M. Laguna, M. L. Castilla, P. G. Jones and K. Meyer-Bäse; *J. Organomet. Chem.*, **1987**, 336, 453.

CHAPTER TWO

The Cycloauration of Iminophosphorane Ligands

2.1 Introduction

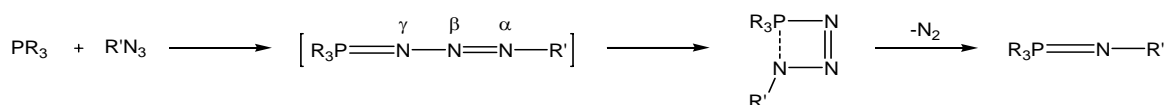
Iminophosphoranes (or phosphorimines, $R_3P=N-R'$), are attractive substrates for cyclometallation reactions. Synthesis is relatively simple and allows various organic functional groups to be introduced easily on both the phosphorus and the nitrogen substituents, therefore tuning the ligand to have the desired steric and electronic properties. The presence of a phosphorus atom in the ligand and the resulting cyclometallated complexes means ^{31}P NMR spectroscopy, a powerful spectroscopic probe, can be used in monitoring the reactions and also in subsequent characterisation of the cyclometallated species. A brief summary of the main synthetic routes to iminophosphoranes and their subsequent properties that relate to this work follows, however more comprehensive reviews are available on the topic.^(1, 2) A discussion on cyclometallated complexes formed from iminophosphorane ligands is also included.

2.1.1 Synthesis of iminophosphorane ligands

Staudinger reaction

The first iminophosphorane, $Ph_3P=N-Ph$, was synthesised by Staudinger and Meyer in 1919. Triphenylphosphine was reacted with phenylazide, and following the evolution of molecular nitrogen the iminophosphorane was obtained as a stable crystalline solid. The aptly named ‘Staudinger reaction’ has since been used to synthesise a number of different iminophosphoranes by varying the tertiary phosphine and/or azide used.

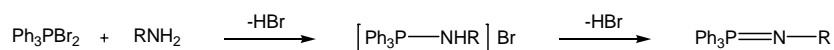
The Staudinger reaction is typically carried out in either diethyl ether or dichloromethane solvent. It is thought to proceed *via* a nucleophilic attack on the terminal nitrogen (N γ) by the phosphine. The resulting linear phosphazide then dissociates to the iminophosphorane and dinitrogen *via* a four-centered transition state, as depicted in Scheme 2.1. Not surprisingly, electron withdrawing groups on the azide facilitate the reaction, as do electron donating groups on the phosphine. Sterically bulky groups on either the azide or the phosphine slow the reaction at the second step – the formation of the four-membered transition state.⁽¹⁾



Scheme 2.1 Proposed mechanism for the Staudinger reaction, involving a four-membered transition state.

Kirsanov reaction

The Kirsanov reaction between R_3PBr_2 and amines is also commonly used in the synthesis of iminophosphoranes and eliminates the use of potentially hazardous organic azides that are a required reagent in the Staudinger reaction. Horner and Oedinger initially discovered that when R_3PBr_2 is reacted with an arylamine and a base (typically triethylamine) an iminophosphorane is formed. Later, Zimmer and Singh continued this initial work to show that aliphatic amines yield the alkylaminophosphonium salts $[\text{R}_3\text{P}-\text{NH}-\text{R}']\text{Br}$. These are simply converted to the iminophosphorane by the addition of a base, usually triethylamine (Scheme 2.2). The reaction is thought to proceed *via* a nucleophilic displacement of the bromide by the amine and again this reaction can lead to the synthesis of a wide variety of iminophosphoranes bearing different functional groups.



Scheme 2.2 Reaction scheme for the Kirsanov reaction.

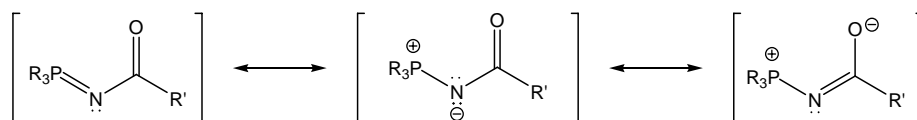
Other synthetic methods

The synthetic pathways to iminophosphoranes are not limited to the Staudinger and Kirsanov reactions. Other, albeit less common, methods of synthesis are available but were not applicable in this work and thus will not be commented on. However, details of these syntheses can be found in reviews by either Johnson⁽¹⁾ or Bestmann.⁽²⁾

2.1.2 Stability of iminophosphorane ligands

Unlike the isoelectronic phosphonium ylides ($\text{Ph}_3\text{P}=\text{CHR}$), the $\text{P}=\text{N}$ bond in iminophosphoranes is relatively stable. The nitrogen atom is trigonally hybridised with one lone pair of electrons in an sp^2 hybridised orbital and the other in a $2p$ orbital. This allows for overlap of a filled $2p$ orbital on the nitrogen with a vacant $3d_{xy}$ or $3d_{xz}$ orbital on the phosphorus thus giving a significant degree of $p\pi-d\pi$ bonding.

Iminophosphoranes are basic and undergo hydrolysis to form phosphine oxides and amines, with the stability of the iminophosphorane largely dependent on the nitrogen substituent. The stability towards hydrolysis is greatest when the nitrogen is substituted with electron-rich or bulky groups *e.g.* the following series increases in stability $-N\text{-alkyl} < -N\text{-aryl} < -N\text{-acyl}$. In addition, the *N*-acyl iminophosphoranes are resonance stabilised (Scheme 2.3).⁽³⁾ The stability of *N*-acyl iminophosphoranes over their *N*-aryl counterparts can be seen in the ^{31}P chemical shifts – because of delocalisation of electron density through the PNCO framework the phosphorus is deshielded thus the chemical shift of *N*-acyl derivatives occurs approximately 20 ppm further downfield than *N*-aryl derivatives.

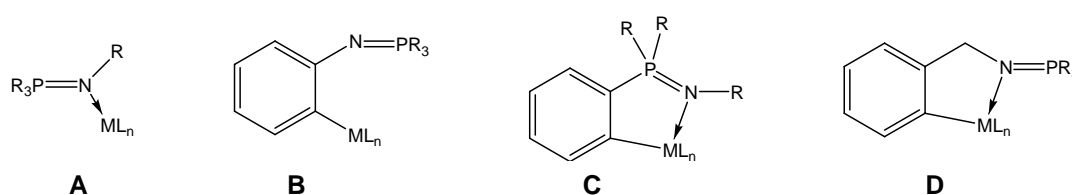


Scheme 2.3 The proposed resonance forms of stabilised iminophosphoranes.

Because triarylphosphine-substituted iminophosphoranes are generally more stable than the tri-alkyl counterparts, the majority of research has been conducted with these derivatives – triphenylphosphine is often used as a starting material because it is commercially available and relatively inexpensive. In addition, the iminophosphoranes with *P*-aryl substituents tend to be crystalline materials, while alkyl substituents on the phosphine tend to result in liquids or oils.

2.1.3 Cyclometallated iminophosphoranes

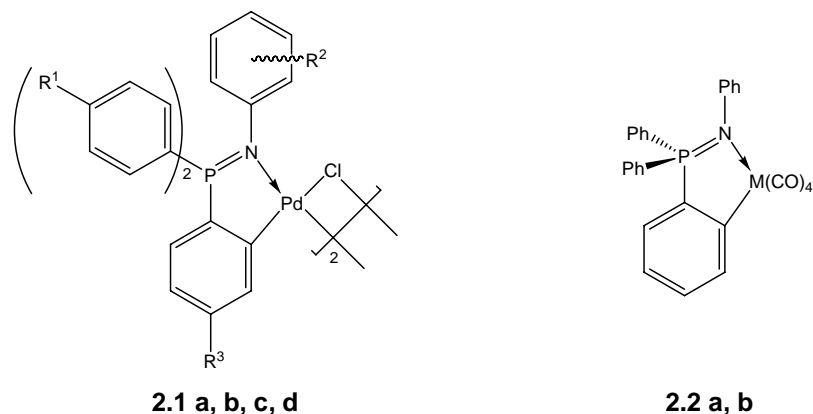
Iminophosphoranes can coordinate to metals in a number of different modes; the classes directly related to this work are shown in Scheme 2.4. The simplest binding mode (**A**) is where the iminophosphorane nitrogen atom acts as a simple two-electron donor to the metal centre. A C-H bond on the nitrogen substituent may be activated by a metal centre giving the simple organometallic complex (**B**). The final binding mode, and the one that is most relevant to this work, is where the iminophosphorane ligand forms a cyclometallated complex *via* a carbon-metal sigma bond and (usually) a nitrogen-metal coordinate bond. Cyclometallated iminophosphoranes can be further subdivided into two classes, that is *endo* (where the P=N bond is included in the cyclometallated ring (**C**)) or *exo* (the P=N bond is outside the ring) type complexes.



Scheme 2.4 Coordination modes of iminophosphorane ligands that relate to this work.

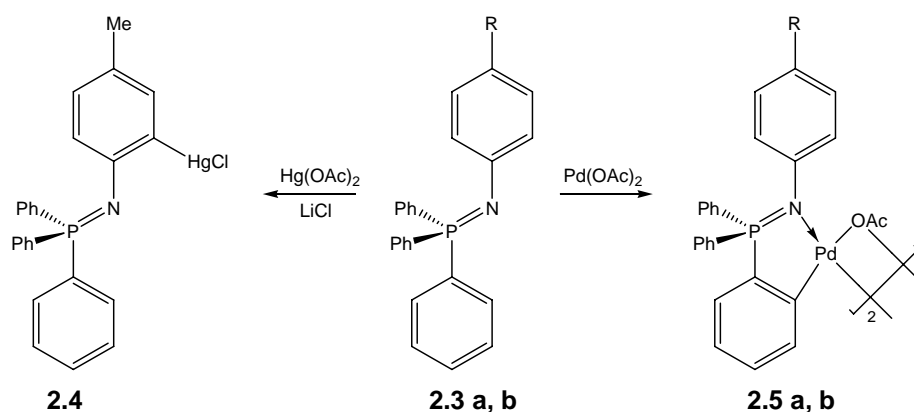
The earliest report on cyclometallated iminophosphoranes came out of Alper's laboratory in 1977. The cyclometallated complexes (**2.1 a-d**, Scheme 2.5) were directly synthesised in good yields by the room temperature reaction of aryl-substituted iminophosphoranes with Na₂PdCl₄.⁽⁴⁾ Interestingly, when the same synthetic procedure was followed with the

unsubstituted iminophosphorane $\text{Ph}_3\text{P}=\text{N}-\text{Ph}$ only the simple coordination complex $[\text{PdCl}_2\{\text{N}(=\text{PPh}_3)\text{Ph}\}]_2$ could be obtained.⁽⁵⁾ After Alper's initial research there was a 20 year 'lull' before Leeson *et al.* reported on the direct *ortho*-metallation of $\text{Ph}_3\text{P}=\text{N}-\text{Ph}$ by $\text{PhCH}_2\text{Mn}(\text{CO})_5$ or $\text{PhCH}_2\text{Re}(\text{CO})_5$ (**2.2a,b**, Scheme 2.5). Interestingly, the *ortho*-manganated complex (**2.2 a**) showed thermochromic properties in solution.⁽⁶⁾



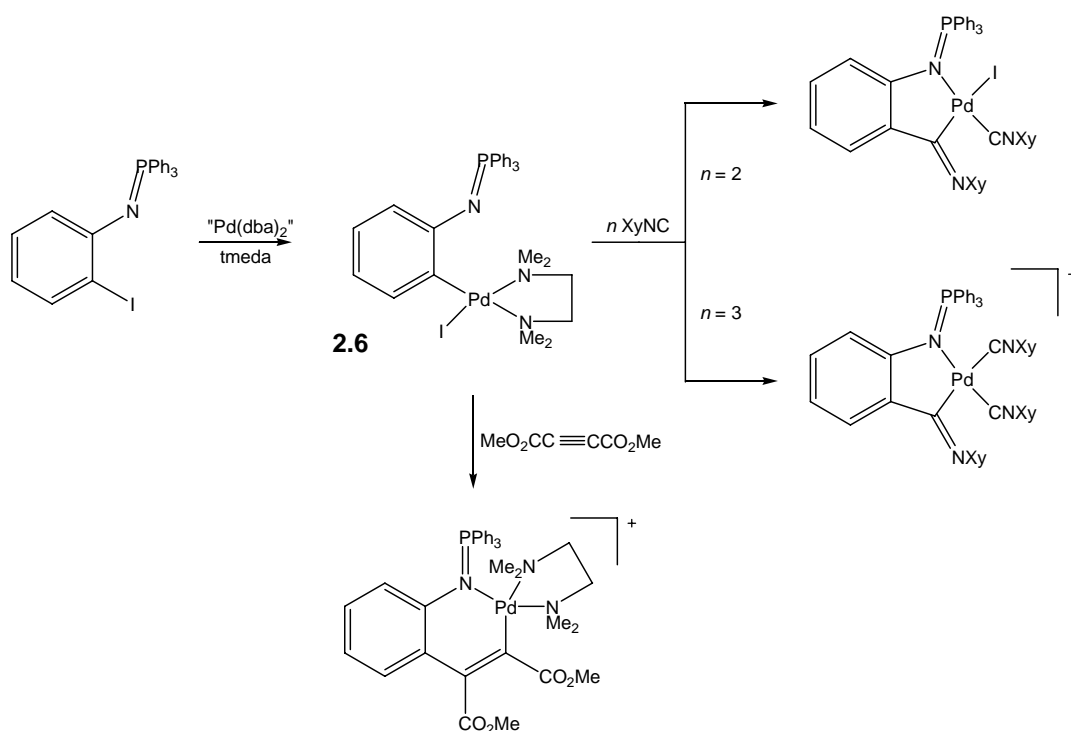
Scheme 2.5 The metal iminophosphorane complexes synthesised directly by Alper **2.1** (**a** $\text{R}^1 = \text{R}^3 = \text{H}$, $\text{R}^2 = m\text{-Me}$; **b** $\text{R}^1 = \text{R}^3 = \text{H}$, $\text{R}^2 = p\text{-Me}$; **c** $\text{R}^1 = \text{R}^3 = \text{H}$, $\text{R}^2 = p\text{-OMe}$; **d** $\text{R}^1 = \text{R}^3 = \text{H}$, $\text{R}^2 = p\text{-OMe}$) and Leeson **2.2** (**a** $\text{M} = \text{Mn}$; **b** $\text{M} = \text{Re}$).

More recently, Vicente *et al.* investigated the direct metallation reactions of *N*-aryl iminophosphoranes (**2.3a** and **2.3b**). Direct mercuration of the iminophosphorane ligand with $\text{Hg}(\text{OAc})_2$ (followed by a metathesis reaction with LiCl) gave the isomer **2.4** where the mercury is coordinated to the *N*-bonded phenyl ring (Scheme 2.6).⁽⁷⁾ This differs from the results that were seen by Zimmer where simple coordination compounds of the type $[\text{HgX}_2\{\text{N}(=\text{PPh}_3)\text{Ar}\}]$ ($\text{X}=\text{Cl}, \text{Br}, \text{I}$) were isolated from the reaction of HgX_2 with *N*-aryl-substituted iminophosphoranes.⁽⁸⁾ Attempted symmetrisation and transmetallation reactions with gold, palladium and platinum were unsuccessful.



Scheme 2.6 Reaction of aryl-iminophosphoranes **2.3** (**a** R = Me; **b** R = OMe) with $\text{Hg}(\text{OAc})_2$ or $\text{Pd}(\text{OAc})_2$ to give mercuration on the *N*-bonded phenyl ring (**2.4**) and palladiation on *P*-bonded aryl rings (**2.5 a** R = Me; **b** R = OMe) respectively.

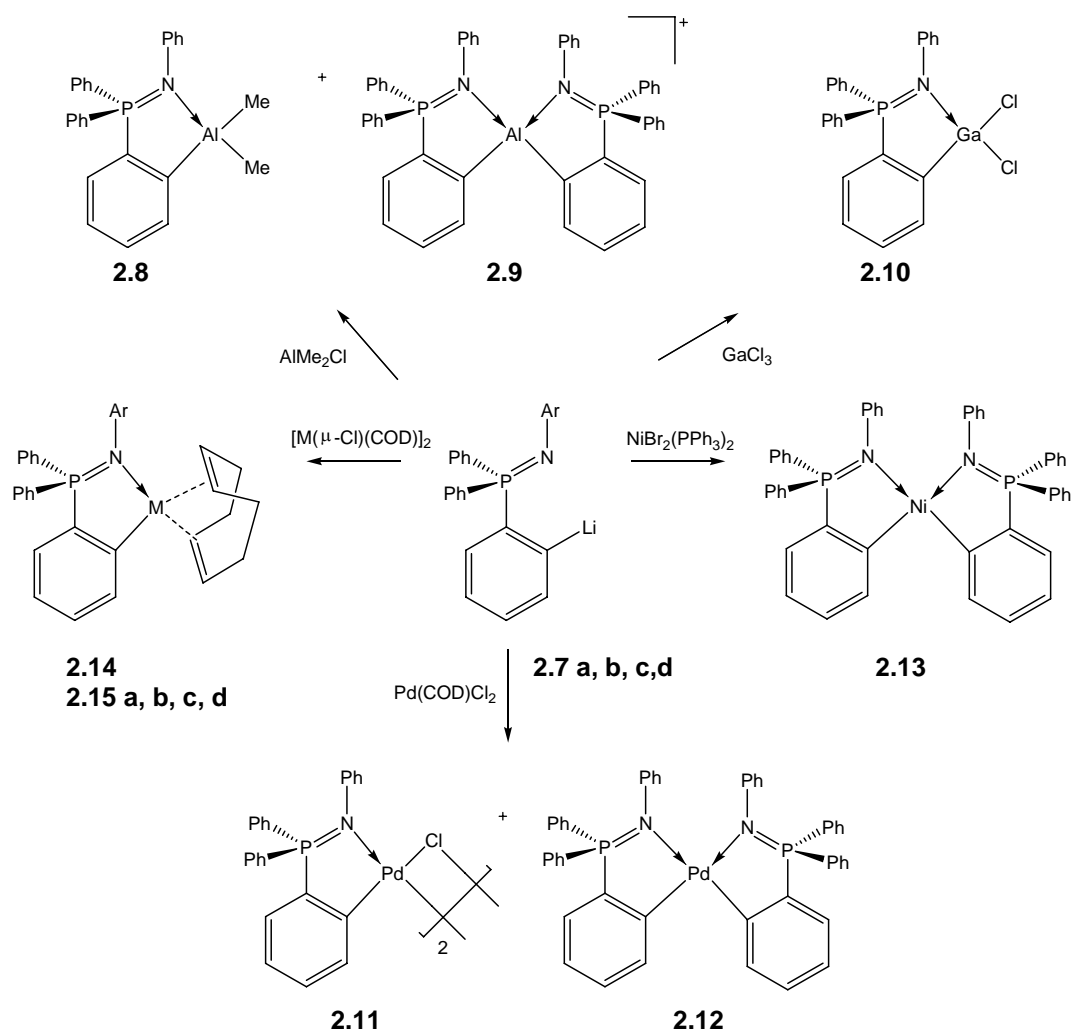
Reaction of **2.3 a, b** with $\text{Pd}(\text{OAc})_2$ in THF (at room temperature) gave the *endo* isomers (**2.5**) with the palladium attached at the *ortho*-position of a *P*-bonded phenyl ring (Scheme 2.6) – the same result as Alper witnessed. Compound **2.6**, with the palladium attached at the *ortho*-position of the *N*-bonded phenyl ring, was synthesised by oxidative addition of $\text{Pd}(0)$ to the *ortho*-iodo complex. Because the nitrogen is no longer coordinated to the metal centre in this complex it was envisioned that it would show interesting chemistry – it was shown that isocyanides or alkynes can be inserted into the palladium-carbon bond to form five- or six-membered rings respectively (Scheme 2.7).⁽⁷⁾



Scheme 2.7 Oxidative addition of the *ortho*-iodiated iminophosphorane to give *exo* isomer **2.6** with Pd attached to *N*-bonded substituent, and the insertion reactions it undergoes ("Pd(dba)₂" = [Pd₂(dba)₃].dba, dba = dibenzylideneacetone; tmeda = *N,N,N',N'*-tetramethylethylenediamine; Xy = 2,6-dimethylphenyl).

The Canadian laboratory of Stephan has looked at transmetallation reactions from *ortho*-lithiated iminophosphoranes, which in turn were first described by Stuckwisch.⁽⁹⁾ That is, reaction of **2.7** with main group (aluminium and gallium) metal complexes gives the *ortho*-metallated complexes **2.8**, **2.9** and **2.10**. In the case of the aluminium complexes, two chemically inseparable compounds **2.8** and **2.9** were formed. Careful crystal selection allowed **2.8** and **2.9** to be distinguished on the basis of X-ray crystallography. The gallium complex **2.10**, also structurally characterised, is interesting as the *N*-bound phenyl ring and the metallated arene ring are co-planar. Furthermore, the palladium and nickel complexes **2.11**, **2.12** and **2.13** were formed upon reaction of **2.7** with Pd(COD)Cl₂ (COD = cyclooctadiene) and NiBr₂(PPh₃)₂ respectively. Minor amounts of **2.11** (14%) were also formed in the reaction with Pd(COD)Cl₂.⁽¹⁰⁾ Rhodium and iridium complexes **2.14** and **2.15**

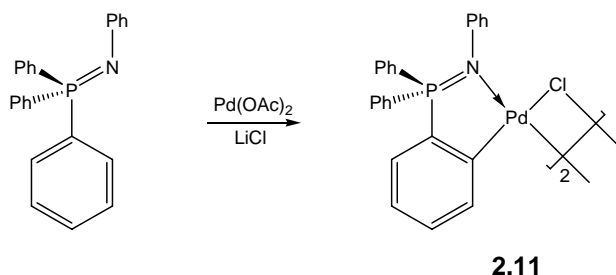
could also be synthesised in a similar manner.⁽¹¹⁾ Scheme 2.8 depicts the transmetalation reactions that were investigated.



Scheme 2.8 Reaction of *ortho*-lithiated iminophosphanes **2.7** (**a** Ar=Ph; **b** Ar=2,6-Me₂C₆H₄; **c** Ar=3,5-Me₂C₆H₄; **d** Ar=2,6-ⁱPr₂C₆H₄) with main-group and transition metal compounds to give aluminium **2.8** and **2.9**, gallium **2.10**, palladium **2.11** and **2.12**, nickel **2.13**, iridium **2.14** (Ar=Ph) and rhodium **2.15** (**a** Ar=Ph; **b** Ar=2,6-Me₂C₆H₄; **c** Ar=3,5-Me₂C₆H₄; **d** Ar=2,6-ⁱPr₂C₆H₄) cyclometallated complexes.

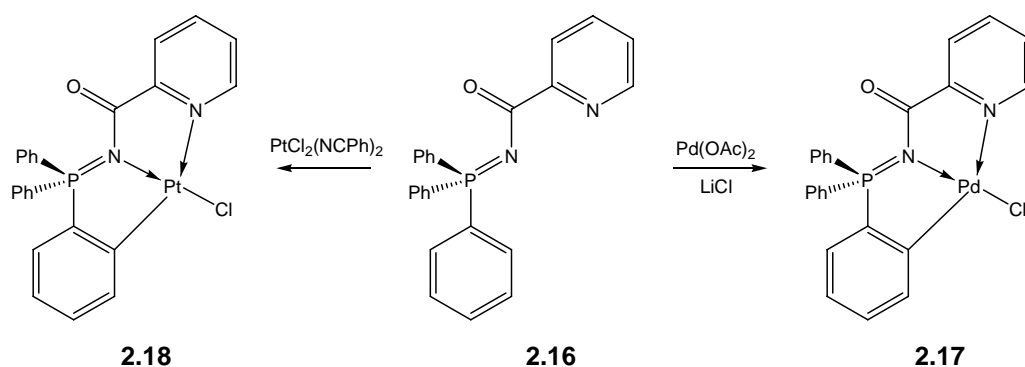
In the last few years the majority of work involving organometallic iminophosphorane complexes, especially palladiated examples, has come out of the laboratory of the Spanish

group of Urriolabeitia. Initial work was conducted treating $\text{Ph}_3\text{P}=\text{N}-\text{Ph}$ with $\text{Pd}(\text{OAc})_2$ in refluxing dichloromethane (Scheme 2.9) – this was found to be a better method for the synthesis of **2.11** than the indirect method involving the *ortho*-lithiated intermediate (Scheme 2.8) and $\text{Pd}(\text{COD})\text{Cl}_2$ (96% compared with 14%). **2.11** could also be formed when $\text{Ph}_3\text{P}=\text{NPh}$ was reacted with $\text{Li}_2[\text{PdCl}_4]$ but it forms an inseparable mixture with the simple *N*-bonded coordination compound $[\text{PdCl}_2\{\text{N}(\text{=PPh}_3)\text{Ph}\}]_2$. Attempts at synthesis of the analogous platinum complex by reaction of $\text{Ph}_3\text{P}=\text{N}-\text{Ph}$ with $\text{PtCl}_2(\text{NCPH})_2$ or $[\text{Pt}(\mu\text{-Cl})(\eta^3\text{-2-MeC}_3\text{H}_4)]_2$ were unsuccessful.⁽¹²⁾ In a similar manner, treatment of the prochiral iminophosphorane $\text{Ph}_2\text{MeP}=\text{NPh}$ with $\text{Pd}(\text{OAc})_2$ gave metallation exclusively on a *P*-bonded phenyl ring, resulting in the phosphorus atom becoming a stereogenic centre.⁽¹³⁾



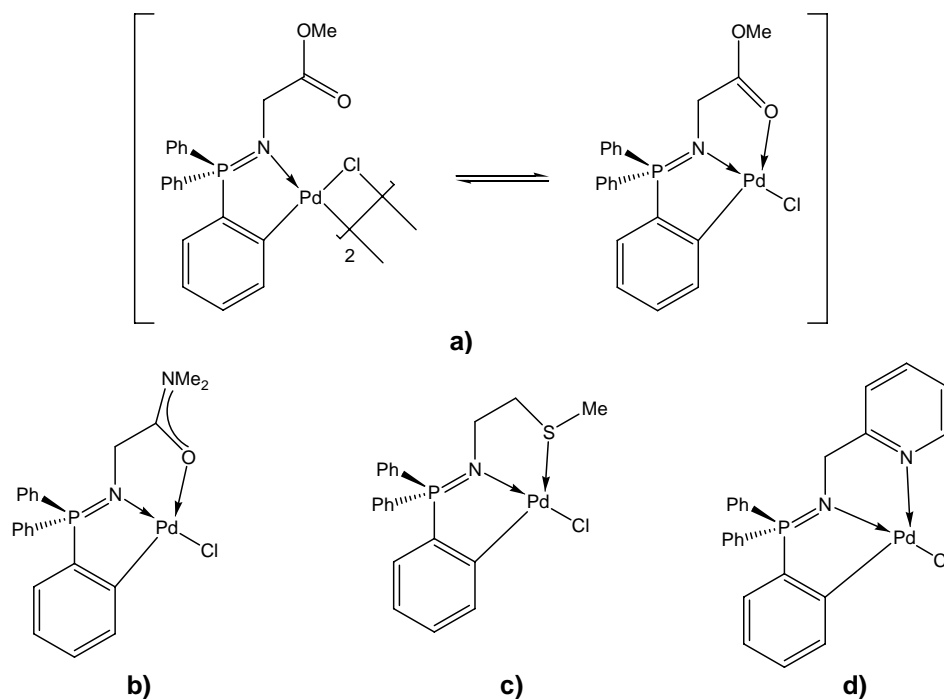
Scheme 2.9 Synthetic route to the *ortho*-palladiated iminophosphorane **2.11** devised by Bielsa *et al.*

The reactivity of the tridentate iminophosphorane ligand **2.16** with platinum and palladium complexes was also investigated. As above, the palladiated complex **2.17** could be formed cleanly when **2.16** was reacted with $\text{Pd}(\text{OAc})_2$ – when $\text{Li}_2[\text{PdCl}_4]$ was used only an inseparable mixture of **2.17** and the *N*-bonded coordination compound could be produced. However, in this case the tridentate platinum iminophosphorane complex **2.18** could be isolated when **2.16** was reacted with $\text{PtCl}_2(\text{NCPH})_2$. It appears that harsher reaction conditions (refluxing 2-methoxyethanol) resulted in cyclometallated complexes – when the same reactions were carried out in less harsh conditions (*i.e.* at room temperature or at low reflux temperatures) only the *N*-bonded coordination compounds could be formed. Subsequent reactions indicated that both the bidentate and tridentate ligands coordinate strongly to the metal centres (Scheme 2.10).⁽¹²⁾



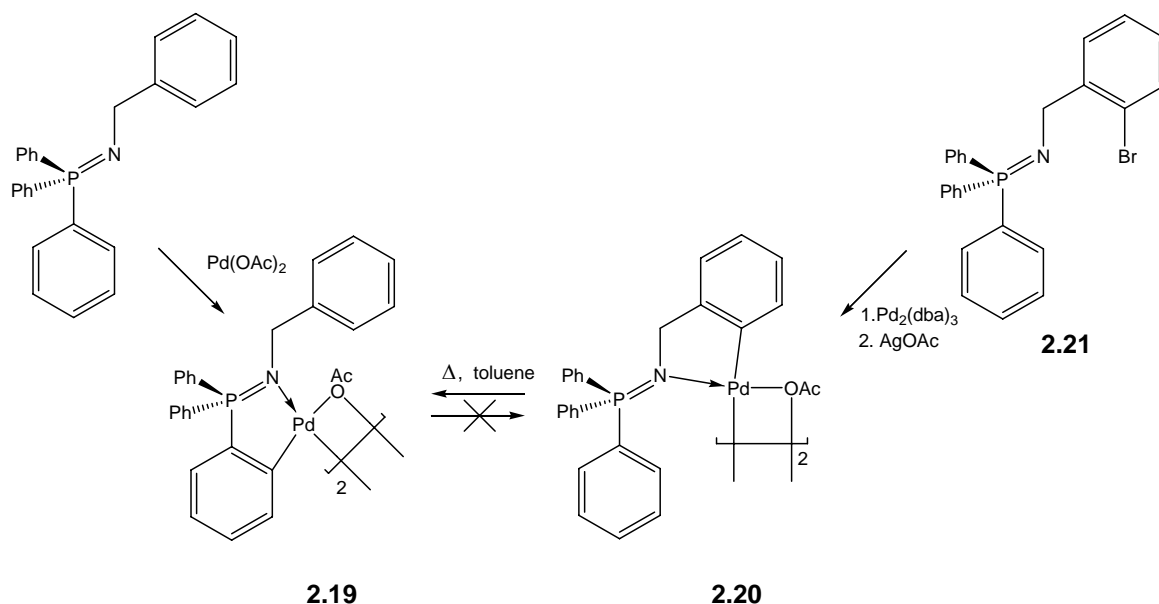
Scheme 2.10 Synthesis of platinum **2.17** and palladium **2.18** iminophosphanes containing tridentate ligands.

The palladiation reactions of other *N*-substituted iminophosphanes capable of a tridentate binding mode have also been investigated. The reaction products of $\text{Ph}_3\text{P}=\text{N}-\text{R}$ ($\text{R} = \text{CH}_2\text{COOMe}$, $\text{CH}_2\text{CONMe}_2$, $(\text{CH}_2)_2\text{SMe}$ and $\text{CH}_2\text{C}_5\text{H}_4\text{N}$) with $\text{Pd}(\text{OAc})_2$ are represented in Scheme 2.11. As shown for **2.17** and **2.18**, the resulting metallacycles show remarkable stability towards substitution with phosphine ligands.⁽¹⁴⁾



Scheme 2.11 Palladium iminophosporane complexes formed from the ligands a) $\text{Ph}_3\text{P}=\text{NCH}_2\text{COOMe}$, b) $\text{Ph}_3\text{P}=\text{NCH}_2\text{CONMe}_2$, c) $\text{Ph}_3\text{P}=\text{N}(\text{CH}_2)_2\text{SMe}$ and d) $\text{Ph}_3\text{P}=\text{NCH}_2\text{C}_5\text{H}_4\text{N}$.

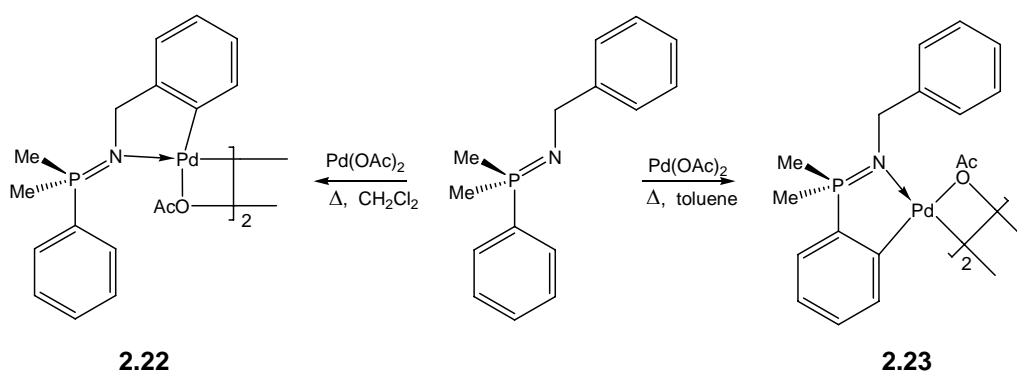
An interesting study was carried out on the palladation of the benzyl substituted iminophosphorane $\text{Ph}_3\text{P}=\text{NCH}_2\text{Ph}$. Such a ligand has two sites for carbon sp^2 bond activation – either on the *P*-substituent (to form the *endo* isomer) or the benzyl *N*-substituent (to form the *exo* isomer) - in both cases five-membered palladacycles result. The reaction of $\text{Ph}_3\text{P}=\text{NCH}_2\text{Ph}$ with $\text{Pd}(\text{OAc})_2$ (followed by treatment with LiCl) showed selective metallation on the *P*-bonded phenyl ring to give the *endo* isomer **2.19**. However, because palladation of aromatic rings occurs by electrophilic substitution, *exo* metallation would be expected to be the favoured pathway (the phosphorus deactivates the *P*-bonded phenyl rings by electron withdrawal). An examination of the *endo* isomer indicated that the resulting cyclometallated ring contained a degree of “metalloaromaticity” – that is aromatic character due to the $\text{C}=\text{C}$ and $\text{P}=\text{N}$ double bonds and the *d* orbitals on the palladium. Such conjugation is not available in the *exo* isomers. Hence it was proposed the site of palladation is controlled by two factors – the electron density on the aromatic rings and the degree of metalloaromaticity in the final products. The *exo* isomer **2.20** could however be formed by oxidative addition of $\text{Pd}(0)$ to the *ortho*-brominated complex **2.21** (again followed by metathesis with LiCl).



Scheme 2.12 Synthesis of *endo* **2.19** and *exo* **2.20** palladated $\text{Ph}_3\text{P}=\text{N}-\text{CH}_2\text{Ph}$ and the interconversion between the two forms.

Heating the *exo* isomer **2.20** resulted in a conversion to the *endo* isomer **2.19** showing that the *endo* isomer is thermodynamically more stable – this process was not reversible (Scheme 2.12). In addition the *endo* isomer was kinetically more stable as no traces of the *exo* isomer could be detected in the synthesis of **2.19**. DFT calculations confirmed these observations.⁽¹⁵⁾

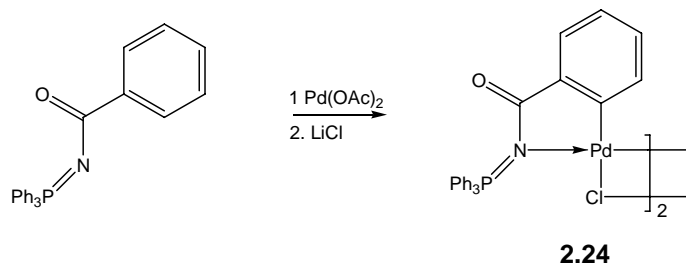
Substitution of electron-donating groups onto both the phenyl and benzyl rings of the iminophosphoranes still resulted in *endo*-metallation indicating that the presence of metalloaromaticity in the final product dominates over both electronic and steric influences. Substitution of groups on the phosphorus (PPhMe₂ compared with PPh₃) produced interesting results. The site of metallation was now temperature dependent – at low temperatures the reaction was under kinetic control and the *exo* isomer **2.22** was formed. At high temperatures the *endo* isomer **2.23** was formed due to thermodynamic control (Scheme 2.13), again DFT calculations were in accordance with experimental observations.⁽¹⁵⁾



Scheme 2.13 Temperature dependent site-selective palladation of the iminophosphorane PhMe₂P=N-CH₂Ph.

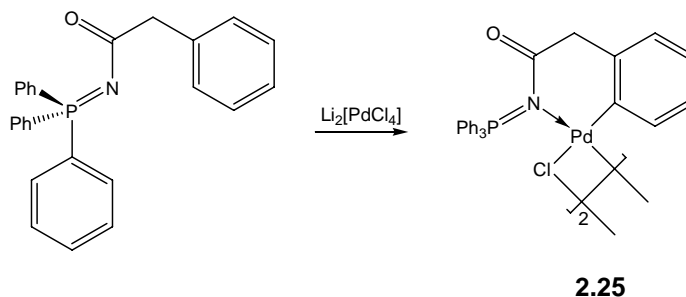
Contrasting results are seen with experiments investigating the cyclopalladation of the stabilised iminophosphorane Ph₃P=NC(O)Ph. For example, when Ph₃P=NC(O)Ph was reacted with Pd(OAc)₂ the *exo* isomer **2.24** was obtained in favour of the *endo* isomer (Scheme 2.14), even though the *endo* isomer would be stabilised by a degree of metalloaromaticity. Aguilar *et al.* proposed that the regioselectivity was due to stabilisation of the *N*-acyl iminophosphorane. Considering the resonance forms shown in Scheme 2.3 – in a solvent such as dichloromethane the two zwitterionic forms will be the most prevalent. The

phosphorus atom would therefore support positive charge so the *P*-bonded phenyl rings would be deactivated towards electrophilic substitution by the palladium. Conversely, the phenacyl ring would be more electron rich thus activated towards electrophilic substitution by the palladium.⁽³⁾ The iminophosphoranes $\text{MePh}_2\text{P}=\text{NC}(\text{O})\text{Ph}$ and $\text{R}_3\text{P}=\text{NC}(\text{O})\text{Ph}$ ($\text{R} = p\text{-tolyl}$ or $m\text{-tolyl}$) also showed metallation on the phenacyl benzene ring even though these substitution patterns activate the *P*-bonded rings towards electrophilic substitution.⁽¹⁶⁾

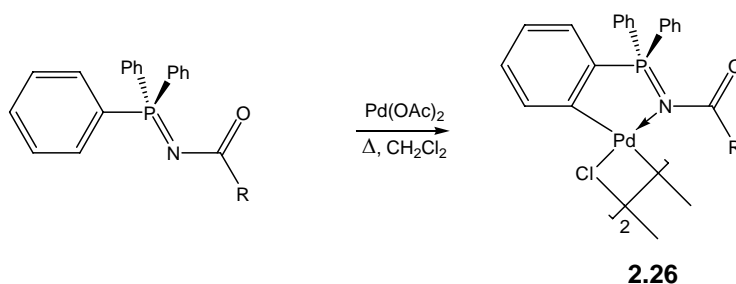


Scheme 2.14 Regioselective cyclopalladation of $\text{Ph}_3\text{P}=\text{NC}(\text{O})\text{Ph}$ to give the *exo* palladacycle **2.24**.

The reactivity of the iminophosphorane $\text{Ph}_3\text{P}=\text{NC}(\text{O})\text{CH}_2\text{Ph}$ towards palladium was also investigated. This time the reaction with $\text{Pd}(\text{OAc})_2$ in refluxing dichloromethane gave the simple coordination complex *trans*- $\text{Cl}_2\text{Pd}\{\text{N}(\text{PPh}_3)\text{C}(\text{O})\text{CH}_2\text{Ph}\}_2$. When $\text{Li}_2[\text{PdCl}_4]$ was used the six-membered palladacycle **2.25** shown in Scheme 2.15 was obtained, somewhat surprisingly, in favour of the five-membered palladacycle that would have formed if metallation had occurred on a *P*-bonded phenyl ring. However, metallation of the *P*-bonded phenyl ring can be forced if the *N*-substituent contains heterocyclic units (derived from pyrrolidine or morpholine groups) that would require sp^3 C-H bond activation (Scheme 2.16).⁽¹⁶⁾

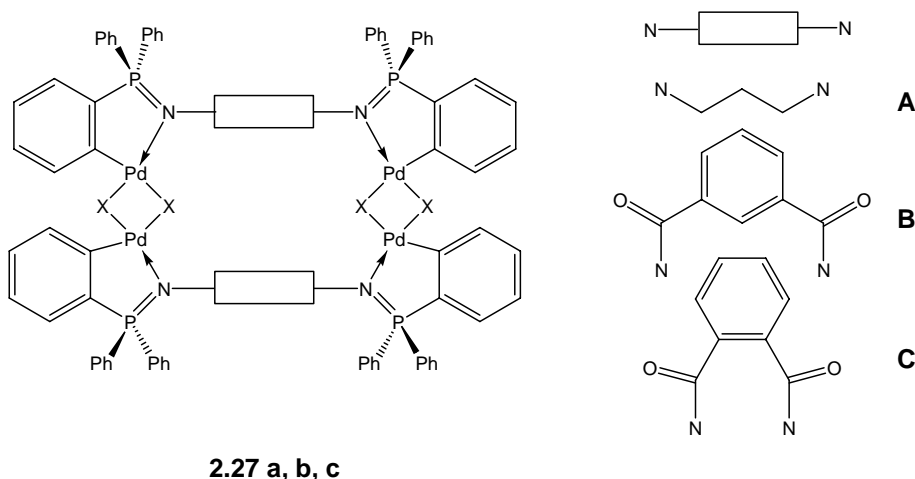


Scheme 2.15 Preferential formation of the six-membered *exo* palladacycle **2.25**.



Scheme 2.16 Formation of endo palladacycles **2.26** (R = *N*-pyrrolidine, *N*-morpholine) by incorporating R groups with alkyl sp^3 carbon atoms.

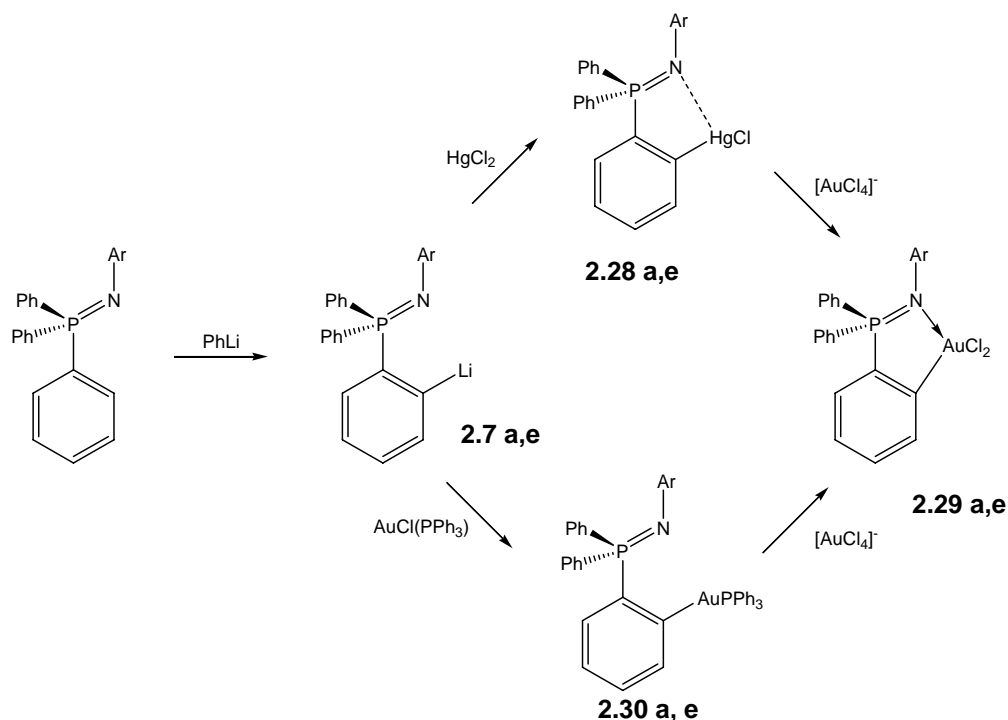
Only recently a report on the palladiation of bis-iminophosphoranes which contain alkyl or aromatic linkers has appeared (Scheme 2.17). Reaction of the alkyl-linked ligands with $\text{Pd}(\text{OAc})_2$ in dichloromethane resulted in tetra-nuclear chloride bridged species **2.27a** – the bridged structure could be cleaved by reaction with $\text{Tl}(\text{acac})$. The *endo* isomer was obtained as palladiation at an sp^2 carbon is preferred over an sp^3 carbon. An analogous reaction with the aromatic linkers was unsuccessful – only when the reaction was carried out in refluxing glacial acetic acid were the products **2.27b** and **2.27c** obtained. The *endo* isomers were obtained exclusively – the reason given is that in acetic acid $\text{Pd}(\text{OAc})_2$ acts as a nucleophile thus attacks at the electron poor (by resonance) *P*-bonded phenyl ring in preference to the electron rich aromatic spacer.⁽¹⁷⁾



Scheme 2.17 Tetranuclear cyclometallated palladium iminophosphoranes **2.27** (a linker = A, X = Cl; b linker = B, X = OAc; c linker = C, X = OAc).

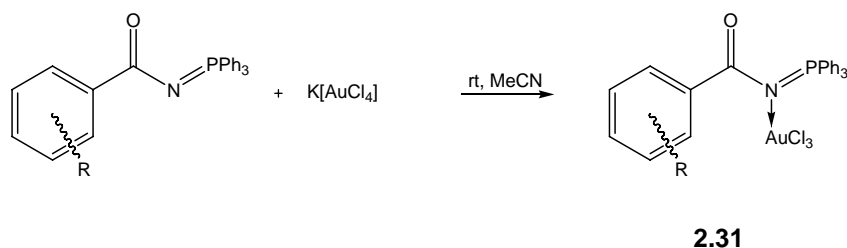
Although the majority of work has been carried out with palladium complexes, both gold(I) and gold(III) complexes have also been investigated. Brown *et al.* found that the reaction of the *ortho*-lithiated iminophosphorane $\text{Ph}_3\text{P}=\text{N}-\text{Ph}$ with HgCl_2 gave the *ortho*-mercurated compound **2.28a** in good yields. The mercury is now attached to a *P*-bonded phenyl ring – the opposite isomer to that obtained by Vicente *et al.* with direct mercuration.⁽⁷⁾ In this case, transmetalation with $[\text{Me}_4\text{N}][\text{AuCl}_4]$ gave the cycloaurated complex **2.29a** in good yields (Scheme 2.18).⁽¹⁸⁾

Independently of this work, Aguilar *et al.* conducted the same experiments but extended it to include the 3-methylphenyl *N*-substituted derivatives **2.28e** and **2.29e**. In addition, they also reported on a ‘greener’ method of synthesis that excluded the use of mercury compounds. That is, reaction of the *ortho*-lithiated intermediates **2.7a** and **2.7e** with $\text{AuCl}(\text{PPh}_3)$ gave the gold(I) complexes **2.30a** and **2.30e**. A transmetalation reaction with $[\text{Me}_4\text{N}][\text{AuCl}_4]$ was used to synthesise the cyclometallated gold(III) complexes **2.29a** and **2.29e** (Scheme 2.18).⁽¹⁹⁾



Scheme 2.18 Synthesis of mercury **2.28** (**a** Ar = Ph; **e** Ar = *m*-tol), gold(I) **2.30** (**a** Ar = Ph; **e** Ar = *m*-tol) and gold(III) **2.29** (**a** Ar = Ph; **e** Ar = *m*-tol) *ortho*-metallated iminophosphoranes from *ortho*-lithiated intermediates **2.7** (**a** Ar = Ph; **e** Ar = *m*-tol)

In addition, Aguilar *et al.* demonstrated that when the stabilised iminophosphanes $\text{Ph}_3\text{P}=\text{NC}(\text{O})\text{R}$ ($\text{R} = o\text{-tolyl}$, $2\text{-OMeC}_6\text{H}_4$ or $2\text{-BrC}_6\text{H}_4$) were reacted with $\text{K}[\text{AuCl}_4]$ (Scheme 2.19) only the *N*-coordinated adducts **2.31** could be obtained. Heating of these adducts did not result in cycloauration.



Scheme 2.19 Reaction of stabilised iminophosphanes with $\text{K}[\text{AuCl}_4]$ to form the simple coordination complexes **2.31** (**a** $\text{R} = 2\text{-Me}$; **b** $\text{R} = 4\text{-OMe}$; **c** $\text{R} = 2\text{-Br}$).

2.1.4 Scope of this work

As mentioned above, work done by Brown (Section 2.1.3) demonstrated that the simple iminophosphorane $\text{Ph}_3\text{P}=\text{N-Ph}$ is capable of forming cycloaurated complexes. The following work expands on the initial investigations and includes the synthesis of cycloaurated (simple) iminophosphanes with *N*-substituents other than a phenyl group. The cycloauration of the stabilised iminophosphorane (to give both the *endo* and *exo* isomers) $\text{Ph}_3\text{P}=\text{NC}(\text{O})\text{Ph}$ is also discussed. In addition, the reactivity and biological activity of the cycloaurated iminophosphanes is evaluated. The catalytic activity of the complexes is discussed separately in Chapter 7.

2.2 Results and Discussion

2.2.1 Synthesis of simple *ortho*-mercurated and cycloaurated iminophosphorane complexes

The Kirsanov reaction (Section 2.1.1) was used to synthesise the alkylaminophosphonium salts ($[\text{R}_3\text{P-NH-R}']\text{Br}$). Subsequent deprotonation of these salts by addition of a base yielded the neutral iminophosphorane ligands. Alternatively, the use of arylamines in the synthesis

gave the iminophosphorane ligand directly. Previously Lee and Singer had reported that the deprotonation of aminophosphonium salts takes place readily and in high yields using KOH as the base.⁽²⁰⁾ However in this work the synthetic yields were often lower than reported and in addition the resulting iminophosphoranes were unstable towards hydrolysis, especially when the *N*-bonded substituent was -CHMePh.

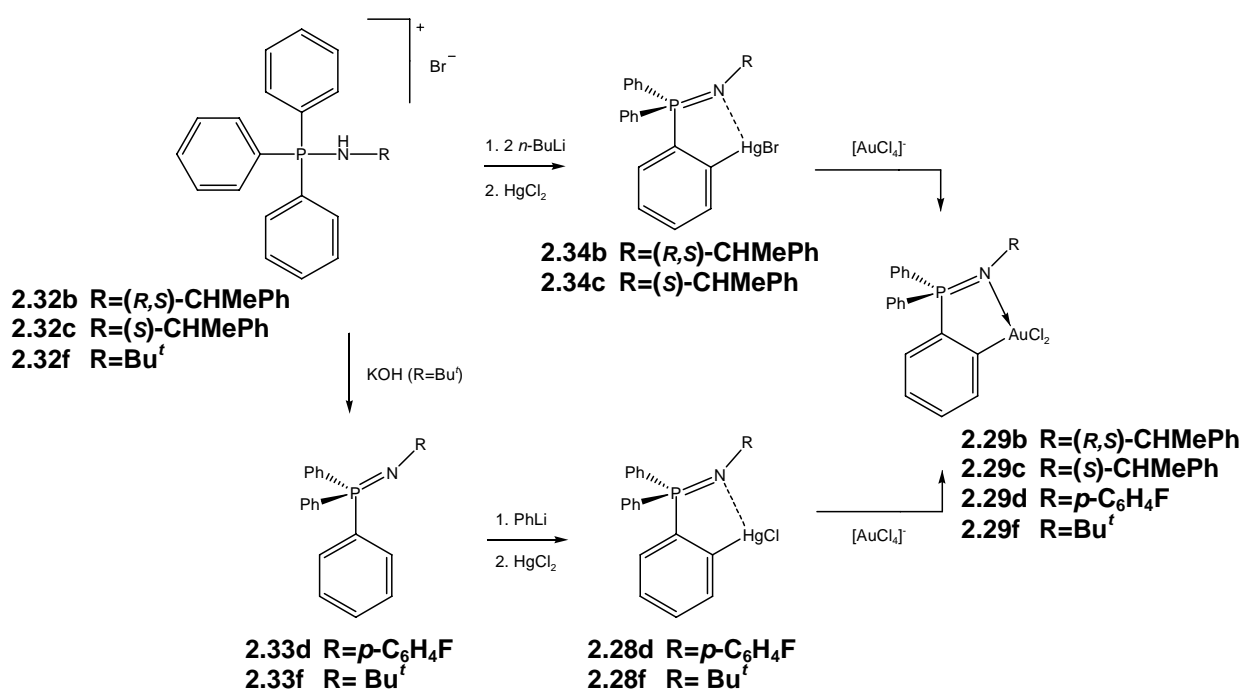
Boubekeur *et al.* have recently shown that reaction of alkylaminophosphonium salts with two equivalents of *n*-butyllithium leads to deprotonation of the phosphonium salt and *ortho*-lithiation of the resulting iminophosphorane in one step.⁽²¹⁾ This methodology was adapted to synthesise *ortho*-mercurated iminophosphoranes in a one-pot reaction without the need to isolate the potentially unstable alkyliminophosphorane ligand. Thus, when the alkylaminophosphonium bromide salts were reacted with two equivalents of *n*-butyllithium followed by HgCl₂, the *ortho*-mercurated bromide compounds were isolated in good yields. In contrast, the aryliminophosphorane ligands were appreciably more stable. They could be isolated in good yields then reacted with PhLi followed by HgCl₂, as previously described,^(18, 19) to give the *ortho*-mercurated compounds, also in good yields.

As previously mentioned in Section 2.1.3, Vicente *et al.*⁽⁷⁾ demonstrated that direct mercuration of Ph₃P=N-C₆H₄-Me gave the *ortho*-mercurated compound with the mercury bound to the *p*-tolyl ring, the wrong isomer for subsequent cycloauration. The use of Ph₃P=N-Bu^{*t*} eliminates the possibility of metallation on the *N*-substituent and when reacted directly with Hg(OAc)₂ in THF it appears that mercuration takes place in the desired position – on the *ortho* position of a *P*-bonded phenyl ring. However, yields were low compared with the synthetic route that proceeds *via* the *ortho*-lithiated intermediate, and appreciable decomposition of the ligand to [Ph₃P-NH-Bu^{*t*}]⁺ and Ph₃P=O was observed (³¹P NMR) during the reaction.

Transmetalation of either the *ortho*-mercurated chloride or bromide species with [Me₄N][AuCl₄] produced the cycloaurated complexes in good yields. It is worthy of note that in all cases the gold(III) dichloride was formed and no evidence of mono- or di-brominated compounds are seen, even when the mercury bromide iminophosphoranes are used. Scheme

2.20 shows the synthetic methods used in the synthesis of both *ortho*-mercurated and cycloaurated iminophosphoranes.

Using the above methodology, the *ortho*-mercurated compounds **2.28d,f** – **2.34b,c** and the cycloaurated complexes **2.29b-d,f** were successfully synthesised. With the exception of **2.29c** which decomposed slowly over time, all the compounds (including the racemic mixture **2.29b**) appear to be stable towards air and light. The compounds were analysed by mass spectrometry, IR, NMR spectroscopy and microelemental analysis. In addition, an X-ray structure determination of the chiral complex **2.29c** was carried out.



Scheme 2.20 Synthetic routes used in the synthesis of the simple *ortho*-mercurated and cycloaurated iminophosphoranes.

2.2.2 X-ray crystal structure of (2-AuCl₂C₆H₄)Ph₂P=N-(*S*)CHMePh, **2.29c**

In order to fully characterise (2-AuCl₂C₆H₄)Ph₂P=N-(*S*)CHMePh **2.29c** and compare it with the *N*-aryl complex **2.29a**, an X-ray crystal structure determination was carried out. Figure 2.1 shows the structure of the complex, and the atom labelling scheme while Table 2.1 gives important bond parameters. Full structural parameters including anisotropic displacement

parameters and atomic coordinates can be found on the enclosed CD. The crystal is a rare example of a molecule crystallised in the P1 space group with $Z = 1$.

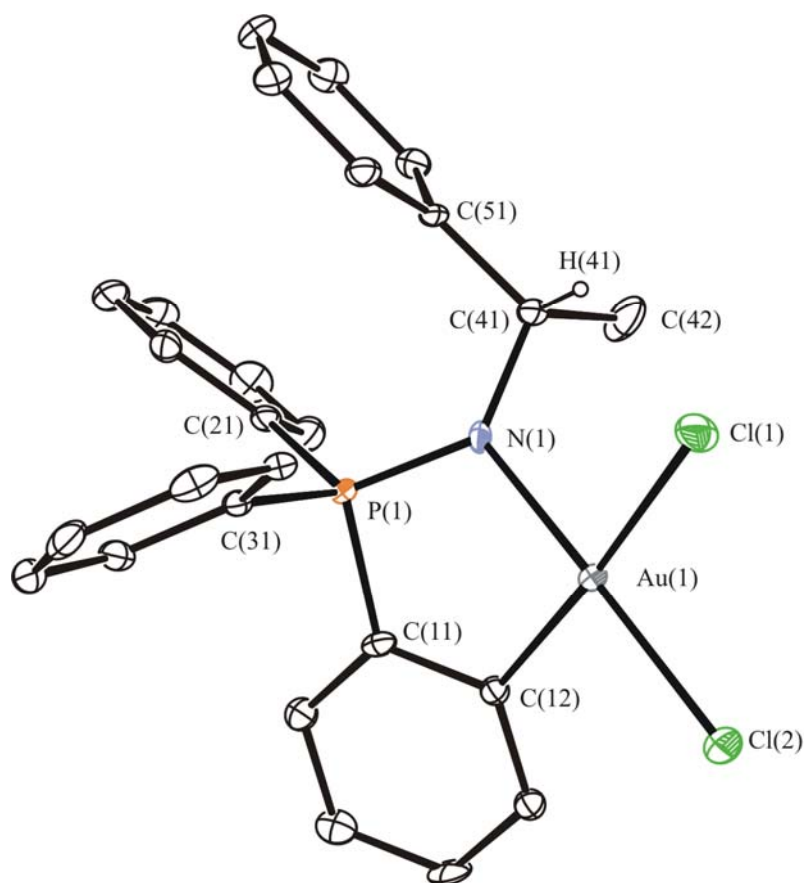


Figure 2.1 Molecular diagram of $(2\text{-AuCl}_2\text{C}_6\text{H}_4)\text{Ph}_2\text{P}=\text{N}-(S)\text{-CHMePh}$ **2.29c**, showing the atom numbering scheme. Hydrogen atoms [with the exception of H(41)] are omitted for clarity, thermal ellipsoids are shown at the 50% probability level.

The structure is as expected; the gold atom is essentially square planar with C(12) showing the greatest deviation from the coordination plane [defined by C(12), N(1), Au(1), Cl(1) and Cl(2)]. Because of the greater *trans* influence of the aryl carbon, the Au-Cl(1) bond length is greater than Au-Cl(2) bond length *trans* to the nitrogen. The metallacyclic ring made up of Au(1), N(1), P(1), C(11) and C(12) is significantly puckered, as in the previously characterised cycloaurated iminophosphorane **2.29a**.⁽¹⁸⁾ Again, the nitrogen atom shows the greatest deviation [0.288(5) Å above the plane]. The bond lengths and angles in **2.29c** are

also very comparable with those in the *N*-phenyl complex **2.29a**. However, the Au-N bond length is longer in **2.29c** than that in **2.29a** [2.072(10) Å compared with 2.034(4) Å] and the Au-Cl bond *trans* to the nitrogen is slightly shorter in **2.29c** than in **2.29a** [2.297(3) Å compared to 2.289(1) Å]. These data indicate that an aryl substituent on the nitrogen results in the nitrogen donor having a lower *trans* influence than if an alkyl substituent was present on the nitrogen.

Table 2.1 Selected structural parameters for (2-AuCl₂C₆H₄)Ph₂P=N-(*S*)-CHMePh, **2.29c**, with esds in parentheses.

Atoms	Lengths (Å)	Atoms	Angles (°)
Au(1) – Cl(1)	2.371(2)	Cl(1) – Au(1) – Cl(2)	89.70(9)
Au(1) – Cl(2)	2.297(3)	N(1) – Au(1) – C(12)	85.1(4)
Au(1) – N(1)	2.072(10)	C(12) – Au(1) – Cl(2)	92.4(3)
Au(1) – C(12)	2.045(8)	N(1) – Au(1) – Cl(1)	93.0(3)
P(1) – N(1)	1.615(10)	N(1) – P(1) – C(11)	101.9(4)
P(1) – C(11)	1.790(6)	P(1) – N(1) – C(41)	131.4(8)
N(1) – C(41)	1.473(12)		

2.2.3 Spectroscopic and mass spectrometric characterisation of simple *ortho*-mercurated and cycloaurated iminophosphanes

NMR spectroscopy

Because of the presence of multiple inequivalent phenyl rings and coupling to phosphorus in the *ortho*-mercurated and cycloaurated complexes, both the ¹H and ¹³C NMR spectra are complex and difficult to fully interpret. ³¹P{¹H} NMR remains the most useful experiment, and Figure 2.2 demonstrates this nicely. Conversion of the aminophosponium salt **2.32** to the neutral iminophosphorane **2.33** results in the phosphorus becoming more shielded and an upfield shift of approximately 40 ppm is seen. A small shift is seen after *ortho*-mercuration and the spectra now contain ¹⁹⁹Hg satellite peaks with ³J_{Hg-P} coupling averaging 330 Hz. Upon transmetalation to the cycloaurated complexes, there is a significant downfield shift in the signal of approximately 40 ppm, consistent with the formation and inclusion of the phosphorus in a five-membered ring.⁽²²⁾

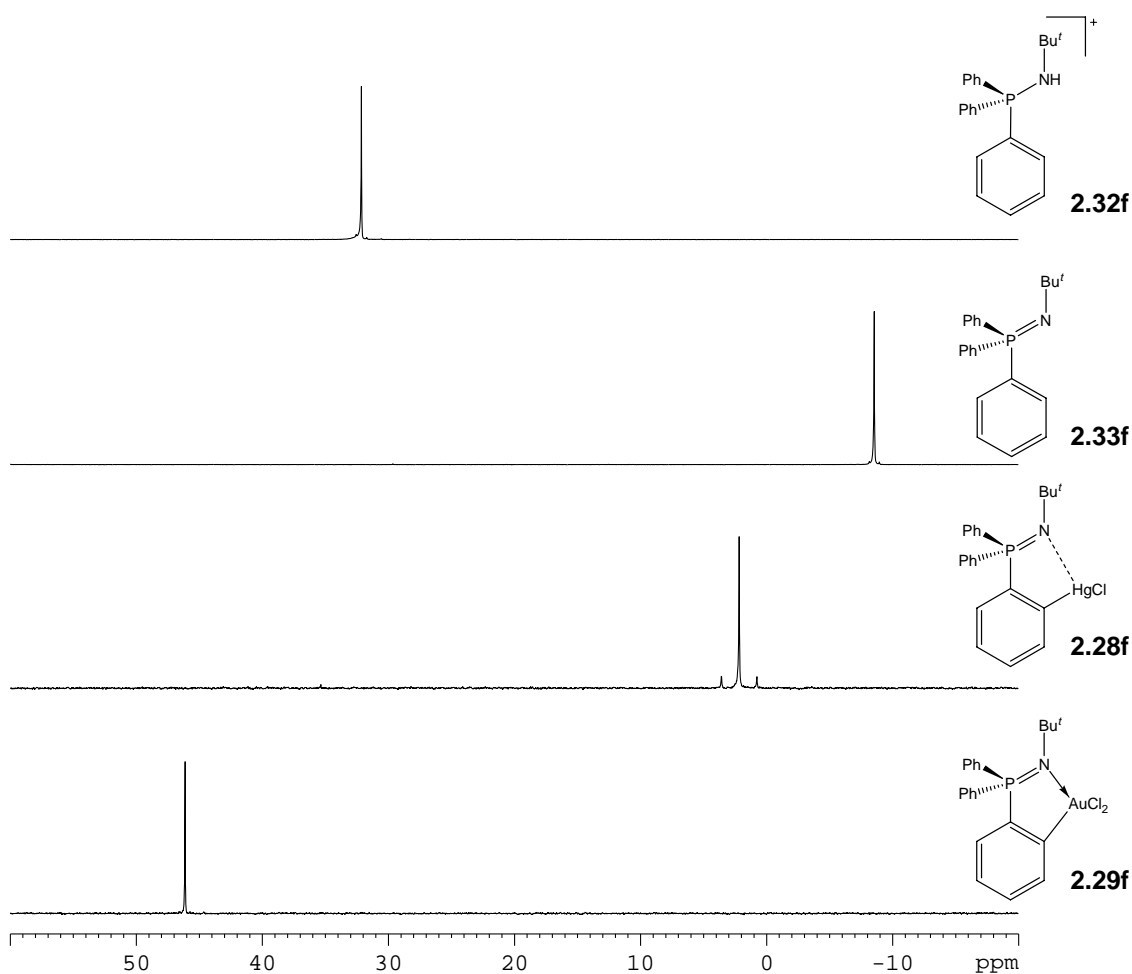


Figure 2.2 $^{31}\text{P}\{^1\text{H}\}$ NMR spectra for the series of simple iminophosphoranes with a Bu^t substituent.

IR Spectroscopy

The IR spectra show a decrease in wavenumber for the $\text{P}=\text{N}$ stretch when moving from the free ligands to the *ortho*-mercurated complexes and on to the cycloaurated complexes. For example, $\text{Ph}_3\text{P}=\text{N}\text{Bu}^t$ has a $\text{P}=\text{N}$ stretch at 1280 cm^{-1} which decreases to 1223 cm^{-1} in **2.28f** and to 1183 cm^{-1} in **2.29f**. This is presumably because electron density is being pulled from the $\text{P}=\text{N}$ bond onto the metal centre through the coordinating nitrogen.

ESI-Mass spectrometry

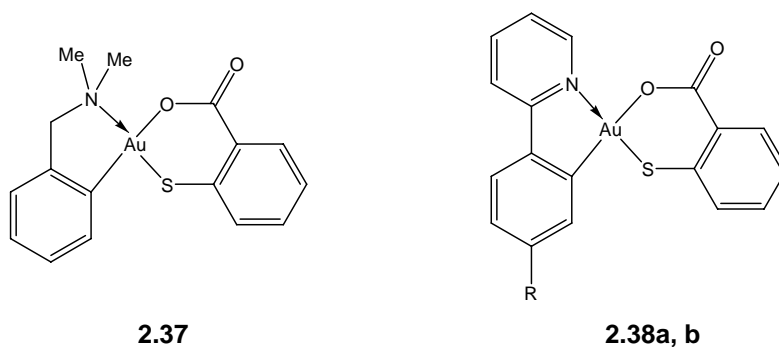
The ESI-MS of the *ortho*-mercurated complexes (**2.34b,c** and **2.28d,f**) all show strong $[M+H]^+$ ions which can easily be identified by the characteristic isotope pattern of mercury. The spectrum of **2.28f** also indicated the presence of the diarylmercury complex $2\text{-Hg}(\{\text{C}_6\text{H}_4\}\text{Ph}_2\text{P}=\text{NBu}^t)_2$ however there was no evidence of this compound in the $^{31}\text{P}\{^1\text{H}\}$ NMR or microelemental analysis. This form of ionisation suggests that there is only a weak N-Hg interaction as the nitrogen is available for protonation.

In contrast, the primary route of ionisation for the cycloaurated complexes appears to be loss of a chloride ligand to give the ions $[M-\text{Cl}]^+$. As previously observed, addition of a small amount of highly coordinating pyridine produces the charged species $[M-\text{Cl}+\text{py}]^+$.⁽²³⁾ Interestingly, the complex **2.29f** also shows the ion $[M+\text{Me}_4\text{N}]^+$ with the cation presumably present due to the use of $[\text{Me}_4\text{N}][\text{AuCl}_4]$ and $[\text{Me}_4\text{N}]\text{Cl}$ in the synthesis. No evidence of $[\text{Me}_4\text{N}]^+$ is observed in NMR spectra, however this type of adduct is also seen as the predominant gold species when monitoring the progression of the transmetallation reaction by ESI-MS.

2.2.4 Reactivity of simple cycloaurated iminophosphorane complexes with dianionic ligands

The chloride ligands on *C,N* cyclometallated Au(III) compounds can be readily replaced by dianionic ligands such as catecholate⁽²⁴⁾ and thiosalicylate, forming new five- and six-membered chelate rings respectively.⁽²⁵⁻²⁷⁾ The iminophosphorane complexes **2.29a** and **2.29f** show analogous behaviour and when reacted with either catechol or thiosalicylic acid in methanol with excess trimethylamine, the cycloaurated complexes **2.35** and **2.36** can easily be isolated in high yields by addition of water to the reaction mixture. NMR spectroscopy, ESI mass spectrometry and elemental microanalysis confirm the formulation. Compound **2.35f** appears to be present with one molecule of water as microanalysis of two independent samples gives a composition which is in agreement with the proposed formula.

and Table 2.2 gives selected bond lengths and angles. A full list of structural parameters can be found on the supplementary CD. As with other gold(III) thiosalicylate complexes⁽²⁵⁻²⁷⁾ the ligand is coordinated to the gold with the two highest *trans* influence donors (aryl carbon and thiolate sulfur) mutually *cis* to each other. The geometry around the gold is square planar with the largest deviation from the N(1), C(12), Au(1), S(1) and O(2) plane being for C(12), which sits 0.1620(7) Å below the plane. The fold angle between the Au coordination plane [defined by Au(1), S(1) and O(2)] and the plane of the thiosalicylate ligand (excluding the oxygen atoms) is 43.34(4)°, which falls in the range of 30.1(8)° (**2.37**) and 59.6° (**2.38a**) previously seen in gold(III) thiosalicylate systems.⁽²⁵⁻²⁷⁾ The bite angle of the thiosalicylate ligand is 91.46(4)°, comparable to those seen in **2.38a** and **2.38b** [89.82(8)° and 90.1(2)° respectively]. The five-membered ring created by the cycloaurated iminophosphorane is also puckered with the greatest deviations for N(1) (0.3226(7) Å above the plane) and P(1) (0.2788(7) Å below the plane). The puckering of the thiosalicylate and the iminophosphorane rings can clearly be seen in Figure 2.4. The fold angle between the gold coordination plane and that of the thiosalicylate ring is 43.3°, towards the lower end of the range found for a series of Pt(II) thiosalicylate complexes.⁽²⁸⁾



Scheme 2.22 Previous cycloaurated thiosalicylate complexes **2.37** and **2.38** (a R = Me; b R = H).

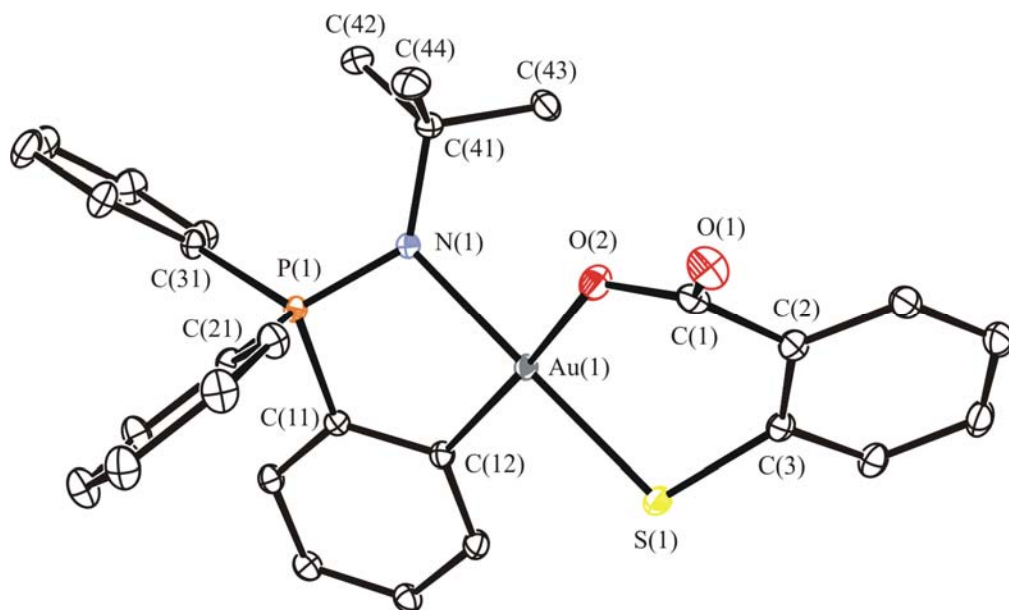


Figure 2.3 Molecular diagram of **2.36f**, showing the atom numbering scheme. Hydrogen atoms are omitted for clarity, thermal ellipsoids are shown at the 50% probability level.

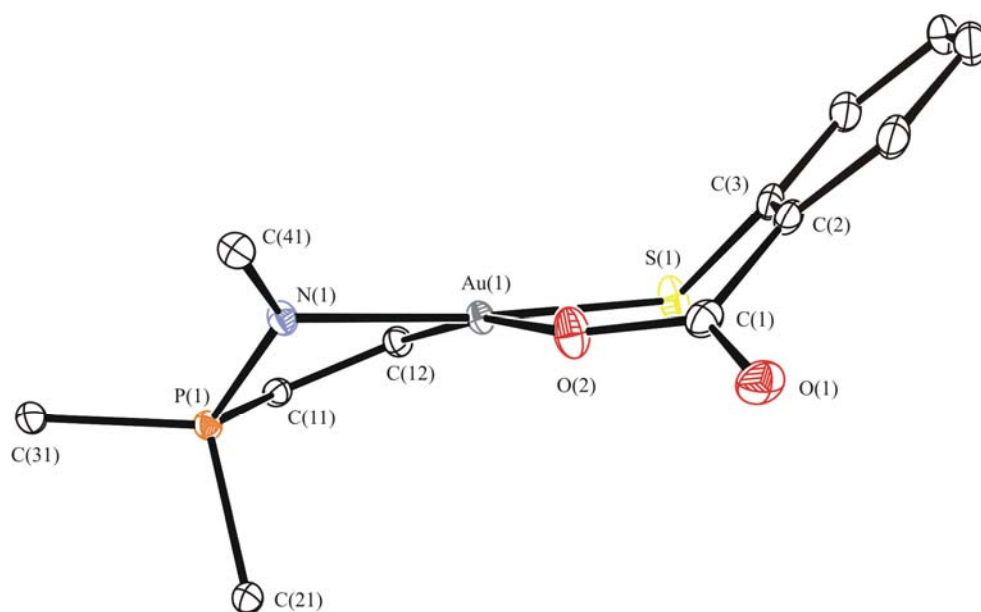


Figure 2.4 Molecular diagram of **2.36f**, showing the fold angle of the thiosalicylate ligand and puckering of the iminophosphorane ring. For clarity, only the *ipso* carbons of the uncoordinated phenyl rings [C(21) and C(31)] and the tertiary carbon of the Bu^t group C(41) are shown. Thermal ellipsoids are shown at the 50% probability level.

Table 2.2 Selected structural parameters for **2.36f**, with esds in parentheses.

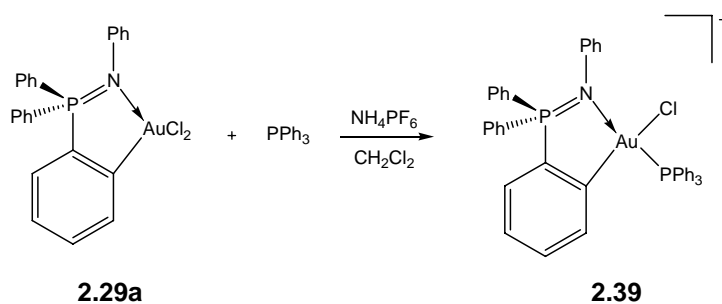
Atoms	Lengths (Å)	Atoms	Angles (°)
N(1) – Au(1)	2.1196(13)	N(1) – Au(1) – C(12)	85.90(6)
C(12) – Au(1)	2.0194(16)	O(2) – Au(1) – S(1)	91.46(4)
O(2) – Au(1)	2.0676(13)	C(3) – S(1) – Au(1)	103.08(6)
S(1) – Au(1)	2.2760(4)	O(1) – C(1) – O(2)	121.52(17)
S(1) – C(3)	1.7618(17)	C(1) – O(2) – Au(1)	130.92(11)
O(1) – C(1)	1.226(2)	O(1) – C(1) – C(2)	119.45(15)
O(2) – C(1)	1.306(2)		

2.2.5 Reactivity of simple cycloaurated iminophosphoranes with phosphines

As described in Chapter One (section 1.2.1), reaction of *C,N* cyclometallated Au(III) dichloride complexes with PPh₃ gives an indication of the relative strength of the N-Au coordinate bond. If the bond is strong, then a chloride ion will be displaced to give a cationic complex. Alternatively, if the N-Au bond is weaker it will be cleaved (with loss of the metallocyclic ring) and coordination of the phosphine will give a neutral phosphine complex.⁽²⁹⁾

To assess the strength of the Au-N bond in Au(III) iminophosphoranes, **2.29a** was reacted with one molar equivalent of PPh₃ together with NH₄PF₆ in dichloromethane, producing the compound **2.39** where the PPh₃ has displaced the chloride ligand (Scheme 2.23). The products were initially characterised by ESI-MS and ³¹P{¹H} NMR. The ³¹P{¹H} NMR shows the expected two signals at 60.6 and 41.0 ppm in a 1:1 ratio. The first arises from the iminophosphorane, and is only slightly shifted from that of the parent dichloride (65.5 ppm) indicating that the phosphorus is still present in a ring. This was unambiguously confirmed by an X-ray crystal structure determination.

The molecular structure of the cation of **2.39** is shown in Figure 2.5, and selected bond parameters are presented in Table 2.3. The geometry around the gold atom is essentially square planar and N(1) shows the greatest deviation [0.113(3) Å] from the coordination plane.



Scheme 2.23 Reaction of the cycloaurated iminophosphorane **2.29a** with PPh_3 .

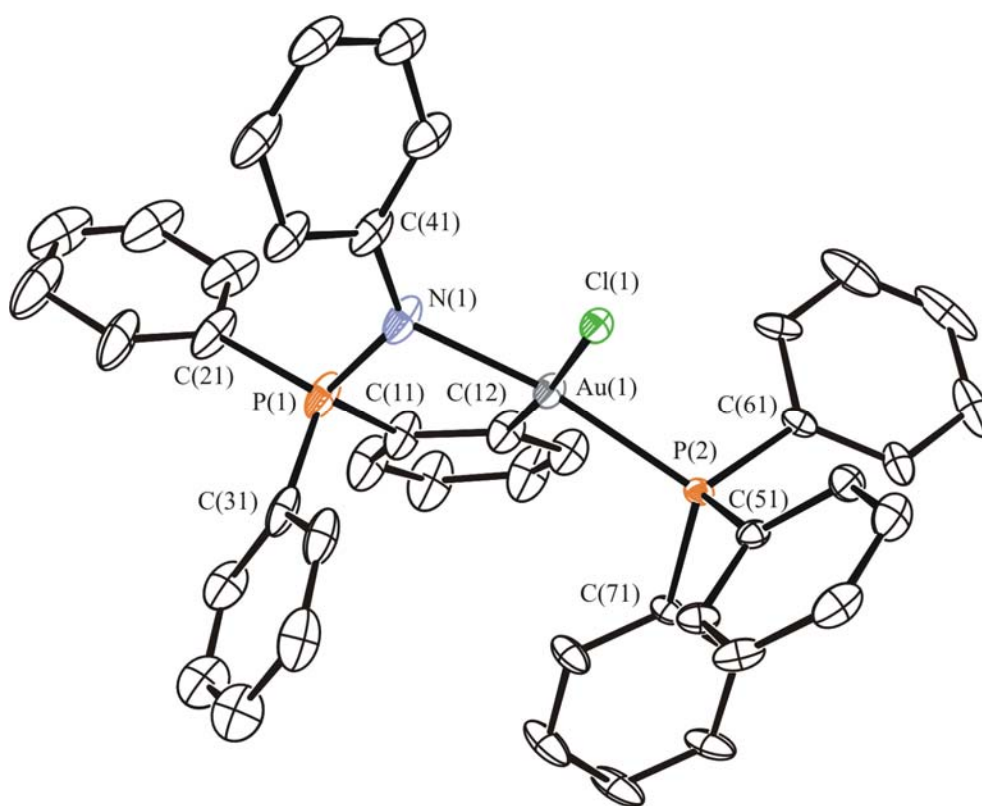


Figure 2.5 Molecular diagram of $[(2\text{-AuCl}(\text{PPh}_3)\text{C}_6\text{H}_4)\text{Ph}_2\text{P}=\text{NPh}]^+$. Hydrogen atoms are omitted for clarity and thermal ellipsoids are shown at the 30% probability level.

The X-ray crystal structure shows that the phosphine is coordinated *trans* to the nitrogen, thus placing the two softest ligands (the phosphine and aryl groups) mutually *cis* to each other, giving the most thermodynamically stable configuration. In addition this configuration is such that steric interactions between the bulky PPh_3 and the N-aryl group are minimised. This

transphobic nature is also observed in other phosphine substituted Au(III) cationic complexes, and the Au-P bond lengths are comparable with those previously seen.⁽³⁰⁻³³⁾ Upon substitution of the chloride with the bulky phosphine group the bond angle between the two monodentate ligands has increased [from 90.70(4)° in **2.29a** to 92.88(17)° in **2.39**] however the change in the bite angle of the iminophosphorane ligand [84.86(17) to 84.0(2)°] is barely noticeable. The ligand remains significantly puckered, with N(1) and P(1) showing the greatest deviation from the mean plane of the ring [defined by N(1), P(1), Au(1), C(11) and C(12)].

Table 2.3 Selected bond parameters for [2-(AuCl(PPh₃)C₆H₄)Ph₂P=NPh]PF₆·0.5Et₂O, **2.39**, with esds in parentheses.

Atoms	Lengths (Å)	Atoms	Angles (°)
Au(1) – Cl(1)	2.3463(11)	N(1) – Au(1) – C(12)	84.0(2)
Au(1) – P(2)	2.30303(12)	C(12) – Au(1) – P(2)	92.88(7)
Au(1) – C(12)	2.057(5)	P(2) – Au(1) – Cl(1)	91.11(4)
Au(1) – N(1)	2.079(5)	Cl(1) – Au(1) – N(1)	92.26(13)
P(1) – N(1)	1.620(6)	Au(1) – N(1) – P(1)	108.3(3)
N(1) – C(41)	1.419(7)	P(1) – N(1) – C(41)	124.9(4)
C(11)–C(12)	1.401(9)	N(1) – P(1) – C(11)	100.6(3)

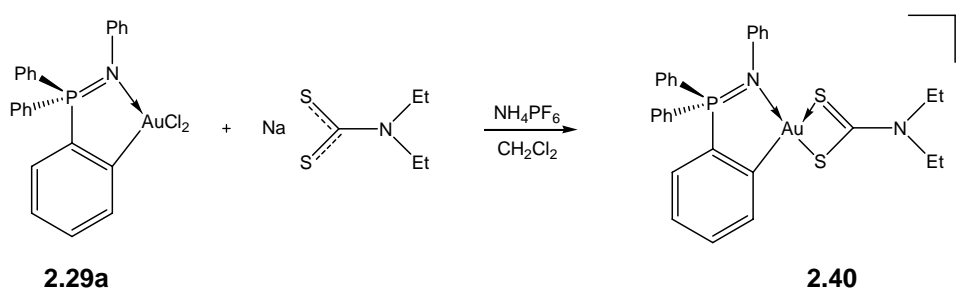
2.2.6 Attempted displacement of the *N*-donor ligand in simple cycloaurated iminophosphanes

In order to evaluate our hypothesis that displacement of the *N*-donor would result in a significant upfield shift in the ³¹P NMR spectra attempts were made to displace the nitrogen. Previously this has been achieved with gold(III) complexes by replacement of the relatively weakly bound chloride ligands with stronger cyanide⁽³⁴⁾ or dithiocarbamate^(34, 35) ligands (see Chapter One).

When **2.29a** was reacted with excess KCN the anion [(2-(CN)₃AuC₆H₄)Ph₂P=NPh]⁻ was observed in the ESI mass spectrum, and an unexpected new peak at 69.5 ppm in the ³¹P{¹H}

is observed. However, isolation and microanalysis of this complex as a white solid produced microelemental data completely inconsistent with the expected formulation.

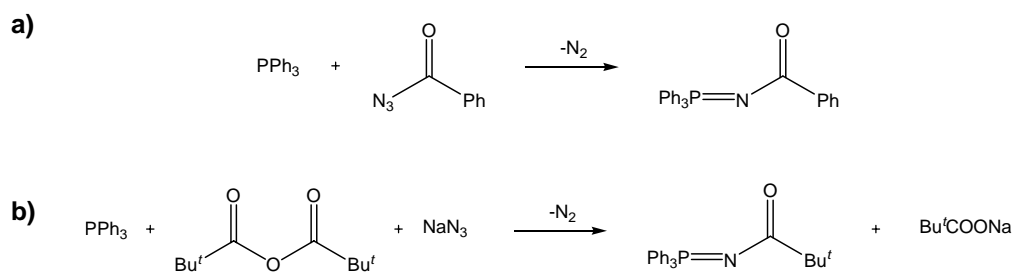
When **2.29a** was reacted with a molar equivalent of $\text{NaS}_2\text{CNEt}_2$ and NH_4PF_6 in dichloromethane the complex **2.40** was obtained as a yellow solid. The analogous reaction with two equivalents of $\text{NaS}_2\text{CNEt}_2$ also gave a yellow complex which was identical to **2.40** (on the basis of ^1H and $^{13}\text{P}\{^1\text{H}\}$ NMR experiments). No evidence of displacement of the nitrogen donor was observed. These observations indicate that the iminophosphorane complexes contain a robust cyclometallated ring.



Scheme 2.24 Reaction of the cycloaurated iminophosphorane **2.29a** with sodium diethyldithiocarbamate

2.2.7 Synthesis of stabilised *ortho*-mercurated and cycloaurated iminophosphoranes

The stabilised iminophosphorane $\text{Ph}_3\text{P}=\text{NC}(\text{O})\text{Ph}$ was synthesised (by Miss Rachael Linklater) from Ph_3P and $\text{N}_3\text{C}(\text{O})\text{Ph}$ using the conventional Staudinger reaction.⁽³⁶⁾ $\text{Ph}_3\text{P}=\text{NC}(\text{O})\text{Bu}^t$ was synthesised by a modified version of the same reaction. Frøyen had previously demonstrated that iminophosphoranes could conveniently be synthesised by the one pot reaction between an acid chloride, sodium azide and triphenylphosphine.⁽³⁷⁾ We have found that exchanging acid chloride for an anhydride gives the same product however the reaction times are longer due to the anhydride being less reactive than the acid chloride. The new stabilised iminophosphorane $\text{Ph}_3\text{P}=\text{NC}(\text{O})\text{Bu}^t$ is an air stable crystalline white solid. The $^{31}\text{P}\{^1\text{H}\}$ NMR and IR data [$\nu(\text{P}=\text{N})$ and $\nu(\text{C}=\text{O})$] are consistent with other stabilised iminophosphoranes.



Scheme 2.25 Synthesis of the stabilised iminophosphanes a) $\text{Ph}_3\text{P=NC(O)Ph}$ and b) $\text{Ph}_3\text{P=NC(O)Bu}^t$.

The cycloauration of stabilised iminophosphanes (to give either the *endo* or *exo* compound) is an interesting synthetic problem. As mentioned in the introduction, Aguilar *et al.* have already shown that the reaction of $\text{Ph}_3\text{P=NC(O)Ph}$ with $\text{K}[\text{AuCl}_4]$ gives the coordination compound where the nitrogen of the iminophosphorane ligand acts as a simple two electron donor to the gold centre (Scheme 2.19).⁽¹⁹⁾ Transmetalation from the corresponding *ortho*-mercurated complex is therefore the only viable option. However, the presence of the carbonyl group on the ligand means that synthesis of the *ortho*-mercurated compound *via* the *ortho*-lithiated compound (*i.e.* the method used for the synthesis of simple *ortho*-mercurated iminophosphanes) is no longer a viable option. Unfortunately, attempts at direct mercuration of the ligand, with $\text{Hg}(\text{OAc})_2$ in refluxing THF, were also unsuccessful. It is possible that the use of a stronger mercurating agent [*e.g.* $\text{Hg}(\text{ClO}_4)_2$ or $\text{Hg}(\text{OTf})_2$] could produce the organomercury complex, however this was not attempted.

Cooney *et al.* have previously demonstrated that the reaction of *ortho*-manganated acetophenone with HgCl_2 gives the *ortho*-mercurated compound in good yields. *Ortho*-mercurated acetophenone can not be synthesised by conventional methods – again the presence of a carbonyl group excludes the use of organolithium reagents and direct mercuration occurs at the methyl carbon due to keto-enol tautomerisation.⁽³⁸⁾ Therefore *ortho*-manganation of the ligand $\text{Ph}_3\text{P=NC(O)Ph}$ may provide an entry point to the *ortho*-mercurated derivative.

As discussed earlier, the simple iminophosphorane $\text{Ph}_3\text{P}=\text{N}-\text{Ph}$ undergoes *ortho*-metallation with $\text{PhCH}_2\text{Mn}(\text{CO})_5$ to give the manganated compound **2.2a** (Scheme 2.5).⁽⁶⁾ Linklater investigated the *ortho*-manganation of the stabilised iminophosphorane $\text{Ph}_3\text{P}=\text{NC}(\text{O})\text{Ph}$ and found that manganation occurred at the *ortho*-position of the *N*-bonded phenyl ring to give the *exo* isomer **2.41**.⁽³⁶⁾ The geometry was initially assigned by NMR and IR spectroscopy. The $^{31}\text{P}\{\text{^1H}\}$ NMR spectrum had a single peak at 23.5 ppm, only slightly shifted from the ligand (21.3 ppm). This pointed strongly towards *ortho*-metallation on the *N*-bonded substituent. Presumably the ^{31}P chemical shift of the *endo* isomer would be further downfield because the phosphorus would be in a five-membered ring.⁽²²⁾ The $^{13}\text{C}\{\text{^1H}\}$ spectrum also had the correct number of signals for metallation of the *N*-bonded substituent. The carbonyl carbon of **2.41** appears at 189.0 ppm – this is slightly different to the free ligand (δ 176.4 ppm) and suggests that the oxygen atom is coordinated to the manganese. The C=O stretching peak in the IR spectrum of the *ortho*-manganated compound **2.41** occurs at 1488 cm^{-1} . When this is compared to the value for the carbonyl stretch in the uncoordinated ligand (1595 cm^{-1}) it also suggests that the oxygen atom is acting as a donor to the manganese. The mechanism of *ortho*-manganation is not well understood so it is unclear why metallation occurs on the *N*-acyl ring with the oxygen atom acting as the neutral donor. However the reaction of *N,N*-dialkylbenzamides with $\text{PhCH}_2\text{Mn}(\text{CO})_5$ also gives the isomer with the oxygen coordinated to the manganese.⁽³⁹⁾

Unambiguous assignment of **2.41** was achieved by an X-ray crystal structure. As the IR and NMR spectroscopic data suggested, the manganese is attached in the *ortho* position of the *N*-bonded phenacyl ring with the carbonyl oxygen acting as a neutral donor. The molecular structure is shown in Figure 2.6.⁽³⁶⁾

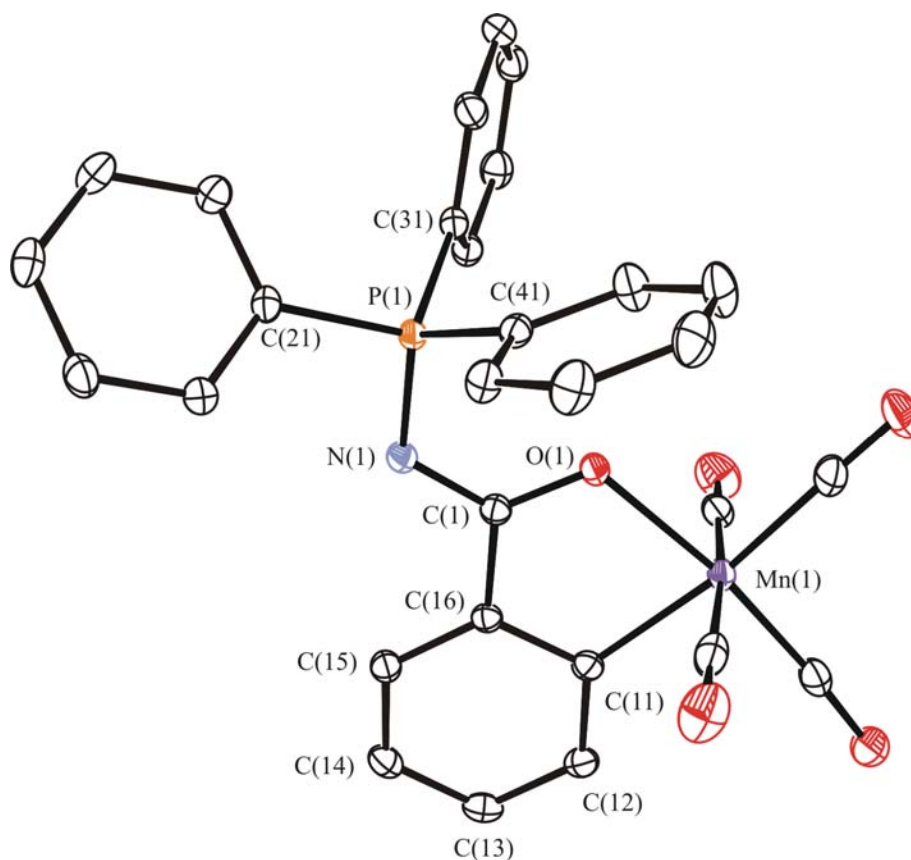
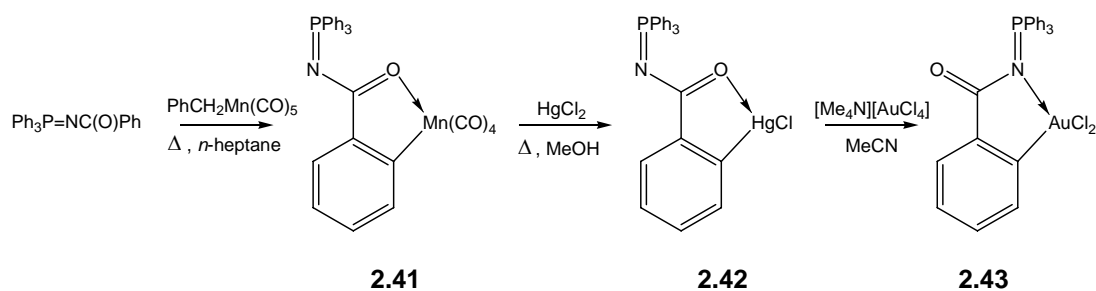


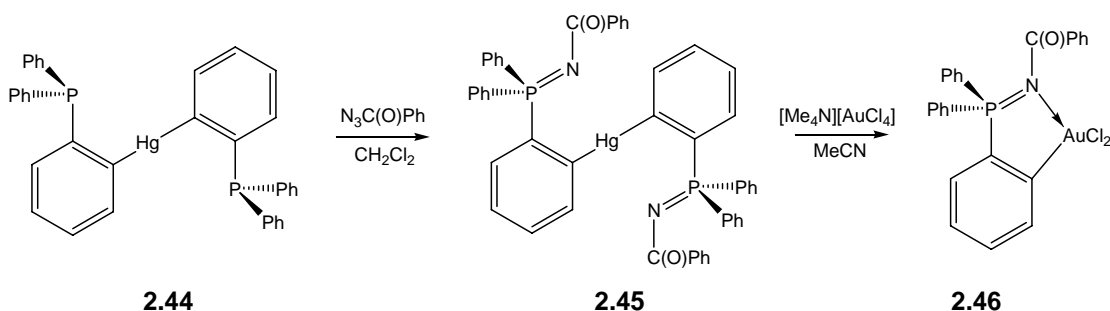
Figure 2.6 Molecular structure of $(2\text{-Mn}(\text{CO})_4\text{C}_6\text{H}_4)\text{C}(\text{O})\text{N}=\text{PPh}_3$, **2.41**. Hydrogen atoms have been excluded for clarity. Thermal ellipsoids are shown at the 50% probability level.

As anticipated, the reaction of **2.41** with HgCl_2 in refluxing methanol gives the *ortho*-mercurated complex **2.42** in a good yield. A transmetallation reaction analogous to that used with the simple iminophosphoranes gives the *exo*-cycloaurated complex **2.43**, also in good yields. Scheme 2.26 depicts the synthetic route to **2.43**. Interestingly, the transmetallation reaction from **2.42** to **2.43** took two days – the corresponding reaction for the simple iminophosphorane only took one. Presumably this is due to the neighbouring carbonyl group pulling electron density away from the nitrogen atom.



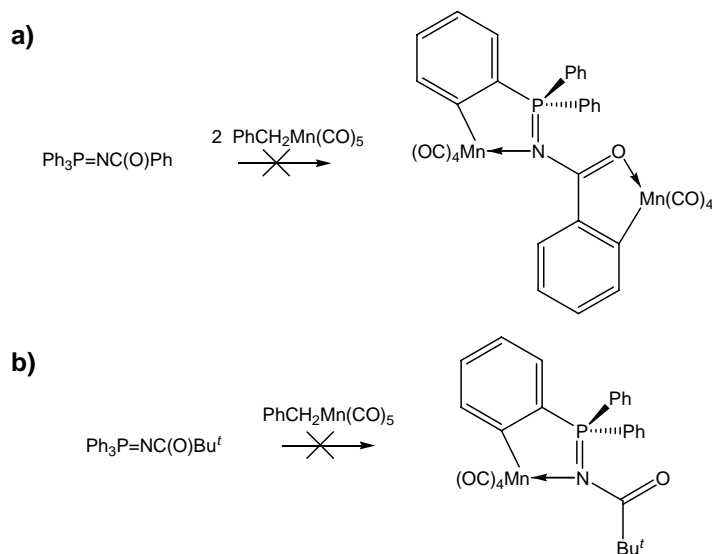
Scheme 2.26 Synthesis of *exo*-cyclometallated complexes from the stabilised iminophosphorane $\text{Ph}_3\text{P}=\text{NC}(\text{O})\text{Ph}$.

Bennett *et al.* have previously derived a synthetic route to the diaryl-mercury(II) compound **2.44**. They subsequently demonstrated that the phosphine groups act in a similar way to simple tertiary phosphines. That is, reaction with H_2O_2 or sulfur led to the phosphine oxide or sulfide respectively and reaction with $\text{BH}_3\cdot\text{SMe}_2$ gave the borane complex.⁽⁴⁰⁾ When **2.44** was reacted with two equivalents of $\text{N}_3\text{C}(\text{O})\text{Ph}$, as per the Staudinger reaction, the iminophosphorane **2.45** was obtained. The reaction however took longer than expected – typically when a phosphine is added to the azide evolution of nitrogen can be seen immediately. When the mechanism of the Staudinger reaction is considered (see Scheme 2.1) it is not surprising that the reaction was sluggish – sterically bulky groups hinder the formation of the four-membered transition state. Again, a transmetalation reaction gave *endo*-cycloaurated compound **2.46**, once more the reaction takes longer than for the simple iminophosphoranes discussed in Section 2.2.1. The synthetic scheme is depicted below (Scheme 2.27).



Scheme 2.27 Synthesis of *endo*-cyclometallated complexes.

When the ligand $\text{Ph}_3\text{P}=\text{NC}(\text{O})\text{Bu}^t$ was reacted with $\text{PhCH}_2\text{Mn}(\text{CO})_5$ in refluxing heptane no reaction occurred, even after 8 hours. In addition, reaction of $\text{Ph}_3\text{P}=\text{NC}(\text{O})\text{Ph}$ with two equivalents of $\text{PhCH}_2\text{Mn}(\text{CO})_5$, in an attempt to make the di-cyclomanganated complex, only afforded the mononuclear compound **2.41**.⁽³⁶⁾ It appears that the *P*-bonded phenyl rings of the stabilised iminophosphoranes are inert towards reaction with manganese.



Scheme 2.28 Attempts to *ortho*-manganate the stabilised iminophosphoranes a) $\text{Ph}_3\text{P}=\text{NC}(\text{O})\text{Ph}$ and b) $\text{Ph}_3\text{P}=\text{NC}(\text{O})\text{Bu}^t$ on the *P*-bonded phenyl ring.

2.2.8 X-ray crystal structures of (2-HgClC₆H₄)C(O)N=PPh₃, **2.42**,

(2-AuCl₂C₆H₄)C(O)N=PPh₃, **2.43** and (2-AuCl₂C₆H₄)Ph₂P=NC(O)Ph, **2.46**

In order to confirm the structures of the **2.42**, **2.43** and **2.46** X-ray crystallography was used. The molecular structures of **2.42**, **2.43** and **2.46** are shown in Figures 2.7, 2.8 and 2.9 respectively and important structural parameters are presented in Tables 2.4, 2.5 and 2.6. Full lists of structural data, atomic coordinates and anisotropic displacement parameters can be located on the supplementary CD.

X-ray crystal structure of (2-HgClC₆H₄)C(O)N=PPh₃, **2.42**

Interestingly, as with the manganese example, it is the oxygen that is interacting with the metal centre. As expected, the coordination around the mercury shows only a slight deviation

from linearity [the C(2)–Hg(1)–C(1) angle is 176.24(6)°]. In this example, the preference for the oxygen atom may be because of steric reasons. The molecules of the mercury complex are packed together so that there are weak intermolecular interactions (3.143 Å) between the metal and a chlorine atom of a neighbouring molecule – in essence a dimeric structure is present in the solid state. If however there was an interaction between the nitrogen and the mercury the bulky triphenylphosphine group would twist around and sit over the metal centre and “clash” with the phenacyl phenyl ring on the adjacent molecule.

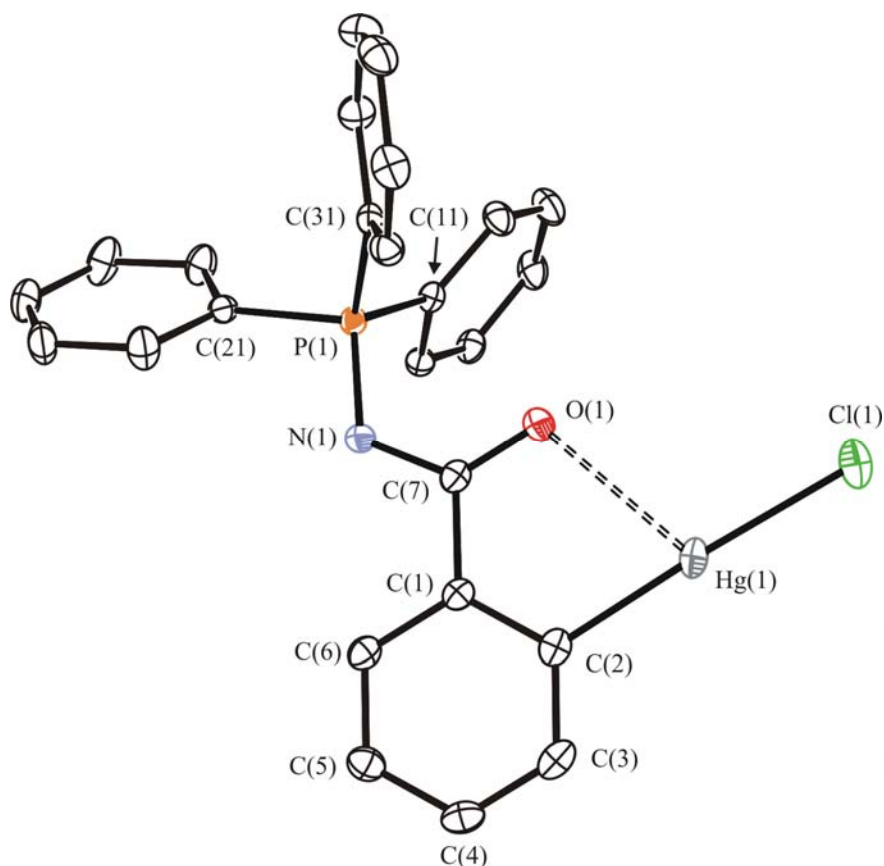


Figure 2.7 Molecular structure of (2-HgClC₆H₄)C(O)N=PPh₃ **2.42** showing the atom numbering scheme. Hydrogen atoms have been omitted for clarity and thermal ellipsoids are shown at the 50% probability level.

Although the mercury–oxygen interaction is weak [the Hg(1)–O(1) bond length is 2.6281(16) Å] it appears that it is keeping the core of the molecule co-planar. Indeed the greatest deviations from the metallacyclic ring are C(1) and C(2) [which sit 0.0254(15) Å and

0.0338(13) Å above and below the plane of the ring respectively]. The PNCO network is also essentially planar but tilted upward at an angle of 6.84(17)° to the metallacyclic ring meaning that the molecule has a slight bow in it. This differs from the free ligand where the phenyl ring is twisted 11.49° from the planar PNCO moiety. Like the uncoordinated ligand the triphenylphosphine groups have a propeller-like arrangement.⁽⁴¹⁾

Table 2.4 Selected bond lengths (Å) and angles (°) for the complex **2.42** with esds in parenthesis.

Atoms	Lengths (Å)	Atoms	Angles (°)
P(1) – N(1)	1.620(2)	C(2) – Hg(1) – Cl(1)	176.24(6)
N(1) – C(7)	1.346(3)	Hg(1) – C(2) – C(1)	118.83(17)
C(7) – O(1)	1.250(3)	C(2) – C(1) – C(7)	120.9(2)
C(7) – C(1)	1.515(3)	C(1) – C(7) – O(1)	119.80(19)
C(1) – C(2)	1.398(3)	C(7) – O(1) – Hg(1)	106.40(14)
C(2) – Hg(1)	2.063(2)	C(1) – C(7) – N(1)	114.86(19)
Hg(1) – Cl(1)	2.3293(6)	C(7) – N(1) – P(1)	118.37(16)
Hg(1) --- O(1)	2.6281(16)	N(1) – C(7) – O(1)	125.3(2)

There is a slight lengthening of the C=O bond upon coordination to the mercury [from 1.2448(3) Å to 1.250(3) Å] which is to be expected if there is a weak interaction between the oxygen atom and the mercury. In addition, both the P=N and N-C bonds have become shorter. Finally, there is only a small change in the C(1)-C(7)-O(1) angle after metallation [119.80(19)° in **2.42** compared with 119.39° in the ligand].

X-ray crystal structure of (2-AuCl₂C₆H₄)C(O)N=PPh₃, **2.43**

As expected, the nitrogen of the iminophosphorane is coordinated to the gold centre. This preference for coordination of the softer nitrogen to the metal centre was also observed in the analogous palladium(II) complex.⁽³⁾ Like the palladium complex the metallacyclic ring is not planar, instead it has an envelope conformation with the gold atom sitting 0.528(5) Å above the ring. Because of this, the PNCO network is no longer planar and has a twist of 19.11°.

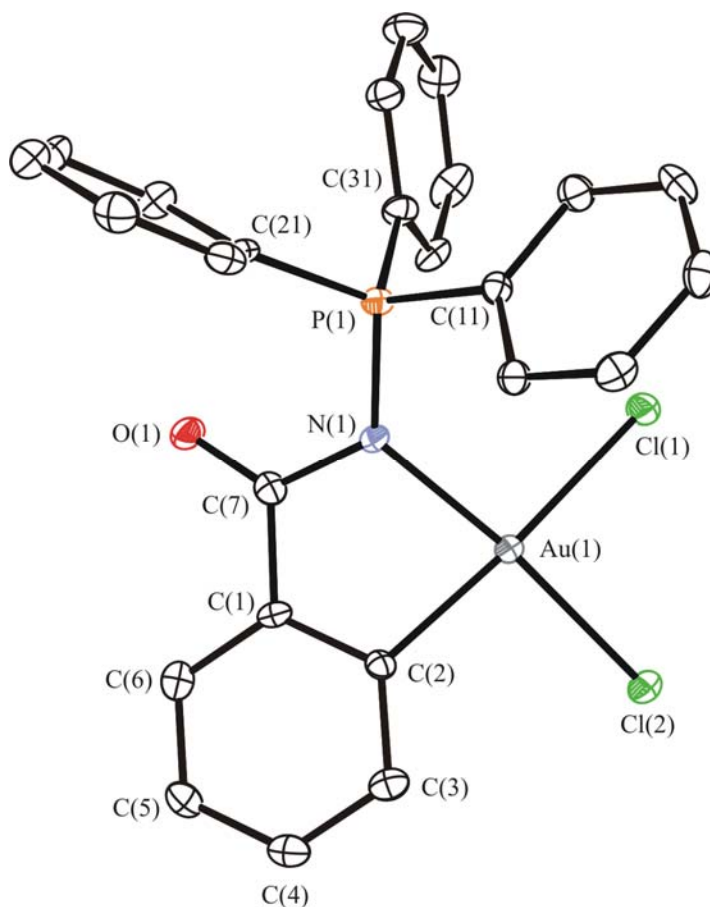


Figure 2.8 Molecular structure of $(2\text{-AuCl}_2\text{C}_6\text{H}_4)\text{C}(\text{O})\text{N}=\text{PPh}_3$ **2.43** showing the atom numbering scheme. The dichloromethane solvent and hydrogen atoms have been omitted for clarity. Thermal ellipsoids are shown at the 50% probability level.

Like the other examples of *exo* metallated iminophosphanes the dangling triphenylphosphine moiety has phenyl groups which are arranged in a propeller-like fashion. Upon coordination to the gold there is an increase in both the P=N and N-C bond lengths when compared to the uncoordinated ligand [P=N: 1.6258(3) Å in ligand, 1.655(3) Å in **2.43**; N-C: 1.3530(4) Å in ligand, 1.401(4) Å in **2.43**]. In addition the C=O bond length has decreased [from 1.2448(3) Å in the ligand to 1.218(4) Å in the cycloaurated complex] – a similar change in bond lengths was observed in the palladium complex.

Table 2.5 Selected bond lengths (Å) and angles (°) for the complex **2.43**, with esds in parenthesis.

Atoms	Lengths (Å)	Atoms	Angles (°)
P(1) – N(1)	1.655(3)	Cl(1) – Au(1) – Cl(2)	90.18(3)
N(1) – C(7)	1.401(4)	Cl(2) – Au(1) – C(2)	93.24(9)
C(7) – O(1)	1.218(4)	C(2) – Au(1) – N(1)	80.90(11)
C(7) – C(1)	1.481(4)	N(1) – Au(1) – Cl(1)	95.55(7)
C(1) – C(2)	1.395(4)	Au(1) – C(2) – C(1)	111.7(2)
C(2) – Au(1)	2.025(3)	C(2) – C(1) – C(7)	117.0(3)
Au(1) – Cl(1)	2.3694(8)	C(1) – C(7) – N(1)	112.0(3)
Au(1) – Cl(2)	2.2798(8)	C(1) – C(7) – O(1)	125.7(3)
Au(1) – N(1)	2.048(3)	O(1) – C(7) – N(1)	122.3(3)
		C(7) – N(1) – Au(1)	112.8(2)
		C(7) – N(1) – P(1)	119.5(2)
		P(1) – N(1) – Au(1)	127.68(16)

The coordination around the gold atom is as expected. It is essentially square planar [the greatest deviation from the mean coordination plane is C(2) which is 0.0906(15) Å below the plane of the atoms]. The bite angle of the ligand is 80.90(11)° and because of the greater *trans* influence of the aryl carbon versus the nitrogen the Au – Cl(1) bond length [2.3694(8) Å] is longer than the Au – Cl(2) distance [2.2798(8) Å].

In addition, the compound also crystallises with a molecule of dichloromethane. This is held in the lattice by an interaction of a proton on the dichloromethane with the two chloride ligands on the gold complex (*i.e.* a bifurcated hydrogen bond).

X-ray crystal structure of (2-AuCl₂C₆H₄)C(O)N=PPh₃, 2.46

The X-ray crystal structure of **2.46** confirms the *endo* isomer with the P=N bond contained in the metallacyclic ring. The environment around the gold is essentially square planar, as expected. Like the simple iminophosphanes, the metallacyclic ring is severely puckered with the phosphorus and the nitrogen atoms showing the greatest deviations from the plane

[P(1) sits 0.2369(9) Å below the plane, N(1) 0.2880(9) Å above the plane]. As a result of the puckering, the PNCO moiety is no longer planar and has a twist of 24.97°. The bite angle of the ligand [84.38(9)°] is similar to what is seen in the simple iminophosphoranes.

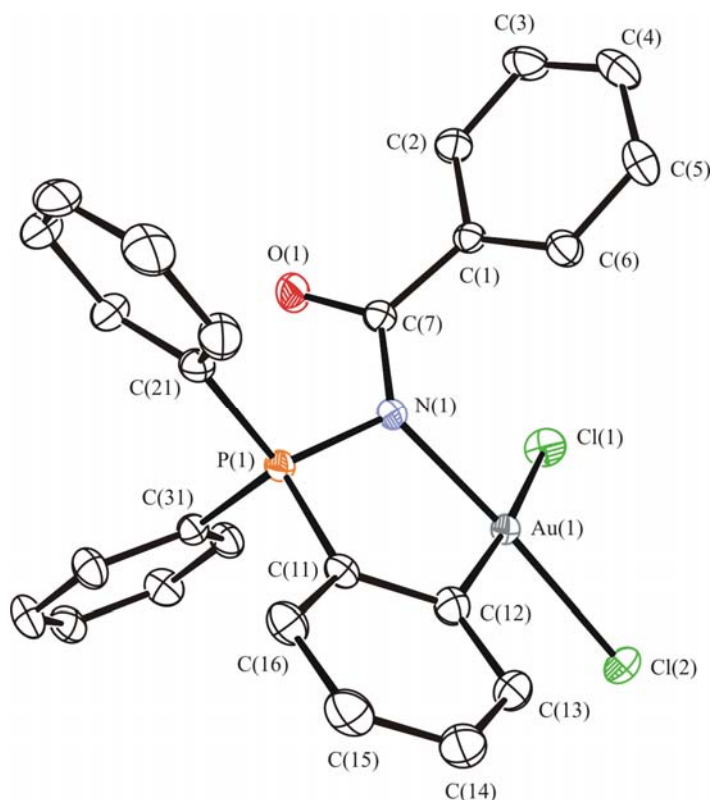


Figure 2.9 Molecular structure of (2-AuCl₂C₆H₄)C(O)N=PPh₃, **2.46** showing the atom numbering scheme. Hydrogen atoms have been omitted for clarity and the thermal ellipsoids are shown at the 50% probability level.

As with the *exo* isomer, the C=O bond length is shorter in the cycloaurated species [1.222(3) Å] than in the free ligand (1.2448(3) Å). This coincides with the P=N and N(1)-C(7) bonds becoming longer and is a result of loss of conjugation as the electron density is pulled onto the gold atom.

As with other crystallographically characterised gold(III) complexes containing *C,N* donor ligands the bond *trans* to the carbon (which has a higher *trans* influence) is longer than the bond *trans* to the nitrogen. Therefore, Au(1)-Cl(1) is longer than Au(1)-N(1) [2.3578(6) Å

versus 2.2721(6) Å]. In addition, the Au-Cl bond *trans* to the nitrogen is shorter in **2.46** than it is in the simple iminophosphoranes indicating that an acyl group on the nitrogen results in the nitrogen having a lower *trans* influence. The Au-N coordinate bond length is significantly shorter in the *endo* complex [2.0321(18) Å] than in the *exo* complex [2.048(3) Å].

Table 2.6 Selected bond lengths (Å) and angles (°) for the complex **2.46**, with esds in parenthesis

Atoms	Lengths (Å)	Atoms	Angles (°)
Au(1) – Cl(1)	2.3578(6)	Cl(1) – Au(1) – Cl(2)	90.89(2)
Au(1) – Cl(2)	2.2721(6)	Cl(2) – Au(1) – C(12)	92.59(7)
Au(1) – C(12)	2.039(3)	C(12) – Au(1) – N(1)	84.38(9)
Au(1) – N(1)	2.0321(18)	N(1) – Au(1) – Cl(1)	91.97(6)
P(1) – N(1)	1.645(2)	C(12) – C(11) – P(1)	115.72(17)
N(1) – C(7)	1.401(3)	C(11) – P(1) – N(1)	99.18(10)
C(7) – O(1)	1.222(3)	P(1) – N(1) – Au(1)	111.98(9)
C(12) – C(11)	1.412(3)	P(1) – N(1) – C(7)	116.59(15)
C(11) – P(1)	1.777(2)	N(1) – C(7) – O(1)	119.1(2)
		N(1) – C(7) – C(1)	118.96(19)

2.2.9 Spectroscopic and mass spectrometric characterisation of *ortho*-mercurated and cycloaurated stabilised iminophosphoranes

NMR spectroscopy of *exo* complexes

Once again, $^{31}\text{P}\{^1\text{H}\}$ NMR spectroscopy is very indicative of what is occurring in the complexes. Figure 2.10 shows the $^{31}\text{P}\{^1\text{H}\}$ NMR spectra of the series of *exo* cyclometallated complexes. The ligand has a chemical shift of 21.3 ppm and the *ortho*-manganated complex **2.41** has a shift of 23.5 ppm – there is essentially no change between the two. As mentioned above, this indicates that the phosphorus atom is not included in the metallacyclic ring. There is little change on transmetallation to the *ortho*-mercurated complex – the chemical shift of **2.42** is 26.6 ppm. Unlike the simple iminophosphoranes there are no ^{199}Hg satellite lines present as the mercury atom is now separated from the phosphorus by five bonds. The cycloaurated complex **2.43** has a chemical shift of 35.8 ppm which is slightly shifted from the

manganese and mercury examples. This is most probably because the nitrogen is now coordinated to the gold so the phosphorus (which is directly bonded to the nitrogen) is slightly more deshielded than in the other examples where the oxygen is coordinated to the metal. In addition, the chemical shift in **2.43** is significantly further upfield than in the simple cycloaurated iminophosphorane **2.29a** (65.5 ppm) where the phosphorus is in the five-membered ring.

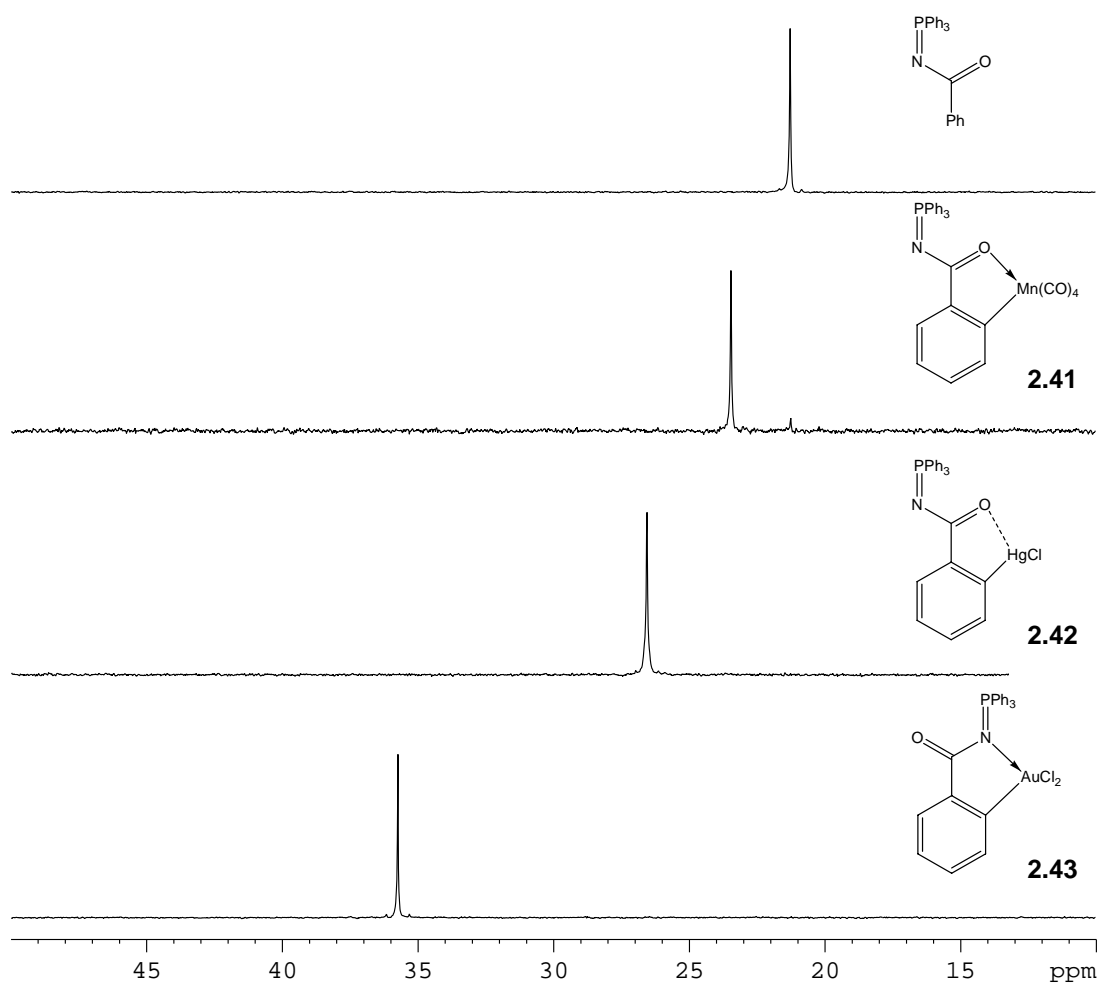


Figure 2.10 $^{31}\text{P}\{^1\text{H}\}$ NMR spectra of the series of exo cyclometallated complexes.

NMR spectroscopy of *endo* complexes

The diaryl mercury complex **2.44** has a $^{31}\text{P}\{^1\text{H}\}$ chemical shift of 0.4 ppm – the diiminophosphorane **2.45** has a chemical shift of 27.4 ppm, so a downfield shift of

approximately 30 ppm has been seen upon oxidation of P(III) to P(V). The chemical shift is very close to the *exo* isomer **2.42** but now ^{199}Hg satellite peaks can also be seen – the $^3J_{\text{PHg}}$ coupling constant indicates that the mercury is attached at the *ortho* position of one of the *P*-bonded phenyl rings. Upon transmetallation to gold there is a significant downfield shift (of approximately 30 ppm) as the phosphorus is now in a five-membered ring **2.46** – the chemical shift of 60.5 ppm is now comparable with the cycloaurated iminophosphorane **2.29a**. Figure 2.11 shows the $^{31}\text{P}\{^1\text{H}\}$ chemical shifts associated with the *endo* complexes.

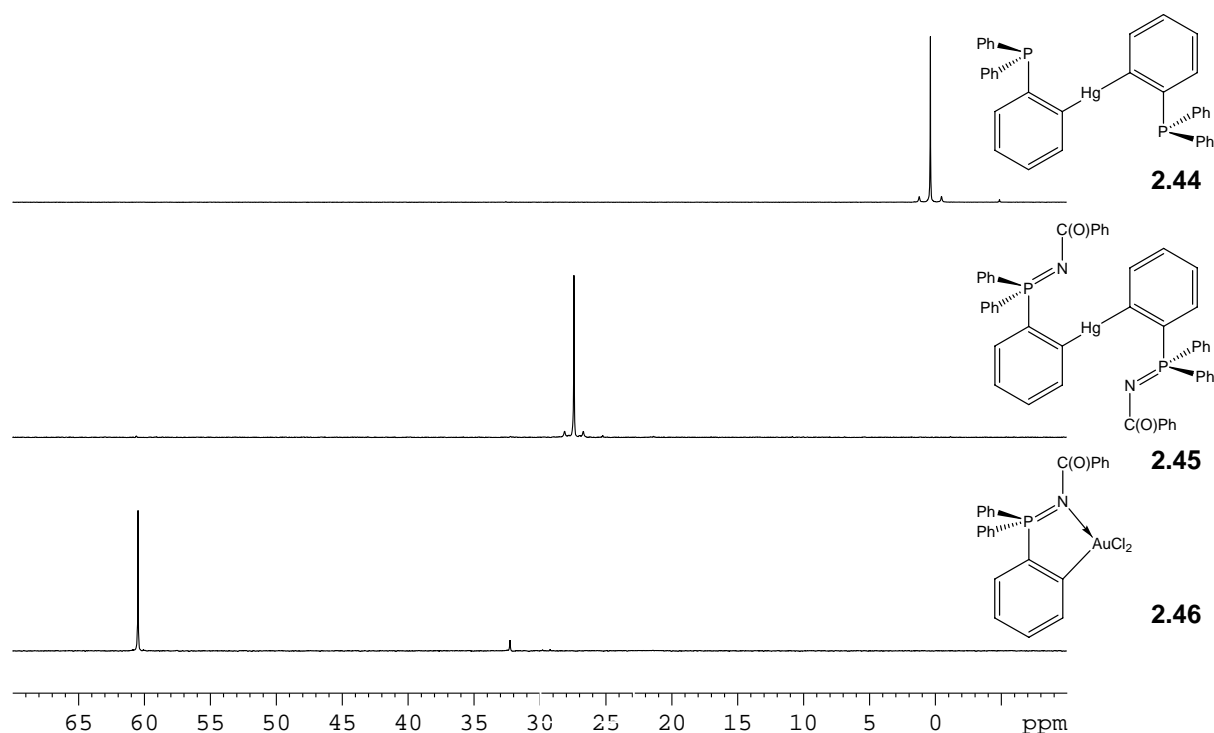


Figure 2.11 $^{31}\text{P}\{^1\text{H}\}$ NMR spectra of the series of *endo* cyclometallated complexes.

Infrared spectroscopy of *exo* complexes

Infrared spectroscopy can also be used to determine the binding mode of iminophosphoranes. It has previously been reported that when the stabilised iminophosphoranes form cyclometallated complexes with a nitrogen-metal bond the P=N stretch moves to lower energies and the C=O stretch moves to slightly higher energies.^(3, 17) In $\text{Ph}_3\text{P}=\text{NC}(\text{O})\text{Ph}$ the P=N stretch occurs at 1341 cm^{-1} and the C=O stretch at 1595 cm^{-1} .⁽³⁶⁾ The *ortho*-mercurated *exo* complex **2.42** (in which the nitrogen is not involved in any interactions with the mercury)

has a P=N stretch at 1340 cm⁻¹ and a C=O stretch at 1532 cm⁻¹. The P=N shift remains relatively unchanged, the C=O shift has moved to lower wavenumbers because of a slight interaction with the mercury. In contrast, in the cycloaurated *exo* complex **2.43** has a P=N stretch at 1285 cm⁻¹; the significant shift to lower wavenumbers indicate that the ligand is coordinated through the nitrogen atom. The C=O stretch occurs at 1684 cm⁻¹, the higher energy stretch associated with the loss of conjugation that is present in the ligand. IR data are displayed in Table 2.7

Infrared spectroscopy of *endo* complexes

The *endo* series of complexes show different IR behaviour to that of the *exo* isomers. The P=N stretch of **2.45** occurs at 1323 cm⁻¹, approximately 20 wavenumbers lower than in the ligand. This suggests an interaction between the nitrogen and the mercury. Upon transmetallation to the gold, there is a further decrease in wavenumber to 1282 cm⁻¹. This pattern is analogous to that seen in the simple iminophosphorane complexes. There is a little change between the C=O stretches in the ligand and the *ortho*-mercurated complex **2.45**, however the in cycloaurated complex **2.46** the C=O stretch occurs at higher wavenumbers, again because of loss of conjugation in the metallacycle. Table 2.7 documents the IR absorbances for the *endo* and *exo* series of complexes.

Table 2.7 Selected IR absorbances (KBr disk) for the metallated iminophosphorane Ph₃P=NC(O)Ph, including *endo* and *exo* isomers.

Complex	IR Absorbances (cm ⁻¹)	
	$\nu(\text{P}=\text{N})$	$\nu(\text{C}=\text{O})$
Ph₃P=NC(O)Ph	1341	1595
2.41	1341	1488
2.42	1340	1532
2.43	1285	1684
2.45	1323	1598
2.46	1282	1641

Mass spectrometry of *exo* and *endo* complexes

The ions seen in the ESI mass spectra of the stabilised iminophosphoranes can not be directly compared to the ions seen for the simple iminophosphoranes because analysis was carried out on two different instruments with different ionisation sources. However, the main ionisation pathway for the mercury complexes was *via* the formation of charged species by picking up a cation from the solution (*e.g.* $[M+Na]^+$). For the gold complexes, a chloride ligand was lost to give a charged species (*e.g.* $[M-Cl]^+$).

2.2.10 Biological activity

The biological activity of **2.29a** has been reported, and showed low anti-tumour activity against the P388 murine leukemia cell line.⁽¹⁸⁾ In order to determine if this is characteristic of cycloaurated iminophosphoranes, the activity of the alkyl compound **2.29f** was evaluated. The bicyclic catecholate (**2.35a** and **2.35f**) and thiosalicylate (**2.36a** and **2.36b**) derivatives were also evaluated, since related derivatives have exhibited higher anti-tumour activity.⁽²⁷⁾ Samples were tested in a 2:1 dichloromethane:methanol solvent system, using the methods described in Appendix I. Results of the assay are given in Table 2.8.

Table 2.8 Anti-tumour (P388 murine leukaemia) activities for selected gold(III) iminophosphoranes and related systems.

Complex	IC ₅₀ ^a	
	ng mL ⁻¹	μM
2.29a	7546	10.7
2.29f	20021	33.4
2.35a	<487	<0.74
2.35f	655	1.03
2.36a	<487	<0.69
2.36f	658	0.97

^a Concentration of sample required to reduce cell growth of the P388 murine leukaemia cell line by 50%.

In contrast to the dichloride complexes **2.29a** and **2.29f** which show low anti-tumour activity, the catecholate and thiosalicylate complexes show a ten-fold increase in the level of activity. In particular the complexes **2.35a** and **2.36a**, originating from complex **2.29a**, show a high level of activity. These preliminary results indicate that these systems (in particular the catecholate and thiosalicylate derivatives) show interesting biological activity and could form the basis for further investigation.

2.3 Conclusions

A range of new *ortho*-mercurated and cycloaurated simple iminophosphoranes, and their derivatives, have been synthesised and fully characterised by NMR spectroscopy and ESI mass spectrometry. X-ray crystal structures of three of these compounds have been carried out. The gold-nitrogen bond is relatively strong because when **2.29a** is reacted with PPh₃ the gold-nitrogen bond remains intact and a chloride ligand is substituted by PPh₃. Attempts at cleaving this bond by reacting **2.29a** with ligands such as cyanide or dithiocarbamates were unsuccessful. Both chloride ligands can be replaced by chelating ligands to give bi-metallacyclic compounds with enhanced anti-tumour activity. In addition, the cycloauration of the stabilised iminophosphorane Ph₃P=NC(O)Ph was investigated. Both the *exo* and the *endo* isomers were obtained, using targeted strategies for each, with their structures confirmed by X-ray crystallography.

2.4 Experimental

2.4.1 General

The known aminophosphonium salts **2.32f** and **2.32b** and the iminophosphoranes **2.33d** and **2.33f** were prepared by literature procedures; **2.32c** was prepared by a completely analogous method to **2.32b**.^(1, 20) Complex **2.29a** was prepared by the literature procedure.⁽¹⁸⁾ The iminophosphoranes **2.33d** and Ph₃P=NC(O)Ph was synthesised by the Staudinger reaction by Miss Frances Gourdie and Miss Rachael Linklater respectively. *n*-Butyllithium (either 1.6 M in hexanes or 2.0 M in cyclohexane, Aldrich), PhBr (AJAX Chemicals), HgCl₂, catechol,

sodium diethyldithiocarbamate trihydrate (BDH), Hg(OAc)₂ (Riedel de Haën) and thiosalicylic acid (Sigma) were used as received. PhCH₂Mn(CO)₅, Hg(C₆H₄PPh₂)₂ were prepared by modifications of the literature procedures, described in Appendix I. Metallation reactions were carried out under a nitrogen atmosphere using standard Schlenk techniques, with light also being excluded in the case of cycloauration reactions.

2.4.2 Syntheses of simple *ortho*-metallated iminophosphanes and the reactions they undergo

Preparation of (2-HgBrC₆H₄)Ph₂P=N-(*R,S*)-CHMePh **2.34b**

[Ph₃P-NH-(*R,S*)-CHMePh]⁺Br⁻ **2.32b** (1.000 g, 2.16 mmol) was suspended in diethyl ether (30 mL) and cooled to -84 °C in an ethyl acetate slush bath. BuⁿLi (1.6 M, 2.7 mL, 4.32 mmol) was added dropwise with stirring. The solution was allowed to warm to room temperature to give a clear orange solution that was stirred for an additional 30 min. HgCl₂ (0.586 g, 2.16 mmol) was added in one portion and after stirring for 1 h the solvent was removed and the solid extracted into dichloromethane (2 × 10 mL), filtered and diethyl ether (20 mL) was added to the filtrate. Storage at -20 °C gave white crystals of (2-HgBrC₆H₄)Ph₂P=N-(*R,S*)-CHMePh **2.34b** (0.606 g, 42%).

Found: C 47.7, H 3.6, N 2.2; C₂₆H₂₃NPBrHg requires C 47.3, H 3.5, N 2.1%.

NMR: ¹H: δ 1.64 (d, CH₃), 4.68 (m, CH), 7.00-7.69 (m, Ar-H); ³¹P{¹H}: δ 14.8, (³J_{HgP} = 317 Hz) ppm.

ESI-MS: *m/z*: 662 (100%, [M+H]⁺).

IR: ν(P=N) = 1163 cm⁻¹ (vs).

Preparation of (2-HgBrC₆H₄)Ph₂P=N-(S)-CHMePh **2.34c**

As for the preparation of **2.34b** above, [Ph₃P-NH-(S)-CHMePh]⁺Br⁻ **2.32c** (2.000 g, 4.34 mmol) was suspended in diethyl ether (30 mL) and BuⁿLi (1.6 M, 5.4 mL, 8.68 mmol) added. After addition of HgCl₂ (1.178 g, 4.34 mmol), work-up as above gave 1.780 g, (62%) of (2-HgBrC₆H₄)Ph₂P=N-(S)-CHMePh **2.34c**. The product was identified by ¹H and ³¹P{¹H} NMR spectroscopy.

Preparation of (2-HgClC₆H₄)Ph₂P=NC₆H₄F **2.28d**

A solution of BuⁿLi (2 mL, 2.69 mmol) was added to a solution of PhBr (0.28 mL, 2.69 mmol) in diethyl ether (20 mL) and stirred for 15 min. Ph₃P=NC₆H₄F **2.33d** (1.000 g, 2.69 mmol) was added to immediately give a dark orange solution. After stirring for 1.5 h a white precipitate had formed. HgCl₂ (0.730 g, 2.69 mmol) was added and the mixture stirred for an additional hour. Workup as for **2.34b** gave crystals of (2-HgClC₆H₄)Ph₂P=NC₆H₄F, **2.28d** (0.927 g, 57%).

Found: C 47.5, H 2.9, N 2.4; C₂₄H₁₈NFPClHg requires C 47.5, H 3.0, N 2.3%.

NMR: ¹H: δ 6.69-6.75, 6.80-6.85, 7.27-7.34, 7.40-7.70 (all m, Ar-H); ³¹P{¹H}: δ 9.0 (br), (³J_{HgP} = 320 Hz) ppm.

ESI-MS: *m/z*: 608 (100%, [M+H]⁺), 943 (35%, [2-Hg({C₆H₄})Ph₂P=NC₆H₄F)₂+H]⁺).

IR: ν(P=N) = 1309 cm⁻¹ (vs).

Preparation of (2-HgClC₆H₄)Ph₂P=NBu^t **2.28f**

As for **2.28d** above, Ph₃P=NBu^t **2.33f** (1.199 g, 3.60 mmol) was added to a solution of PhBr (0.38 mL, 3.60 mmol) and BuⁿLi (1.6 M, 2.25 mL, 3.60 mmol) in diethyl ether (20 mL). Addition of HgCl₂ (0.977 g, 3.60 mmol) followed by workup gave (2-HgClC₆H₄)Ph₂P=NBu^t **2.28f** (0.909 g, 44%).

Found: C 46.0, H 4.1, N 2.5; C₂₂H₂₃NPClHg requires C 46.5, H 4.1, N 2.5%.

NMR: ¹H: δ 1.29 (s, CH₃), 7.13-7.19, 7.31-7.64, 7.74-7.81 (all m, Ar-H); ³¹P{¹H}: δ 2.2, (³J_{HgP} = 341 Hz) ppm.

ESI-MS: *m/z*: 570 (100%, [M+H]⁺).

IR: ν(P=N) = 1223 cm⁻¹ (vs).

Alternative synthesis:

Ph₃P=Nbu' **2.33f** (0.300 g, 0.90 mmol) and Hg(OAc)₂ (0.288 g, 0.90 mmol) were refluxed under nitrogen in dry degassed THF (20 mL) for 16 h. The solution was allowed to cool, LiCl (0.076 g, 1.79 mmol) was added and stirred for an additional 4 h. The solution was filtered and evaporated to dryness. The filtrate was redissolved in dichloromethane (2 × 10 mL) and diethyl ether (20 mL) was added. Storage at -20 °C gave crystals of (2-HgClC₆H₄)Ph₂P=Nbu' **2.28f** (0.128 g, 25%), identified by ¹H and ³¹P{¹H} NMR spectroscopy.

Preparation of (2-AuCl₂C₆H₄)Ph₂P=N-(*R,S*)-CHMePh **2.29b**

The complex (2-HgBrC₆H₄)Ph₂P=N-(*R,S*)-CHMePh **2.34b** (0.100 g, 0.15 mmol), [Me₄N][AuCl₄] (0.062 g, 0.15 mmol) and [Me₄N]Cl (0.016 g, 0.15 mmol) were added to degassed acetonitrile (15 mL) and stirred in a foil-covered flask for 48 h. The solvent was removed and the yellow solid extracted into dichloromethane (2 × 10 mL), filtered and diethyl ether was added to the filtrate. Storage at -20 °C gave yellow crystals of (2-AuCl₂C₆H₄)Ph₂P=N-(*R,S*)-CHMePh **2.29b** (0.062 g, 64%).

Found: C 47.2, H 3.5, N 2.1; C₂₆H₂₃NPCl₂Au requires C 48.2, H 3.6, N 2.2%.

NMR: ¹H: δ 1.62 (d, CH₃), 5.85 (m, CH), 6.92-7.01, 7.05-7.08, 7.18-7.23, 7.32-7.53, 7.58-7.67, 8.17-8.21 (all m, Ar-H); ³¹P{¹H}: δ 59.0 ppm.

ESI-MS: pyridine doped m/z : 653 (100%, $[M-Cl+MeCN]^+$), 691 (85%, $[M-Cl+py]^+$), 612 (53%, $[M-Cl]^+$).

IR: $\nu(P=N) = 1138 \text{ cm}^{-1}$ (s).

Preparation of (2-AuCl₂C₆H₄)Ph₂P=N-(S)-CHMePh 2.29c

Analogous to **2.29b**, (2-HgBrC₆H₄)Ph₂P=N-(S)-CHMePh **2.34c** (1.000 g, 1.51 mmol), [Me₄N][AuCl₄] (0.623 g, 1.51 mmol) and [Me₄N]Cl (0.166 g, 1.51 mmol) were reacted in acetonitrile (30 mL) for 48 h. Workup gave (2-AuCl₂C₆H₄)Ph₂P=N-(S)-CHMePh as pale yellow crystals (0.139 g, 14%). The product was identified as **2.29c** by ¹H and ³¹P{¹H} NMR spectroscopy.

Preparation of (2-AuCl₂C₆H₄)Ph₂P=NC₆H₄F 2.29d

As for **2.29b**, (2-HgClC₆H₄)Ph₂P=NC₆H₄F **2.28d** (0.174 g, 0.29 mmol), [Me₄N][AuCl₄] (0.119 g, 0.29 mmol) and [Me₄N]Cl (0.032 g, 0.29 mmol) in acetonitrile (20 mL) for 24 h. Work-up gave (2-AuCl₂C₆H₄)Ph₂P=NC₆H₄F, **2.29d** as bright yellow crystals (0.074 g, 40%).

Found: C 45.2, H 3.1, N 2.2; C₂₄H₁₈NFPCl₂Au requires C 45.2, H 2.8, N 2.2%.

NMR: ¹H: δ 6.73-6.80, 6.92-6.97, 7.10-7.17, 7.33-7.38, 7.49-7.62, 7.71-7.78, 8.41-8.46 (all m, Ar-H); ³¹P{¹H}: δ 66.9 ppm.

ESI-MS: m/z : 602 (100%, $[M-Cl]^+$), 1241 (80%, $[2M-Cl]^+$); pyridine doped m/z : 681 (100%, $[M-Cl+py]^+$).

IR: $\nu(P=N) = 1219 \text{ cm}^{-1}$ (s).

Preparation of (2-AuCl₂C₆H₄)Ph₂P=NBu^t **2.29f**

As for **2.29b**, (2-HgClC₆H₄)Ph₂P=NBu^t **2.28f** (0.400 g, 0.70 mmol), [Me₄N][AuCl₄] (0.291 g, 0.70 mmol) and [Me₄N]Cl (0.077 g, 0.70 mmol) were reacted in acetonitrile (20 mL) for 24 h. Workup gave yellow crystals of (2-AuCl₂C₆H₄)Ph₂P=NBu^t **2.29f** (0.312 g, 74%).

Found: C 44.2, H 3.9, N 2.4; C₂₂H₂₃NPCL₂Au requires C 44.0, H 3.9, N 2.3%.

NMR: ¹H: δ 1.34 (s, CH₃), 7.31-7.40, 7.55-7.62, 7.67-7.72, 7.85-7.91, 8.04-8.07 (all m, Ar-H); ³¹P{¹H}: δ 46.1 ppm.

ESI-MS: *m/z*: 564 (100%, [M-Cl]⁺), 673 (35%, [M+Me₄N]⁺), 1165 (30%, [2M-Cl]⁺); pyridine doped *m/z*: 643 (100%, [M-Cl+py]⁺), 564 (60%, [M-Cl]⁺).

IR: ν(P=N) = 1183 cm⁻¹ (m).

Synthesis of **2.35a**

The complex (2-AuCl₂C₆H₄)Ph₂P=NPh **2.29a** (0.100 g, 0.16 mmol) and catechol (0.018 g, 0.16 mmol) were refluxed in methanol (20 mL). With stirring, Me₃N (1 mL, excess) was added resulting in the yellow solution immediately turning dark orange. After refluxing for a further 20 min. the solution was allowed to cool, water (20 mL) was added and stirring continued overnight. The precipitate that had formed was filtered, washed with water (2 × 10 mL) and diethyl ether (10 mL) and dried under vacuum to give **2.35a** (0.085 g, 81%) as a rose-coloured solid.

Found: C 54.8, H 3.6, N 2.2; C₃₀H₂₃NO₂PAu requires C 54.8, H 3.5, N 2.1%.

NMR: ¹H: δ 6.42-6.47, 6.73-6.76, 7.01-7.15, 7.29-7.36, 7.49-7.57, 7.66-7.79, 8.19-8.22 (all m, Ar-H); ³¹P{¹H}: δ 60.9 ppm.

ESI-MS: m/z : 658 (100%, $[M+H]^+$), 1315 (60%, $[2M+H]^+$); NaCl doped m/z : 680 (100%, $[M+Na]^+$), 1337 (34%, $[2M+Na]^+$), 658 (28%, $[M+H]^+$), 1315 (12%, $[2M+H]^+$).

IR: $\nu(P=N) = 1254 \text{ cm}^{-1}$ (m).

Synthesis of **2.35f**

The complex $(2\text{-AuCl}_2\text{C}_6\text{H}_4)\text{Ph}_2\text{P}=\text{NBu}^t$ **2.29f** (0.100 g, 0.17 mmol) and catechol (0.019 g, 0.17 mmol) were brought to reflux in methanol (15 mL). With stirring, Me_3N (1 mL, excess) was added resulting in the yellow solution turning dark orange. After refluxing for a further 15 minutes the now purple solution was allowed to cool, water (20 mL) was added, and stirring continued overnight. The precipitate that had formed was filtered, washed with water ($3 \times 10 \text{ mL}$) and diethyl ether (20 mL) and dried under vacuum to give **2.35f** (0.067 g, 62%) as a rose-coloured solid. A sample for microanalysis was recrystallised from dichloromethane/diethyl ether.

Found: C 51.3, H 4.2, N 2.2; $\text{C}_{28}\text{H}_{27}\text{NO}_2\text{PAu}$ requires C 52.8, H 4.3, N 2.2; $\text{C}_{28}\text{H}_{27}\text{AuNO}_2\text{P} \cdot \text{H}_2\text{O}$ requires C 51.3, H 4.5, N 2.1%.

NMR: ^1H : δ 1.52 (s, CH_3), 6.45-6.50, 6.53-6.58, 6.67-6.79, 7.13-7.20, 7.34-7.39, 7.56-7.62, 7.66-7.71, 7.91-7.98, 8.11-8.14 (all m, Ar-H) $^{31}\text{P}\{^1\text{H}\}$: δ 55.7 ppm.

ESI-MS: m/z : 638 (100%, $[M+H]^+$), 1275 (30%, $[2M+H]^+$); NaCl doped m/z : 660 (100%, $[M+Na]^+$), 1297 (60%, $[2M+Na]^+$), 638 (40% $[M+H]^+$).

IR: $\nu(P=N) = 1254 \text{ cm}^{-1}$ (m).

Synthesis of **2.36a**

To a stirred methanolic solution (15 mL) of $(2\text{-AuCl}_2\text{C}_6\text{H}_4)\text{Ph}_2\text{P}=\text{NPh}$ **2.29a** (0.100 g, 0.16 mmol) and thiosalicylic acid (0.025 g, 0.16 mmol), Me_3N (1 mL, excess) was added, resulting

in the pale yellow solution immediately becoming darker. Stirring was continued in the dark for a further 90 minutes before water (20 mL) was added. The fine yellow precipitate that had formed was filtered and washed with water (3×10 mL) and diethyl ether (1×10 mL) and dried under vacuum to give **2.36a** (0.099 g, 88%).

Found: C 53.1, H 3.4, N 2.0; $C_{31}H_{23}NO_2PSAu$ requires C 53.1, H 3.3, N 2.0%.

NMR: 1H : δ 6.88-6.92, 7.01-7.21, 7.28-7.35, 7.46-7.57, 7.64-7.75, 8.00-8.04, 8.15-8.20 (all m, Ar-H); $^{31}P\{^1H\}$: δ 54.1 ppm

ESI-MS: m/z : 901 (100%, $[2-Au(\{C_6H_4\}Ph_2P=NPh)_2]^+$), 702 (30%, $[M+H]^+$), 1404 (25%, $[2M+H]^+$); NaCl doped m/z : 901 (100%, $[2-Au(\{C_6H_4\}Ph_2P=NPh)_2]^+$), 1425 (85%, $[2M+Na]^+$), 724 (40%, $[M+Na]^+$), 702 (10%, $[M+H]^+$), 1403 (7%, $[2M+H]^+$).

IR: $\nu(P=N) = 1316$ (m), $\nu(C=O) = 1626$ (vs) cm^{-1} .

Synthesis of **2.36f**

As for **2.36a**, $(2-AuCl_2C_6H_4)Ph_2P=NBU^t$ **2.29f** (0.101 g, 0.17 mmol) and thiosalicylic acid (0.026 g, 0.17 mmol) were reacted in methanol (15 mL). Addition of Me_3N (1 mL, excess) and water (20 mL) followed by workup gave 0.085 g (73%) of **2.36f** as a yellow solid.

Found: C 51.0, H 4.0, N 2.0; $C_{29}H_{27}NO_2PSAu$ requires C 51.1, H 4.0, N 2.1%.

NMR: 1H : δ 1.40 (s, CH_3), 7.01-7.05, 7.15-7.25, 7.32-7.38, 7.43-7.47, 7.53-7.59, 7.63-7.69, 7.86-7.99, 8.14-8.19 (all m, Ar-H); $^{31}P\{^1H\}$: δ 43.2 ppm.

ESI-MS: m/z : 682 (100%, $[M+H]^+$), 1212 (52%, unidentified), 1363 (30%, $[2M+H]^+$); NaCl doped m/z : 704 (100%, $[M+Na]^+$), 1385 (87%, $[2M+Na]^+$).

IR: $\nu(P=N) = 1310$ (m), $\nu(C=O) = 1626$ (vs) cm^{-1} .

Synthesis of [(2-AuCl(PPh₃)C₆H₄)Ph₂P=NPh]PF₆ **2.39**

The complex (2-AuCl₂C₆H₄)Ph₂P=NPh **2.29a** (0.104 g, 0.17 mmol), PPh₃ (0.045 g, 0.17 mmol) and NH₄PF₆ (0.111 g, 0.68 mmol) were stirred in dichloromethane (10 mL) for 4 h. The solution was filtered and the dark orange filtrate reduced in volume (~2 mL). Diethyl ether was added until the solution went cloudy. Storage at -20 °C gave yellow crystals of [(2-AuCl(PPh₃)C₆H₄)Ph₂P=NPh]PF₆ (0.088 g, 52%).

Found: C 50.2, H 3.5, N 1.5; C₄₂H₃₄NF₆P₃ClAu requires C 50.9, H 3.5, N 1.4%.

NMR: ¹H: δ 6.90-7.03, 7.09-7.14, 7.30-7.34, 7.51-7.57, 7.61-7.71, 7.78-7.87 (all m, Ar-H);
³¹P{¹H}: δ 60.6 (P=N), 41.0 (PPh₃) (1:1 ratio) ppm.

ESI-MS: *m/z*: 846 (100%, [(2-Cl(PPh₃)AuC₆H₄)Ph₂P=NPh]⁺).

IR: ν(P=N) = 1253 cm⁻¹ (w).

Synthesis of **2.40**

The complex (2-AuCl₂C₆H₄)Ph₂P=NPh **2.29a** (0.100 g, 0.16 mmol) and NaS₂CNEt₂·3H₂O (0.036 g, 0.16 mmol) were stirred in dichloromethane (10 mL) for 2.5 h. NH₄PF₆ (0.065 g, 0.40 mmol) was added and the solution stirred for an additional 18 h. The insoluble material was removed by filtration and the yellow solution reduced in volume (~2 mL). Diethyl ether was added until the solution went cloudy. Storage at -20 °C gave yellow microcrystals (0.099 g, 73%) of **2.40**.

Found: C 41.8, H 3.6, N 3.2; C₂₉H₂₉N₂F₆P₂S₂Au requires C 41.3, H 3.5, N 3.3%.

NMR: ¹H: δ 1.30 (t, CH₃), 1.43 (t, CH₃), 3.71 (q, CH₂), 3.82 (q, CH₂), 6.83-6.86, 7.06-7.12, 7.17-7.23, 7.28-7.35, 7.39-7.43, 7.47-7.54, 7.57-7.80 (all m, Ar-H); ³¹P{¹H}: δ 65.9 ppm.

ESI-MS: m/z : 697 (100%, $[M]^+$).

IR: $\nu(\text{P}=\text{N}) = 1232 \text{ cm}^{-1}$ (w).

2.4.3 Syntheses of *ortho*-metallated stabilised iminophosphoranes

Preparation of $\text{Ph}_3\text{P}=\text{NC}(\text{O})\text{Bu}^t$

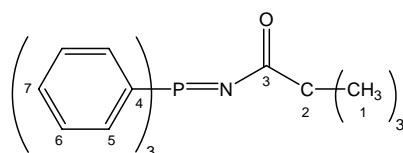
Pivalic anhydride (2.0 mL, 9.9 mmol) and sodium azide (0.769 g, 11.8 mmol) were stirred in dry, degassed acetone (100 mL) for 10 minutes. PPh_3 (2.59 g, 9.9 mmol) was added in one portion and the resulting solution was stirred at room temperature for 72 hours. The solvent was removed under reduced pressure and the solid extracted into dichloromethane (40 mL) and filtered. Diethyl ether (60 mL) was added and the solution was stored at $-25 \text{ }^\circ\text{C}$. $\text{Ph}_3\text{P}=\text{NC}(\text{O})\text{Bu}^t$ crystallised out as white crystals (2.20 g, 62%).

Found: C 76.3, H 6.8, N 3.8; $\text{C}_{23}\text{H}_{24}\text{NOP}$ requires C 76.4, H 6.7, N 3.9%.

NMR: ^1H δ 1.29 (s, 9H, H-1), 7.44 (m, 6H, H-5), 7.53 (m, 3H, H-7), 7.74 (m, 6H, H-6); $^{13}\text{C}\{^1\text{H}\}$ δ 28.8 (s, C-1), 41.4 (d, $^3J_{\text{PC}} = 17.2 \text{ Hz}$, C-2), 128.6 (d, $^3J_{\text{PC}} = 12.0 \text{ Hz}$, C-6), 129.2 (d, $^1J_{\text{PC}} = 98.8 \text{ Hz}$, C-4), 131.9 (d, $^4J_{\text{PC}} = 2.9 \text{ Hz}$, C-7), 133.1 (d, $^2J_{\text{PC}} = 9.8 \text{ Hz}$, C-5), 190.6 (d, $^2J_{\text{PC}} = 11.0 \text{ Hz}$, C-3); $^{31}\text{P}\{^1\text{H}\}$ δ 18.3 ppm (see Scheme 2.29 for NMR labelling scheme).

ESI-MS: m/z : 362.167 (100%, $[\text{M}+\text{H}]^+$, calc 362.169), 384.148 (47%, $[\text{M}+\text{Na}]^+$, calc 384.149), 745.308 (21%, $[2\text{M}+\text{Na}]^+$, calc 745.308).

IR: $\nu(\text{P}=\text{N}) = 1322$ (vs), $\nu(\text{C}=\text{O}) = 1580$ (s) cm^{-1} .



Scheme 2.29 NMR labelling scheme for complexes $\text{Ph}_3\text{P}=\text{NC}(\text{O})\text{Bu}^t$.

Preparation of (2-Mn(CO)₄C₆H₄)C(O)N=PPh₃ **2.41**

PhCH₂Mn(CO)₅ (0.200 g, 0.70 mmol) and Ph₃P=NC(O)Ph (0.268 g, 0.70 mmol) were refluxed in *n*-heptane (30 mL) for 2 hours. While hot the solution was filtered and the yellow filtrate reduced in volume until signs of crystallisation. Storage at -20 °C gave yellow crystals of (2-Mn(CO)₄C₆H₄)C(O)N=PPh₃ (0.246 g, 65%).

Found: C 64.8, H 3.8, N 2.6; C₂₉H₁₉NO₅PMn requires C 63.6, H 3.5, N 2.6%.

NMR: ¹H δ 7.13 (t, 1H, H-5), 7.33 (t, 1H, H-4), 7.51 (m, 6H, H-10), 7.62 (m, 3H, H-11), 7.75 (m, 6H, H-9), 7.90 (d, 1H, H-3), 8.09 (d, 1H, H-6); ¹³C{¹H} δ 123.1 (C-5), 127.2 (d, ¹J_{PC} = 100.1 Hz, C-8), 128.9 (d, ³J_{PC} = 12.6 Hz, C-10), 129.3 (C-6), 131.8 (C-4), 132.9 (d, ⁴J_{PC} = 3.1 Hz, C-11), 133.2 (d, ²J_{PC} = 10.1 Hz, C-9), 140.9 (C-3), 143.3 (d, ³J_{PC} = 16.6 Hz, C-1), 181.2 (d, ⁴J_{PC} = 2.8 Hz, C-2), 189.0 (d, ²J_{PC} = 10.7 Hz, C-7), 213.4 (C=O), 214.8 (C=O), 221.8 (C=O); ³¹P{¹H} δ 23.5 ppm (see Scheme 2.30 for the NMR labelling system).

ESI-MS (-ve): *m/z*: 553.958 (100%, [M-CO+Cl]⁻, calc 554.012), 581.949 (90%, [M+Cl]⁻, calc 582.007), 525.968 (25%, [M-2CO+Cl]⁻, calc 526.017).

IR: ν(P=N) = 1341 (vs), ν(C=O) = 1488 (s) cm⁻¹.

Preparation of (2-HgClC₆H₄)C(O)N=PPh₃ **2.42**

(2-Mn(CO)₄C₆H₄)C(O)N=PPh₃ **2.41** (0.200 g, 0.37 mmol) and HgCl₂ (0.199 g, 0.73 mmol) were refluxed in methanol (20 mL) for 5 hours during which time the yellow solution became colourless and a white solid formed. The solution was cooled in ice then filtered and the white solid washed well with cold methanol. The solid was redissolved in dichloromethane (50 mL) and filtered through a column of celite. The resulting clear solution was reduced in volume (~5 mL) and diethyl ether was added dropwise until the solution went cloudy. Storage at -20 °C gave white crystals of (2-HgClC₆H₄)C(O)N=PPh₃ (0.129 g, 57%).

Found: C 48.9, H 3.1, N 2.3; C₂₅H₁₉NO₅ClHg requires C 48.7, H 3.1, N 2.3%.

NMR: ^1H δ 7.36 (m, 1H, H-5), 7.38 (m, 1H, H-3), 7.48 (m, 1H, H-4), 7.51 (m, 6H, H-10), 7.60 (m, 3H, H-11), 7.79 (m, 6H, H-9), 8.49 (m, 1H, H-6); $^{13}\text{C}\{^1\text{H}\}$ δ 127.5 (d, $^1J_{\text{PC}} = 99.9$ Hz, C-8), 128.3 (C-5), 129.0 (d, $^3J_{\text{PC}} = 12.3$ Hz, C-10), 130.8 (C-6), 131.5 (C-4), 132.7 (d, $^4J_{\text{PC}} = 2.5$ Hz, C-11), 133.5 (d, $^2J_{\text{PC}} = 10.5$ Hz, C-9) 136.2 (C-3), 142.9 (d, $^3J_{\text{PC}} = 18.5$ Hz, C-1), 150.1 (d, $^4J_{\text{PC}} = 3.7$ Hz, C-2), 177.6 (d, $^2J_{\text{PC}} = 7.7$ Hz, C-7); $^{31}\text{P}\{^1\text{H}\}$ δ 26.6 ppm (see Scheme 2.30 for NMR labelling system).

ESI-MS: m/z : 640.044 (100%, $[\text{M}+\text{Na}]^+$, calc 640.049), 656.018 (60%, $[\text{M}+\text{K}]^+$, calc 656.022), 618.062 (20%, $[\text{M}+\text{H}]^+$, calc 618.067), 1255.097 (8%, $[2\text{M}+\text{Na}]^+$, calc 1255.106), 1197.140 (4%, $[2\text{M}-\text{Cl}]^+$, calc 1197.149).

IR: $\nu(\text{P}=\text{N}) = 1340$ (vs), $\nu(\text{C}=\text{O}) = 1532$ (s) cm^{-1} .

Preparation of (2-AuCl₂C₆H₄)C(O)N=PPh₃ 2.43

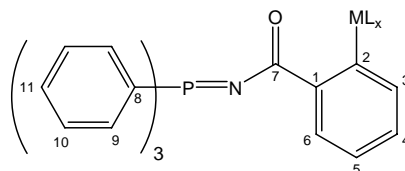
(2-HgClC₆H₄)C(O)N=PPh₃ 2.42 (0.100 g, 0.16 mmol), $[\text{Me}_4\text{N}][\text{AuCl}_4]$ (0.067 g, 0.16 mmol) and $[\text{Me}_4\text{N}]\text{Cl}$ (0.018 g, 0.17 mmol) were stirred in acetonitrile (10 mL) for 2 days in a foil-covered flask. The solvent was removed under reduced pressure and the yellow solid extracted into dichloromethane (3×10 mL) and filtered. The yellow solution was reduced in volume (~5 mL) and subsequent addition of diethyl ether and storage at -20 °C gave pale yellow crystals of (2-AuCl₂C₆H₄)C(O)N=PPh₃ (0.065 g, 62%).

Found: C 42.7, H 2.9, N 1.9, C₂₅H₁₉NOPCl₂Au · CH₂Cl₂ requires C 42.6, H 2.9, N 1.9%.

NMR: ^1H δ 7.29 (d, 1H, H-6), 7.37 (m, 1H, H-4), 7.40 (m, 1H, H-5), 7.58 (m, 6H, H-10) 7.69 (m, 3H, H-11), 7.95 (m, 6H, H-9) 8.10 (d, 1H, H-3); $^{13}\text{C}\{^1\text{H}\}$ δ 124.0 (d, $^1J_{\text{PC}} = 103.3$ Hz, C-8), 128.5 (C-6), 129.2 (d, $^3J_{\text{PC}} = 13.6$ Hz, C-10), 130.1 (C-3), 130.3 (C-5 and C-2), 133.6 (C-4), 133.8 (d, $^4J_{\text{PC}} = 2.6$ Hz, C-11), 133.9 (d, $^2J_{\text{PC}} = 10.6$ Hz, C-9), 144.9 (C-1), 179.5 (d, $^2J_{\text{PC}} = 3.9$ Hz, C-7); $^{31}\text{P}\{^1\text{H}\}$ δ 35.8 ppm (see Scheme 2.30 for the NMR labelling scheme).

ESI-MS: m/z : 612.059 (100%, $[\text{M}-\text{Cl}]^+$, calc 612.055).

IR: $\nu(\text{P}=\text{N}) = 1285$ (vs), $\nu(\text{C}=\text{O}) = 1684$ (s) cm^{-1} .



Scheme 2.30 NMR labelling scheme for complexes **2.41** ($\text{ML}_x = \text{Mn}(\text{CO})_4$), **2.42** ($\text{ML}_x = \text{HgCl}$) and **2.43** ($\text{ML}_x = \text{AuCl}_2$).

Preparation of 2-Hg($\text{C}_6\text{H}_4\text{P}(\text{=NCOPh})\text{Ph}_2$)₂ **2.45**

To a degassed solution of $\text{N}_3\text{C}(\text{O})\text{Ph}$ (0.081 g, 0.55 mmol) in dry dichloromethane (10 mL) 2-Hg($\text{C}_6\text{H}_4\text{PPh}_2$)₂ **2.44** (0.200 g, 0.28 mmol) was added and the resulting was stirred at room temperature under nitrogen for 24 hours. The solution was reduced in volume and diethyl ether was added until signs of crystallisation. Storage at $-20\text{ }^\circ\text{C}$ gave white microcrystals of 2-Hg($\text{C}_6\text{H}_4\text{P}(\text{=NCOPh})\text{Ph}_2$)₂ (0.207 g, 77%).

Found: C 62.2, H 4.1, N 2.8; $\text{C}_{50}\text{H}_{38}\text{P}_2\text{N}_2\text{O}_2\text{Hg}$ requires C 62.5, H 4.0, N 2.9%.

NMR: ^1H δ 7.09 (m, 3H), 7.22 (m, 4H), 7.40 (m, 4H), 7.51 (m, 2H), 7.72 (m, 4H), 8.12 (d, 2H); $^{31}\text{P}\{^1\text{H}\}$ δ 27.4 ($^3J_{\text{HgP}} = 171$ Hz) ppm.

ESI-MS: m/z : 985.205 (100%, $[\text{M}+\text{Na}]^+$, calc 985.202), 963.224 (21%, $[\text{M}+\text{H}]^+$, calc 963.220).

IR: $\nu(\text{P}=\text{N}) = 1323$ (vs), $\nu(\text{C}=\text{O}) = 1598$ (s) cm^{-1} .

Preparation of (2-AuCl₂C₆H₄)Ph₂P=NCOPh **2.46**

2-Hg($\text{C}_6\text{H}_4\text{P}(\text{=NCOPh})\text{Ph}_2$)₂ **2.45** (0.100 g, 0.10 mmol), $[\text{Me}_4\text{N}][\text{AuCl}_4]$ (0.086 g, 0.21 mmol) and $[\text{Me}_4\text{N}][\text{AuCl}_4]$ (0.011g, 0.10 mmol) were stirred in acetonitrile (10 mL) for seven days in a foil-covered flask. Work-up as for **2.43** gave yellow microcrystals (0.091 g, 68%).

NMR: ^1H δ 7.18 (m, 1H), 7.41 (m, 3H), 7.51 (m, 2H), 7.60 (m, 4H), 7.72 (m, 2H), 7.88 (m, 4H), 8.01 (d, 2H), 8.26 (d, 1H); $^{31}\text{P}\{^1\text{H}\}$ δ 60.5 ppm.

ESI-MS: m/z : 612.052 (100%, $[\text{M}-\text{Cl}]^+$, calc 612.055), 1319 (36%, $[2\text{M}+\text{Na}]^+$, calc 1319.037), 670.013 (16%, $[\text{M}+\text{Na}]^+$, calc 670.020)

IR: $\nu(\text{P}=\text{N}) = 1282$ (vs), $\nu(\text{C}=\text{O}) = 1641$ (vs) cm^{-1} .

2.4.4 X-ray crystal structure determinations

Single crystals of X-ray quality were grown by vapour diffusion of either diethyl ether (**2.29c**, **2.39** and **2.46**) or pentane (**2.36f**) into a dichloromethane solution of the compound at room temperature. Crystals of **2.42** and **2.43** were grown by adding diethyl ether to a dichloromethane solution of the compound and storing at -20 °C. Compounds **2.29c** and **2.39** crystallised as yellow blocks, **2.36f** as orange plates, **2.42** as colourless plates and **2.43** (the dichloromethane solvate) as pale yellow blocks.

Data collection

Unit cell dimensions and intensity data (Table 2.7) were collected at either the University of Canterbury on a Bruker Nonius Apex II CCD diffractometer (**2.29c**, **2.36f**, **2.39** and **2.46**) or the University of Auckland on a Bruker Smart CCD diffractometer (**2.42** and **2.43**). Absorption correction of the data was carried out by semi-empirical methods (SADABS⁽⁴²⁾).

Solution and refinement

Structures were solved by either the Direct Methods (**2.39**) or Patterson (**2.29c**, **2.36f**, **2.42**, **2.43** and **2.46**) options of SHELXS-97.⁽⁴³⁾ In all cases the heavy atom (either the gold or mercury) was initially located followed by all other atoms from a series of difference maps. Full-matrix least-squares refinement (SHELXL-97⁽⁴⁴⁾) was based upon F_o^2 with all non-

Table 2.9 Crystallographic data for the complexes **2.29c**, **2.36f**, **2.39**, **2.42**, **2.43** and **2.46**.

Complex	2.29c	2.36f	2.39 .0.5Et ₂ O	2.42	2.43 .CH ₂ Cl ₂	2.46
Formula	C ₂₆ H ₂₃ NPCl ₂ Au	C ₂₉ H ₂₇ NO ₂ PSAu	C ₄₄ H ₃₉ NO _{0.5} F ₆ PClAu	C ₂₅ H ₁₉ NOPClHg	C ₂₆ H ₂₁ NOPCl ₄ Au	C ₂₅ H ₁₉ NOPCl ₂ Au
Molecular Weight	648.29	681.51	1029.09	616.42	733.17	648.25
<i>T</i> /K	93	93	93	89	89	93
Crystal system	Triclinic	Monoclinic	Monoclinic	Triclinic	Monoclinic	Tetragonal
Space group	<i>P</i> 1	<i>P</i> 2 ₁ / <i>n</i>	<i>C</i> 2/ <i>c</i>	<i>P</i> -1	<i>P</i> 2 ₁ / <i>n</i>	<i>I</i> -4
<i>a</i> (Å)	9.0297(4)	9.0966(2)	50.109(2)	8.7828(3)	10.4176(3)	21.4348(6)
<i>b</i> (Å)	9.2152(4)	17.4390(4)	9.8843(5)	10.6870(3)	17.6738(4)	21.4348(6)
<i>c</i> (Å)	9.3699(4)	15.6240(4)	18.3601(8)	12.5133(4)	15.0557(5)	9.7613(3)
<i>α</i> (°)	61.462(2)	90	90	105.335(1)	90	90
<i>β</i> (°)	63.334(2)	93.998(1)	111.043(2)	104.864(1)	110.231(2)	90
<i>γ</i> (°)	61.134(2)	90	90	90.765(2)	90	90
<i>V</i> (Å ³)	575.22(4)	2472.49(1)	8487.2(7)	1090.64(6)	2601.02(13)	4484.8(2)
<i>Z</i>	1	4	8	2	4	8
<i>D</i> _{calc} (g cm ⁻³)	1.871	1.831	1.611	1.877	1.872	1.920
<i>T</i> _{max,min}	0.5534, 0.0508	0.5267, 0.2164	0.530, 0.327	0.5301, 0.3545	0.6390, 0.5257	0.3396, 0.1159
Number of unique reflections	5778	10185	13986	5239	6087	8411
Number of observed reflections	5273	8940	11379	4927	4985	8021
[<i>I</i> > 2σ(<i>I</i>)]						
R[<i>I</i> > 2σ(<i>I</i>)]	0.0319	0.0198	0.0536	0.0171	0.0252	0.0193
wR ₂ (all data)	0.077	0.0454	0.1385	0.0422	0.0503	0.0401
Goodness of Fit	1.062	1.016	1.142	1.077	0.996	1.011
Flack <i>x</i> parameter	-0.005(7)	-	-	-	-	0.017(3)

hydrogen atoms refined anisotropically (with the exceptions of the cases mentioned below) and hydrogen atoms in calculated positions.

Complex **2.39** crystallised with the phosphorus of one PF_6^- falling on a crystallographic inversion centre. The other half of the anion was in a hole which contained either a PF_6^- or a diethyl ether molecule (50:50) occupancy). Both the PF_6^- and the diethyl ether showed considerable disorder and as a result were not refined anisotropically and the hydrogen atoms were excluded from the diethyl ether. Bond lengths in these species were constrained.

After the final refinement complex **2.29c** showed significant ripples around the gold. As a result the anisotropic displacement parameters for C(12) and C(13) were unrealistic and thus were refined isotropically.

2.5 References

1. A. W. Johnson; *Ylides and Imines of Phosphorus*, Wiley, New York, **1993**.
2. H. J. Bestmann and R. Zimmerman, *Phosphine Alkylenes and Other Phosphorus Ylides* In: *Organic Phosphorus Compounds*, Vol 3, Wiley Interscience, page 1, **1972**.
3. D. Aguilar, M. A. Aragüés, R. Bielsa, E. Serrano, R. Navarro and E. P. Urriolabeitia; *Organometallics*, **2007**, 26, 3541.
4. H. Alper; *J. Organomet. Chem.*, **1977**, 127, 385.
5. D. Comrie; *Undergraduate Laboratory Report*, **2000**, University of Waikato.
6. M. A. Leeson, B. K. Nicholson and M. R. Olsen; *J. Organomet. Chem.*, **1999**, 579, 243.
7. J. Vicente, J. A. Abad, R. Clemente, J. López-Serrano, M. C. Ramírez de Arellano, P. G. Jones and D. Bautista; *Organometallics*, **2003**, 22, 4248.
8. T. P. Braun, P. A. Gutsch and H. Zimmer; *Z. Naturforsch., B: Chem. Sci.*, **1999**, 54, 858.
9. C. G. Stuckwisch; *J. Org. Chem.*, **1976**, 41, 1173.
10. P. Wei, K. T. K. Chan and D. W. Stephan; *Dalton Trans.*, **2003**, 3804.
11. K. T. K. Chan, L. P. Spencer, J. D. Masuda, J. S. J. McCahill, P. Wei and D. W. Stephan; *Organometallics*, **2004**, 23, 381.
12. R. Bielsa, A. Larrea, R. Navarro, T. Soler and E. P. Urriolabeitia; *Eur. J. Inorg. Chem.*, **2005**, 1724.

13. D. Aguilar, M. A. Aragüés, R. Bielsa, E. Serrano, T. Soler, R. Navarro and E. P. Urriolabeitia; *J. Organomet. Chem.*, **2008**, 693, 417.
14. R. Bielsa, R. Navarro, T. Soler and E. P. Urriolabeitia; *Dalton Trans.*, **2008**, 1203.
15. R. Bielsa, R. Navarro, E. P. Urriolabeitia and A. Lledós; *Inorg. Chem.*, **2007**, 46, 10133.
16. D. Aguilar, R. Bielsa, M. A. Contel, A. Lledós, R. Navarro, T. Soler and E. P. Urriolabeitia; *Organometallics*, **2008**, 27, 2929.
17. R. Bielsa, R. Navarro, T. Soler and E. P. Urriolabeitia; *Dalton Trans.*, **2008**, 1787.
18. S. D. J. Brown, W. Henderson, K. J. Kilpin and B. K. Nicholson; *Inorg. Chim. Acta*, **2007**, 360, 1310.
19. D. Aguilar, M. Contel, R. Navarro and E. P. Urriolabeitia; *Organometallics*, **2007**, 26, 4604.
20. K.-W. Lee and L. A. Singer; *J. Org. Chem.*, **1974**, 39, 3780.
21. L. Boubekeur, L. Ricard, N. Mézailles, M. Demange, A. Auffrant and P. Le Floch; *Organometallics*, **2006**, 25, 3091.
22. P. E. Garrou; *Chem. Rev.*, **1981**, 81, 229.
23. W. Henderson and C. Evans; *Inorg. Chim. Acta*, **1999**, 294, 183.
24. C. H. A. Goss, W. Henderson, A. L. Wilkins and C. Evans; *J. Organomet. Chem.*, **2003**, 679, 194.
25. W. Henderson, B. K. Nicholson, S. J. Faville, D. Fan and J. D. Ranford; *J. Organomet. Chem.*, **2001**, 631, 41.
26. D. Fan, C.-T. Yang, J. D. Ranford, J. J. Vittal and P. F. Lee; *Dalton Trans.*, **2003**, 3376.
27. M. B. Dinger and W. Henderson; *J. Organomet. Chem.*, **1998**, 560, 233.
28. W. Henderson, L. J. McCaffrey and B. K. Nicholson; *J. Chem. Soc., Dalton Trans.*, **2000**, 2753.
29. W. Henderson; *Adv. Organomet. Chem.*, **2006**, 54, 207.
30. Y. Fuchita, H. Ieda, A. Kayama, J. Kinoshita-Nagaoka, H. Kawano, S. Kameda and M. Mikuriya; *J. Chem. Soc., Dalton Trans.*, **1998**, 4095.
31. Y. Fuchita, H. Ieda, Y. Tsunemune, J. Kinoshita-Nagaoka and H. Kawano; *J. Chem. Soc., Dalton Trans.*, **1998**, 791.
32. Y. Fuchita, H. Ieda, S. Wada, S. Kameda and M. Mikuriya; *J. Chem. Soc., Dalton Trans.*, **1999**, 4431.
33. Y. Fuchita, H. Ieda and M. Yasutake; *J. Chem. Soc., Dalton Trans.*, **2000**, 271.
34. R. V. Parish, B. P. Howe, J. P. Wright, J. Mack, R. G. Pritchard, R. G. Buckley, A. M. Elsome and S. P. Fricker; *Inorg. Chem.*, **1996**, 35, 1659.
35. P. A. Bonnardel, R. V. Parish and R. G. Pritchard; *J. Chem. Soc., Dalton Trans.*, **1996**, 3185.
36. R. Linklater; *Undergraduate Laboratory Report*, **2008**, University of Waikato.

37. P. Frøyen; *Phosphorus, Sulfur and Silicon*, **1993**, 78, 161.
38. J. M. Cooney, L. H. P. Gommans, L. Main and B. K. Nicholson; *J. Organomet. Chem.*, **1987**, 336, 293.
39. N. P. Robinson, L. Main and B. K. Nicholson; *J. Organomet. Chem.*, **1988**, 349, 209.
40. M. A. Bennett, M. Contel, D. C. R. Hockless, L. L. Welling and A. C. Willis; *Inorg. Chem.*, **2002**, 41, 844.
41. I. Bar and J. Bernstein; *Acta Cryst. Sect. B*, **1980**, 36, 1962.
42. R. H. Blessing; *Acta Cryst. Sect. A*, **1995**, 51, 33.
43. G. M. Sheldrick, SHELXS-97 - A Program for the Solution of Crystal Structures, University of Göttingen, Germany, **1997**.
44. G. M. Sheldrick, SHELXL-97 - A Program for the Refinement of Crystal Structures, University of Göttingen, Germany, **1997**.

CHAPTER THREE

The Cycloauration of Phosphine Chalcogenides

3.1 Introduction

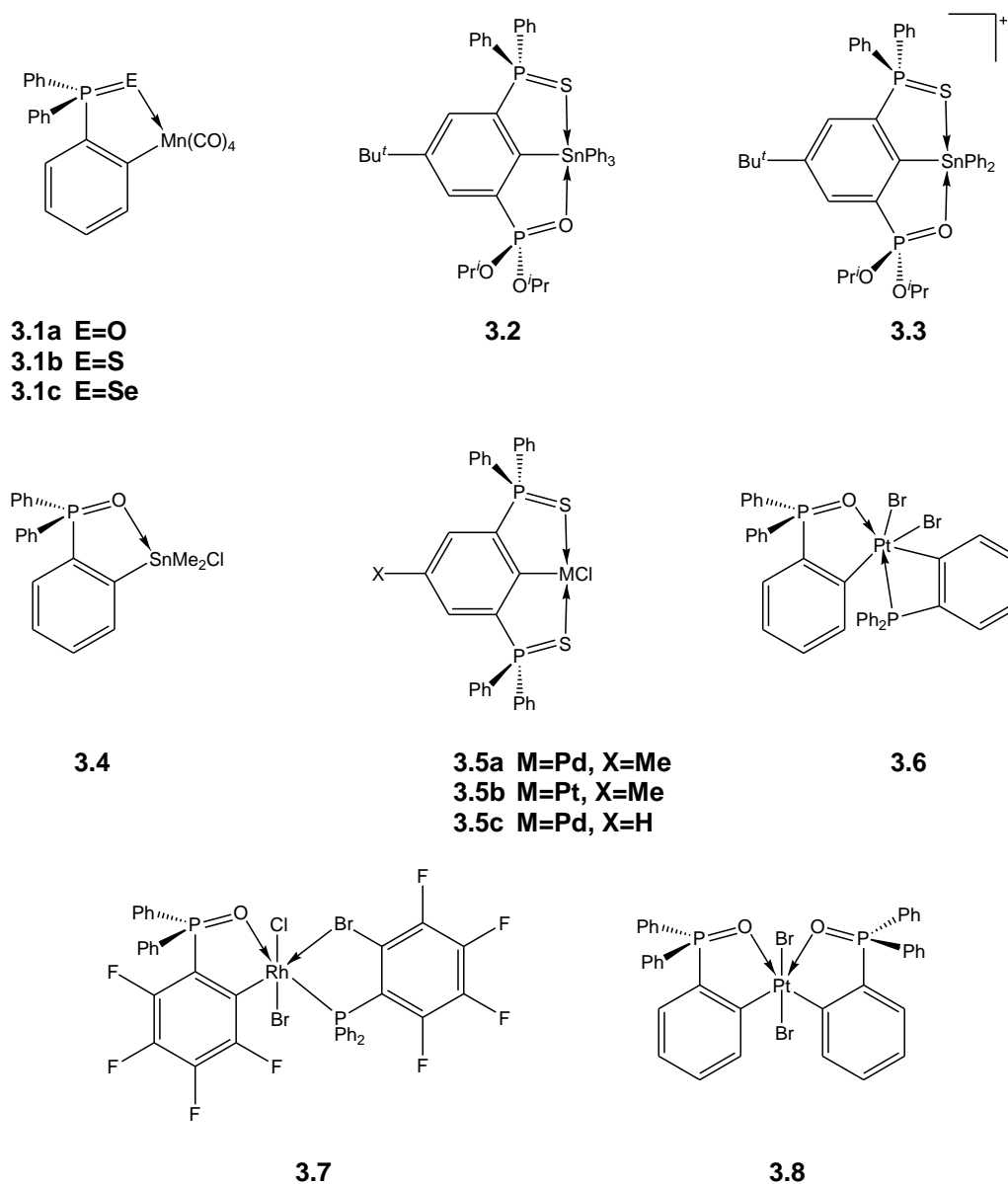
3.1.1 Metal complexes of phosphine chalcogenides

Metal coordination compounds of tertiary phosphine chalcogenides are well known and a number of reviews are dedicated to complexes with either the oxygen, sulfur or selenium atom of the ligand acting as a neutral donor to the metal centre (*i.e.* binding to the metal in an η^1 fashion).^(1, 2) Both $\text{Ph}_3\text{P}=\text{O}$ ⁽³⁻⁵⁾ (a hard donor ligand) and $\text{Ph}_3\text{P}=\text{S}$ ⁽³⁻⁶⁾ (a soft donor ligand) form complexes with Au(III) (a soft metal centre) *via* the electron rich chalcogen atom. To the best of our knowledge, there are no examples of cycloaurated phosphine chalcogenides.

Examples of orthometallated phosphine chalcogenide ligands in general are rare in the literature. The series of *ortho*-manganated complexes of $\text{Ph}_3\text{P}=\text{O}$, $\text{Ph}_3\text{P}=\text{S}$ and $\text{Ph}_3\text{P}=\text{Se}$ have been studied (**3.1a-c**, Scheme 3.1) with the sulfide and selenide complexes structurally characterised. Yields of the sulfide complex **3.1c** were excellent (90%) but both the selenide **3.1c** (22%) and the oxide **3.1a** (41% as an oil) were only obtained in moderate yields because of either the instability of the P=Se bond or the unfavourable bond angle that is formed at the oxygen in the cyclometallated complex. In addition, the metallacyclic ring in the sulfide complex was shown to be relatively stable as the displacement of two carbonyl ligands by $\text{P}(\text{OMe})_3$ was favoured over cleavage of the metallacyclic ring (the S-Mn bond).⁽⁷⁾

The tin complex **3.2** could be synthesised in poor yields by reaction of the free ligand with Ph_3SnCl *via* an *ortho*-lithiated intermediate. The resulting complex had weak O-Sn and S-Sn interactions both in the solid state and in solution. However, the cationic complex **3.3**, formed by the reaction of **3.2** with $\text{CPh}_3^+\text{PF}_6^-$ had much stronger O-Sn and S-Sn interactions.⁽⁸⁾ In

addition *ortho*-stannated $\text{Ph}_3\text{P}=\text{O}$ **3.4**, which has been structurally characterised, has been synthesised indirectly.⁽⁹⁾



Scheme 3.1 Cyclometallated triphenylphosphine chalcogenide ligands that have been reported in the literature.

With the exception of the Pt(II) and Pd(II) compounds (**3.5a,b**, Scheme 3.1) containing tridentate *S, C, S'* pincer ligands⁽¹⁰⁾ (of which **3.5c** was shown to be an efficient catalyst in the allylation of aldehydes with allyltributyltin⁽¹¹⁾), a selection of indirectly synthesised Pt(IV)⁽¹²⁾

(**3.6** and **3.8**, Scheme 3.1) and Rh⁽¹³⁾ (**3.7**, Scheme 3.1) compounds containing Ph₃P=O moieties, and *ortho*-mercurated Ph₃P=O and Ph₃P=S^(14, 15) cyclometallated complexes containing the heavier transition metal elements have thus far been largely neglected.

3.1.2 Scope of this work

Because of the interesting and successful results we had seen with the cycloauration of iminophosphorane ligands (Chapter Two) we wished to investigate cycloauration of the isoelectronic phosphine chalcogenide (Group 16) ligands. The resulting *ortho*-metallated compounds were expected to be interesting as in addition to a carbon-gold sigma bond they would also contain a chalcogenide-gold coordinate bond – an unusual combination of a highly oxidising metal centre and a potentially reducing ligand.

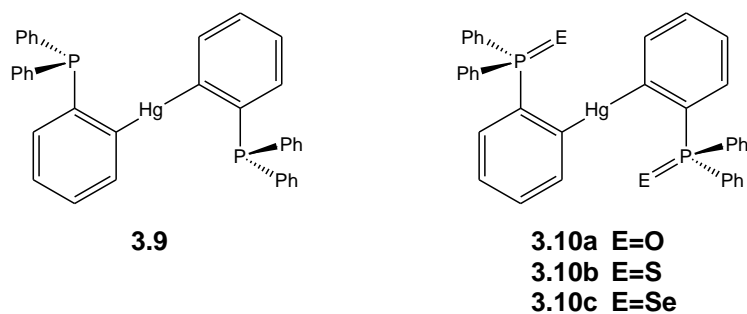
The following chapter reports on the synthesis of a new *ortho*-mercurated phosphine chalcogenide and the first examples of cycloaurated Ph₃P=S and Ph₃P=Se. *Ortho*-mercuration and cycloauration of the related amino-phosphine sulfide ligand PhP(S)(NEt₂)₂ is also reported. All complexes have been fully characterised.

3.2 Results and Discussion

3.2.1 Synthesis and properties of *ortho*-mercurated phosphine chalcogenide complexes

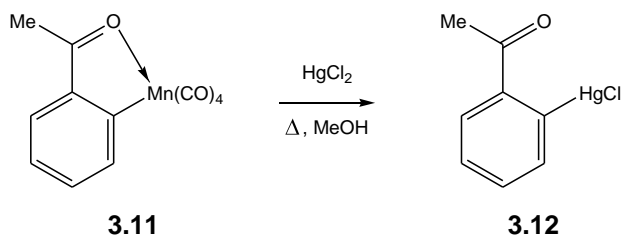
Cycloaurated complexes are typically synthesized either by direct C-H bond activation of the ligand by a gold reagent (*e.g.* H[AuCl₄]) or by transmetallation from the corresponding *ortho*-mercurated compound (see Chapter One).⁽¹⁶⁾ With the phosphine chalcogenide ligands utilised in this study direct cyclometallation with gold was not possible [because of reduction of the gold(III)] so the transmetallation route from the *ortho*-mercurated complexes needed to be employed (and hence prior synthesis of these compounds was required).

Bennett *et al.* have shown that the *ortho*-mercurated bisphosphine complex **3.9** reacts with either hydrogen peroxide or sulfur to yield the bisphosphine-dioxide **3.10a** or -disulfide **3.10b** complexes respectively.^(14, 15) We have extended this series of compounds to the diselenide analogue **3.10c** by reaction of the bis-phosphine **3.9** with (grey) selenium powder under ultrasonic conditions (Scheme 3.2). The synthesis of phosphine chalcogenides using ultrasonic techniques has been investigated previously in this laboratory and shows many benefits over traditional preparative methods.⁽¹⁷⁾ For example, reactions times are typically shorter and the high temperatures that are often needed can be avoided. Like **3.10a** and **3.10b**, the selenide derivative **3.10c** is a white solid that is stable in air. The $^{31}\text{P}\{^1\text{H}\}$ NMR spectrum of **3.10c** gives a singlet at 41.4 ppm with the expected coupling to both the ^{199}Hg (284 Hz) and the ^{77}Se (684 Hz) nuclei observed. Mass spectrometry confirmed that both phosphine groups had been converted to the corresponding selenide, however ions due to mixed oxide/selenide species were also present. As only one compound was observed in the $^{31}\text{P}\{^1\text{H}\}$ NMR spectrum it is possible that loss of selenium and subsequent oxidation is occurring inside the spectrometer. Alternatively, if very small traces of the mixed oxide/selenide species were present in the sample then they would ionise more efficiently than **3.10c**. The addition of AgNO_3 solution to **3.10c** prior to ESI-MS analysis resulted in silver adducts in the spectrum (*e.g.* $[\mathbf{3.10}+\text{Ag}]^+$), however the mixed oxide/selenide species was still present. The use of silver salts to aid in the analysis of phosphine and phosphine chalcogenide compounds is well documented.⁽¹⁸⁾



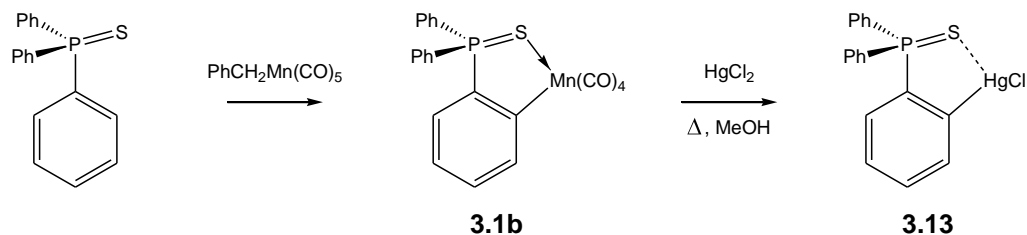
Scheme 3.2 Bennett's diarylmercury complex **3.9** with two pendant phosphine groups and the oxide **3.10a**, sulfide **3.10b** and selenide **3.10c** derivatives that can subsequently be synthesised.

Synthesis of *ortho*-mercurated complexes is commonly achieved by either direct mercuriation of the substrate or transmetallation reactions from *ortho*-lithiated or Grignard intermediates, with the choice of method often limited by the functional groups present on the ligand.⁽¹⁹⁾ This laboratory has previously been interested in *ortho*-manganated complexes and the subsequent reactions of these compounds.⁽²⁰⁾ In 1987, Cooney *et al.* demonstrated that reaction of *ortho*-manganated acetophenone **3.11** with HgCl₂ yielded the *ortho*-mercurated derivative **3.12** (Scheme 3.3) – a compound that can not be formed by the classical methods of mercuriation.⁽²¹⁾ The use of lithium or Grignard reagents is excluded due to the ketone functionality and direct mercuriation occurs at the methyl carbon (as a result of keto-enol tautomerisation).



Scheme 3.3 Cooney's synthesis of *ortho*-mercurated acetophenone **3.12** from *ortho*-manganated acetophenone **3.11**.

As mentioned previously, *ortho*-manganated Ph₃P=S **3.1b** (Scheme 3.1) can be synthesised in high yields (*ca.* 90%) by the reaction of Ph₃P=S with PhCH₂Mn(CO)₅⁽⁷⁾ so we decided to investigate whether transmetallation from **3.1b** would produce the *ortho*-mercurated complex **3.13**, an analogous reaction to that shown in Scheme 3.3. In addition, it was shown in Chapter Two (Section 2.2.7) that a manganese reagent can be used to transfer an iminophosphorane ligand onto a mercury centre. Indeed, the desired compound is formed cleanly and in high yields upon refluxing **3.1b** with a slight excess of HgCl₂ in methanol (Scheme 3.4). The ³¹P{¹H} NMR spectrum of **3.13** (in CDCl₃) has a single peak at 48.2 ppm, which is close to the literature value of the bis-phosphine sulfide **3.10b** (47.7 ppm, acquired in CD₂Cl₂).⁽¹⁵⁾



Scheme 3.4 Synthesis of *ortho*-mercured triphenylphosphine sulfide **3.13** from triphenylphosphine sulfide, *via* *ortho*-manganated triphenylphosphine sulfide **3.1b**.

Although mass spectrometry indicated the diaryl-mercury complex **3.10b** had also been formed (by an ion at m/z 789.093 corresponding to $[\mathbf{3.10b}+\text{H}]^+$, 100%), an X-ray crystal structure unambiguously showed that the complex has the formulation consistent with **3.13**. The molecular structure and the atom labelling scheme are shown in Figure 3.1 and selected bond lengths and angles in Table 3.1. Full tables of structural parameters along with atomic coordinates and anisotropic displacement parameters can be found on the supplementary CD.

The mercury atom is bonded to the *ortho* carbon of one of the phenyl rings showing that transmetallation from the manganese compound has occurred. In other structurally characterised complexes where tertiary phosphine sulfides are coordinated to Hg(II) the S-Hg bond lengths range from 2.500 Å to 2.761 Å, and the P-S-Hg angles are in the range of 99.31-110.99°. ^(22, 23) The P-S-Hg angle in **3.13** is 86.58° which is extremely acute as most P-S-M angles in coordinated phosphine sulfides fall within the range of 96-120° (see Table 3.3). The P(1)-S(1) bond length in **3.13** [1.9745(11) Å] is longer than in Ph₃P=S (1.950 Å), ⁽²⁴⁾ and the coordination around the mercury atom slightly deviates from linear geometry [C(12)-Hg(1)-Cl(1) angle of 173.34(9)°]. These observations indicate that the interaction between the mercury and sulfur [the Hg(1)-S(1) distance is 2.9585(8) Å] is substantial enough to hold the compound in a pseudo-cyclic structure.

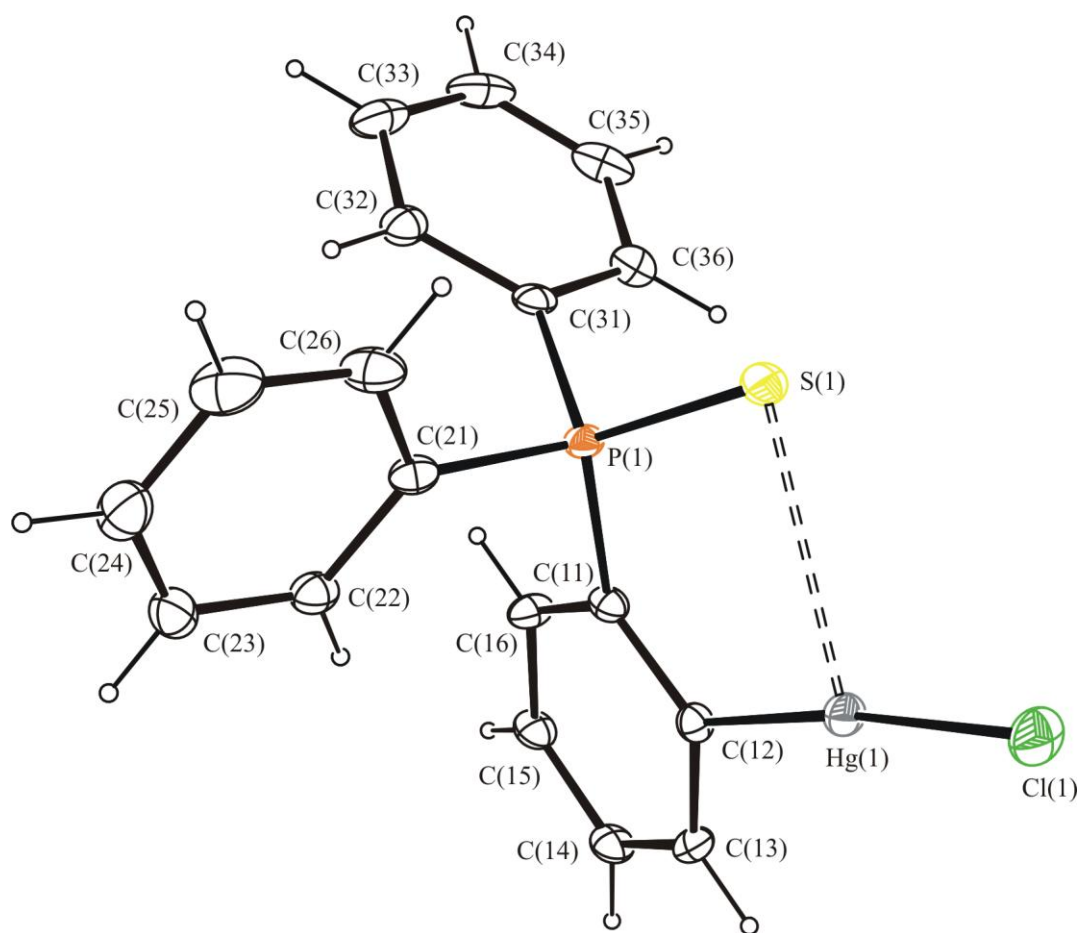
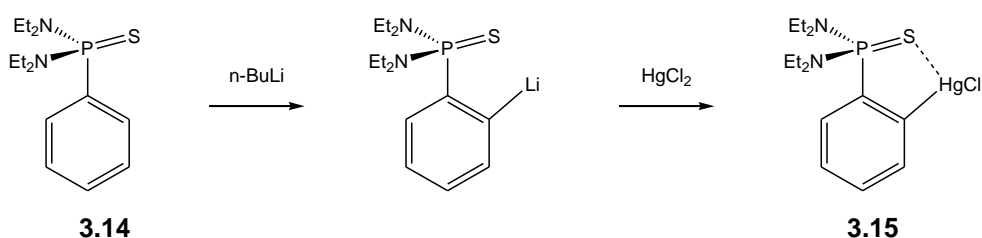


Figure 3.1 Structure of the complex $(2\text{-HgClC}_6\text{H}_4)\text{P}(\text{S})\text{Ph}_2$ **3.13** showing the atom numbering scheme. Thermal ellipsoids are shown at the 50% probability level.

Table 3.1 Selected structural parameters for the complex $(2\text{-HgClC}_6\text{H}_4)\text{P}(\text{S})\text{Ph}_2$ **3.13**.

Atoms	Lengths (Å)	Atoms	Angles (°)
P(1) – S(1)	1.9745(11)	S(1) – P(1) – C(11)	114.51(11)
P(1) – C(11)	1.824(3)	P(1) – C(11) – C(12)	121.3(2)
C(11) – C(12)	1.400(4)	C(11) – C(12) – Hg(1)	121.7(2)
C(12) – Hg(1)	2.068(3)	C(12) – Hg(1) – Cl(1)	173.34(9)
Hg(1) – Cl(1)	2.3273(8)	C(11) – P(1) – C(31)	106.25(14)
S(1)---Hg(1)	2.9585(8)	C(21) – P(1) – C(11)	105.86(14)

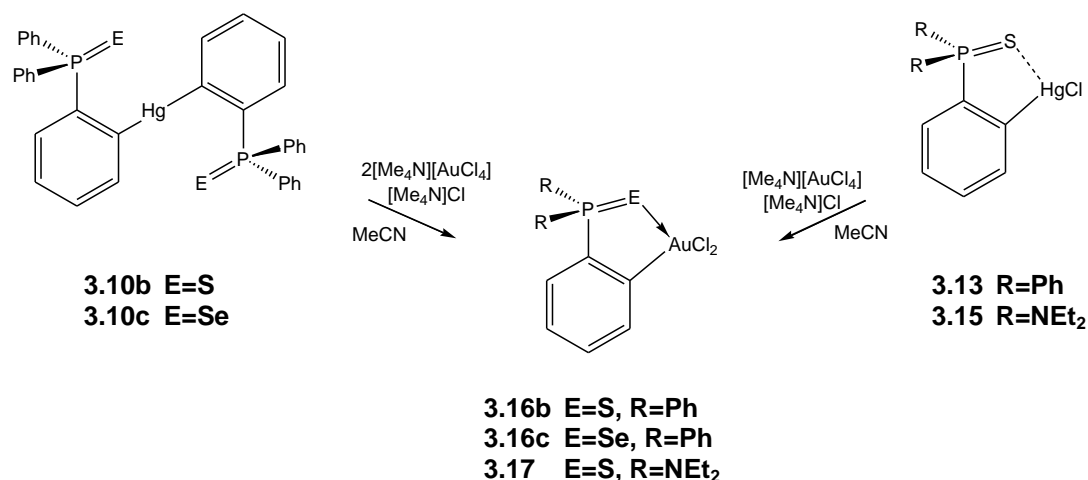
In order to continue our investigations into ligands which contain soft donor ligands we decided to investigate the cyclometallation of $\text{PhP(S)(NEt}_2)_2$ **3.14**, which is capable of forming a five-membered metallacyclic ring *via* coordination of either the nitrogen or the softer sulfur atom. Craig *et al.*⁽²⁵⁾ have previously shown that the ligand $\text{PhP(S)(NMe}_2)_2$ undergoes *ortho*-lithiation on the phenyl ring. The ethyl analogue **3.14** behaves in an identical manner and the resulting *ortho*-lithiated compound can be further reacted with HgCl_2 to give the *ortho*-mercurated compound **3.15** in good yields (Scheme 3.5). Like **3.13**, there is a peak in the mass spectrum (m/z 769.266) corresponding to the diaryl mercury complex ($[\text{2-Hg}(\text{C}_6\text{H}_4\text{P(S)(NEt}_2)_2)_2+\text{H}]^+$). However, the $^{31}\text{P}\{^1\text{H}\}$ NMR spectrum shows a ^{31}P - ^{199}Hg coupling of 414 Hz, very similar to the coupling seen in **3.13**. Microelemental analysis supports the structure being the mercury chloride species **3.15**.



Scheme 3.5 Scheme for the synthesis of **3.15**, *via* the *ortho*-lithiated intermediate.

3.2.2 Synthesis of cycloaurated gold(III) phosphine chalcogenides

The reaction of both the *ortho*-mercurated sulfide complexes **3.10b** and **3.13**, and the selenide complex **3.10c**, with $[\text{Me}_4\text{N}][\text{AuCl}_4]$ and $[\text{Me}_4\text{N}]\text{Cl}$ in acetonitrile gave the cycloaurated complexes **3.16b** and **3.16c** in moderate yields (Scheme 3.6). When the donor atom was selenium, the transmetallation reaction proceeded in three hours compared to the 24 hours required with the sulfur donor. Both **3.16b** and **3.16c** are yellow micro-crystalline compounds; however **3.16c** appears to be moisture sensitive and when isolated in the solid form it decomposes over time (even in darkness) to give a black powder. Complex **3.15** also readily transmetallates in an analogous manner; when reacted with $[\text{Me}_4\text{N}][\text{AuCl}_4]$ the cycloaurated complex **3.17** was isolated as a fluffy pale yellow solid. All of the transmetallation reactions gave adequate to good yields of cycloaurated product.



Scheme 3.6 Scheme for the synthesis of cycloaurated phosphine chalcogenides **3.16b**, **3.16c** and **3.17**.

Attempts at synthesising cycloaurated Ph₃P=O *via* transmetalation from **3.10a** were unsuccessful. The same synthetic methodology as for **3.10b** and **3.10c** gave a variety of unidentified compounds that were observed by ³¹P{¹H} NMR spectroscopy of the reaction mixture. Longer reaction times and changing the solvent from acetonitrile to DMSO resulted in complete loss of **3.10a** and evidence of the cycloaurated product in ESI mass spectrometry. Unfortunately, despite numerous attempts, the cycloaurated species could not be isolated. In the early studies on transmetalation reactions, Parish proposed that the initial step involves coordination of the neutral donor to the gold atom to form a bimetallic species (see Scheme 1.8, Chapter One).⁽²⁶⁾ Considering the hard oxygen of Ph₃P=O is a poor donor to Au(III) it is not surprising that the reaction is sluggish as the initial coordination step would not occur easily. In the earlier work on *ortho*-manganated triphenylphosphine chalcogenides Depree *et al.* suggested that incorporation of Ph₃P=O into a five-membered ring results in an unfavourable bond angle at the oxygen (the P-O-M angle).⁽⁷⁾ This may also be a factor in the inability to isolate cycloaurated Ph₃P=O.

3.2.3 X-ray crystal structures of 2-AuCl₂(C₆H₄)P(S)Ph₂ **3.16b**, 2-AuCl₂(C₆H₄)P(Se)Ph₂ **3.16c** and 2-AuCl₂(C₆H₄)P(S)(NEt₂)₂ **3.17**

X-ray crystal structure analyses on both **3.16b** and **3.16c** were carried out, and the compounds are iso-structural and isomorphous. The molecular structures and atom numbering schemes are shown in Figures 3.2 and 3.3 respectively, with important bond parameters presented in Table 3.2. Full tables of structural parameters along with atomic coordinates and anisotropic displacement parameters can be found on the supplementary CD.

In each case, a new five-membered metallacyclic ring has formed with the gold bonded in the *ortho* position of one of the phenyl rings and either a sulfur or a selenium atom as the neutral donor. Two chloride ligands complete the coordination sphere around the metal. As expected, the geometry around the gold atom is essentially square planar. The greatest deviations from the gold coordination planes are 0.0681(14) Å (C12) for **3.16b** and 0.0643(8) Å (C12) for **3.16c**. Because of the greater *trans* influence of the carbon-bonded phenyl ring, the Au(1)-Cl(1) bonds [2.3635(11) and 2.3628(6) Å] are longer than the Au(1)-Cl(2) bonds [2.3094(12) and 2.3222(6) Å for **3.16b** and **3.16c** respectively]. In addition, the Au-Cl bond *trans* to the selenium atom [2.3222(6) Å] is longer than the Au-Cl bond *trans* to the sulfur atom [2.3094(12) Å] owing to the greater *trans* influence of the P=Se group.

Coordination to the metal has lengthened the P=E bond [(from 1.950(3) Å in Ph₃P=S⁽²⁴⁾ to 2.0324(16) Å in **3.16b** and from 2.112(1) Å in Ph₃P=Se⁽²⁷⁾ to 2.1839(6) in **3.16c**]. The Au-S bond is 2.3073(11) Å and this is comparable with other Au(III)-S bond lengths where the sulfur originates from a tertiary phosphine sulfide group.^(28, 29) Likewise, the Au-Se bond in **3.16c** is comparable with similar complexes⁽³⁰⁾ and in conjunction with the P-Se bond length suggests a strong gold-selenium interaction. The bite angle of the ligand is close to 90° for both **3.16b** and **3.16c**. The metallacyclic rings of both the sulfide **3.16b** and the selenide **3.16c** complex are significantly puckered, which contrasts to the *ortho*-manganated analogues **3.1b** and **3.1c**, where the metallacyclic rings are planar. The greatest deviations from the mean metallacyclic plane are P(1) [0.3002(14) Å above the plane] and S(1) [0.3016(11) Å below the plane]. Likewise, for the selenide complex, P(1) and Se(1) show the greatest deviations from the mean plane [+0.3114(8) and -0.2976(6) Å respectively].

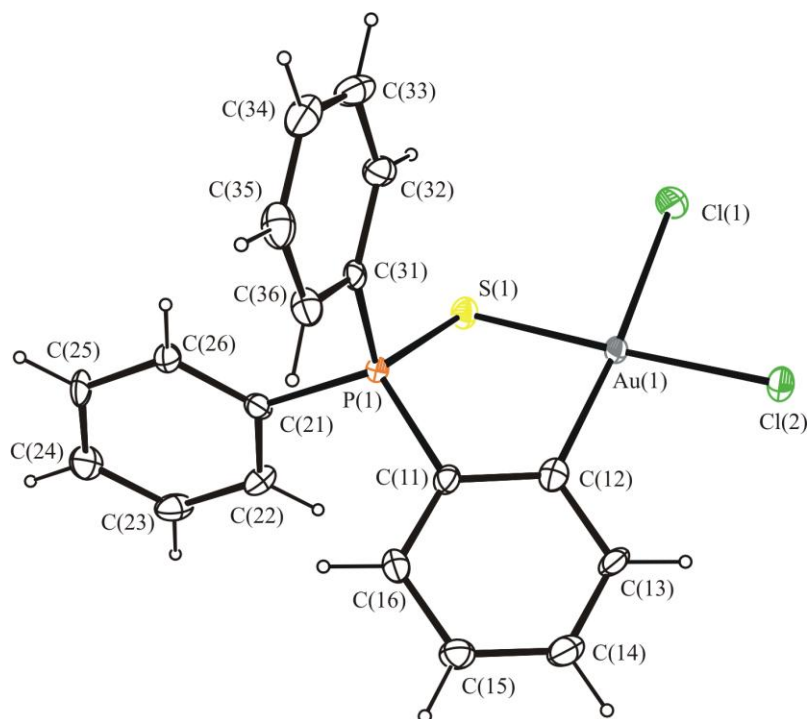


Figure 3.2 Molecular diagram of $(2\text{-AuCl}_2\text{C}_6\text{H}_4)\text{P}(\text{S})\text{Ph}_2$ **3.16b** showing the atom labelling scheme. Thermal ellipsoids are shown at the 50% probability level.

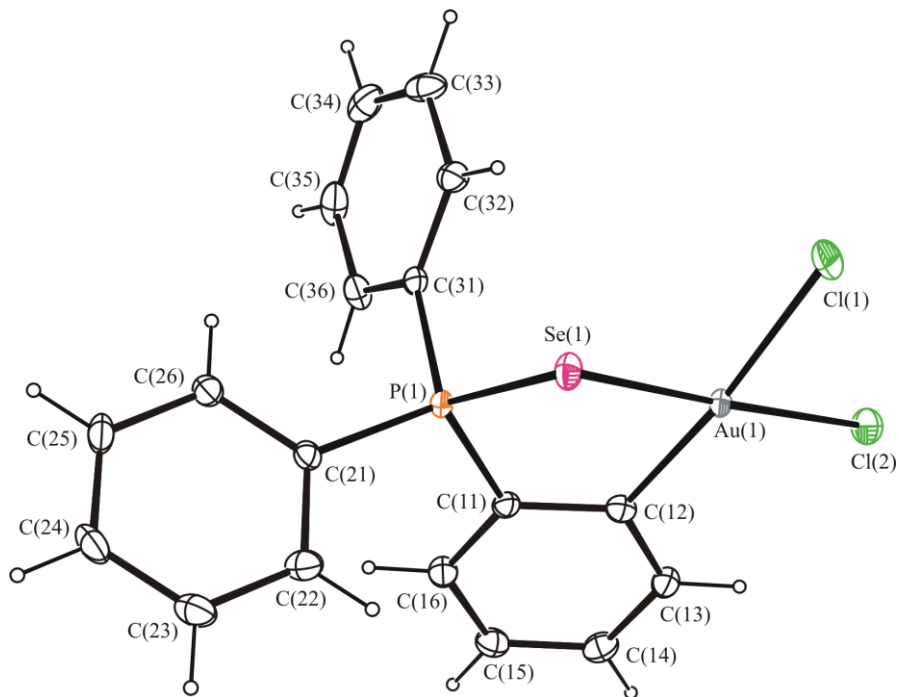


Figure 3.3 Molecular diagram of $(2\text{-AuCl}_2\text{C}_6\text{H}_4)\text{P}(\text{Se})\text{Ph}_2$ **3.16c** indicating the atom numbering scheme, with thermal ellipsoids at the 50% probability level.

Table 3.2 Selected structural parameters for the complexes **3.16b** and **3.16c**.

	3.16b (E=S)	3.16c (E=Se)
<i>Bond lengths (Å)</i>		
Au(1) – Cl(1)	2.3635(11)	2.3628(6)
Au(1) – Cl(2)	2.3094(12)	2.3222(6)
C(12) – Au(1)	2.045(5)	2.049(2)
E(1) – Au(1)	2.3073(11)	2.4091(3)
P(1) – E(1)	2.0324(16)	2.1839(6)
P(1) – C(11)	1.794(4)	1.783(2)
C(11) – C(12)	1.401(6)	1.406(3)
<i>Bond angles (°)</i>		
Cl(1) – Au(1) – Cl(2)	90.64(4)	90.52(2)
Cl(1) – Au(1) – E(1)	86.25(4)	84.876(18)
E(1) – Au(1) – C(12)	90.02(13)	91.16(7)
C(12) – Au(1) – Cl(2)	93.23(13)	93.60(7)
Au(1) – E(1) – P(1)	95.24(5)	91.759(18)
E(1) – P(1) – C(11)	104.57(15)	104.17(8)
C(11) – C(12) – Au(1)	120.2(3)	120.99(18)

Table 3.3 gives the results of a search of the Cambridge Crystallographic Database for structures of triphenylphosphine chalcogenide ligands where the chalcogenide atom acts as an η^1 donor.⁽³¹⁾ In these complexes the chalcogenide atom is not constrained so the preferred geometry around the chalcogenide atom can be ascertained. Inspection of Table 3.3 shows that as a result of cycloauration the angles at the chalcogenide atoms (P-E-Au) in the gold complexes are extremely acute – they fall well below the mean P-E-M angles. This further supports the suggestion that the analogous $\text{Ph}_3\text{P}=\text{O}$ complex could not be formed because of an unfavourable angle at the oxygen when $\text{Ph}_3\text{P}=\text{O}$ is constrained in a ring system.

Table 3.3 Results of a search of the Cambridge Crystallographic Database for η^1 coordinated $\text{Ph}_3\text{P}=\text{E}$ ligands.

	$\text{Ph}_3\text{P}=\text{O}$	$\text{Ph}_3\text{P}=\text{S}$	$\text{Ph}_3\text{P}=\text{Se}$
Sample number	317	21	10
Independent XPPH_3 moieties	543	23	11
Mean P-E-M angle ($^\circ$)	158.36	108.13	105.00
Std deviation in P-E-M angle ($^\circ$)	10.85	5.13	4.08
Range P-E-M angle ($^\circ$)	124-180	95-116	100-111
P-E-Au angle ($^\circ$)		95.24 (3.16b)	91.759 (3.16c)

In order to confirm that in **3.17** the neutral coordinating donor atom is the soft sulfur, an X-ray crystallographic study was carried out. The compound crystallised in the space group $Pna2_1$, with two unique molecules in the asymmetric unit. One of these molecules is depicted in Figure 3.4, clearly showing that the neutral donor is the sulfur and not the nitrogen. The atom labelling scheme is also shown in Figure 3.4, with important bond parameters of both molecules in Table 3.4.

In both cases the coordination around the gold atom is essentially square planar, with the largest deviations from the coordination plane of the metal 0.0183(17) Å (C2, molecule A) and 0.0181(11) Å (Au1, molecule B). Like **3.16b** and **3.16c** the bite angle of the ligand is approximately 90°. The P-S-Au angles are 94.58(6)° (molecule 1) and 95.30(6)° (molecule 2) which are again severely acute and leads to the metallacyclic ring being extremely puckered.

In both molecules it is the sulfur and phosphorus atoms that show the greatest deviation from the metallacyclic ring. The Au-S bond lengths are 2.3108(14) Å (molecule A) and 2.3064(13) Å (molecule B), which are comparable to the Au-S bond length in **3.16b** (2.3073(11) Å). As expected, the Au-Cl bonds *trans* to the carbon [2.3700(13), 2.3715(12) Å] are longer than those *trans* to the sulfur [2.3178(13), 2.3205(13) Å].

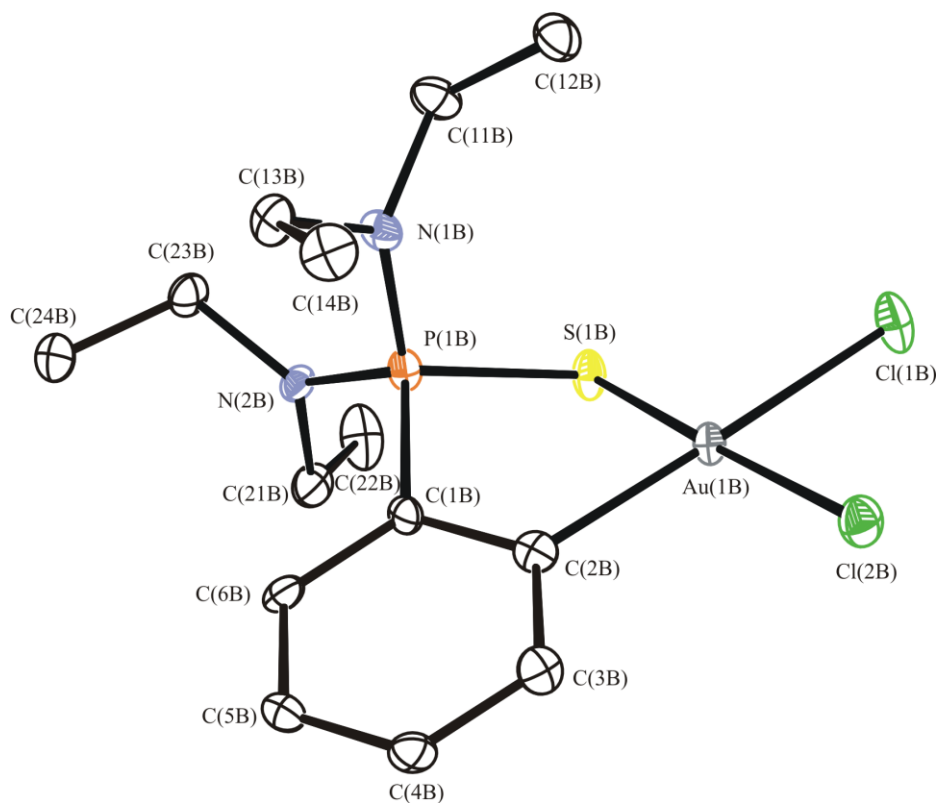


Figure 3.4 Molecular structure of $(2\text{-AuCl}_2\text{C}_6\text{H}_4)\text{P}(\text{S})(\text{NEt}_2)_2$ **3.17** showing one of the unique molecules in the asymmetric unit. Hydrogen atoms have been excluded for clarity and thermal ellipsoids are shown at the 50% probability level.

Interestingly, substituting two phenyl groups (**3.16b**) for amine groups (**3.17**) results in an increase in Au-Cl bond lengths. The Au-Cl bond *trans* to the sulfur in **3.16b** is 2.3094(12) Å – this increases to 2.3178(13) and 2.3205(13) Å in **3.17** indicating that the amine substituted ligand has a greater *trans* influence than the phenyl substituted ligand.

Table 3.4 Selected structural parameters for the complex (2-AuCl₂C₆H₄)P(S)(NEt₂)₂ **3.17**.

	Molecule A	Molecule B
<i>Bond lengths (Å)</i>		
Au(1) – Cl(1)	2.3700(13)	2.3715(12)
Au(1) – Cl(2)	2.3178(13)	2.3205(13)
Au(1) – S(1)	2.3108(14)	2.3064(13)
Au(1) – C(2)	2.059(5)	2.051(5)
P(1) – S(1)	2.0403(19)	2.0451(18)
P(1) – C(1)	1.781(5)	1.776(5)
C(1) – C(2)	1.398(7)	1.414(7)
P(1) – N(1)	1.628(5)	1.638(5)
P(1) – N(2)	1.623(4)	1.619(4)
<i>Bond angles (°)</i>		
Cl(1) – Au(1) – Cl(2)	91.49(5)	90.28(5)
Cl(2) – Au(1) – C(2)	93.21(15)	92.90(15)
Cl(1) – Au(1) – S(1)	85.88(5)	86.43(5)
C(2) – Au(1) – S(1)	89.42(14)	90.37(15)
Au(1) – S(1) – P(1)	94.58(6)	95.30(6)
S(1) – P(1) – C(1)	102.91(17)	102.68(17)
P(1) – C(1) – C(2)	116.2(4)	117.1(4)
C(1) – C(2) – Au(1)	119.3(4)	118.6(4)

3.2.4 Spectroscopic and mass spectrometric characterisation of cycloaurated triphenylphosphine chalcogenides

The presence of phosphorus in these compounds introduces a powerful (³¹P) NMR spectroscopic probe which aids in both characterisation of the final products and in monitoring the extent of (*e.g.* transmetallation) reactions. In the iso-electronic iminophosphorane complexes we have seen a small change in chemical shift of the compounds upon *ortho*-mercuration of the ligand followed by a larger predictable downfield shift of approximately 40 ppm after transmetallation to the gold,^(32, 33) attributed to the phosphorus entering a cyclic

environment.⁽³⁴⁾ The trend is not as obvious in this series, with only small unpredictable changes between the ligand, *ortho*-mercurated and cycloaurated complexes hence other effects must also be contributing to the ³¹P chemical shift. Table 3.5 presents the ³¹P{¹H} NMR data for the complexes studied.

As discussed by Glidewell *et al.*,⁽³⁵⁾ the coordination of phosphine selenides to metal centres results in significant deshielding of the selenium nucleus and a decrease in the ¹J_{Se-P} coupling constant – this is observed in the series of Ph₃P=Se complexes. There is only a small change (47 Hz) upon mercuration which indicates little interaction between the selenium and the mercury atom. Transmetallation to gold sees a decrease in the value of ¹J_{P-Se} by 259 Hz which indicates a strong selenium – gold interaction. In addition, the value of ¹J_{P-Se} is related to P-Se bond lengths in the solid state – the longer the P-Se bond the smaller ¹J_{P-Se} is. This is in accordance with X-ray crystallographic data – the P-Se bond length in Ph₃P=Se is 2.112(1) Å and ¹J_{P-Se} is 731 Hz and in the cycloaurated complex the P-Se bond length is 2.1839(6) Å with ¹J_{P-Se} = 425 Hz.

Table 3.5 ³¹P{¹H} NMR chemical shifts (ppm) of the metallated phosphine chalcogenide ligands used in this study (300 MHz, CDCl₃).

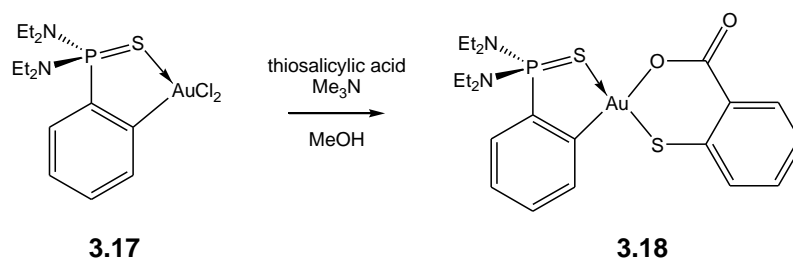
Ligand	<i>Ortho</i> -mercurated complex	Cycloaurated complex
Ph ₃ P=S	44.0	48.2 (³ J _{P-Hg} = 385 Hz)
Ph ₃ P=Se	36.0 (¹ J _{P-Se} = 731 Hz)	56.4
		38.8 (¹ J _{P-Se} = 425 Hz)
		(³ J _{P-Hg} = 284 Hz)
PhP(S)(NEt ₂) ₂	78.4	83.1 (³ J _{P-Hg} = 414 Hz)
		79.4

The P=E vibrations in Ph₃P=S and Ph₃P=Se occur at 638 cm⁻¹ and 561 cm⁻¹ respectively. Upon coordination to the metal this value decreases to 603 cm⁻¹ for **3.13** and further still to 597 cm⁻¹ for **3.16b**. In the case of the selenide derivatives, the mercury compound **3.10c** shows no change in the P=Se vibration upon metallation, however coordination to the gold (**3.16c**) gives a shift to 545 cm⁻¹. This further supports the inference from the NMR data that there is little interaction between the selenium and mercury. Likewise, the ligand

PhP(S)(NEt₂)₂ **3.14** has a P=S vibration at 604 cm⁻¹ which moves to lower wavenumbers for the mercury complex **3.15** (597 cm⁻¹) and the cycloaurated species **3.17** (586 cm⁻¹). These decreases mirror those seen by King and McQuillan, and are attributed to a weakening of the P-E π bonds upon coordination to the metal.⁽³⁶⁾

3.2.5 Reaction of (2-AuCl₂C₆H₄)P(S)(NEt₂)₂, **3.17**, with thiosalicylic acid

Because gold(III) thiosalicylate derivatives often show a greater biological activity than the parent dichloride complex,⁽³⁷⁻⁴⁰⁾ compound **3.17** was reacted with a molar equivalent of thiosalicylic acid and excess Me₃N in methanol to give the thiosalicylate complex **3.18** in good yields (Scheme 3.7). Previously with gold(III) and other transition metal complexes the dianionic thiosalicylate ligand is coordinated so that the two soft sigma donor ligands are mutually *cis* to each other due to the *anti*-sympiotic effect.^(41, 42) Therefore, it is assumed that **3.18** is the isomer where the carbon and the thiosalicylate sulfur are *cis* to each other as opposed to the thermodynamically less favoured isomer with the carbon and oxygen in *cis* arrangement.



Scheme 3.7 Scheme for the synthesis of the thiosalicylate derivative of the cycloaurated phosphine sulfide (2-AuCl₂C₆H₄)P(S)(NEt₂)₂ **3.18**.

3.2.6 Biological activity

Since the discovery of the anticancer activity of *cisplatin*, Au(III) complexes, which are both isoelectronic and isosteric with Pt(II) have routinely been screened for biological activity with some showing promising results.⁽⁴³⁻⁴⁵⁾ For this reason, compounds **3.16b** and **3.17** were screened for anti-tumour activity against the P388 murine leukemia cell line, using the methods described in Appendix 1. Compound **3.16b** shows poor activity with an IC₅₀ >12500

ng/mL, however the activity of **3.17** is more promising with an IC_{50} value of 3474 ng/mL. Replacement of the *cis* chloride ligands of **3.17** with the chelating dianionic thiosalicylate ligand (**3.18**) results in an increase in biological activity ($IC_{50} = 1522$ ng/mL).

3.3 Conclusions

Three new *ortho*-metallated gold(III) complexes containing phosphine chalcogenide ligands have been synthesised and fully characterised – these are rare examples of cycloaurated complexes which contain a neutral donor ligand other than nitrogen. The complexes with the neutral sulfur donors show a similar stability to the cycloaurated *C,N'* complexes, which is interesting as they contain a oxidising gold(III) centre and a reducing phosphine chalcogenide ligand. Reactivity is also similar to the *C,N'* auracycles - the *cis* chloride ligands can be replaced by the chelating dianionic thiosalicylate ligand to give a bi-metallacyclic complex which shows better biological activity than the parent complex against the P388 murine leukemia cell line.

3.4 Experimental

3.4.1 General

The compounds **3.9**, **3.10a**, **3.10b** and **3.1b** were prepared by literature procedures.^(15, 46) $HgCl_2$, $PhP(NEt_2)_2$ (Aldrich) and *n*-butyllithium (2.0 M in cyclohexane, Aldrich) were used as received. $[Me_4N][AuCl_4]$ was prepared by the addition of $[Me_4N]Cl$ to $H[AuCl_4]$, as described in Appendix 1, where the general characterisation conditions can also be located.

3.4.2 Syntheses

Preparation of 2- $Hg(C_6H_4P(Se)Ph_2)_2$ **3.10c**

2- $Hg(C_6H_4PPh_2)_2$ **3.9** (0.300 g, 0.42 mmol) and grey selenium powder (0.066 g, 0.84 mmol) were added to dry degassed toluene (50 mL) and placed in an ultrasonic bath at 50 °C until the

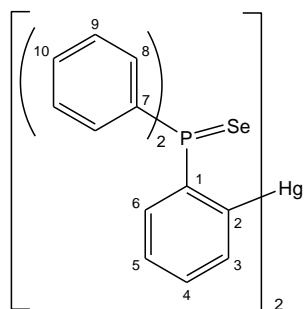
majority of the Se had disappeared (~16 hours). The toluene was removed under vacuum and the white solid extracted into dichloromethane (3×10 mL). Petroleum spirits (30 mL) was added to the filtrate and storage at -20 °C gave $2\text{-Hg}(\text{C}_6\text{H}_4\text{P}(\text{Se})\text{Ph}_2)_2$ **3.10c** as a white solid (0.225 g, 61%).

Found: C 49.1, H 3.3, N <0.2, $\text{C}_{36}\text{H}_{28}\text{P}_2\text{Se}_2\text{Hg}$ requires C 49.1, H 3.2, N 0.0%.

NMR: ^1H : δ 7.05 (m, 4H, H-5 and H-6), 7.40 (m, 2H, H-4), 7.42 (m, 8H, H-9), 7.47 (m, 4H, H-10), 7.68 (m, 8H, H-8), 7.78 (m, 2H, H-3); $^{13}\text{C}\{^1\text{H}\}$: δ 125.6 (d, $^3J_{\text{PC}} = 12.6$ Hz, C-5), 128.6 (d, $^3J_{\text{PC}} = 12.6$ Hz, C-9), 130.3 (d, $^4J_{\text{PC}} = 3.6$ Hz, C-4), 131.6 (d, $^4J_{\text{PC}} = 2.4$ Hz, C-10), 132.3 (d, $^2J_{\text{PC}} = 15.8$ Hz, C-6), 132.4 (d, $^1J_{\text{PC}} = 75.2$ Hz, C-7), 133.2 (d, $^2J_{\text{PC}} = 9.7$ Hz, C-8), 140.2 (d, $^1J_{\text{PC}} = 84.9$ Hz, C-1), 140.8 (d, $^3J_{\text{PC}} = 19.4$ Hz, C-3), 175.4 (d, $^2J_{\text{PC}} = 25.1$ Hz, C-2); $^{31}\text{P}\{^1\text{H}\}$: δ 41.4 ($^3J_{\text{HgP}} = 284$ Hz, $^1J_{\text{SeP}} = 684$ Hz) ppm. See Scheme 3.8 for the NMR numbering system.

ESI-MS: m/z : 904.964 (100%, $[\text{M}+\text{Na}]^+$, calc 904.960), 841.040 (44%, $[\text{M}-\text{Se}+\text{O}+\text{Na}]^+$, calc 841.038), 819.064 (20%, $[\text{M}-\text{Se}+\text{O}+\text{H}]$, calc 819.056), 882.981 (15%, $[\text{M}+\text{H}]^+$, calc 882.978); AgNO_3 added: 988.880 (100%, $[\text{M}+\text{Ag}]^+$, calc 988.876), 926.957 (25%, $[\text{M}-\text{Se}+\text{O}+\text{Ag}]^+$, calc 926.954).

IR: $\nu(\text{P}=\text{Se})$ 562 (m) cm^{-1} .



Scheme 3.8 NMR numbering scheme for $2\text{-Hg}(\text{C}_6\text{H}_4\text{P}(\text{Se})\text{Ph}_2)_2$ **3.10c**.

Preparation of (2-HgClC₆H₄)P(S)Ph₂ **3.13**

(2-Mn(CO)₄C₆H₄)P(S)Ph₂ **3.1b** (0.406 g, 0.88 mmol) and HgCl₂ (0.477 g, 1.77 mmol) were refluxed in methanol (15 mL) for 3 hours. The white solid that formed was removed by filtration and the filtrate reduced in volume to give a white solid. This was subsequently redissolved in minimal dichloromethane and passed through a column of Celite. Removal of the dichloromethane gave (2-HgClC₆H₄)P(S)Ph₂ **3.13** as a white solid (0.339 g, 73%).

Found: C 40.8, H 2.7, N 0.0; C₁₈H₁₄PSClHg requires C 40.8, H 2.7, N 0.0%.

NMR: ¹H: δ 7.30 (m, 1H, H-5), 7.39 (m, 1H, H-6), 7.47 (m, 4H, H-9), 7.55 (m, 3H, H-4 and H-10), 7.63 (m, 4H, H-8), 7.70 (m, 1H, H-3); ³¹C{¹H}: δ 127.5 (d, ³J_{PC} = 11.8 Hz, C-5), 129.0 (d, ³J_{PC} = 12.7 Hz, C-9), 131.6 (d, ⁴J_{PC} = 3.5 Hz, C-4), 132.1 (d, ¹J_{PC} = 86.3 Hz, C-7), 132.3 (d, ⁴J_{PC} = 3 Hz, C-10), 132.6 (d, ²J_{PC} = 10.6 Hz, C-8), 133.5 (d, ²J_{PC} = 13.8 Hz, C-6), 136.8 (d, ¹J_{PC} = 89.0 Hz, C-1), 138.9 (d, ³J_{PC} = 17.1 Hz, C-3), 155.8 (d, ²J_{PC} = 19.8 Hz, C-2); ³¹P{¹H}: δ 48.2 (³J_{HgP} = 385 Hz) ppm (see Scheme 3.9 for the NMR numbering system).

ESI-MS: *m/z*: 789.093 (100%, [2-Hg(C₆H₄P(S)Ph₂)₂+H]⁺, calc 789.089), 1023.016 (20%, [2M-Cl]⁺, calc 1023.018), 552.980 (9%, [M+Na]⁺, calc 552.983).

IR: ν(P=S) 603 (m) cm⁻¹.

Preparation of (2-AuCl₂C₆H₄)P(S)Ph₂ **3.16b**

2-Hg[(C₆H₄)P(S)Ph₂]₂ **3.10b** (0.100 g, 0.13 mmol), [Me₄N][AuCl₄] (0.105 g, 0.26 mmol) and [Me₄N]Cl (0.014 g, 0.13 mmol) were stirred overnight in degassed acetonitrile (15 mL) in a foil-covered flask. The acetonitrile was removed under vacuum and the residue extracted into dichloromethane (2 × 10 mL) and filtered. Slow addition of diethyl ether to the filtrate produced yellow crystals of (2-AuCl₂C₆H₄)P(S)Ph₂ **3.16b** (0.060 g, 42%).

Found: C 38.4, H 2.6, N 0.0; C₁₈H₁₄PSCl₂Au requires C 38.5, H 2.5, N 0.0%.

NMR: ^1H : δ 6.97 (m, 1H, H-6), 7.30 (m, 1H, H-5), 7.45 (m, 1H, H-4), 7.64 (m, 4H, H-9), 7.72 (m, 2H, H-10), 7.76 (m, 4H, H-8) 8.46 (m, 1H, H-3); $^{13}\text{C}\{^1\text{H}\}$: δ 125.0 (d, $^1J_{\text{PC}} = 83.4$ Hz, C-7), 127.9 (d, $^3J_{\text{PC}} = 12.6$ Hz, C-5), 130.2 (d, $^3J_{\text{PC}} = 13.7$, C-9), 131.9 (d, $^2J_{\text{PC}} = 14.3$ Hz, C-6), 133.2 (d, $^2J_{\text{PC}} = 11.5$ Hz, C-8), 134.9 (d, $^4J_{\text{PC}} = 3.3$ Hz, C-4), 135.0 (d, $^4J_{\text{PC}} = 2.7$ Hz, C-10), 137.2 (d, $^3J_{\text{PC}} = 14.8$ Hz, C-3), 140.5 (d, $^1J_{\text{PC}} = 100.0$ Hz, C-1), 152.0 (d, $^2J_{\text{PC}} = 16.1$ Hz, C-2); $^{31}\text{P}\{^1\text{H}\}$: δ 56.4 ppm (see Scheme 3.9 for the NMR numbering system).

ESI-MS: m/z : 578.999 (100%, $[\text{M}-\text{Cl}+\text{OMe}+\text{Na}]^+$, calc 578.998), 1081.002 (15%, $[\text{2M}-2\text{Cl}+\text{OMe}]^+$, calc 1080.999), 1135.010 (14%, $[\text{2M}-2\text{Cl}+2\text{OMe}+\text{Na}]^+$, calc 1135.008)

IR: $\nu(\text{P}=\text{S})$ 597 (m) cm^{-1} .

Alternative synthesis:

(2-HgClC₆H₄)P(S)Ph₂ **3.13** (0.250 g, 0.47 mmol), [Me₄N][AuCl₄] (0.195 g, 0.47 mmol) and [Me₄N]Cl (0.052 g, 0.47 mmol) were stirred in degassed acetonitrile (20 mL) for 24 hours in a foil-covered flask. The acetonitrile was removed under vacuum and the residue extracted into dichloromethane (2 × 10 mL) and filtered. Slow addition of diethyl ether to the filtrate produced yellow crystals of (2-AuCl₂C₆H₄)P(S)Ph₂ **3.16b** (0.121 g, 46%). The product was identified by NMR and ESI mass spectrometry.

Preparation of (2-AuCl₂C₆H₄)P(Se)Ph₂ 3.16c

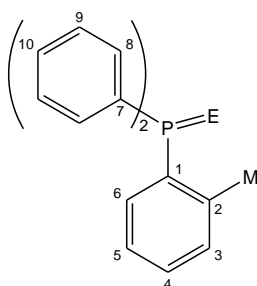
2-Hg[(C₆H₄)P(Se)Ph₂]₂ **3.10c** (0.100 g, 0.11 mmol), [Me₄N][AuCl₄] (0.094 g, 0.22 mmol) and [Me₄N]Cl (0.012 g, 0.11 mmol) were stirred in degassed acetonitrile (10 mL) for 3 hours in a foil covered flask. The solvent was removed under reduced pressure and the resulting yellow solid extracted into dichloromethane (2 × 10 mL) and filtered. The resulting filtrate was treated with diethyl ether (20 mL) and storage at -20 °C gave yellow crystals of (2-AuCl₂C₆H₄)P(Se)Ph₂ **3.16c** (0.082 g, 61%).

NMR: ^1H : δ 6.87 (m, 1H, H-6), 7.29 (m, 1H, H-5), 7.45 (m, 1H, H-4), 7.64 (m, 4H, H-9), 7.71 (m, 2H, H-10), 7.75 (m, 4H, H-8), 8.51 (m, 1H, H-3); $^{13}\text{C}\{^1\text{H}\}$: δ 124.5 (d, $^1J_{\text{PC}} = 75.4$

Hz, C-7), 127.5 (d, $^3J_{PC} = 13.0$ Hz, C-5), 130.2 (d, $^3J_{PC} = 13.4$ Hz, C-9), 132.6 (d, $^2J_{PC} = 13.9$ Hz, C-6), 133.5 (d, $^2J_{PC} = 11.9$ Hz, C-8), 134.8 (d, $^4J_{PC} = 3.0$ Hz, C-4), 134.9 (d, $^4J_{PC} = 3.0$ Hz, C-10), 138.5 (d, $^3J_{PC} = 14.8$ Hz, C-3), 140.9 (d, $^1J_{PC} = 96.0$ Hz, C-1), 150.2 (d, $^2J_{PC} = 19.4$ Hz, C-2); $^{31}\text{P}\{^1\text{H}\}$ δ 38.8 ($^1J_{\text{SeP}} = 425$ Hz) ppm (see Scheme 3.9 for the NMR labelling system).

ESI-MS: m/z : 630.890 (100%, $[\text{M}+\text{Na}]^+$, calc 630.893), 1238.793 (28%, $[2\text{M}+\text{Na}]^+$, calc 1238.797), 1180.838 (9%, $[2\text{M}-\text{Cl}]^+$, calc 1180.838).

IR: $\nu(\text{P}=\text{Se})$ 562 (m) cm^{-1} .



Scheme 3.9 NMR numbering scheme for **3.13** (M = Hg, E = S), **3.16b** (M = Au, E = S) and **3.16c** (M = Au, E = Se).

Preparation of $\text{PhP}(\text{S})(\text{NEt}_2)_2$ **3.14**

$\text{PhP}(\text{NEt}_2)_2$ (2 mL, 7.9 mmol) and sulfur (0.275 g, 8.6 mmol) were stirred under a nitrogen environment overnight in dry degassed hexanes (50 mL). The solvent was removed under reduced pressure to give a pale yellow oil that failed to crystallise (1.40 g, 62%).

Found: C 59.3, H 9.1, N 9.9; $\text{C}_{14}\text{H}_{25}\text{N}_2\text{PS}$ requires C 59.1, H 8.9, N 9.9%

NMR: ^1H : δ 1.04 (t, 12H, H-8), 3.13 (m, 8H, H-7), 7.42 (m, 3H, H-3, H-4 and H-5), 7.93 (m, 2H, H-2 and H-6); $^{13}\text{C}\{^1\text{H}\}$: δ 13.5 (d, $^3J_{PC} = 4$ Hz, C-8), 39.4 (d, $^2J_{PC} = 4$ Hz, C-7), 128.2 (d, $^3J_{PC} = 14$ Hz, C-3 and C-5), 130.9 (d, $^4J_{PC} = 3$ Hz, C-4), 131.7 (d, $^2J_{PC} = 10$ Hz, C-2 and C-6), 135.7 (d, $^1J_{PC} = 123$ Hz, C-1); $^{31}\text{P}\{^1\text{H}\}$: δ 78.4 ppm (see Scheme 3.10 for the NMR numbering system).

ESI-MS: m/z : 307.138 (100%, $[M+Na]^+$, calc 307.137), 591.287 (5%, $[2M+Na]^+$, calc 591.284).

IR: $\nu(P=S) = 604 \text{ cm}^{-1}$.

Preparation of (2-HgClC₆H₄)P(S)(NEt₂)₂ **3.15**

PhP(S)(NEt₂)₂ **3.14** (0.500 g, 1.76 mmol) was dissolved in dry, degassed diethyl ether (20 mL). *n*-Butyllithium (0.9 mL, 1.76 mmol) was added dropwise to give a yellow solution that was stirred for 22 hours. HgCl₂ (0.478 g, 1.76 mmol) in THF (5 mL) was added dropwise and the resulting grey solution stirred for a further 4 hours. The grey solid that had formed was filtered off and the solvent removed under reduced pressure. The residue was redissolved in dichloromethane (20 mL) and refiltered. The solvent was reduced in volume (to ~ 5 mL) and hexanes were added until the solution went cloudy. Storage at -20 °C gave white crystals of (2-HgClC₆H₄)P(S)(NEt₂)₂ **3.15** (0.503 g, 55%).

Found: C 32.6, H 4.6, N 5.3; C₁₄H₂₄N₂PSClHg requires C 32.4, H 4.7, N 5.4%.

NMR: ¹H: δ 1.05 (t, 12H, H-8), 3.12 (m, 8H, H-7), 7.32 (m, 1H, H-5), 7.47 (m, 1H, H-4), 7.57 (m, 1H, H-3), 7.84 (m, 1H, H-6); ¹³C{¹H}: δ 13.6 (d, ³J_{PC} = 3.1 Hz, C-8), 39.9 (d, ²J_{PC} = 3.6 Hz, C-7), 127.1 (d, ³J_{PC} = 11.4 Hz, C-5), 130.8 (d, ²J_{PC} = 9.3 Hz, C-6), 131.0 (d, ⁴J_{PC} = 3.4 Hz, C-4), 138.7 (d, ³J_{PC} = 20.5 Hz, C-3), 139.7 (d, ¹J_{PC} = 132.1 Hz, C-1), 156.9 (d, ²J_{PC} = 22.8 Hz, C-2); ³¹P{¹H}: δ 83.1 (³J_{HgP} = 414 Hz) ppm (see Scheme 3.10 for the NMR labelling system).

ESI-MS: m/z : 1003.188 (100%, $[2M-Cl]^+$, calc 1003.186), 769.266 (55%, $[2\text{-Hg}(\text{C}_6\text{H}_4\text{P}(\text{S})(\text{NEt}_2)_2)_2\text{H}]^+$, calc 769.258), 543.071 (24%, $[M+Na]^+$, calc 543.068).

IR: $\nu(P=S) = 597 \text{ (s)} \text{ cm}^{-1}$.

Preparation of (2-AuCl₂C₆H₄)P(S)(NEt₂)₂ **3.17**

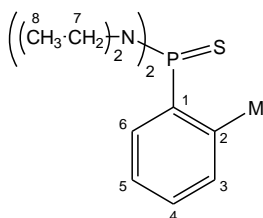
(2-HgCl₂C₆H₄)P(S)(NEt₂)₂ **3.15** (0.150 g, 0.29 mmol), [Me₄N][AuCl₄] (0.119 g, 0.29 mmol) and [Me₄N]Cl (0.032 g, 0.29 mmol) were stirred overnight in a foil-covered flask of degassed acetonitrile (15 mL), under a nitrogen atmosphere. The acetonitrile was removed under reduced pressure and the residue extracted into dichloromethane (2 × 10 mL). Hexanes (20 mL) were added and the solution stored at -20 °C to give fluffy yellow crystals of (2-AuCl₂C₆H₄)P(S)(NEt₂)₂ **3.17** (0.106 g, 66%).

Found: C 30.0, H 4.5, N 4.9; C₁₄H₂₄N₂PSCl₂Au requires 30.5, H 4.4, N 5.1%.

NMR: ¹H: δ 1.20 (t, 12H, H-8), 3.25 (m, 8H, H-7), 7.11 (m, 1H, H-6), 7.30 (m, 1H, H-5), 7.40 (m, 1H, H-4), 8.39 (m, 1H, H-3); ¹³C{¹H}: δ 13.9 (³J_{PC} = 2.5 Hz, C-8), 40.7 (²J_{PC} = 4.7 Hz, C-7), 127.4 (³J_{PC} = 13.1 Hz, C-5), 129.9 (²J_{PC} = 11.5 Hz, C-6), 134.7 (⁴J_{PC} = 2.9 Hz, C-4), 135.8 (¹J_{PC} = 139.0 Hz, C-1), 136.2 (³J_{PC} = 17.3 Hz, C-3), 144.0 (²J_{PC} = 24.6 Hz, C-2); ³¹P{¹H}: δ 79.4 ppm (see Scheme 3.10 for the NMR numbering system).

ESI-MS: *m/z*: 1067.114 (100%, [2M-Cl]⁺, calc 1067.116), 573.033 (95%, [M+Na]⁺, calc 573.033), 1061.166 (73%, [2M-2Cl+OMe]⁺, 1061.168), 1125.072 (58%, [2M+Na]⁺, calc 1125.075), 515.074 (38%, [M-Cl]⁺, calc 515.075).

IR: ν(P=S) = 586 (m) cm⁻¹.



Scheme 3.10 NMR numbering scheme for **3.14** (M=H), **3.15** (M=Hg) and **3.17** (M=Au).

Reaction of (2-AuCl₂C₆H₄)P(S)(NEt₂)₂ **3.17** with thiosalicylic acid

(2-AuCl₂C₆H₄)P(S)(NEt₂)₂ **3.17** (0.051 g, 0.09 mmol) and thiosalicylic acid (0.014 g, 0.09 mmol) were stirred in methanol (10 mL). To the dark orange solution Me₃N (1 mL, excess) was added resulting in the solution becoming immediately lighter. The solution was stirred

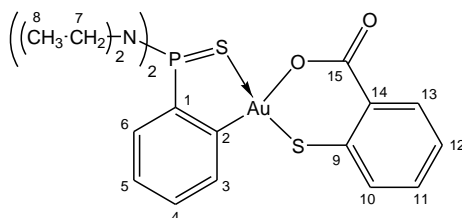
for 90 minutes in a foil covered flask before water (50 mL) was added to produce a fine precipitate. Stirring was continued for a further 12 hours, the solution was filtered and the yellow solid washed well with water (2×10 mL) and diethyl ether (1×10 mL). Drying under vacuum gave 0.043 g (76%) of the thiosalicylate derivative **3.18**.

Found: C 39.9, H 4.5, N 4.5, $C_{21}H_{28}N_2O_2PS_2Au$ requires C 39.9, H 4.5, N 4.4%.

NMR: 1H : δ 1.14 (t, 12H, H-8), 3.25 (m, 8H, H-7), 7.12 (m, 1H, H-6), 7.18 (m, 2H, H-11 and H-12), 7.27 (m, 1H, H-5), 7.39 (m, 2H, H-4 and H-10), 7.93 (m, 1H, H-3), 8.16 (m, 1H, H-13); $^{13}C\{^1H\}$: δ 13.7 ($^3J_{PC} = 2.8$ Hz, C-8), 40.4 ($^2J_{PC} = 4.5$ Hz, C-7), 125.4 (C-12), 127.0 ($^3J_{PC} = 13.0$ Hz, C-5), 129.9 (C-10 and C-11), 130.4 ($^2J_{PC} = 10.8$ Hz, C-6), 133.2 (C-13), 134.0 ($^4J_{PC} = 3.3$ Hz, C-4), 134.1 (C-14), 134.2 ($^3J_{PC} = 16.1$ Hz, C-3), 134.7 ($^2J_{PC} = 21.5$ Hz, C-2), 136.8 (C-9), 141.6 ($^1J_{PC} = 138.0$ Hz, C-1), 168.6 (C-15); $^{31}P\{^1H\}$: δ 75.0 ppm (see Scheme 3.11 for the NMR labelling system).

ESI-MS: m/z : 633.109 (100%, $[M+H]^+$, calc 633.107), 655.092 (64%, $[M+Na]^+$, calc 655.089), 763.254 (27%, $[2-Au(C_6H_4P(S)(NEt_2)_2)_2]^+$, calc 763.247), 1287.192 (21%, $[2M+Na]^+$, calc 1287.188), 1265.210 (6%, $[2M+H]^+$, calc 1265.206).

IR: $\nu(P=S) = 587$ (m); $\nu(C=O) = 1624$ (vs) cm^{-1} .



Scheme 3.11 NMR numbering scheme for **3.18**.

3.4.3 X-ray crystal structure determinations of 3.13, 3.16b, 3.16c and 3.17

In all cases single crystals suitable for X-ray diffraction were grown by vapour diffusion of diethyl ether into a dichloromethane solution of the compound at room temperature.

Data collection

Unit cell and intensity data were collected at the University of Auckland on a Bruker Smart CCD Diffractometer, operating at 89 K; crystallographic details are presented in Table 3.6. Absorption corrections were applied by semi-empirical methods (SADABS⁽⁴⁷⁾). The crystallographic information files for the structures can be located on the supplementary CD.

Solution and refinement

The structures **3.13** and **3.17** were solved by the direct methods option of SHELXL-97, **3.16b** and **3.16c** by the Patterson methods option.⁽⁴⁸⁾ In all cases the heavy metal was initially located and all other non-hydrogen atoms by a series of difference maps.⁽⁴⁹⁾ Hydrogen atoms were placed in calculated positions. In addition, **3.17** was refined as a racemic twin with occupancy 0.76/0.24.

An initial inspection of **3.17** indicated that the two independent molecules were related by an inversion point. A closer examination showed that the heavy atoms (Au, P, N, S and Cl) appeared to be related by symmetry whereas the lighter atoms were not. In order to confirm that the structure was not only one unique molecule with disordered ethyl arms the data was reprocessed in the higher symmetry space group *Pnma*. The data could not be solved in this space group so we are confident that *Pna2₁* is the correct space group.

Table 3.6 Crystal and refinement data for the complexes **3.13**, **3.16b**, **3.16c** and **3.17**.

Complex	3.13	3.16b	3.16c	3.17
Formula	C ₁₈ H ₁₄ PSClHg	C ₁₈ H ₁₄ PSCl ₂ Au	C ₁₈ H ₁₄ PCl ₂ SeAu	C ₁₄ H ₂₄ N ₂ PSCl ₂ Au
Molecular Weight	529.36	561.19	608.09	551.25
<i>T</i> /K	89	89	89	89
Crystal system	Monoclinic	Triclinic	Triclinic	Orthorhombic
Space group	<i>P</i> 2 ₁ / <i>c</i>	<i>P</i> -1	<i>P</i> -1	<i>Pna</i> 2 ₁
<i>a</i> (Å)	8.8845(1)	8.1875(1)	8.1506(1)	27.3998(9)
<i>b</i> (Å)	17.2034(1)	9.1443(1)	9.2374(1)	7.9520(3)
<i>c</i> (Å)	11.2712(2)	12.4011(1)	12.4369(2)	17.1925(6)
α (°)	90	98.705(1)	80.142(1)	90
β (°)	101.8490(1)	102.795(1)	76.934(1)	90
γ (°)	90	90.484(1)	89.994(1)	90
<i>V</i> (Å ³)	1686.02(4)	894.124(16)	897.94(2)	3746.0(2)
<i>Z</i>	4	2	2	8
<i>D</i> _{calc} (g cm ⁻³)	2.085	2.084	2.249	1.955
<i>T</i> _{max,min}	0.2524, 0.1026	0.2742, 0.2285	0.4170, 0.1553	0.2397, 0.2038
Number of unique reflections	3430	3657	4284	7379
Number of observed reflections [<i>I</i> >2σ(<i>I</i>)]	3258	3562	4147	6979
R[<i>I</i> >2σ(<i>I</i>)]	0.0200	0.0274	0.0152	0.0216
<i>w</i> R ₂ (all data)	0.0525	0.0717	0.0360	0.0457
Goodness of Fit	1.060	1.106	1.073	1.130
Flack <i>x</i> parameter				0.2364(4) [*]

^{*} Racemic twin (occupancy 0.76/0.24)

3.5 References

1. T. S. Lobana; *Prog. Inorg. Chem.*, **1989**, 37, 495.
2. T. S. Lobana, *Coordination Chemistry of Phosphine Chalcogenides and Their Analytical and Catalytic Applications* In: *The Chemistry of Organophosphorus Compounds*, Vol 2, John Wiley and Sons Ltd, page 409 (Chapter 8), **1992**.
3. R. Usón, A. Laguna and J. L. Sanjoaquin; *J. Organomet. Chem.*, **1974**, 80, 147.
4. R. Usón, A. Laguna, M. Laguna, J. Jiménez and M. E. Durana; *Inorg. Chim. Acta*, **1990**, 168, 89.
5. A. Laguna, M. Laguna, J. Jiménez and A. J. Fumanal; *J. Organomet. Chem.*, **1990**, 396, 121.
6. M. Contel, A. J. Edwards, J. Garrido, M. B. Hursthouse, M. Laguna and R. Terroba; *J. Organomet. Chem.*, **2000**, 607, 129.
7. G. J. Depree, N. D. Childerhouse and B. K. Nicholson; *J. Organomet. Chem.*, **1997**, 533, 143.
8. J. Fischer, M. Schürmann, M. Mehring, U. Zachwieja and K. Jurkschat; *Organometallics*, **2006**, 25, 2886.
9. H. Hartung, D. Petrick, C. Schmoll and H. Weichmann; *Z. Anorg. Allg. Chem.*, **1987**, 550, 140.
10. T. Kanbara and T. Yamamoto; *J. Organomet. Chem.*, **2003**, 688, 15.
11. O. Piechaczyk, T. Cantat, N. Mézailles and P. Le Floch; *J. Org. Chem.*, **2007**, 72, 4228.
12. M. A. Bennett, S. K. Bhargava, M. Ke and A. C. Willis; *J. Chem. Soc., Dalton Trans.*, **2000**, 3537.
13. X. Solans, M. Font-Altaba, M. Aguilo, C. Miravittles, J. C. Besteiro and P. Lahuerta; *Acta Cryst. Sect. C*, **1985**, 41, 841.
14. M. A. Bennett, M. Contel, D. C. R. Hockless and L. L. Welling; *Chem. Comm.*, **1998**, 2401.
15. M. A. Bennett, M. Contel, D. C. R. Hockless, L. L. Welling and A. C. Willis; *Inorg. Chem.*, **2002**, 41, 844.
16. W. Henderson; *Adv. Organomet. Chem.*, **2006**, 54, 207.
17. J. B. Cook; *M. Sc Thesis*, **1999**, University of Waikato.
18. W. Henderson, B. K. Nicholson and L. J. McCaffrey; *Polyhedron*, **1998**, 17, 4291.
19. R. C. Larock; *Organomercury Compounds in Synthesis*, Springer-Verlag, Berlin, **1985**
20. L. Main and B. K. Nicholson; *Adv. Metal-Org. Chem.*, **1994**, 3, 1.
21. J. M. Cooney, L. H. P. Gommans, L. Main and B. K. Nicholson; *J. Organomet. Chem.*, **1987**, 336, 293.

22. T. S. Lobana, M. K. Sandhu, M. J. Liddell and E. R. T. Tiekink; *J. Chem. Soc., Dalton Trans.*, **1990**, 691.
23. T. S. Lobana, R. Verma, A. Singh, M. Shikha and A. Castiñeiras; *Polyhedron*, **2002**, 21, 205.
24. P. W. Coddling and K. A. Kerr; *Acta Cryst. Sect. B*, **1978**, 34, 3785.
25. D. C. Craig, N. K. Roberts and J. L. Tanswell; *Aust. J. Chem.*, **1990**, 43, 1487.
26. P. A. Bonnardel, R. V. Parish and R. G. Pritchard; *J. Chem. Soc., Dalton Trans.*, **1996**, 3185.
27. P. G. Jones, C. Kienitz and C. Thoene; *Z. Kristallogr.*, **1994**, 209, 80.
28. M. C. Gimeno, P. G. Jones, A. Laguna and C. Sarroca; *J. Organomet. Chem.*, **2000**, 596, 10.
29. H. H. Murray, G. Garzón, R. G. Raptis, A. M. Mazany, L. C. Porter and J. P. Fackler Jr.; *Inorg. Chem.*, **1988**, 27, 836.
30. S. Canales, O. Crespo, M. C. Gimeno, P. G. Jones and A. Laguna; *Z. Naturf.*, **2007**, 62b, 407.
31. CCDC; *Version 5.29, November 2007*.
32. S. D. J. Brown, W. Henderson, K. J. Kilpin and B. K. Nicholson; *Inorg. Chim. Acta*, **2007**, 360, 1310.
33. K. J. Kilpin, W. Henderson and B. K. Nicholson; *submitted*, **2008**.
34. P. E. Garrou; *Chem. Rev.*, **1981**, 81, 229.
35. C. Glidewell and E. J. Leslie; *J. Chem. Soc., Dalton Trans.*, **1977**, 527.
36. M. G. King and G. P. McQuillan; *J. Chem. Soc. A*, **1967**, 898.
37. K. J. Kilpin, W. Henderson and B. K. Nicholson; *Polyhedron*, **2007**, 26, 434.
38. M. B. Dinger and W. Henderson; *J. Organomet. Chem.*, **1998**, 560, 233.
39. W. Henderson, B. K. Nicholson, S. J. Faville, D. Fan and J. D. Ranford; *J. Organomet. Chem.*, **2001**, 631, 41.
40. D. Fan, C.-T. Yang, J. D. Ranford, J. J. Vittal and P. F. Lee; *Dalton Trans.*, **2003**, 3376.
41. T. G. Appleton, H. C. Clark and L. E. Manzer; *Co-ord. Chem. Rev.*, **1973**, 10, 335.
42. R. G. Pearson; *Inorg. Chem.*, **1973**, 12, 712.
43. E. R. T. Tiekink; *Critical Rev. Onc./Hem.*, **2002**, 42, 225.
44. R. V. Parish; *Met.-Based Drugs*, **1999**, 6, 271.
45. C. Gabbiani, A. Casini and L. Messori; *Gold Bull.*, **2007**, 40, 73.
46. M. I. Bruce, M. J. Liddell and G. N. Pain; *Inorg. Synth.*, **1989**, 26, 172.
47. R. H. Blessing; *Acta Cryst. Sect. A*, **1995**, 51, 33.

48. G. M. Sheldrick, SHELXS-97 - A Program for the Solution of Crystal Structures, University of Göttingen, Germany, **1997**.
49. G. M. Sheldrick, SHELXL-97 - A Program for the Refinement of Crystal Structures, University of Göttingen, Germany, **1997**.

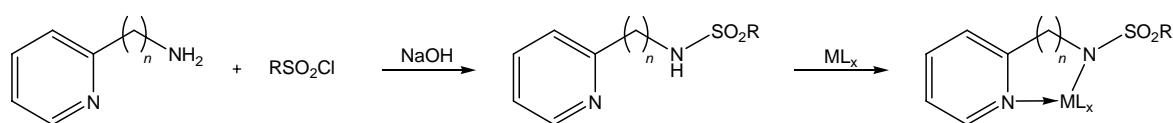
CHAPTER FOUR

The Cycloauration of Pyridyl Sulfonamides

4.1 Introduction

4.1.1 2-Pyridyl derived sulfonamides as bidentate ligands

Sulfonamide ligands derived from 2-pyridylamines are attractive bidentate N,N' donor ligands because of their facile synthesis and the relatively low cost of the starting materials. Synthesis can be achieved by a convenient condensation reaction between a pyridylamine (such as 2-picolylamine or 2-(2-aminoethyl)pyridine) and an organic sulfonyl chloride in the presence of a base (Scheme 4.1). This allows the introduction of different functional groups to tune both the steric and electronic properties of the ligand. Deprotonation of these ligands at the sulfonamide nitrogen can lead to a sigma bond to the metal centre, with a dative bond provided by the pyridyl nitrogen. Depending on the length of the spacer in the parent amine, cyclometallated compounds containing four-, five- or six-membered rings can potentially result.



Scheme 4.1 Synthesis of 2-pyridyl derived sulfonamide ligands and the subsequent reaction to give cyclometallated complexes.

4.1.2 Examples of complexes of bidentate sulfonamide ligands

The first report on the coordination of pyridyl sulfonamide ligands to metal centres appeared in 1962, when Billman and Chernin discussed the use of 8-(sulfonamido)quinoline derivatives as selective metal chelating agents for Ag^+ , Cu^{2+} , Zn^{2+} , Pb^{2+} , Co^{2+} and Hg^{2+} ions. The resulting metal-ligand chelates were highly coloured solids which were insoluble in all

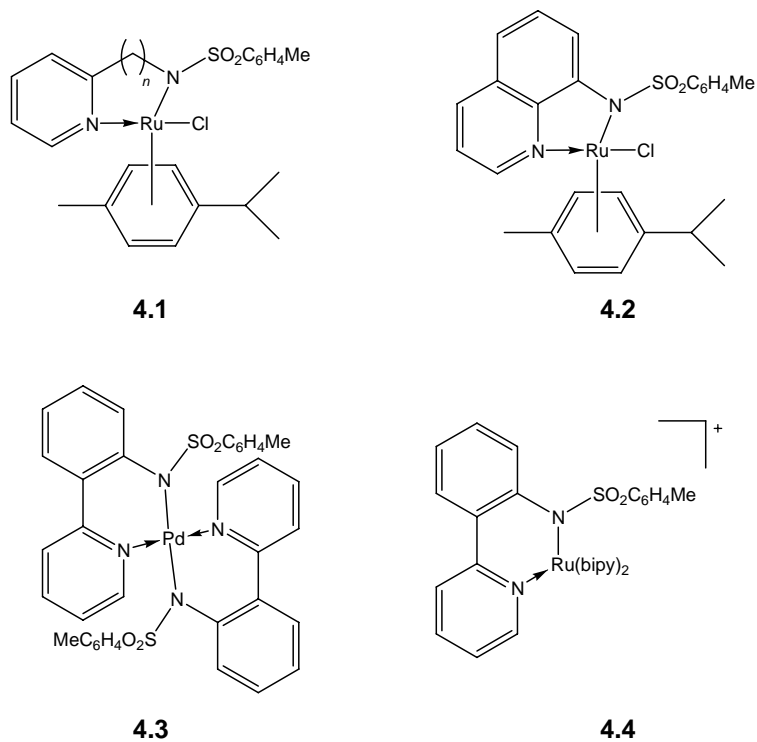
common organic solvents. Unfortunately they were not structurally characterised but on the basis of infra-red and elemental data the complexes were assumed to contain the deprotonated ligand coordinated to the metal ion *via* two nitrogen atoms.⁽¹⁾

More recently, the bulk of the literature explores the coordination of first row transition metal ions to these types of ligands, forming bis(sulfonamide) complexes of the type ML_2 . The vast majority of the research is centred around the redox chemistry of copper(II) complexes⁽²⁻⁶⁾ with a number of examples showing interesting biological properties.⁽⁷⁻¹¹⁾ Similarly the chemistry of nickel(II)^(2, 5, 12) and cobalt(II)^(5, 13) bis(sulfonamide) complexes has been explored, and zinc(II) analogues containing fluorescent substituents on the sulfonamide ligands have been used to study intracellular zinc chemistry.^(6, 15, 16)

Although much more scarce, studies on the coordination of second row transition metal ions to deprotonated sulfonamide ligands have also been conducted. Ruthenium(II) complexes with *N*-(*p*-toluenesulfonyl)diamine ligands **4.1** and **4.2** were found to be catalytically active in the insertion of carbenes into alcoholic O-H bonds⁽¹⁴⁾. Palladium(II)⁽¹⁵⁾ **4.3** and ruthenium(II)⁽¹⁶⁾ **4.4** complexes of the sulfonamide ligand derived from 2-(2-aminophenyl)pyridine have been synthesised and structurally characterised. Both contain puckered six-membered metallacyclic rings, and because of the bridge between the pyridyl and phenyl rings in the ligand these two moieties are not co-planar.

4.1.3 Scope of this work

To date, gold(III) cyclometallated complexes with pyridyl sulfonamide ligands are unknown, and as mentioned in Chapter One, cycloaurated complexes containing monoanionic bidentate ligands with donor atoms other than the *C,N* pair are rare. The following work details the synthesis and the resulting properties of cycloaurated compounds containing deprotonated 2-pyridyl sulfonamide ligands acting as *N,N'* monoanionic donor ligands to the gold(III) centre.

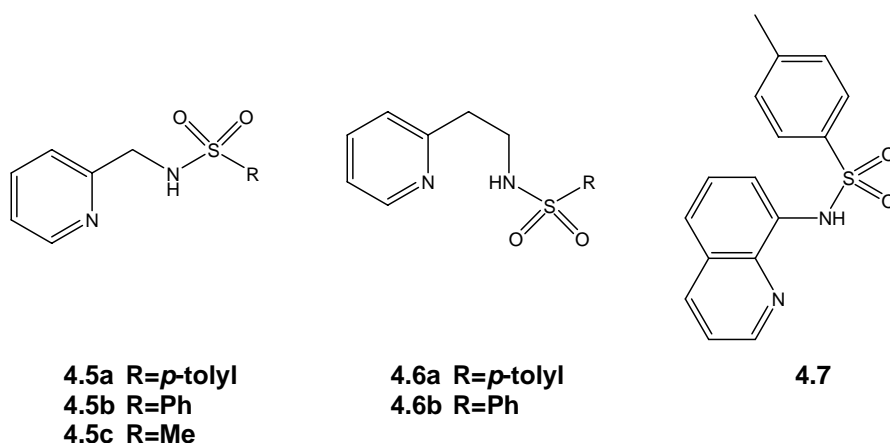


Scheme 4.2 Literature examples of sulfonamide complexes formed with second row transition metals.

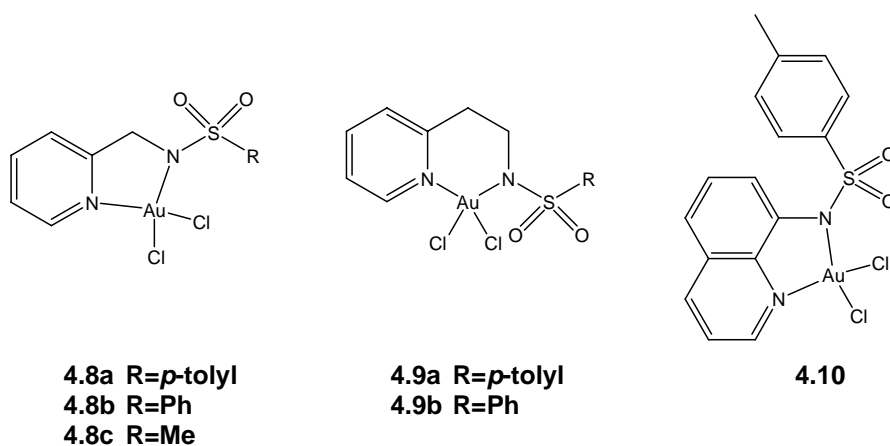
4.2 Results and Discussion

4.2.1 Syntheses

When the ligands **4.5** – **4.7** (Scheme 4.3) were refluxed in aqueous $\text{H}[\text{AuCl}_4]$ in a 1:1 mole ratio, the auracyclic compounds **4.8** – **4.10** (Scheme 4.4) were easily isolated in excellent yields by filtration of the yellow to brown solid that was present throughout the reaction, the exception being **4.8c** which required cooling to induce crystallisation.

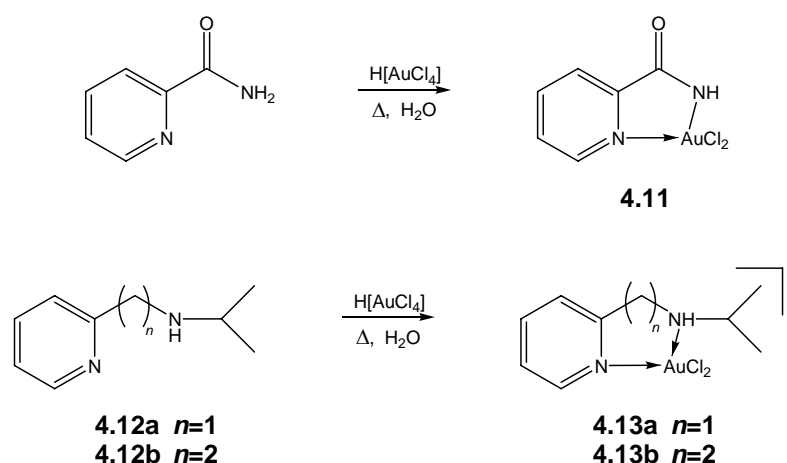


Scheme 4.3 Sulfonamide ligands used in the study.



Scheme 4.4 Cycloaurated complexes formed from deprotonated sulfonamide ligands.

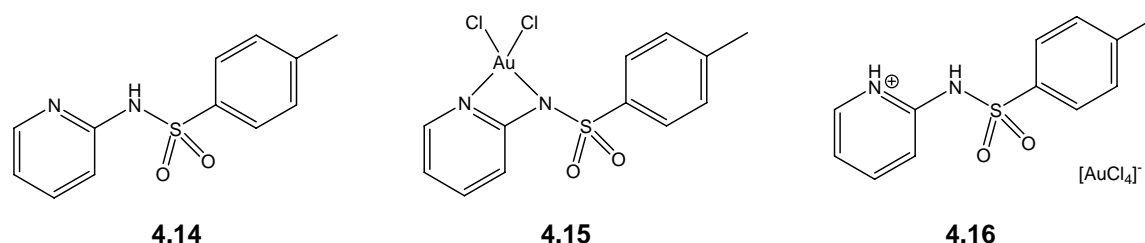
This synthetic procedure is analogous to the preparation of **4.11**,^(17, 18) however, similar reactions of the secondary amines **4.12a** and **4.12b** with $[\text{AuCl}_4]^-$ only afforded the salts **4.13a** and **4.13b** (Scheme 4.5).⁽¹⁹⁾ The difference in the reactivity (*i.e.* no deprotonation of the sulfonamide ligand and the formation of a cationic cycloaurated product) can be attributed to the decreased acidity of the NH protons in the ligands **4.12a** and **4.12b** relative to the sulfonamide counterparts.



Scheme 4.5 Synthesis of similar cycloaurated N,N' complexes which have been reported in the literature.

NMR and IR spectroscopy, along with ESI mass spectrometry indicate the nitrogen donor ligands in **4.8** – **4.10** are coordinated to gold through a neutral pyridyl donor and an anionic amido group (see below). The formulation was confirmed by X-ray crystal structures of the complexes **4.8c** and **4.10**.

Attempted preparation of the analogous four-membered auracyclic system **4.15** from **4.14** proved unsuccessful. When **4.14** was refluxed with H[AuCl₄] in either an aqueous or an acetonitrile/water (1:1) solution, or alternatively when **4.14** was added to an aqueous acetonitrile solution of H[AuCl₄] at room temperature, the only product was the salt **4.16**. This was identified by NMR spectroscopy and the presence of both the [4.14+H]⁺ and [AuCl₄]⁻ ions in positive and negative ESI mass spectra respectively.



Scheme 4.6 The sulfonamide ligand derived from 2-aminopyridine and the possible products formed when reacted with H[AuCl₄].

4.2.2 X-ray crystal structures of **4.8c** and **4.10** · CH₂Cl₂

Single crystal X-ray structure analyses of **4.8c** and **4.10** were carried out in order to confirm the bonding of the ligand to the gold. In both cases, the ligands are deprotonated at the sulfonamide nitrogen and bonded to the gold through the two nitrogen atoms, with the remaining sites on the metal occupied by two *cis* chloride ligands. Complex **4.8c** crystallises with two independent molecules per asymmetric unit and **4.10** as a CH₂Cl₂ solvate. Diagrams of the crystal structures of **4.8c** and **4.10** · CH₂Cl₂, along with the atom numbering schemes, are shown in Figures 4.1 and 4.2 respectively. Selected bond lengths and angles are presented in Tables 4.1 and 4.2. A full list of structural parameters, atomic coordinates and anisotropic displacement parameters can be found on the supplementary CD.

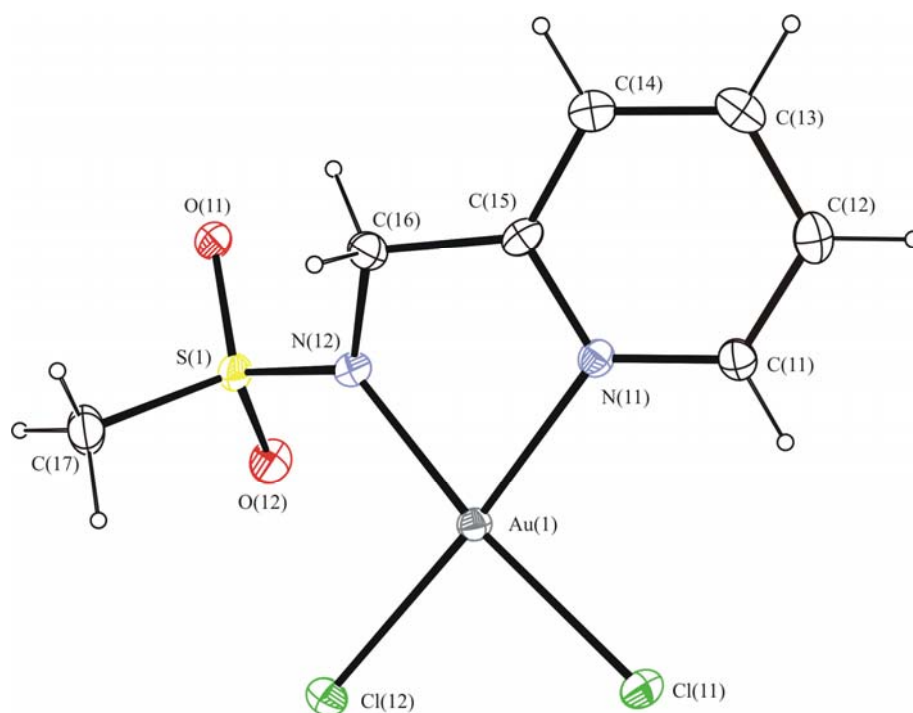


Figure 4.1 Molecular structure of **4.8c**, showing one of the unique molecules in the asymmetric unit, and the atom numbering scheme. Thermal ellipsoids are shown at the 50% probability level.

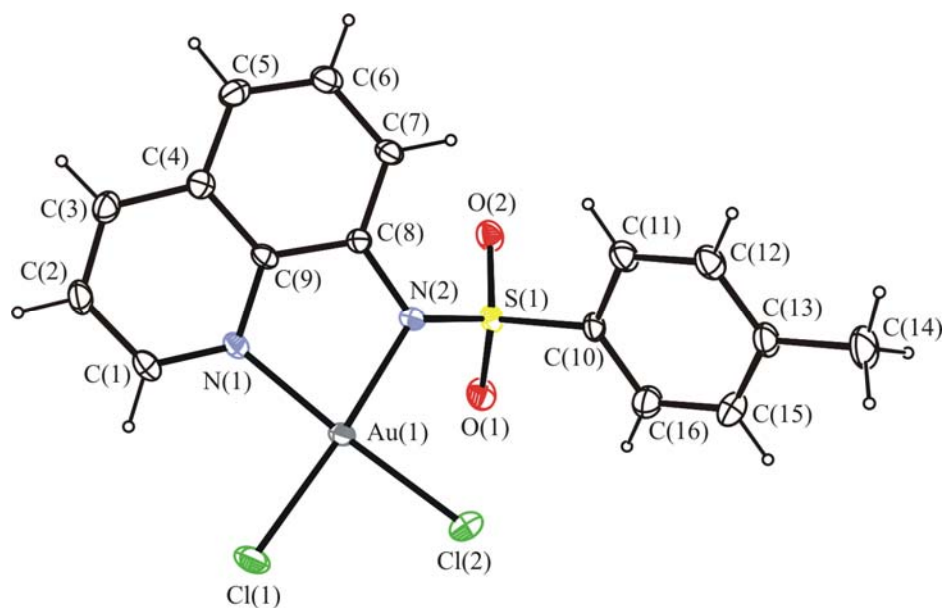


Figure 4.2 Molecular structure of **4.10** · CH₂Cl₂, showing the atom numbering scheme. The dichloromethane solvent has been omitted for clarity and thermal ellipsoids are shown at the 50% probability level.

For both **4.8c** and **4.10** · CH₂Cl₂, the geometry around the d^8 gold centre is essentially square planar, with the bite angle of the sulfonamide ligand less than 90° in both cases (Table 4.2). In **4.8c**, the atom with the greatest deviation from the metallic coordination plane [defined by Au(1), N(1), N(2), Cl(1) and Cl(2)] is N(1) (0.0817(15) Å) and Au(1) (0.0280(10) Å) for molecules 1 and 2 respectively. For **4.10** · CH₂Cl₂, the gold atom shows the greatest deviation from the coordination plane [defined by Au(1), N(1), N(2), Cl(1) and Cl(2)], sitting 0.0514(8) Å above the plane.

Table 4.1 A comparison of selected bond lengths (Å) for the crystal structures of **4.8c** (two independent molecules) and **4.10** · CH₂Cl₂ (esds in parentheses).

	4.8c		4.10 · CH ₂ Cl ₂
	Molecule 1	Molecule 2	
Au(1) – Cl(1)	2.2872(10)	2.2807(10)	2.2789(8)
Au(1) – Cl(2)	2.2720(10)	2.2800(10)	2.2637(9)
Au(1) – N(ex py)	2.046(3)	2.037(3)	2.026(3)
Au(1) – N(ex NH)	2.006(3)	2.021(3)	2.038(3)

Table 4.2 A comparison of selected bond angles (°) for the crystal structures of **4.8c** (including the two independent molecules) and **4.10** · CH₂Cl₂ (esds in parentheses).

	4.8c		4.10 · CH ₂ Cl ₂
	Molecule 1	Molecule 2	
Cl(1) – Au(1) – Cl(2)	89.09(4)	90.17(4)	88.13(3)
Cl(1) – Au(1) – N(ex py)	94.08(10)	93.89(10)	94.36(8)
N(ex py) – Au(1) – N(ex NH)	78.98(13)	82.09(13)	81.48(11)
N(ex NH) – Au(1) – Cl(2)	98.02(10)	93.79(10)	95.88(8)

In all cases, the coordination around the deprotonated sulfonamide nitrogen N(2) is not planar, but is slightly distorted towards tetrahedral geometry, with the angles around the nitrogen adding to 358.6° (molecule 1) and 344.2° (molecule 2) for **4.8c**, and 353.7° for **4.10** · CH₂Cl₂. Similar cyclometallated gold(III)⁽²⁰⁾ and platinum(II)⁽²¹⁾ compounds have also shown this behaviour.

In both molecules of **4.8c**, the cycloaurated ring [defined by Au(1), C(1), C(5), N(1) and N(2)] is in an envelope conformation with N(2) sitting above the ring (by 0.2858(22) Å and 0.2060(22) Å for molecules 1 and 2 respectively). Due to the increased rigidity imposed by the aromatic ring system, in **4.10** · CH₂Cl₂ it is Au(1) that shows the greatest deviation from the plane [defined by C(1)-C(9), N(1) and N(2)], sitting 0.3388(25) Å below the plane of the quinoline ring system (Figure 4.3).

In **4.8c** the gold – sulfonamide nitrogen bond length is shorter than the gold – pyridyl nitrogen bond length, but the opposite is observed in the structure of **4.10** · CH₂Cl₂. The rigidity imposed on the system by the quinoline moiety in **4.10** · CH₂Cl₂, in comparison to the flexibility of **4.8c** system, is the probable cause of this discrepancy.

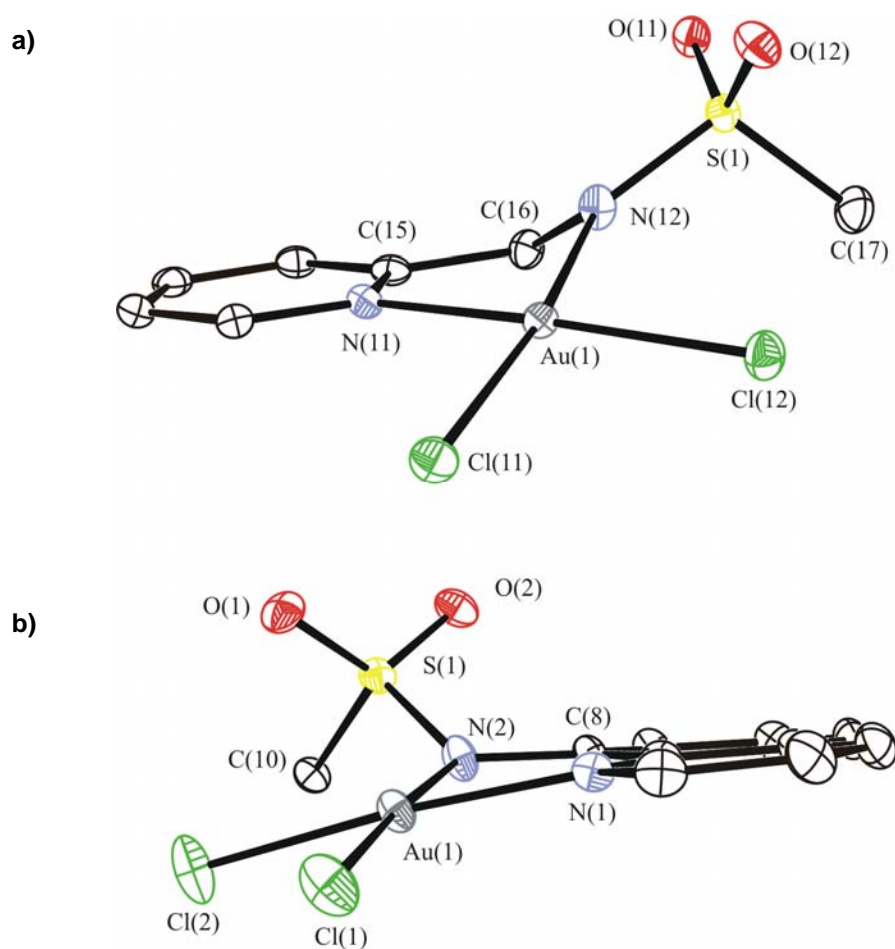


Figure 4.3 (a) Structure of **4.8c** (molecule 1) showing the envelope conformation of the cycloaurated ring with N(2) sitting above the plane of the ring; (b) structure of **4.10** · CH₂Cl₂, showing the planarity of the quinoline group, with Au(1) sitting below the plane. For clarity, only the *ipso* carbon of the *p*-tolyl group (C(10)) of **4.10** · CH₂Cl₂ is shown and the hydrogen atoms are omitted. Thermal ellipsoids are shown at the 50% probability level.

4.2.3 NMR and IR spectroscopic characterisation

The compounds **4.8** – **4.10** were most suited to analysis by NMR spectroscopy. The effect of coordination of the gold to the ligand through the deprotonated sulfonamide nitrogen and pyridyl nitrogen could clearly be seen. The methylene protons of the ligands **4.5a-c** appear as a doublet due to coupling to the NH proton of the sulfonamide group, whereas for **4.6a** and **4.6b** a triplet and a quartet arise from the two methylene groups. Upon coordination to the gold, the methylene signals become either a singlet (five-membered ring systems) or two

triplets (six-membered ring systems) which provides unambiguous evidence for loss of the sulfonamide proton.

Coordination to the gold can clearly be seen in compounds **4.8a** (Figure 4.4) and **4.8b**. A downfield shift of approximately 0.7 ppm is seen for H-1 (the proton adjacent to the coordinated pyridyl nitrogen) upon coordination to the gold, most probably due to the proximity of the gold atom and the increased deshielding produced by the electronegative metal centre. Lesser shifts are seen for the remaining three complexes. This could be explained by the spectra of the ligands being acquired in a different solvent to the complexes (for solubility reasons).

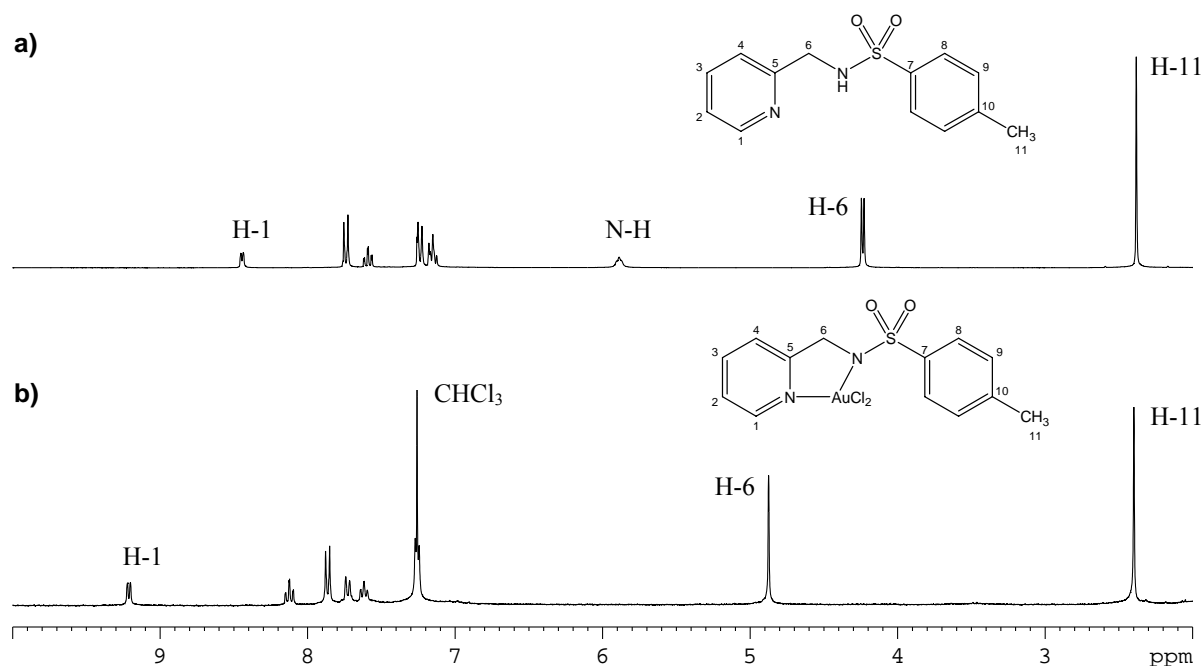


Figure 4.4 ^1H NMR spectra (CDCl_3) of (a) **4.5a** and (b) **4.8a**, showing changes in the spectra upon coordination of the ligand to gold.

For the complexes **4.9a** and **4.9b** there appears to be fluxionality in the six-membered auracyclic rings at 30 °C. There is the possibility that this may be due to inversion of the amide nitrogen which is distorted from planarity, however this seems unlikely. The two

methylene signals are seen as broad triplets – presumably if the ring was not fluxional the multiplets would be much more complex due to the different stereochemical environment each proton inhabits.

Upon coordination of the ligand to the gold centre, the main points of interest in the IR spectra are the loss of NH stretching frequencies ($\sim 3100\text{ cm}^{-1}$) and a shift to lower wavenumbers for the SO_2 stretching modes, consistent with lengthening of the S=O bonds through movement of electrons onto the sulfonyl oxygen atoms. For example, the SO_2 stretches shift from 1164 cm^{-1} and 1327 cm^{-1} (for the asymmetric and symmetric stretches respectively) in **4.5a** to 1146 cm^{-1} and 1306 cm^{-1} in the cycloaurated complex **4.5b**.

4.2.4 ESI mass spectrometric characterisation

Analysis of the compounds **4.8** – **4.10** by ESI-MS was not overly effective. Because the compounds are neutral they must form a complex with an ion (*e.g.* H^+ or Na^+) to be observed in the mass spectra, alternatively the displacement of a chloride ligand by a neutral species (*e.g.* pyridine) also produces a cation.⁽²²⁾ The low ionisation ability of the neutral species, means that cationic impurity ions (namely the bis(cycloaurated) species $[(\text{L})_2\text{Au}]^+$ where L is the deprotonated ligand, also see Figure 4.5) dominate the spectra as a result of their high ionisation efficiency. This phenomenon has been observed previously in cyclometallated gold(III) dichloride species.⁽²³⁾

For example, when **4.8b** (=M) is analysed without ionisation aids (Figure 4.5a), the spectrum is dominated by the ion at m/z 691 ($[(\text{L})_2\text{Au}]^+$), although there is no evidence for the presence of this species in either the ^1H NMR spectrum or microanalytical results. Addition of NaCl to the sample before analysis (Figure 4.5b) produces ions at m/z 537 (21%) and 1051 (10%) corresponding to $[\text{M}+\text{Na}]^+$ and $[2\text{M}+\text{Na}]^+$ respectively, however the species ($[(\text{L})_2\text{Au}]^+$) is still the dominant peak. Addition of pyridine (py), a strongly coordinating species, to a solution of the compound in methanol (Figure 4.5c) forms species identified as $[\text{M}-\text{Cl}+\text{py}]^+$ and $[\text{M}-2\text{Cl}+\text{py}+\text{OMe}]^+$ at m/z 558 and 554 respectively, however the ion at m/z 691 (40%) is still present. Identification and confirmation of these ions is aided by the presence of chlorine(s)

and thus unique isotope patterns. A similar pattern of behaviour was seen for all members of this family of compounds.

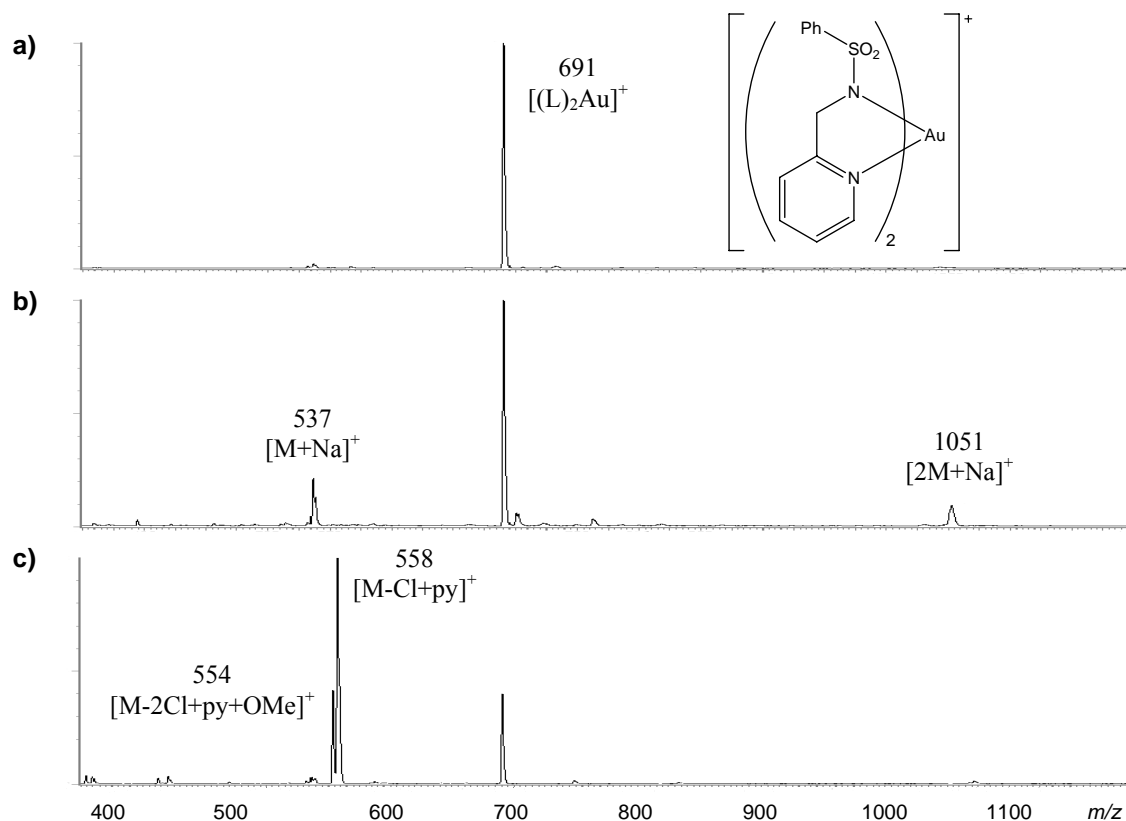


Figure 4.5 Positive ion ESI mass spectra (cone voltage 20 V, MeOH solvent) of **4.8b** (=M) showing the observed ions under different ionisation conditions: (a) neat solution; (b) with addition of NaCl; (c) with addition of pyridine (py).

4.2.5 Biological activity

Previously *C,N* cycloaurated complexes, in particular the compound (damp)AuCl₂, (damp = 2-[(dimethylamino)methyl]phenyl) and its derivatives have shown promising anti-tumour activity.⁽²⁴⁾ Little data exist on *N,N'* stabilised cycloaurated complexes and for this reason complexes **4.8a-c** – **4.8a-b** were evaluated for anti-tumour activity against the P388 murine leukemia cell line. Samples were analysed as 1:1 dichloromethane/methanol solutions; the method of analysis is described in Appendix 1. Results indicate an IC₅₀ value of greater than 12500 ng mL⁻¹ for all compounds, indicating little activity against this particular cell line.

4.2.6 Reactivity

As discussed previously in Chapter 1, the reaction of *C,N* cycloaurated dichloride species with tertiary phosphines may result in displacement of the chloride ligands by coordination of the neutral phosphines to the gold or conversely, cleavage of the Au–N bond may occur with both Au–Cl bonds remaining intact – in both cases gold(III) products are formed. Such reactions can give an indication of the strength of the gold-nitrogen bond and are dependent on the cycloaurated ligand present.⁽²⁵⁾

Reaction of the auracyclic species **4.8a** with PPh₃ in a 1:1 molar ratio in dichloromethane resulted in the yellow solution becoming lighter. ESI-MS of the solution showed ions corresponding to the gold(I) species [Au(PPh₃)₂]⁺ (*m/z* 721), PPh₃ and Ph₃P=O. ³¹P NMR spectroscopy of the solution gave peaks at δ 30 (br s) and 34 (s) ppm, the first of which arises from Ph₃P=O, the second an average of rapidly exchanging [Au(PPh₃)₂]⁺ with free PPh₃.⁽²⁶⁾ Likewise, when **4.8a** was reacted with PPh₃ in a 1:2 molar ratio, ESI-MS gave ions due to [Au(PPh₃)₂]⁺, PPh₃ and Ph₃P=O; the ³¹P NMR spectrum again showed peaks at δ 30 (s) and 34 (s) ppm. Reaction of **4.8a** with thiosalicylic acid using previously established methods for *C,N* cycloaurated complexes⁽²⁷⁾ resulted in immediate reduction and decomposition of the gold species to elemental gold. These results indicate that the *N,N'* cycloaurated ligands do not stabilise the Au(III) centre as effectively as *C,N* cycloaurated species, and reaction with phosphines gives reduction of the gold(III).

4.3 Conclusions

Six new cycloaurated gold(III) complexes containing *N,N'* cyclometallated ligands have been synthesised and fully characterised, including the X-ray crystal structures of two of these complexes. Coordination to the gold is through a pyridyl and deprotonated amide nitrogen atom. Compared with the more common analogous *C,N* cyclometallated compounds, these complexes do not appear to show as much stability, as reactions with reducing agents leads to reduction of Au(III) to Au(I) and elemental gold. The biological activity of these complexes against murine leukaemia cell lines is also low – possibly due to this lack of stability towards reduction. These results indicate that the anionic nitrogen is not as efficient at stabilising the

electron deficient gold(III) centre as the carbon. This is possibly because of the difference in the electronegativity of carbon (2.55) and nitrogen (3.04).

4.4 Experimental

4.4.1 General

2-Picolylamine, 2-(2-aminoethyl)pyridine and 8-(tosylamino)quinoline (Aldrich) were used as supplied, as were *p*-toluenesulfonylchloride (BDH), benzenesulfonylchloride (BDH) and methanesulfonylchloride (Riedel-de Haën). The sulfonamide ligands (all previously reported compounds)^(3, 28, 29) were synthesised by the condensation of the sulfonyl chloride with the amine, following the procedure reported for **4.5a** and **4.6a**.⁽³⁰⁾ Details of the general characterisation conditions can be found in Appendix 1. For the ESI-MS assignment $M = LAuCl_2$ where L is the deprotonated sulfonamide ligand.

4.4.2 Syntheses

Synthesis of **4.8a**

4.5a (0.560 g, 2.13 mmol) and $H[AuCl_4] \cdot 4H_2O$ (0.877 g, 2.13 mmol) were added to water (75 mL) to give an orange suspension. This was refluxed with stirring for 3 hours and then cooled to room temperature. The orange precipitate that was present throughout the reaction was filtered and washed with water (2×10 mL) and isopropanol (2×10 mL) and air dried to give 0.918 g (82%) of **4.8a** as an orange solid.

Found: C 29.6, H 2.5, N 5.3; $C_{13}H_{13}N_2O_2SCl_2Au$ requires C 29.5, H 2.5, N 5.3%.

NMR ($CDCl_3$): 1H : δ 2.40 (s, 3H, H-11), 4.88 (s, 2H, H-6), 7.26 (d, $^3J_{9,8} = 8.5$ Hz, 2H, H-9), 7.62 (ddd, $^3J_{2,1} = 6.1$ Hz, $^3J_{2,3} = 7.7$ Hz, $^4J_{2,4} = 1.6$ Hz, 1H, H-2), 7.73 (dd, $^3J_{4,3} = 7.8$ Hz, $^4J_{4,2} = 1.6$ Hz, 1H, H-4), 7.87 (d, $^3J_{8,9} = 8.5$ Hz, 2H, H-8), 8.13 (td, $^3J_{3,2} = 7.7$ Hz, $^3J_{3,4} = 7.8$ Hz, $^4J_{3,1} = 1.5$ Hz, 1H, H-3), 9.22 (dd, $^3J_{1,2} = 6.1$ Hz, $^4J_{1,3} = 1.5$ Hz, 1H, H-1); $^{13}C\{^1H\}$: δ 21.7

(C-11), 61.6 (C-6), 121.7 (C-4), 125.5 (C-2), 127.8 (C-8), 129.7 (C-9), 138.0 (C-7), 143.2 (C-3), 143.6 (C-10), 147.5 (C-1), 166.9 (C-5) ppm (see Scheme 4.7 for the NMR numbering scheme).

ESI-MS: NaCl added: m/z : 551 (32%, $[M+Na]^+$), 719 (100%, $[(L)_2Au]^+$), 1079 (10%, $[2M+Na]^+$); pyridine added: m/z : 568 (28%, $[M-2Cl+py+OMe]^+$), 572 (100%, $[M-Cl+py]^+$), 719 (25%, $[(L)_2Au]^+$).

IR: $\nu(\text{SO}_2 \text{ sym})$ 1306 (s), $\nu(\text{SO}_2 \text{ asym})$ = 1146 (vs) cm^{-1} .

Synthesis of 4.8b

As for the synthesis of **4.8a**, the ligand **4.5b** (0.566 g, 2.28 mmol) was suspended in an aqueous (50 mL) solution of $\text{H}[\text{AuCl}_4] \cdot 4\text{H}_2\text{O}$ (0.939 g, 2.28 mmol) and refluxed with stirring for 3 hours. The precipitate that was present throughout was filtered and washed with water (2×10 mL) and isopropanol (2×10 mL). The yellow/brown solid was air dried to give 0.964 g (82%) of **4.8b**.

Found: C 27.9, H 2.1, N 5.4; $\text{C}_{12}\text{H}_{11}\text{N}_2\text{O}_2\text{SCl}_2\text{Au}$ requires C 28.0, H 2.2, N 5.4%.

NMR (CDCl_3): ^1H : δ 4.91 (s, 2H, H-6), 7.47 (t, $^3J_{9,10} = 8.0$ Hz, $^3J_{9,8} = 7.2$ Hz, 2H, H-9), 7.53 (t, $^3J_{10,9} = 8.0$ Hz, 1H, H-10), 7.63 (ddd, $^3J_{2,1} = 6.1$ Hz, $^3J_{2,3} = 7.6$ Hz, $^4J_{2,4} = 1.6$ Hz, 1H, H-2), 7.74 (dd, $^3J_{4,3} = 7.8$ Hz, $^4J_{4,2} = 1.6$ Hz, 1H, H-4), 7.99 (d, $^3J_{8,9} = 7.2$ Hz, 2H, H-8), 8.13 (td, $^3J_{3,2} = 7.6$ Hz, $^3J_{3,4} = 7.8$ Hz, $^4J_{3,1} = 1.5$ Hz, 1H, H-3), 9.22 (dd, $^3J_{1,2} = 6.1$ Hz, $^4J_{1,3} = 1.5$ Hz, 1H, H-1); $^{13}\text{C}\{^1\text{H}\}$: δ 61.6 (C-6), 121.7 (C-4), 125.5 (C-2), 127.7 (C-8), 129.0 (C-9), 141.2 (C-7), 143.2 (C-3), 132.7 (C-10), 147.5 (C-1), 166.7 (C-5) ppm (see Scheme 4.7 for the NMR numbering scheme).

ESI-MS: NaCl added: m/z : 537 (21%, $[M+Na]^+$), 691 (100 %, $[(L)_2Au]^+$), 1051 (10% $[2M+Na]^+$); pyridine added: m/z : 554 (40%, $[M-2Cl+py+OMe]^+$), 558 (100% $[M-Cl+py]^+$), 691 (40%, $[(L)_2Au]^+$).

IR: $\nu(\text{SO}_2 \text{ sym}) = 1313 \text{ (s)}$, $\nu(\text{SO}_2 \text{ asym}) = 1155 \text{ (vs)} \text{ cm}^{-1}$.

Synthesis of 4.8c

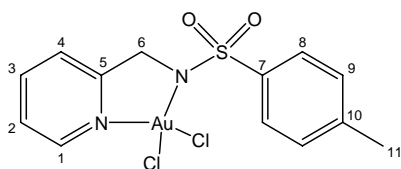
4.5c (0.200 g, 1.07 mmol) was dissolved in a solution of $\text{H}[\text{AuCl}_4] \cdot 4\text{H}_2\text{O}$ (0.441 g, 1.07 mmol) in water (30 mL). Upon reaching reflux temperature, the yellow solution turned deep orange and remained this colour for the duration of the reflux (2 hours). The clear solution was cooled in an ice bath which resulted in the deposition of orange/red microcrystals. These were filtered and washed with water ($2 \times 10 \text{ mL}$) and isopropanol ($2 \times 10 \text{ mL}$) and air dried to give 0.266 g (55%) of **4.8c**.

Found: C 18.1, H 1.9, N 6.0; $\text{C}_7\text{H}_9\text{N}_2\text{O}_2\text{SCl}_2\text{Au}$ requires C 18.6, H 2.0, N 6.2%.

NMR (d_6 -DMSO): ^1H : δ 3.10 (s, 3H, H-7), 4.96 (s, 2H, H-6), 7.80 (ddd, $^3J_{2,1} = 6.2 \text{ Hz}$, $^3J_{2,3} = 7.6 \text{ Hz}$, $^4J_{2,4} = 1.2 \text{ Hz}$, 1H, H-2), 8.05 (dd, $^3J_{4,3} = 7.7 \text{ Hz}$, $^4J_{4,2} = 1.2 \text{ Hz}$, 1H, H-4), 8.33 (td, $^3J_{3,2} = 7.6 \text{ Hz}$, $^3J_{3,4} = 7.7 \text{ Hz}$, $^4J_{3,1} = 1.4 \text{ Hz}$, 1H, H-3), 9.04 (dd, $^3J_{1,2} = 6.2 \text{ Hz}$, $^4J_{1,3} = 1.4 \text{ Hz}$, 1H, H-1); $^{13}\text{C}\{^1\text{H}\}$: δ 41.9 (C-7), 61.1 (C-6), 122.1 (C-4), 125.6 (C-2), 143.8 (C-3), 146.5 (C-1), 166.2 (C-5) ppm (see Scheme 4.7 for the NMR numbering scheme).

ESI-MS: NaCl added: 475 (100%, $[\text{M}+\text{Na}]^+$), 567 (84%, $[(\text{L})_2\text{Au}]^+$), 927 (56%, $[2\text{M}+\text{Na}]^+$); pyridine added: 492 (45%, $[\text{M}-2\text{Cl}+\text{py}+\text{OMe}]^+$), 496 (100%, $[\text{M}-\text{Cl}+\text{py}]^+$).

IR: $\nu(\text{SO}_2 \text{ sym}) = 1306 \text{ (s)}$, $\nu(\text{SO}_2 \text{ asym}) = 1132 \text{ (vs)} \text{ cm}^{-1}$.



Scheme 4.7 NMR numbering scheme for **4.8a-c**. For complex **4.8c** the methyl carbon is labelled C-7.

Synthesis of 4.9a

To an aqueous (30 mL) solution of H[AuCl₄].4H₂O (0.531 g, 1.29 mmol), **4.6a** (0.357 g, 1.29 mmol) was added and the yellow solution refluxed with stirring for 3.5 hours. During this time a brown solid formed, which after cooling was filtered, dried and washed with water (2 × 10 mL) and ether (1 × 10 mL) to give 0.542 g (78%) of **4.9a**.

Found: C 31.1, H 2.9, N 5.3; C₁₄H₁₅N₂O₂SCl₂Au requires C 31.0, H 2.8, N 5.2%.

NMR (d₆-DMSO): ¹H: δ 2.31 (s, 3H, H-12), 3.23 (br t, 2H, H-7), 3.47 (t, ³J_{6,7} = 6.3 Hz, 2H, H-6), 7.19 (d, ³J_{10,9} = 8.2 Hz, 2H, H-10), 7.57 (d, ³J_{9,10} = 8.2 Hz, 2H, H-9), 7.74 (ddd, ³J_{2,1} = 6.0 Hz, ³J_{2,3} = 7.7 Hz, ⁴J_{2,4} = 1.5 Hz, 1H, H-2), 7.77 (dd, ³J_{4,3} = 7.8 Hz, ⁴J_{4,2} = 1.5 Hz, 1H, H-4), 8.26 (td, 1H, ³J_{3,2} = 7.7 Hz, ³J_{3,4} = 7.8 Hz, ⁴J_{3,1} = 1.4 Hz, 1H, H-3), 8.91 (dd, ³J_{1,2} = 6.0 Hz, ⁴J_{1,3} = 1.4 Hz, 1H, H-1); ¹³C {¹H}: δ 20.8 (C-12), 37.6 (C-6), 42.4 (C-7), 126.0 (C-2), 126.8 (C-9), 127.7 (C-4), 129.4 (C-10), 137.8 (C-8), 142.2 (C-11), 143.8 (C-3), 149.7 (C-1), 155.5 (C-5) ppm (see Scheme 4.8 for the NMR numbering scheme).

ESI-MS: NaCl added: 565 (100%, [M+Na]⁺), 747 (91%, [(L)₂Au]⁺), 1107 (19%, [2M+Na]⁺); pyridine added: 582 (50%, [M-2Cl+py+OMe]⁺), 586 (100%, [M-Cl+py]⁺).

IR: ν(SO₂ sym) = 1311 (s), ν(SO₂ asym) = 1148 (vs) cm⁻¹.

Synthesis of 4.9b

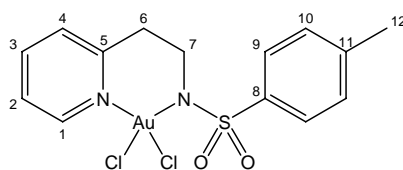
4.6b (0.329 g, 1.25 mmol) and aqueous (30 mL) H[AuCl₄].4H₂O (0.515 g, 1.25 mmol) were refluxed with stirring for 3 hours, resulting in the formation of a red/orange precipitate. This was filtered, washed with water (2 × 10 mL) and isopropanol (1 × 10 mL). The crude product was recrystallised by dissolving in minimal dichloromethane, filtering off the insoluble yellow precipitate, and adding diethyl ether to the filtrate until the solution went cloudy. The resulting dark red crystals were filtered and washed with diethyl ether (2 × 10 mL) and dried to give 0.436 g (66%) of **4.9b**.

Found: C 29.7, H 2.6, N 5.4; C₁₃H₁₃N₂O₂SCl₂Au requires C 29.5, H 2.5, N 5.3%.

NMR (d₆-DMSO): ¹H: δ 3.25 (br t, 2H, H-7), 3.48 (t, ³J_{6,7} = 6.4 Hz, 2H, H-6), 7.41 (t, ³J_{10,11} = 7.5 Hz, ³J_{10,9} = 7.0 Hz, 2H, H-10), 7.48 (t, ³J_{11,10} = 7.5 Hz, 1H, H-11), 7.70 (d, ³J_{9,10} = 7.0 Hz, 2H, H-9), 7.75 (ddd, ³J_{2,1} = 6.0 Hz, ³J_{2,3} = 7.8 Hz, ⁴J_{2,4} = 1.7 Hz, 1H, H-2), 7.77 (dd, ³J_{4,3} = 7.7 Hz, ⁴J_{4,2} = 1.7 Hz, 1H, H-4), 8.25 (td, ³J_{3,2} = 7.8 Hz, ³J_{3,4} = 7.7 Hz, ⁴J_{3,1} = 1.4 Hz, 1H, H-3), 8.95 (dd, ³J_{1,2} = 6.0 Hz, ⁴J_{1,3} = 1.4 Hz, 1H, H-1); ¹³C{¹H}: δ 37.6 (C-6), 42.4 (C-7), 126.0 (C-2), 126.7 (C-9), 127.7 (C-4), 128.9 (C-10), 131.9 (C-11), 140.6 (C-8), 143.9 (C-3), 149.7 (C-1), 155.5 (C-5) ppm (see Scheme 4.8 for the NMR numbering scheme).

ESI-MS: NaCl added: 547 (55%, [M-Cl+OMe+Na]⁺), 551 (100%, [M+Na]⁺), 1079 (25%, [2M+Na]⁺); pyridine added: 568 (100%, [M-2Cl+py+OMe]⁺), 572 (78%, [M-Cl+py]⁺).

IR: ν(SO₂ sym) = 1320 (s), ν(SO₂ asym) = 1149 (vs) cm⁻¹.



Scheme 4.8 NMR numbering scheme for **4.9a** and **4.9b**.

Synthesis of **4.10**

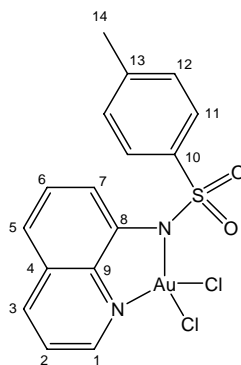
8-(*p*-Tosylamino)quinoline **4.7** (0.176 g, 0.590 mmol) was suspended in aqueous (30 mL) H[AuCl₄].4H₂O (0.243 g, 0.590 mmol) and refluxed with stirring for 8 hours. When the mixture reached reflux temperature, a brown solid formed that remained present throughout the duration of the reaction. The mixture was allowed to cool before being filtered, washed with H₂O (2 × 10 mL) and isopropanol (2 × 10 mL) and dried under vacuum, to give **4.10** as a brown solid (0.241 g, 72 %).

Found: C 33.9, H 2.3, N 5.0; C₁₆H₁₃N₂O₂SCl₂Au requires C 34.0, H 2.3, N 5.0%.

NMR (d₆-DMSO): ¹H: δ 2.30 (s, 3H, H-14), 7.26 (d, ³J_{12,11} = 8.3 Hz, 2H, H-12), 7.67 (d, ³J_{11,12} = 8.3 Hz 2H, H-11), 7.76 (t, ³J_{6,7/5} = 7.7 Hz, 1H, H-6), 7.81 (dd, ³J_{7,6} = 7.7 Hz, ⁴J_{7,5} = 1.6 Hz, 1H, H-7), 7.86 (dd, ³J_{5,6} = 7.7 Hz, ⁴J_{5,7} = 1.6 Hz, 1H, H-5), 7.93 (dd, ³J_{2,1} = 5.6 Hz, ³J_{2,3} = 8.3 Hz, 1H, H-2), 8.92 (dd, ³J_{3,2} = 8.3 Hz, ⁴J_{3,1} = 1.1 Hz, 1H, H-3), 9.21 (dd, ³J_{1,2} = 5.6 Hz, ⁴J_{1,3} = 1.1 Hz, 1H, H-1); ¹³C{¹H}: δ 21.1 (C-14), 123.5 (C-2), 124.3 (C-5), 125.9 (C-7), 126.8 (C-11), 129.7 (C-12), 130.0 (C-6), 130.7 (C-4), 138.8 (C-10), 143.3 (C-13), 143.7 (C-9), 144.0 (C-3), 146.0 (C-8), 148.1 (C-1) ppm (see Scheme 4.9 for the NMR numbering scheme).

ESI-MS: NaCl added: 587 (100%, [M+Na]⁺); pyridine added: 608 (100%, [M-Cl+py]⁺), 604 (35%, [M-2Cl+py+OMe]⁺).

IR: ν(SO₂ sym) = 1326 (s), ν(SO₂ asym) = 1158 (vs) cm⁻¹.



Scheme 4.9 NMR numbering scheme for **4.10**.

Attempted preparation of **4.15**

(i) **Reflux with H[AuCl₄] in water.** **4.14** (0.310 g, 1.25 mmol) was refluxed with stirring in aqueous (30 mL) H[AuCl₄].4H₂O (0.515 g, 1.25 mmol) for 1 hour, after which a brown solid had formed. When cool, the solution was filtered and the solid washed with water (2 × 10 mL) and isopropanol (1 × 10 mL) to give 0.188 g (26%) of a brown solid, which was identified as the salt **4.16**.

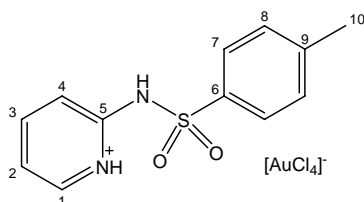
NMR (CDCl₃): ¹H δ 2.38 (s, 3H, H-10), 6.80 (ddd, ³J_{2,1} = 5.9 Hz, ³J_{2,3} = 7.1 Hz, ⁴J_{2,4} = 1.1 Hz, 1H, H-2), 7.24 (d, ³J_{8,7} = 8.1 Hz, 2H, H-8), 7.40 (dd, ³J_{4,3} = 8.9 Hz, ⁴J_{4,2} = 1.1 Hz, 1H,

H-4), 7.64 (ddd, $^3J_{3,2} = 7.1$ Hz, $^3J_{3,4} = 8.9$ Hz, $^4J_{3,1} = 1.9$ Hz, 1H, H-3), 7.79 (d, $^3J_{7,8} = 8.1$ Hz, 2H, H-7), 8.34 (dd, $^3J_{1,2} = 5.9$ Hz, $^4J_{1,3} = 1.9$ Hz, 1H, H-1), NH not observed; $^{13}\text{C}\{^1\text{H}\}$: δ 21.6 (C-10), 114.7 (C-2), 115.1 (C-4), 127.0 (C-7), 129.7 (C-8), 138.8 (C-6), 141.5 (C-1), 141.9 (C-3), 143.1 (C-9), 155.0 (C-5) ppm (see Scheme 4.10 for the NMR numbering scheme).

ESI-MS: (+ve): 249 (100%, [**4.14**+H] $^+$); (-ve): 339 (100%, [AuCl_4] $^-$).

(ii) **Standing with H[AuCl₄] in MeCN/H₂O solution.** **4.14** (0.108 g, 0.43 mmol) was dissolved in MeCN (5 mL) and added dropwise to aqueous (20 mL) H[AuCl₄].4H₂O (0.177 g, 0.43 mmol). The solution was left to stand and after 2 weeks a light brown solid had formed. This was filtered and washed with water (2 × 10 mL) and ether (1 × 10 mL), to give 0.078 g (31%) of **4.16**, which was identified by ESI-MS and ^1H NMR spectroscopy.

(iii) **Refluxing in MeCN/H₂O.** **4.14** (0.050 g, 0.20 mmol) and H[AuCl₄].4H₂O (0.082 g, 0.20 mmol) were refluxed in aqueous (20 mL) MeCN (1:1) with stirring for 3 hours. The solution was left to stand overnight and brown crystals were formed. These were subsequently identified as **4.16** (0.037g, 31%).



Scheme 4.10 NMR numbering scheme for **4.16**.

4.4.3 X-ray crystal structure determinations of **4.8c** and **4.10** · CH₂Cl₂

Single crystals of **4.8c** and **4.10** · CH₂Cl₂ suitable for X-ray structure analysis were obtained by slow diffusion of diethyl ether into a dichloromethane solution of the compound, at room temperature and -20 °C respectively. Complex **4.8c** crystallised as orange prisms with two independent molecules per asymmetric unit and **4.10** · CH₂Cl₂ as brown blocks as a dichloromethane solvate.

Table 4.3 Crystal and refinement data for the complexes **4.8c** and **4.10** · CH₂Cl₂.

Complex	4.8c	4.10 · CH ₂ Cl ₂
Formula	C ₇ H ₉ AuCl ₂ N ₂ O ₂ S	C ₁₆ H ₁₃ AuCl ₂ N ₂ O ₂ S · CH ₂ Cl ₂
Molecular Weight	453.09	650.14
<i>T</i> /K	89	93
Crystal system	Triclinic	Monoclinic
Space group	<i>P</i> -1	<i>P</i> 2 ₁ / <i>n</i>
<i>a</i> (Å)	7.3424(1)	14.1782(6)
<i>b</i> (Å)	9.281(1)	10.6792(5)
<i>c</i> (Å)	17.2700(2)	14.4771(6)
α (°)	99.383(1)	90
β (°)	95.785(1)	115.147(2)
γ (°)	102.127(1)	90
<i>V</i> (Å ³)	1124.06(2)	1984.2(2)
<i>Z</i>	4	4
<i>D</i> _{calc} (g cm ⁻³)	2.677	2.176
<i>T</i> _{max,min}	0.1699, 0.1138	0.2950, 0.0597
Number of unique reflections	4562	6252
Number of observed reflections [<i>I</i> >2σ(<i>I</i>)]	4360	5476
R[<i>I</i> >2σ(<i>I</i>)]	0.0203	0.0293
wR ₂ (all data)	0.0512	0.0868
Goodness of Fit	1.117	1.046

Data Collection

Intensity data and unit cell dimensions were obtained at the University of Auckland on a Bruker Smart CCD Diffractometer (**4.8c**) and at the University of Canterbury on a Bruker Apex II Diffractometer (**4.10** · CH₂Cl₂). The data were corrected for absorption using SADABS.⁽³¹⁾ Crystal and refinement data for the complexes are presented in Table 4.3. The crystallographic information files for the complexes are included on the supplementary CD.

Solution and refinement

The structures of **4.8c** and **4.10** · CH₂Cl₂ were solved using the Patterson and Direct methods options of SHELXS-97⁽³²⁾ respectively. The gold atom was initially located, followed by the

location of all other non-hydrogen atoms by a series of difference maps. Full-matrix least-squares refinement (SHELXL-97)⁽³³⁾ was based upon F_o^2 with all non-hydrogen atoms anisotropic, and hydrogen atoms in calculated positions.

4.5 References

1. J. H. Billman and R. Chernin; *Analyt. Chem.*, **1962**, 34, 408.
2. M. L. Durán, J. A. García-Vázquez, J. Romero, A. Castiñeiras, A. Sousa, A. D. Garnovskii and D. A. Garnovskii; *Polyhedron*, **1997**, 16, 1707.
3. L. Gutierrez, G. Alzuet, J. Borrás, M. Liu-González, F. Sanz and A. Castiñeiras; *Polyhedron*, **2001**, 20, 703.
4. E. V. Rybak-Akimova, A. Y. Nazarenko, L. Chen, P. W. Krieger, A. M. Herrera, V. V. Tarasov and P. D. Robinson; *Inorg. Chim. Acta*, **2001**, 324, 1.
5. A. Congreve, R. Katakya, M. Knell, D. Parker, H. Puschmann, K. Senanayake and L. Wylie; *New. J. Chem.*, **2003**, 27, 98.
6. J. P. Malval, R. Lapouyade, J.-M. Léger and C. Jarry; *Photochem. Photobiol. Sci.*, **2003**, 2, 259.
7. B. Macías, M. V. Villa, E. Fiz, I. García, A. Castiñeiras, M. González-Álvarez and J. Borrás; *J. Inorg. Biochem.*, **2002**, 88, 101.
8. B. Macías, M. V. Villa, I. García, A. Castiñeiras, J. Borrás and R. Cejudo-Marin; *Inorg. Chim. Acta*, **2003**, 342, 241.
9. B. Macías, I. García, M. V. Villa, J. Borrás, M. González-Álvarez and A. Castiñeiras; *J. Inorg. Biochem.*, **2003**, 96, 367.
10. B. Macías, M. V. Villa, M. Salgado, J. Borrás, M. González-Álvarez and F. Sanz; *Inorg. Chim. Acta*, **2006**, 359, 1465.
11. M. González-Álvarez, G. Alzuet, J. Borrás, B. Macías and A. Castiñeiras; *Inorg. Chem.*, **2003**, 42, 2992.
12. B. Macías, I. García, M. V. Villa, J. Borrás, A. Castiñeiras and F. Sanz; *Polyhedron*, **2002**, 21, 1229.
13. M. L. Durán, J. A. García-Vázquez, C. Gómez, A. Sousa-Pedrares, J. Romero and A. Sousa; *Eur. J. Inorg. Chem.*, **2002**, 2348.
14. F. Simal, A. Demonceau and A. F. Noels; *Tetrahedron Lett.*, **1999**, 40, 63.
15. C. A. Otter, S. M. Couchman, J. C. Jeffery, K. L. V. Mann, E. Psillakis and M. D. Ward; *Inorg. Chim. Acta*, **1998**, 278, 178.
16. S. M. Couchman, J. M. Dominguez-Vera, J. C. Jeffery, C. A. McKee, S. Nevitt, M. Pohlman, C. M. White and M. D. Ward; *Polyhedron*, **1998**, 17, 3541.

17. D. T. Hill, K. Burns, D. D. Titus, G. R. Girard, W. M. Reiff and L. M. Mascavage; *Inorg. Chim. Acta*, **2003**, 346, 1.
18. D. Fan, C.-T. Yang, J. D. Ranford and J. J. Vittal; *Dalton Trans.*, **2003**, 4749.
19. S. Schouteeten, O. R. Allen, A. D. Haley, G. L. Ong, G. D. Jones and D. A. Vivic; *J. Organomet. Chem.*, **2006**, 691, 4975.
20. K. J. Kilpin, W. Henderson and B. K. Nicholson; *Polyhedron*, **2007**, 26, 434.
21. C. Evans, W. Henderson and B. K. Nicholson; *Inorg. Chim. Acta*, **2001**, 314, 42.
22. W. Henderson and C. Evans; *Inorg. Chim. Acta*, **1999**, 294, 183.
23. M. B. Dinger and W. Henderson; *J. Organomet. Chem.*, **1998**, 560, 233.
24. R. G. Buckley, A. M. Elsome, S. P. Fricker, G. R. Henderson, B. R. C. Theobald, R. V. Parish, B. P. Howe and L. R. Kelland; *J. Med. Chem.*, **1996**, 39, 5208.
25. W. Henderson; *Adv. Organomet. Chem.*, **2006**, 54, 207.
26. B. D. Alexander, P. D. Boyle, B. J. Johnson, J. A. Casalnuovo, S. M. Johnson, A. M. Mueting and L. H. Pignolet; *Inorg. Chem.*, **1987**, 26, 2547.
27. W. Henderson, B. K. Nicholson, S. J. Faville, D. Fan and J. D. Ranford; *J. Organomet. Chem.*, **2001**, 631, 41.
28. W. J. Houlihan, S. H. Cheon, D. A. Handley and D. A. Larson; *J. Lipid Mediator.*, **1991**, 3, 91.
29. M. Doering, E. Mueller, E. Uhlig and B. Undeutsch; *Z. Anorg. Allg. Chem.*, **1987**, 547, 7.
30. M. H. Klingele, B. Moubaraki, K. S. Murray and S. Brooker; *Chem-Eur. J.*, **2005**, 11, 6962.
31. R. H. Blessing; *Acta Cryst. Sect. A*, **1995**, 51, 33.
32. G. M. Sheldrick, SHELXS-97 - A Program for the Solution of Crystal Structures, University of Göttingen, Germany, **1997**.
33. G. M. Sheldrick, SHELXL-97 - A Program for the Refinement of Crystal Structures, University of Göttingen, Germany, **1997**.

CHAPTER FIVE

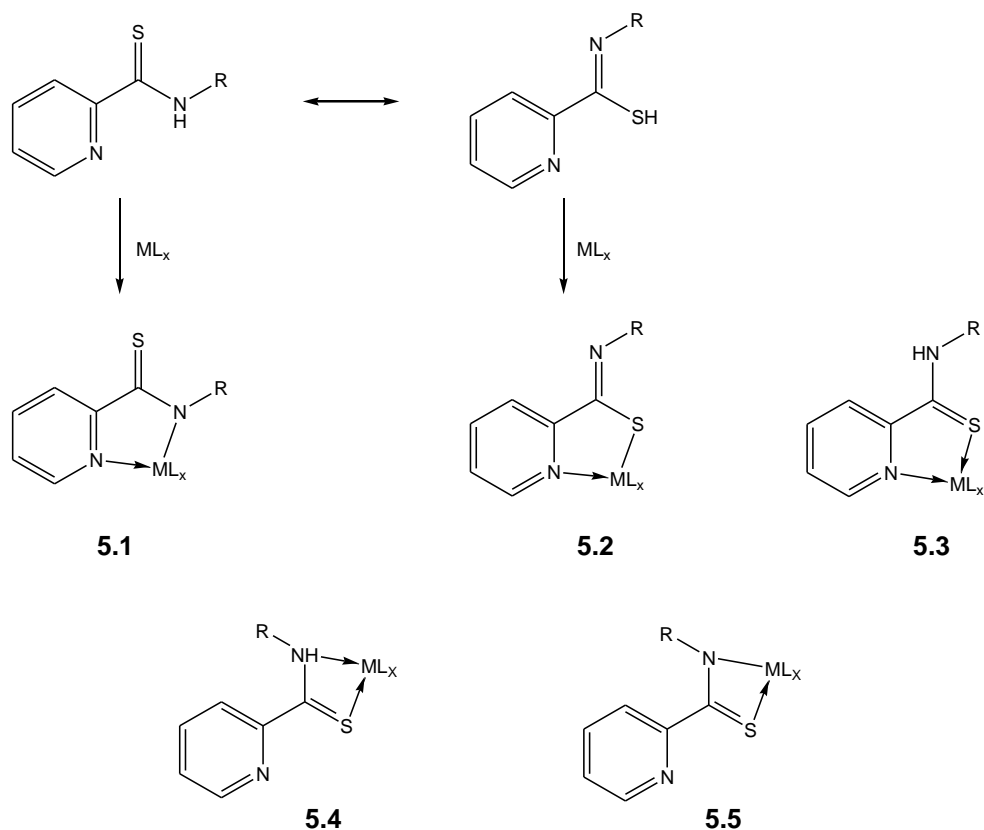
The Cycloauration of Pyridine-2-Thiocarboxamide Ligands

5.1 Introduction

5.1.1 *N*-Substituted pyridine-2-thiocarboxamides as bidentate ligands

N-Substituted pyridine-2-thiocarboxamides are interesting bidentate ligands as they have the potential to coordinate to metal centres in a number of different ways, as depicted in Scheme 5.1. Firstly, deprotonation of the ligand may occur prior to coordination and because thioamides have two tautomeric forms they may act as either a monoanionic *N, N'* (coordination of thioketo tautomer **5.1**) or *S, N* (coordination of the thiol form **5.2**) bidentate ligand. Alternatively, the neutral ligand may coordinate to the metal centre *via* the pyridyl nitrogen and sulfur atoms **5.3**. In these cases, five-membered chelates result. However, coordination *via* the amide nitrogen and the sulfur (either as the neutral ligand **5.4** or after deprotonation **5.5**) would give four-membered metallacycles. In the case of the deprotonated ligand both tautomeric forms will again be present, only the thioketo isomer **5.5** is shown in Scheme 5.1.

Although there are a number of synthetic routes to *N*-substituted pyridine-2-thiocarboxamides, the most attractive preparative method involves the reaction of an amine with sulfur in refluxing 2-methylpyridine in the presence of a catalytic amount (2 mol %) of sodium sulfide nonahydrate (a modified Willgerodt-Kindler reaction).⁽¹⁾ Yields of the thioamides are excellent (>70 %) and there is the opportunity to tune the steric and electronic properties of the products easily by varying the amines used.



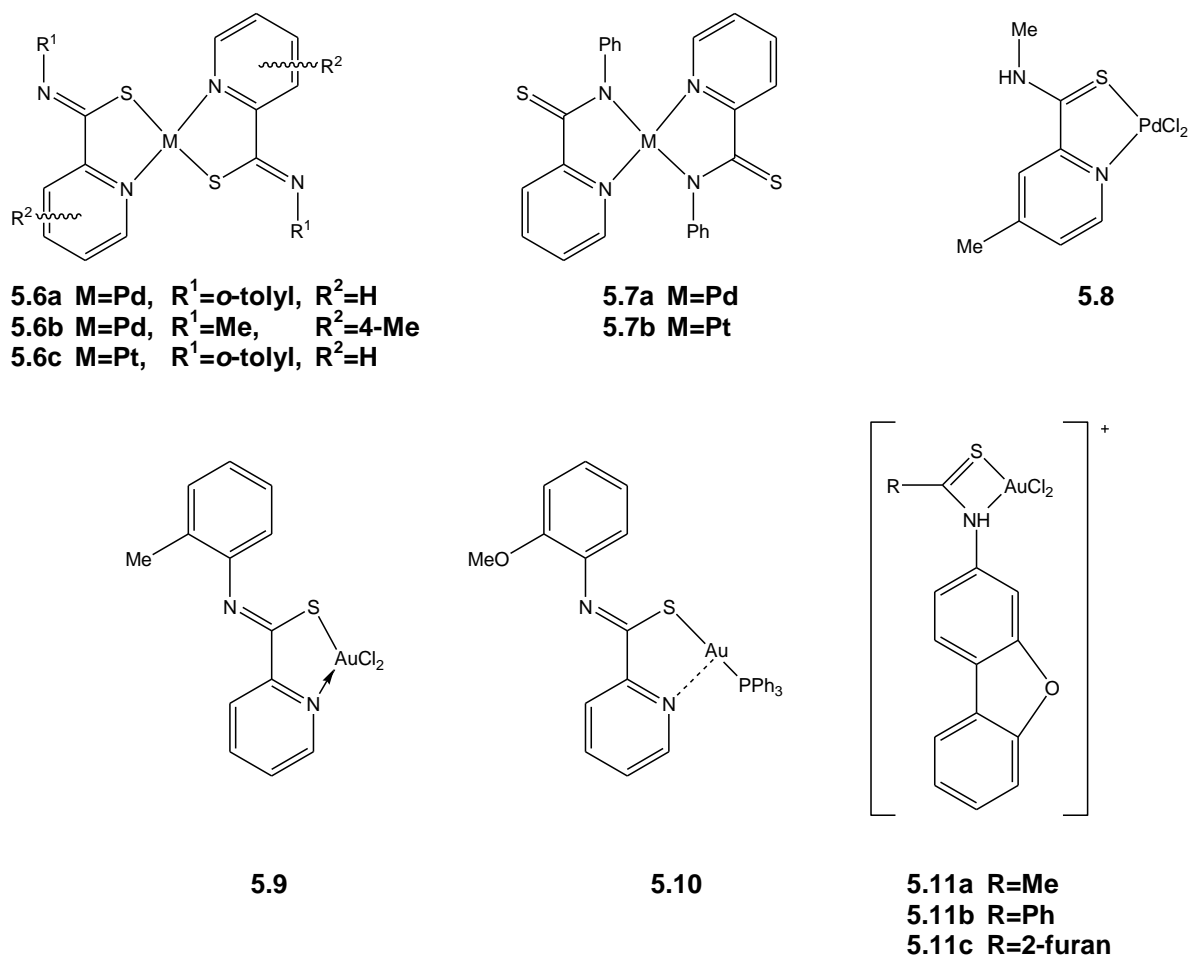
Scheme 5.1 Possible bidentate coordination modes of *N*-substituted pyridine-2-thiocarboxamide ligands.

5.1.2 Coordination complexes of *N*-substituted pyridine-2-thiocarboxamides with heavy transition metals

The literature contains a vast number of examples of *N*-substituted pyridine-2-thiocarboxamide coordination compounds, mostly containing copper(II) metal centres. Therefore this introduction will only briefly cover the coordination compounds that contain either palladium, platinum or gold d^8 metal centres. Unfortunately, most examples appear in the non-English literature (*i.e.* either Russian or German language publications) so a full review could not be carried out.

Palladium(II) complexes of *N*-substituted pyridine-2-thiocarboxamides have been reported for the three coordination modes that are described in Scheme 5.1 (**5.6a, b**, **5.7a**, **5.8**, Scheme 5.2).⁽²⁻⁴⁾ Examples of platinum(II) complexes also exist, with the ligand coordinated *via* either the *S, N* (**5.6c**)⁽²⁾ or *N, N'* (**5.7b**)⁽⁴⁾ binding modes. One example **5.9** of an *S, N* coordinated

gold(III) complex is reported, synthesised by the extraction of gold(III) from an HCl solution by the ligand.⁽²⁾ Although structural characterisation by X-ray crystallography was not reported for any of the above complexes, the coordination mode of the ligand was assigned using IR, UV-Vis and NMR spectroscopy. There is however, an example of a gold(I) complex where the structure has been elucidated by X-ray crystallography **5.10**. Not surprisingly, the thiol tautomer is deprotonated and the ligand is coordinated to the gold through the sulfur atom, with a weak interaction between the gold and the pyridyl nitrogen.⁽⁵⁾



Scheme 5.2 Examples of palladium, platinum and gold coordination complexes formed with *N*-substituted pyridine-2-thiocarboxamide ligands.

To the best of our knowledge, there are no examples of palladium, platinum and gold four-membered ring systems formed from *N*-substituted pyridine-2-thiocarboxamide ligands,

however the Polish literature cites several examples of four-membered cationic auracycles formed from the coordination of neutral thiocarboxamides ligands (**5.11a-c**, Scheme 5.2). Again the binding mode was proposed on the basis of elemental analysis and spectroscopy⁽⁶⁾ Scheme 5.2 depicts the complexes described above.

5.1.3 Scope of this work

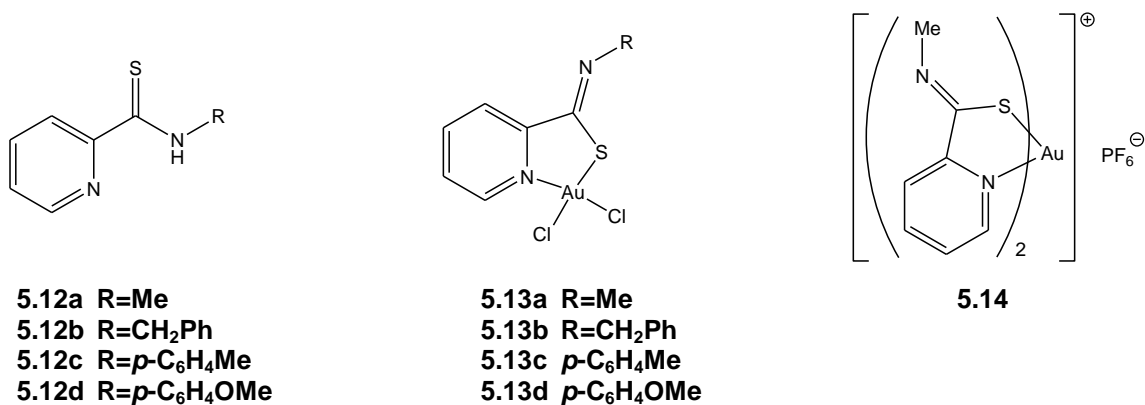
Although there are precedents in the literature for a cycloaurated *N*-substituted pyridine-2-thiocarboxamide ligand, structures have not been fully characterised. We wished to investigate the synthesis of these compounds *via* direct reaction with gold sources and subsequently fully characterise the compounds and assess their properties. Therefore, this Chapter describes the synthesis and characterisation of *N*-substituted pyridine-2-thiocarboxamide complexes.

5.2 Results and Discussion

5.2.1 Reaction of *N*-substituted pyridine-2-thiocarboxamide ligands **5.12a-d** with H[AuCl₄]

Reaction of the *N*-substituted pyridine-2-thiocarboxamide ligands **5.12a-d** with one molar equivalent of H[AuCl₄] in water gave the cycloaurated compounds **5.13a-d** in moderate to good yields. The reactivity of the ligands towards H[AuCl₄] was dependent on the *N*-substituent. For the methyl derivative (**5.12a**), the reaction took place rapidly (15 minutes) at room temperature. However, when the *N*-substituent was more electron withdrawing (*e.g.* **5.12c** and **5.12d**) the reaction needed more forcing conditions and the solution had to be refluxed before any reaction was observed. The intermediate benzyl substituted ligand **5.12b** required stirring at room temperature for five hours and any heating of this solution to reflux resulted in the reduction of the gold (observed as a gold mirror on the flask). In addition, when two equivalents of **5.12a** were reacted with H[AuCl₄] and NH₄PF₆ the complex **5.14** was formed in moderate yields.

The gold complexes **5.13a-c** were poorly soluble in MeOH, CH₂Cl₂, CHCl₃ and acetone. They were however soluble in DMSO but decomposition occurred after approximately six hours in solution. Complex **5.13d**, which contains a methoxy substituted phenyl ring was much more soluble in CH₂Cl₂, CHCl₃ and acetone. The complexes were characterised by NMR spectroscopy and microanalytical data. In addition an X-ray crystal structure of **5.13b** was obtained.



Scheme 5.3 *N*-substituted pyridine-2-thiocarboxamide ligands used in this study and the resulting thiocarboxamide complexes formed.

5.2.2 X-ray crystal structure of **5.13b**

An X-ray crystal structure determination of **5.13b** confirms that the thiol tautomer has been deprotonated which allows for the ligand to coordinate to the gold *via* the anionic sulfur and the neutral pyridyl nitrogen. The remaining two coordination sites on the square planar gold are occupied by *cis* chloride ligands. The compound has crystallised with two independent molecules in the asymmetric unit, which differ mainly in the conformation of the benzyl groups. The molecular structure and atom labelling scheme of one molecule is shown in Figure 5.1 and selected bond parameters are presented in Table 5.1. A full list of structural parameters, atomic coordinates and anisotropic displacement parameters can be found on the supplementary CD.

Excluding the benzyl moiety, the core of the molecule is essentially planar. In molecule 1 the benzyl ring is tilted from the main plane of the molecule at an angle of 18.88(8)°, however in molecule 2 the benzyl ring is twisted out of the plane of the molecule by 58.80(4)°. The two

molecules in the asymmetric unit pack together in such a way that there are two intermolecular Au-S interactions, with distances of 3.498 Å and 3.556 Å (Figure 5.2). However, this packing is only between the two molecules in the asymmetric unit and these dimers do not extend into chains that run throughout the structure. Presumably the planar nature of the two molecules allows such interactions in the solid state.

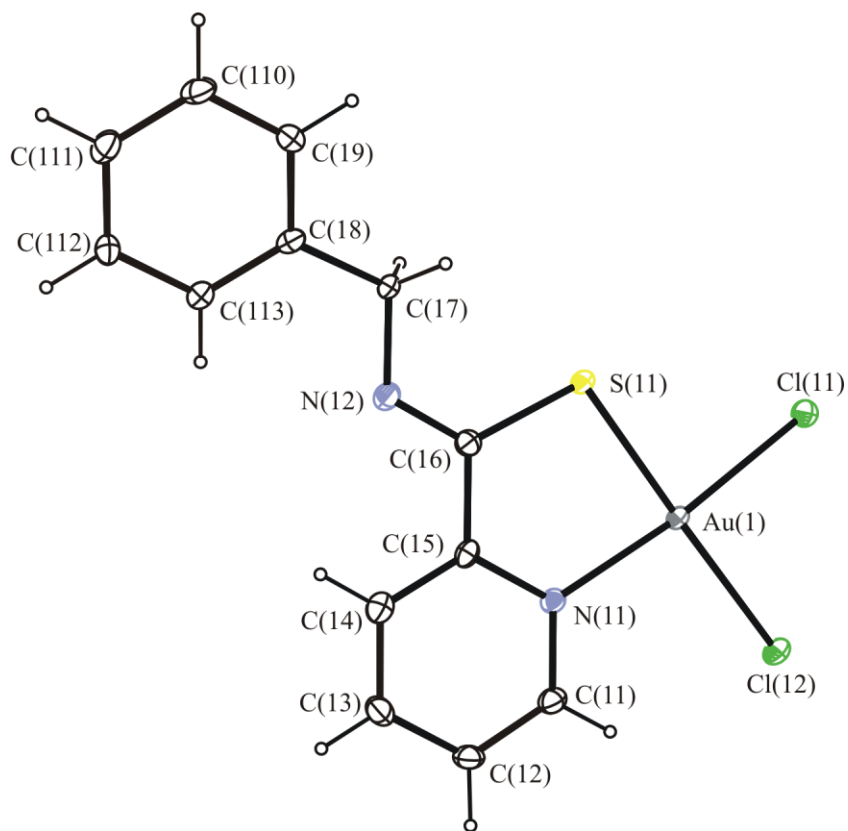


Figure 5.1 Molecular diagram of **5.13b** showing one of the unique molecules present in the asymmetric unit, and the atom numbering scheme. Thermal ellipsoids are shown at the 50% probability level.

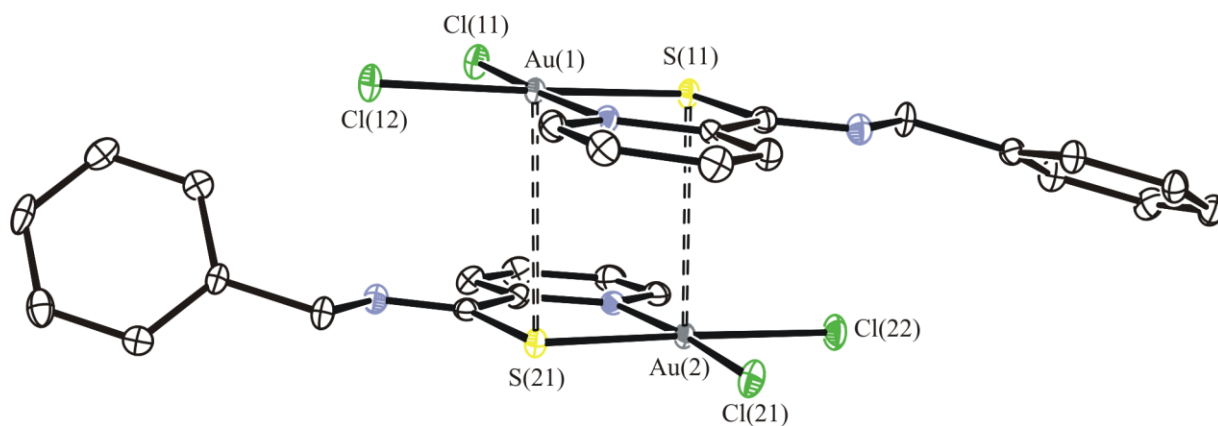


Figure 5.2 Diagram of showing the gold-sulfur interactions between the two molecules in the asymmetric unit of **5.13b**. The different orientations of the phenyl rings can also clearly be seen. Hydrogen atoms have been omitted for clarity and thermal ellipsoids are shown at the 50% probability level.

The C(6)-S(1) bond lengths of 1.772(3) Å (molecule 1) and 1.767(3) Å (molecule 2) in the gold complexes are longer than the C=S bond length (*ca.* 1.64 Å) in previously characterised *N*-substituted pyridine-2-thiocarboxamide ligands.^(7, 8) This is not surprising as the free ligands contain a formal C=S bond, in the gold complexes the bond order is reduced as it is the thiol tautomer that is coordinated. In addition, the C(6)-N(2) bond lengths in the cycloaurated complexes are 1.273(3) Å (molecule 1) 1.278(3) Å (molecule 2) and are shorter than in the free ligands (where they are *ca.* 1.33 Å).

The bite angles of the ligands in the complexes are 86.42(6)° and 86.71(6)° for molecule 1 and 2 respectively, and are comparable to deprotonated thioamides coordinated to square-planar Cu(II) or Ni(II) centres through a sulfur and pyridyl nitrogen.^(9, 10) As a result, the S(1)-C(6)-C(5) angles in the complexes are more acute than in the free ligands where they are *ca.* 121°. A gold(I) complex has been formed from the *N*-(2-methoxyphenyl)pyridine-2-thiocarboxamide ligand (**5.10**, Scheme 5.2). The sulfur is acting as an anionic donor, with enough of an interaction between the nitrogen of the 2-pyridyl group and the gold to hold the ligand in a pseudo-cyclic structure. However, the bite angle of the ligand is much less (78.82°).⁽⁵⁾

Table 5.1 Selected structural parameters for **5.13b** (both molecules), with esds in parentheses.

	Molecule 1	Molecule 2
<i>Bond lengths (Å)</i>		
Au(1) – Cl(1)	2.2709(6)	2.2746(7)
Au(1) – Cl(2)	2.3289(6)	2.3353(6)
Au(1) – S(1)	2.2747(6)	2.2723(6)
Au(1) – N(1)	2.051(2)	2.050(2)
N(1) – C(5)	1.359(3)	1.365(3)
C(5) – C(6)	1.479(3)	1.479(3)
C(6) – S(1)	1.772(3)	1.767(3)
C(6) – N(2)	1.273(3)	1.278(3)
N(2) – C(7)	1.454(3)	1.459(3)
<i>Bond angles (°)</i>		
Cl(1) – Au – Cl(2)	90.58(2)	91.35(2)
Cl(2) – Au – N(1)	95.29(6)	95.45(6)
Cl(1) – Au – S(1)	87.70(2)	86.48(2)
S(1) – Au – N(1)	86.42(6)	86.71(6)
Au – N(1) – C(5)	118.95(16)	118.58(16)
N(1) – C(5) – C(6)	118.1(2)	118.0(2)
C(5) – C(6) – S(1)	117.69(18)	117.98(18)
C(6) – S(1) – Au	98.77(8)	98.59(8)
C(6) – N(2) – C(7)	118.6(2)	117.6(2)

5.2.3 Spectroscopic characterisation of complexes **5.13a** – **5.13d**

Cycloauration of the ligands results in three main changes to the NMR spectra. Firstly, coordination of the electron-withdrawing gold atom to the pyridyl nitrogen causes a significant downfield shift of approximately 1.4 ppm for the proton adjacent to the nitrogen (H-1, Figure 5.3) when the spectra are acquired in CDCl₃ (in d₆-DMSO there is only 1 ppm difference). The amide proton (N-H) is lost upon coordination and is therefore not observed in the spectra of the cyclometallated complexes. Because of this, in **5.13a** and **5.13b** the H-7 protons change

from a doublet in the ligand to a singlet in the metallacycle as they are no longer coupled to the NH proton (*e.g.* H-7 in Figure 5.3). The most obvious change in the $^{13}\text{C}\{^1\text{H}\}$ spectra is the signal assigned to the thioketone carbon (C-6), which moves upfield by approximately 30 ppm (~ 190 ppm in the ligand to ~ 160 ppm in the metallacycle) upon coordination to the gold. This observation is in accordance with the suggestion that upon coordination of the sulfur to the gold the bond order of the C=S bond is reduced.

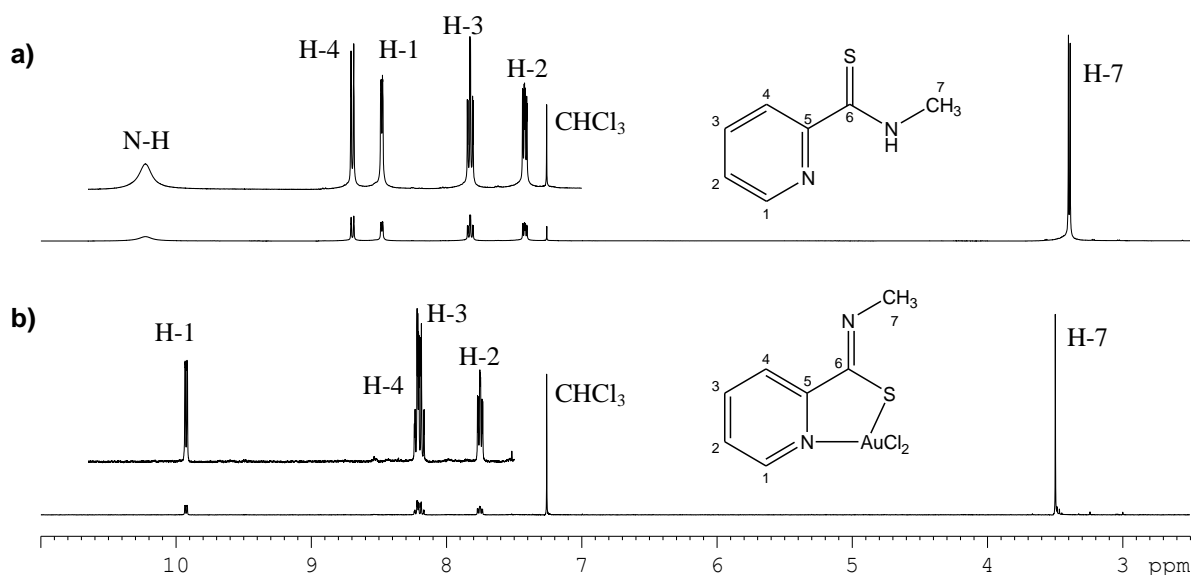


Figure 5.3 ^1H NMR spectra (CDCl_3) of (a) **5.12a** and (b) **5.13a**, showing the changes in the spectra upon coordination of the ligand to gold. The insets show the expanded aromatic regions (ligand assignment from reference 1).

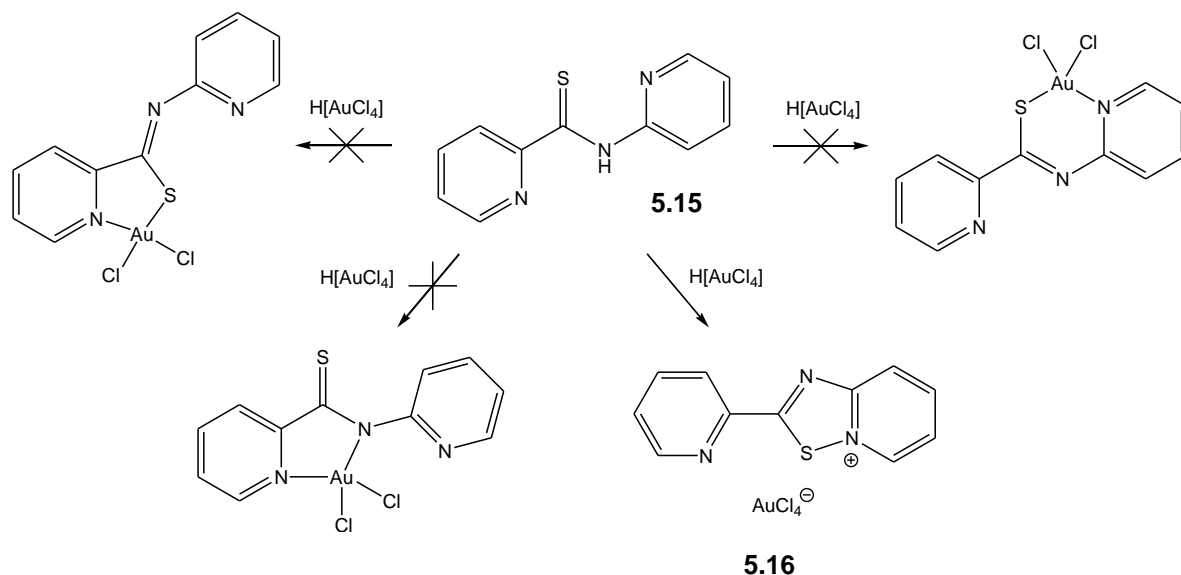
Characterisation of cycloaurated complexes by infrared spectroscopy is of little use. Other than the loss of the N-H stretch that is present in the ligand the main diagnostic band in the cycloaurated complexes would be in the C-S stretching region. However, the C-S stretch occurs in the region of $600\text{-}700\text{ cm}^{-1}$ and is weak and difficult to assign due to the multitude of other vibrations that occur in this region (*e.g.* aromatic C-H bending vibrations).⁽¹¹⁾ Therefore, this raises queries as to the mode of bonding in the previous cyclometallated *N*-substituted pyridine-2-thiocarboxamide complexes (mentioned in Section 5.1.2) that were assigned on the basis of IR spectroscopy.

5.2.4 Mass spectrometric characterisation of complexes 5.13a – 5.13d

Because of the lack of ionisable groups on the cycloaurated complexes they were not overly visible in ESI mass spectrometry experiments. Although small peaks are seen that arise from $[M+Na]^+$ cations, the main peak in the spectra were from the cationic species $[(L)_2Au]^+$, analogous to **5.14**, which was presumably only present in trace amounts as neither NMR or microanalysis found any evidence of it. We have previously seen this type of ion before as the most abundant in poorly ionising Au(III) dichloride complexes and found that addition of pyridine to the sample immediately before analysis results in substitution of a chloride ligand giving a cationic species which is easily visible.⁽¹²⁾ However when this method was applied to the cycloaurated complexes **5.13a** - **5.13d** the number of peaks present in the spectra (none of which were easily identifiable) increased substantially – it appears in this case the addition of pyridine causes rapid decomposition of the metallacycle.

5.2.5 Reaction of *N*-(2-pyridyl)pyridine-2-thiocarboxamide (**5.15**) with $H[AuCl_4]$

The ligand **5.15** was investigated as there was the possibility of forming either a five- or six-membered cyclometallated ring with the thioamide acting as a *S,N* donor ligand. In addition, deprotonation of the ligand may give a *N,N'* coordinated five-membered auracycle, as shown in Scheme 5.4. However, when **5.15** was reacted with one equivalent of $H[AuCl_4]$ the result was not as expected. Instead of cycloauration, the ligand was oxidised by the gold followed by internal cyclisation to form a 1,2,4-thiadiazolo[2,3-*a*]pyridinium heterocyclic ring system, with an $[AuCl_4]^-$ counter ion **5.16**. The structure was elucidated by an X-ray crystallographic study, with the molecular structure shown in Figure 5.4. Selected bond lengths and angles can be found in Table 5.2, full structural parameters along with atomic coordinates and anisotropic displacement factors can be found on the supplementary CD.



Scheme 5.4 Possible reactions products of the ligand **5.15** with $\text{H}[\text{AuCl}_4]$, including the salt obtained by oxidation and ring closure of the ligand **5.16**.

X-ray quality crystals of **5.16** were grown by diffusion of methanol into a DMSO solution of the crude sample. However, microanalysis of the crystals was inconsistent with this formulation and the crystal chosen for the diffraction study may not have been representative of the entire sample. Indeed, the crude yield is also inconsistent with the formulation **5.16** and it is likely that $[\text{AuCl}_2]^-$ and Cl^- anions are also present in the sample. Because both $[\text{AuCl}_2]^-$ and Cl^- are inherently present in the ESI mass spectrum of $[\text{AuCl}_4]^-$ it is difficult to confirm this assumption.

Few X-ray structural studies have been carried out on 1,2,4-thiadiazolo[2,3-*a*]pyridine ring systems. Compound **5.17** and the copper complex **5.18** (Scheme 5.5) represent the closest examples of structurally characterised compounds. As with the neutral species **5.17**⁽¹³⁾ and **5.18**^(14, 15) the cationic moiety of **5.16** is essentially planar. The C(6)–N(2) bond is 1.293(13) Å, very close to what is expected for a C=N bond. The bonds C(5)–C(6), C(7)–N(2) and C(6)–S(1) all have distances which fall between the values expected for either a double or a single bond suggesting some conjugation is present in the system. The $[\text{AuCl}_4]^-$ anion has a regular square planar geometry as expected.

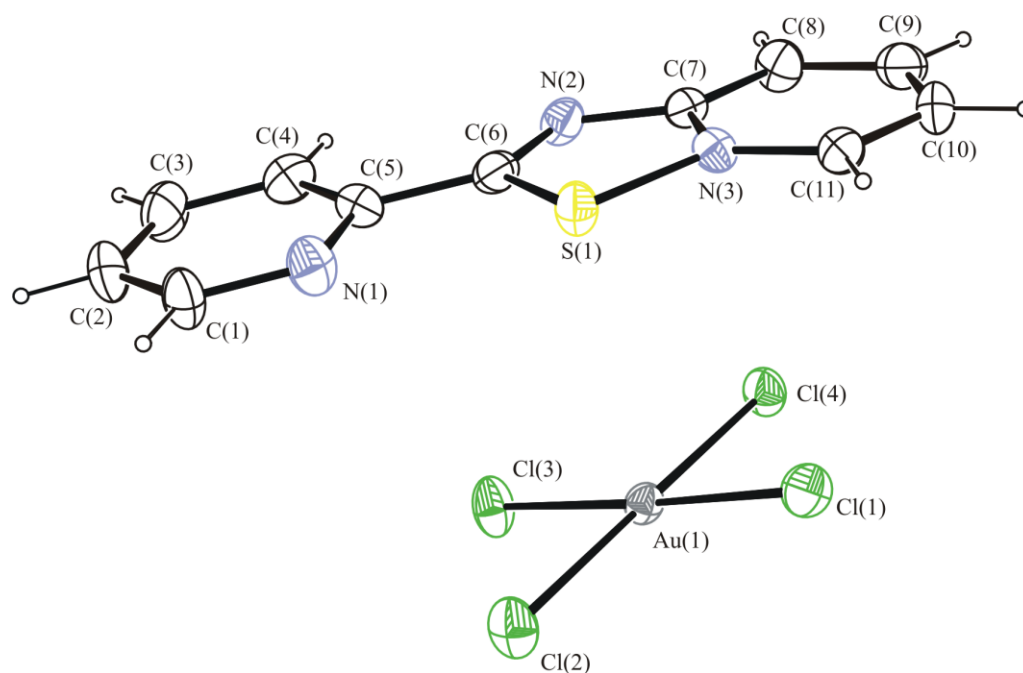
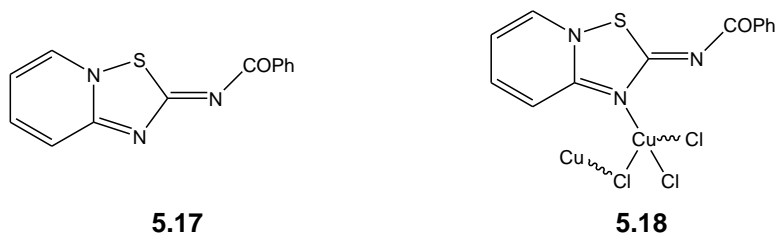


Figure 5.4 Molecular diagram of **5.16** showing the atom labelling scheme. Thermal ellipsoids are shown at the 50% probability level.

Table 5.2 Selected structural parameters for **5.16** (esds in parentheses)

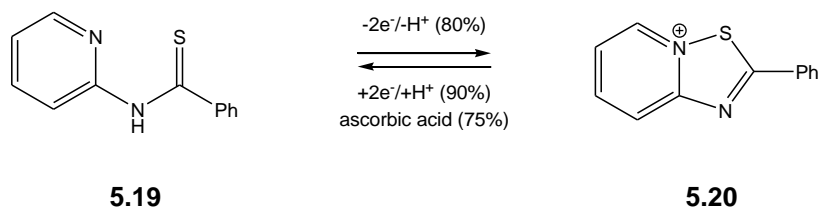
Atoms	Lengths (Å)	Atoms	Angles (°)
N(3) – C(7)	1.378(12)	C(4) – C(5) – C(6)	123.0(9)
C(7) – N(2)	1.376(12)	N(1) – C(5) – C(6)	113.0(9)
N(2) – C(6)	1.293(13)	C(5) – C(6) – S(1)	115.5(7)
C(6) – S(1)	1.727(10)	C(5) – C(6) – N(2)	127.4(9)
S(1) – N(3)	1.704(8)	N(2) – C(6) – S(1)	117.1(8)
C(5) – C(6)	1.462(14)	C(6) – S(1) – N(3)	87.2(4)
		S(1) – N(3) – C(7)	112.3(6)
		N(3) – C(7) – N(2)	113.3(8)
		C(7) – N(2) – C(6)	110.1(8)



Scheme 5.5 Structurally characterised compounds that contain a 1,2,4-thiadiazolo[2,3-*a*]pyridine heterocyclic ring

NMR spectroscopy and ESI mass spectrometry are consistent with the X-ray structural analysis. The proton adjacent to the pyridinium nitrogen (H-11) is further downfield (~0.7 ppm) than the equivalent proton in the free ligand, however a greater shift (~1 ppm) would be expected if a cycloaurated complex had formed. In addition, the carbon arising from the thioketone group (C-6) has shifted upfield from 188.2 ppm in the ligand to 181.9 ppm in the cation. In the cycloaurated complexes, the shift has been much more significant (~30 ppm) and is further evidence for some conjugation in the system. The ESI mass spectrum shows a single peak at m/z 214.043 which corresponds to the pyridinium cation.

In hindsight it is not surprising that oxidation and cyclisation of **5.15** has occurred. Both chemical and electrochemical oxidation of *N*-(2-pyridyl)thiocarboxamides has previously been used in the synthesis of 1,2,4-thiadiazolo[2,3-*a*]pyridinium species. For example, Tabakovič *et al.* have shown that oxidation of **5.19** at a graphite anode gives the cation **5.20**, with the process being reversible either by reduction at a platinum cathode or by reaction with ascorbic acid (Scheme 5.6).⁽¹⁶⁾ Other reagents such as nitrosobenzene,⁽¹⁷⁾ sulfonyl chloride⁽¹⁸⁾ and Cu(III) ions⁽¹⁹⁾ have also been shown to oxidise species containing the 2-pyridylthioamide moiety to heterocyclic species



Scheme 5.6 Electrochemical synthesis 1,2,4-thiadiazolo[2,3-*a*]pyridinium species that was demonstrated by Tabakovič *et al.*

5.3 Conclusions

Five new cyclometallated gold(III) complexes containing mono-anionic *N*-substituted pyridine-2-thiocarboxamide donor ligands have been synthesised and fully characterised, including the X-ray crystal structure of one of the complexes. This unambiguously shows that the thiol tautomer (*i.e.* the deprotonated sulfur) has coordinated to the metal centre *via* the sulfur and nitrogen atoms. Unlike the more common cycloaurated complexes that contain mono-anionic *C,N* donor ligands these compounds show poor stability and decompose over a short period of time (approximately six hours in solution). This is not surprising; in the cycloaurated thiocarboxamide complexes described above there is an easily oxidised sulfur centre neighbouring a highly reducible gold(III) centre. Therefore, although the synthesis of these cycloaurated complexes is facile, they appear to have limited applications because of the inherent instability they possess. Interestingly, the 2-pyridyl substituted ligand does not undergo analogous cyclometallation. Instead, the ligand is oxidised and an internal cyclisation occurs to give a 1,2,4-thiadiazolo[2,3-*a*]pyridinium heterocyclic ring.

5.4 Experimental

5.4.1 General

The *N*-substituted pyridine-2-thiocarboxamides used in this study were prepared by literature the methods⁽¹⁾, with their purity assessed by ¹H NMR spectroscopy. Ligands **5.12a**, **5.12b** and **5.12c** were synthesised by Mr. Scott Carter. H[AuCl₄] was prepared by the method described in Appendix 1.

5.4.2 Syntheses

Synthesis of **5.13a**

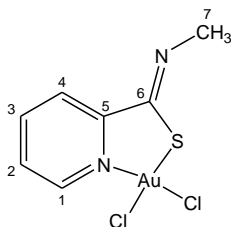
5.12a (0.200 g, 1.30 mol) and H[AuCl₄].4H₂O (0.536 g, 1.30 mol) were stirred in water (20 mL) for 20 minutes during which time a brown solid formed. The solution was filtered and

the brown solid washed with water (2 × 10 mL) and isopropanol (1 × 10 mL) and air dried to give 0.413 g (76%) of **5.13a** as a brown solid.

Found: C 20.4, H 1.9, N 6.4; C₇H₇N₂SCl₂Au requires C 20.1, H 1.7, N 6.7%.

NMR (CDCl₃): ¹H δ 3.50 (s, 3H, H-7), 7.75 (ddd, ³J_{2,1} = 6.1 Hz, ³J_{2,3} = 7.0 Hz, ⁴J_{2,4} = 2.1 Hz, 1H, H-2), 8.19 (ddd, ³J_{3,2} = 7.0 Hz, ³J_{3,4} = 8.1 Hz, ⁴J_{3,1} = 1.4 Hz, 1H, H-3), 8.23 (dd, ³J_{4,3} = 8.1 Hz, ⁴J_{4,2} = 2.1 Hz, 1H, H-4), 9.93 (dd, ³J_{1,2} = 6.1 Hz, ⁴J_{1,3} = 1.4 Hz, 1H, H-1); ¹³C{¹H} δ 40.8 (C-7), 127.0 (C-3), 128.5 (C-2), 142.3 (C-4), 148.3 (C-1), 158.6 (C-5), 162.3 (C-6) ppm (see Scheme 5.7 for the NMR numbering scheme).

ESI-MS: *m/z*: 499.034 (100%, [(L)₂Au]⁺, calc 499.032), 440.930 (78%, [M+Na]⁺, calc 440.927), 418.947 (65%, [M+H]⁺, calc 418.945).



Scheme 5.7 NMR numbering scheme for **5.13a**.

Synthesis of **5.13b**

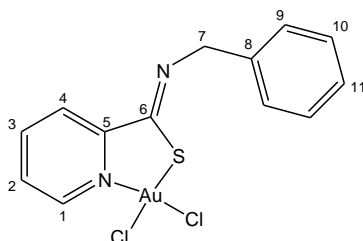
5.12b (0.100 g, 0.44 mmol) and H[AuCl₄].4H₂O (0.180 g, 0.44 mmol) were stirred in water (10 mL) for 5.5 hours during which time a pale yellow solid formed. The solution was filtered and the light yellow solid washed with water (2 × 10 mL) and isopropanol (1 × 10 mL) and air dried to give 0.107 g (49%) of **5.13b** as a pale yellow solid.

Found: C 31.8, H 2.3, N 5.5; C₁₃H₁₁N₂SCl₂Au requires C 31.5, H 2.2, N 5.7%.

NMR (*d*₆-DMSO): ¹H δ 4.79 (s, 2H, H-7), 7.31 (d, ³J_{11,10} = 7.4 Hz, 1H, H-11), 7.38 (t, ³J_{10,9/11} = 7.4 Hz, 2H, H-10), 7.47 (d, ³J_{9,10} = 7.4 Hz, 2H, H-9), 8.02 (ddd, ³J_{2,1} = 6.0 Hz, ³J_{2,3} = 7.7 Hz, ⁴J_{2,4} = 1.7 Hz, 1H, H-2), 8.23 (dd, ³J_{4,3} = 8.0 Hz, ⁴J_{4,2} = 1.7 Hz, 1H, H-4), 8.41 (ddd, ³J_{3,2} = 7.7

Hz, $^3J_{3,4} = 8.0$ Hz, $^4J_{3,1} = 1.4$ Hz, 1H, H-3), 9.66 (dd, $^3J_{1,2} = 6.0$ Hz, $^4J_{1,3} = 1.4$ Hz, 1H, H-1); $^{13}\text{C}\{^1\text{H}\}$ δ 55.8 (C-7), 126.6 (C-4), 127.0 (C-11), 127.8 (C-9), 128.4(C-10), 129.6 (C-2), 138.6 (C-8), 143.5 (C-3), 148.2 (C-1), 157.1 (C-5), 161.5 (C-6) ppm (See Scheme 5.8 for the NMR numbering scheme).

ESI-MS: m/z : 651.099 (100%, $[(\text{L})_2\text{Au}]^+$, calc 651.095), 516.962 (5%, $[\text{M}+\text{Na}]^+$, calc 516.958).



Scheme 5.8 NMR numbering scheme for **5.13b**.

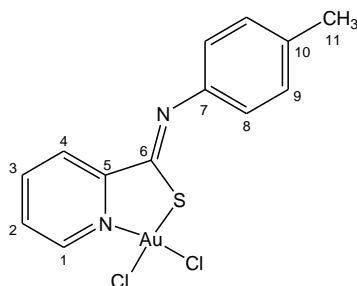
Synthesis of 5.13c

5.12c (0.200 g, 0.88 mmol) and $\text{H}[\text{AuCl}_4] \cdot 4\text{H}_2\text{O}$ (0.362 g, 0.88 mmol) were refluxed in water (20 mL) for 1 hour during which time a dark brown solid formed. The solution was filtered and the dark brown solid was washed with water (2×10 mL) and isopropanol (1×10 mL) and air dried to give 0.385 g (88%) of **5.13c** as a dark brown solid.

Found: C 31.9, H 2.2, N 5.6; $\text{C}_{13}\text{H}_{11}\text{N}_2\text{SCl}_2\text{Au}$ requires C 31.5, H 2.2, N 5.7%.

NMR (d_6 -DMSO): ^1H δ 2.34 (s, 3H, H-11), 7.00 (d, $^3J_{8,9} = 8.4$ Hz, 2H, H-8), 7.29 (d, $^3J_{9,8} = 8.4$ Hz, 2H, H-9), 8.08 (ddd, $^3J_{2,1} = 6.0$ Hz, $^3J_{2,3} = 7.6$ Hz, $^4J_{2,4} = 1.4$ Hz, 1H, H-2), 8.34 (dd, $^3J_{4,3} = 7.9$ Hz, $^4J_{4,2} = 1.4$ Hz, 1H, H-4), 8.48 (ddd, $^3J_{3,2} = 7.6$ Hz, $^3J_{3,4} = 7.9$ Hz, $^4J_{3,1} = 1.1$ Hz, 1H, H-3), 9.69 (dd, $^3J_{1,2} = 6.0$ Hz, $^4J_{1,3} = 1.1$ Hz, 1H, H-1); $^{13}\text{C}\{^1\text{H}\}$ δ 20.6 (C-11), 120.3 (C-8), 126.7 (C-4), 129.8 (C-9), 130.0 (C-2), 135.6 (C-10), 143.6 (C-3), 144.6 (C-7), 148.5 (C-1), 157.2 (C-5), 161.9 (C-6) ppm (see Scheme 5.9 for the NMR numbering scheme).

ESI-MS: m/z 516.957 (100%, $[M+Na]^+$, calc 516.958), 651.095 (49%, $[(L)_2Au]^+$, calc 651.095), 494.971 (14%, $[M+H]^+$, calc 494.976).



Scheme 5.9 NMR numbering scheme for **5.13c**.

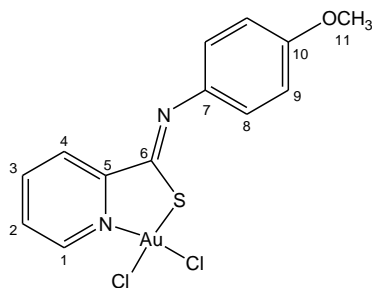
Synthesis of **5.13d**

5.12d (0.100 g, 0.41 mmol) and $H[AuCl_4] \cdot 4H_2O$ (0.169 g, 0.41 mmol) were refluxed in water (15 mL) for 1 hour during which time a dark coloured solid formed. The solution was cooled and filtered and the solid washed with water (2×10 mL) and isopropanol (1×10 mL). Air drying gave 0.107 g (51%) of **5.13d** as a dark brown solid.

Found: C 29.8, H 2.2, N 5.1; $C_{13}H_{11}N_2OSCl_2Au$ requires C 30.6, H 2.2, N 5.5%.

NMR ($CDCl_3$): δ 3.85 (s, 3H, H-11), 6.97 (d, $^3J_{9,8} = 9.0$ Hz, 2H, H-9), 7.22 (d, $^3J_{8,9} = 9.0$ Hz, 2H, H-8), 7.77 (ddd, $^3J_{2,1} = 6.0$ Hz, $^3J_{2,3} = 7.6$ Hz, $^4J_{2,4} = 1.6$ Hz, 1H, H-2), 8.23 (ddd, $^3J_{3,2} = 7.6$ Hz, $^3J_{3,4} = 8.1$ Hz, $^4J_{3,1} = 1.3$ Hz, 1H, H-3), 8.43 (dd, $^3J_{4,3} = 8.1$ Hz, $^4J_{4,2} = 1.6$ Hz, 1H, H-4), 9.96 (dd, $^3J_{1,2} = 6.0$ Hz, $^4J_{1,3} = 1.3$ Hz, 1H, H-1); $^{13}C\{^1H\}$ δ 55.7 (C-11), 114.6 (C-9), 124.1 (C-8), 127.4 (C-4), 128.5 (C-2), 140.4 (C-7), 142.1 (C-3), 148.6 (C-1), 158.4 (C-6), 158.9 (C-10), 159.8 (C-5) ppm (see Scheme 5.10 for the NMR numbering scheme).

ESI-MS: m/z 683.088 (100%, $[(L)_2Au]^+$, calc 683.084), 532.957 (10%, $[M+Na]^+$, calc 532.953).



Scheme 5.10 NMR numbering scheme for **5.13d**.

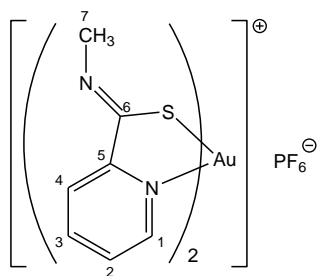
Synthesis of **5.14**

5.12a (0.050 g, 0.33 mmol), H[AuCl₄].4H₂O (0.066 g, 0.16 mmol) and NH₄PF₆ (0.054 g, 0.33 mmol) were stirred in water (10 mL) for 20 minutes. The pale brown solid that formed during this time was filtered off and washed with water (2 × 10 mL) and isopropanol (10 mL) to give 0.081 g (79%) of **5.14**.

Found: C 25.5, H 2.2, N 8.3; C₁₄H₁₄N₄F₆PS₂Au requires C 26.1, H 2.2, N 8.7%.

NMR (*d*₆-DMSO): ¹H δ 3.56 (s, 3H, H-7), 8.07 (ddd, ³J_{2,1} = 5.6 Hz, ³J_{2,3} = 7.6 Hz, ⁴J_{2,4} = 1.4 Hz, 1H, H-2), 8.28 (dd, ³J_{4,3} = 7.9 Hz, ⁴J_{4,2} = 1.4 Hz, 1H, H-4), 8.49 (ddd, ³J_{3,2} = 7.6 Hz, ³J_{3,4} = 7.9 Hz, ⁴J_{3,1} = 1.0 Hz, 1H, H-3), 8.89 (d, ³J_{1,2} = 5.6 Hz, 1H, H-1); ¹³C{¹H} δ 41.2 (C-7), 125.5 (C-4), 129.9 (C-2), 143.5 (C-3), 148.1 (C-1), 154.4 (C-5), 160.7 (C-6) ppm (see Scheme 5.11 for the NMR numbering scheme).

ESI-MS: *m/z* 499.033 (100%, [(L)₂Au]⁺, calc 499.032).



Scheme 5.11 NMR numbering scheme for **5.14**.

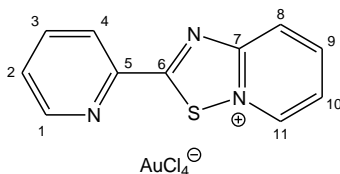
Reaction of 5.15 with H[AuCl₄]

5.15 (0.100 g, 0.46 mmol) was stirred in aqueous (15 mL) H[AuCl₄].4H₂O (0.190 g, 0.46 mmol) for 1 hour. The solution was filtered leaving a brown/orange solid that was washed with water (2 × 10 mL) and isopropanol (1 × 10 mL) and dried to give 0.144 g of **5.16**.

Found: C 26.8, H 1.8, N 6.9; C₁₁H₈N₃SCl₄Au requires C 23.9, H 1.5, N 7.6% (see section 5.2.5 for discussion).

NMR (*d*₆-DMSO): ¹H: δ 7.90 (dd, ³J_{2,1} = 4.6 Hz, ³J_{2,3} = 7.6 Hz, 1H, H-2), 8.04 (dd, ³J_{10,11} = 6.6 Hz, ³J_{10,9} = 7.4 Hz, 1H, H-10), 8.28 (dd, ³J_{3,2} = 7.6 Hz, ³J_{3,4} = 7.7 Hz, 1H, H-3), 8.42 (d, ³J_{4,3} = 7.7 Hz, 1H, H-4), 8.60 (dd, ³J_{9,10} = 7.4 Hz, ³J_{9,8} = 8.5 Hz, 1H, H-9), 8.73 (d, ³J_{8,9} = 8.5 Hz, 1H, H-8), 8.88 (d, ³J_{1,2} = 4.6 Hz, 1H, H-1), 9.75 (d, ³J_{11,10} = 6.6 Hz, 1H, H-11); ¹³C{¹H} δ 121.6 (C-4), 122.8 (C-10), 123.2 (C-8), 130.2 (C-2), 138.6 (C-11), 139.6 (C-3), 142.9 (C-9), 146.2 (C-5), 151.0 (C-1), 161.2 (C-7), 181.9 (C-6) ppm (see Scheme 5.12 for the NMR numbering scheme).

ESI-MS: *m/z* 214.043 (100%, [**5.15-H**]⁺, calc 214.043).



Scheme 5.12 NMR numbering scheme for **5.16**.

5.4.3 X-ray crystal structure determinations of 5.13b and 5.16

Crystals of **5.13b** were grown by slow diffusion of diethyl ether into a dichloromethane solution of the compound and **5.16** was crystallised by slow diffusion of methanol into a solution of the compound in DMSO, both at room temperature.

Data collection

Unit cell dimensions and reflection data for **5.13b** was collected at the University of Auckland on a Bruker Smart CCD Diffractometer and for **5.16** at the University of Canterbury on a Bruker Apex II Diffractometer. Semi-empirical absorption corrections were applied by SADABS.⁽²⁰⁾ Crystal and refinement data for the two complexes are presented in Table 5.3.

Table 5.3 Unit cell and crystallographic refinement data for the complexes **5.13b** and **5.16**.

Complex	5.13b	5.16
Formula	C ₁₃ H ₁₁ AuCl ₂ N ₂ S	C ₁₁ H ₈ AuCl ₄ N ₃ S
Molecular Weight	495.16	553.03
<i>T</i> /K	90	90
Crystal system	Triclinic	Monoclinic
Space group	<i>P</i> -1	<i>P</i> 2 ₁ / <i>c</i>
<i>a</i> (Å)	7.6029(1)	7.8738(4)
<i>b</i> (Å)	13.6803(2)	28.0459(14)
<i>c</i> (Å)	13.7727(2)	7.2397(4)
α (°)	90.542(1)	90
β (°)	103.635(1)	108.677(3)
γ (°)	91.901(1)	90
<i>V</i> (Å ³)	1391.14(3)	1514.54(14)
<i>Z</i>	4	4
<i>D</i> _{calc} (g cm ⁻³)	2.364	2.425
<i>T</i> _{max,min}	0.5557, 0.1356	0.1239, 0.0460
Number of unique reflections	6673	2679
Number of observed reflections [<i>I</i> >2σ(<i>I</i>)]	5957	2594
R[<i>I</i> >2σ(<i>I</i>)]	0.0156	0.0369
wR ₂ (all data)	0.0361	0.0910
Goodness of Fit	1.039	1.082

Solution and refinement

Both structures were solved by Patterson methods of SHELXS-97.⁽²¹⁾ The gold atoms were initially located, and all other non-hydrogen atoms were found by a series of difference maps (SHELXL-97⁽²²⁾) and refined anisotropically. Hydrogen atoms were placed in calculated positions. Because of the pseudo symmetry present in the free pyridyl ring of **5.16** an inspection of temperature factors was used to assign N(1) and C(4). The pyridyl ring is orientated so that N(1) and S(1) are *cis* to each other. In addition, inversion of C(4) and N(1) (so that N(1) and N(2) are *cis* to each other) resulted in increases in both R_1 and wR_2 . After a final refinement cycle of **5.16** there was still a significant amount of residual electron density present. Refinement excluding the high angle data (above 50°) reduced, but did not totally eliminate, this problem. A peak ($2.05 \text{ e } \text{\AA}^{-3}$) remained approximately 1.6 \AA from S(1) and this was assigned as an artefact as it could not be modelled in any way that made chemical sense.

5.5 References

1. M. H. Klingele and S. Brooker; *Eur. J. Org. Chem.*, **2004**, 3422.
2. A. N. Shkil, Y. A. Zolotov and E. G. Rukhadze; *Koordinats. Khim.*, **1987**, 13, 1352.
3. E. Gagliardi and H. Zechmann; *Mikrochim. Acta*, **1976**, 2, 377.
4. G. Bahr and E. Scholz; *Z. Anorg. Allg. Chem.*, **1959**, 299, 281.
5. L. G. Kuz'mina, K. I. Grandberg and L. G. Il'ina; *Zh. Neorg. Khim.*, **1995**, 40, 1827.
6. V. Muresan, N. Muresan and A. Resiss; *Pol. J. Chem.*, **1993**, 67, 2113.
7. M. Chen, M. Huang and S. Hu; *Jiegou Huaxue (Chin. J. Struct. Chem.)*, **1992**, 11, 12.
8. S. Hu, D. Shi, T. Huang, J. Wan and Z. Huang; *Jiegou Huaxue (Chin. J. Struct. Chem.)*, **1991**, 10, 110.
9. B. F. Hoskins and F. D. Whillans; *J. Chem. Soc., Dalton Trans.*, **1974**, 2112.
10. Z. G. Aliev, L. O. Atovmyan, A. P. Ranskii, B. A. Bovykin and V. I. Kolyada; *Zh. Strukt. Khim.*, **1994**, 35, 138.
11. R. M. Silverstein and F. X. Webster; *Spectrometric Identification of Organic Compounds (Sixth Edition)*, John Wiley & Sons, Inc., New York, **1998**.
12. W. Henderson and C. Evans; *Inorg. Chim. Acta*, **1999**, 294, 183.
13. V. B. Rybakov, L. G. Boboshko, N. I. Burakov, M. Y. Zubritsky, V. I. Kovalenko, V. A. Savelova, A. F. Popov and V. A. Mikhailov; *Kristallografiya*, **2003**, 48, 627.

14. D.-J. Che, G. Li, Z. Yu, D.-P. Zou and C.-X. Du; *Inorg. Chem. Comm.*, **2000**, 3, 537.
15. G. Li, D.-J. Che, Z.-F. Li, Y. Zhu and D.-P. Zou; *New. J. Chem.*, **2002**, 26, 1629.
16. I. Tabakovič, M. Trkovnik, M. Batušič and K. Tabakovič; *Synthesis*, **1979**, 8, 590.
17. B. Zaleska, B. Trzewik, E. Stodolak, J. Grochowski and P. Serda; *Synthesis*, **2004**, 18, 2975.
18. R. L. N. Harris; *Aust. J. Chem.*, **1972**, 25, 993.
19. P. Iliopoulos and K. S. Murray; *J. Chem. Soc., Dalton Trans.*, **1988**, 433.
20. R. H. Blessing; *Acta Cryst. Sect. A*, **1995**, 51, 33.
21. G. M. Sheldrick, SHELXS-97 - A Program for the Solution of Crystal Structures, University of Göttingen, Germany, **1997**.
22. G. M. Sheldrick, SHELXL-97 - A Program for the Refinement of Crystal Structures, University of Göttingen, Germany, **1997**.

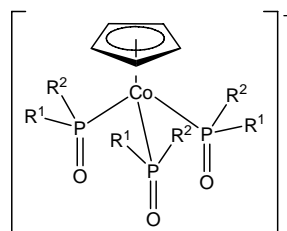
CHAPTER SIX

Gold(III) Complexes formed with Kläui Ligands

6.1 Introduction

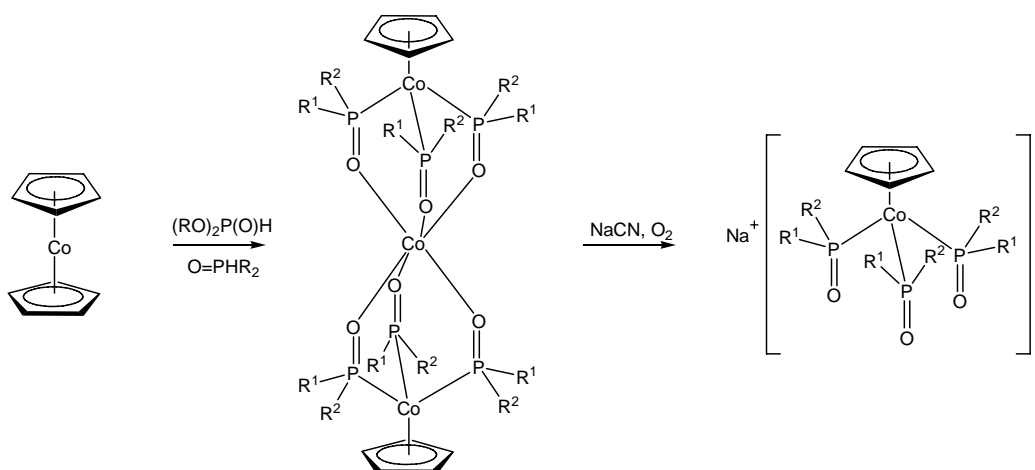
6.1.1 Synthesis and properties of the Kläui ligand

The Kläui ligands have the general formula $[(C_5R_5)Co\{P(O)R^1R^2\}_3]^-$ (Scheme 6.1) and were first synthesised in 1977. These ligands are examples of monoanionic tridentate six-electron ligands able to coordinate to metal centres through three oxygen donor atoms.⁽¹⁾ The following is only a brief introduction to the Kläui ligand, however two comprehensive reviews are available which cover the chemistry in detail.^(2, 3)



Scheme 6.1 Schematic of a general Kläui ligand, L⁻.

The synthesis of Kläui ligands can be carried out in a one-pot reaction, depicted in Scheme 6.2. When cobaltocene is heated (without solvent) to approximately 100 °C with diesters of phosphorous acid ((RO)₂P(O)H) or secondary phosphane oxides (HP(O)R₂) the complex containing two Kläui ligands (L₂Co) is obtained. The free anionic ligand L⁻ can be acquired by the cleavage of L₂Co with cyanide in the presence of atmospheric oxygen. Using this strategy, ligands with R = alkyl, aryl or *O*-alkyl substituents can be synthesised. In addition, the analogous rhodium⁽⁴⁾ and iridium based ligands⁽⁵⁾ have also been synthesised.



Scheme 6.2 Synthesis of Kläui ligands from cobaltocene.

Even though the ligands are examples of ‘half-sandwich’ complexes they are extremely robust and can be dissolved in aqueous sulfuric acid without decomposition. In addition they are inert to oxidation by atmospheric oxygen and they show interesting solubility. For example, the sodium salts are readily soluble in both water and pentane.⁽²⁾

The Kläui ligands fall between F^- and DMSO in the spectrochemical series making them weak oxygen ligands; in the nephelauxetic series the ligands fall between water and DMSO making them hard ligands. Therefore, the electronic properties of the ligands are approximately equal to that of fluoride or oxide anions. Kläui has stated that these observations may be because the presence of the $CpCo$ means there is no opportunity for delocalisation of the d electrons of the coordinated metal ions through the $P=O$ bridges.⁽²⁾

6.1.2 Scope of this work

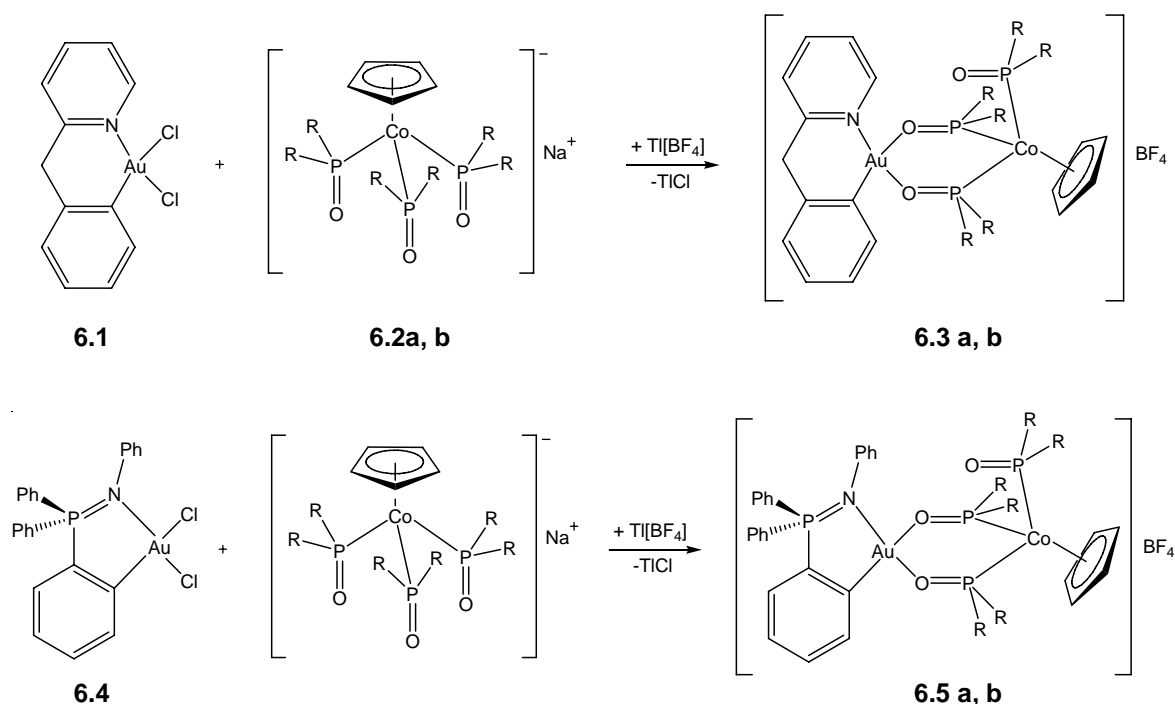
In a 1990 review on the chemistry of these ligands it was pointed out that Kläui complexes can be formed with almost every metal ion and a selection of non-metals (boron) as well.⁽²⁾ As the Kläui ligands favour octahedral coordination it is not surprising that gold complexes are missing. Complexes with the square planar platinum(II) centres are known - in these examples the Kläui ligand is only coordinated *via* two oxygen atoms.^(6, 7) This laboratory has

previously been interested in the coordination of Kläui ligands to metal centres^(8, 9) therefore it was decided to investigate complexes with gold(III).

6.2 Results and Discussion

6.2.1 Syntheses

When cycloaurated 2-benzylpyridine gold(III) dichloride **6.1** was reacted with the Kläui ligands **6.2** (**a** R = OMe, **b** R = OEt) in dichloromethane in the presence of Ti[BF₄] for 24 hours, the complexes **6.3a** and **6.3b** were isolated as yellow [BF₄] salts in adequate yields (Scheme 6.3). Varying the reaction times (to either six or 48 hours) did not improve the yields and there was evidence for the decomposition of the gold(III) starting material to elemental gold. A similar reaction with a cycloaurated iminophosphorane **6.4** gave the analogous complexes **6.5a** and **6.5b**, again in adequate yields (Scheme 6.3).



Scheme 6.3 Synthesis of Au(III) Kläui complexes **6.3** and **6.5** (**a** R = OMe; **b** R = OEt).

The resulting complexes were analysed by ESI mass spectrometry and variable temperature NMR analysis. Satisfactory microelemental data could be obtained for three of the complexes. Unfortunately, after several attempts, satisfactory data could not be obtained for **6.5a**. Even after successive recrystallisations the ^1H NMR spectrum showed traces of an impurity that could not be removed. In addition, an X-ray crystal structure of **6.5b** was determined.

6.2.2 X-ray crystal structure of **6.5b**

An X-ray crystal structure of **6.5b** was carried out in order to characterise the bonding of Kläui compound to the gold(III) complex. The structure shows that the complex is bound to the gold centre through two oxygen atoms with the third ‘dangling’ above the gold coordination plane. Figure 6.1 shows the molecular structure and Table 6.1 gives important bond lengths and angles. Full structural parameters can be found on the supplementary CD.

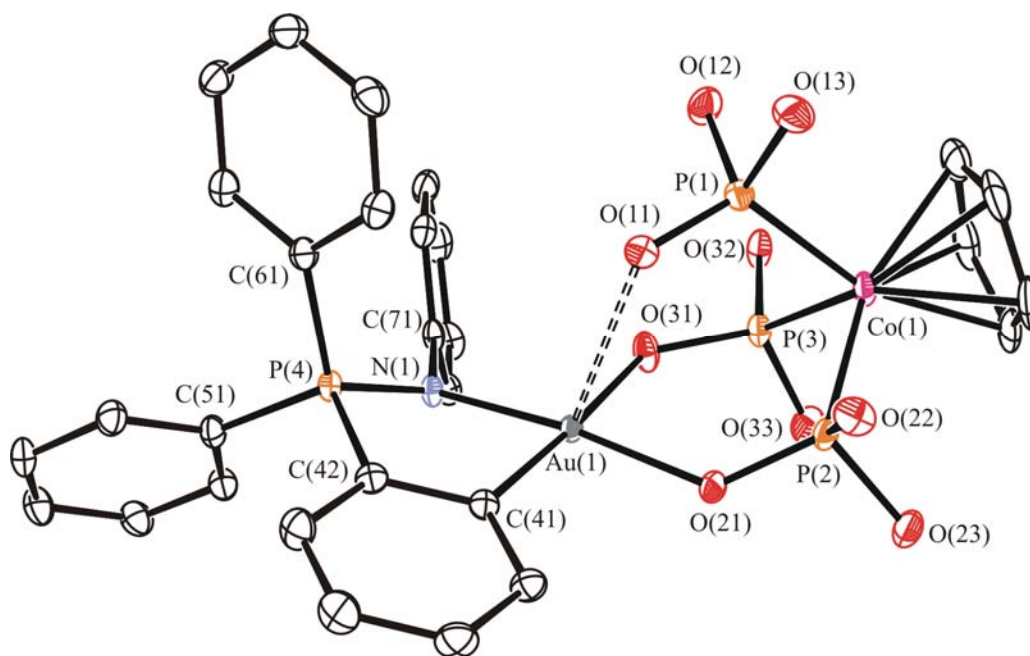
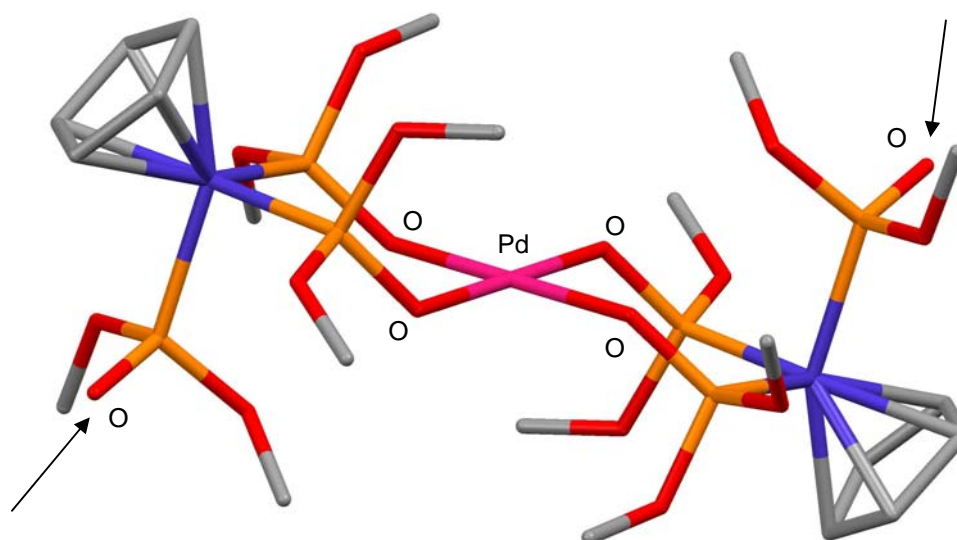


Figure 6.1 Molecular diagram of the cationic moiety of **6.5b**. For clarity, the hydrogen atoms, $[\text{BF}_4]^-$ anion and the ethyl arms of the Kläui ligand have been excluded. Thermal ellipsoids are shown at the 50% probability level.

Table 6.1 Selected bond lengths (Å) and angles (°) for the complex **6.5b**.

Atoms	Lengths (Å)	Atoms	Angles (°)
Au(1) – O(11)	2.722(2)	O(31) – Au(1) – O(21)	91.82(9)
Au(1) – O(21)	2.023(2)	O(31) – Au(1) – N(1)	90.54(9)
Au(1) – O(31)	2.083(2)	N(1) – Au(1) – C(41)	85.55(11)
O(11) – P(1)	1.487(2)	C(41) – Au(1) – O(21)	92.08(11)
O(21) – P(2)	1.537(2)		
O(31) – P(3)	1.522(2)		
Au(1) – C(41)	1.995(3)		
Au(1) – N(1)	2.008(2)		
P(4) – N(1)	1.636(3)		

This geometrical arrangement differs from what is seen in the palladium(II) Kläui complex **6.6**. In this case the two non-coordinating P=O oxygen atoms are twisted away from the palladium centre (Figure 6.2).⁽⁶⁾ In the palladium(II) π -allyl Kläui complex **6.7** the non-coordinating oxygen sits over the palladium centre, and forms a hydrogen bond with a water molecule.⁽⁷⁾

**Figure 6.2** Molecular structure of the palladium Kläui complex **6.6**. Only the oxygen atoms from the P=O moieties are labelled. The non-coordinated oxygen atoms can clearly be seen pointing away from the palladium centre.

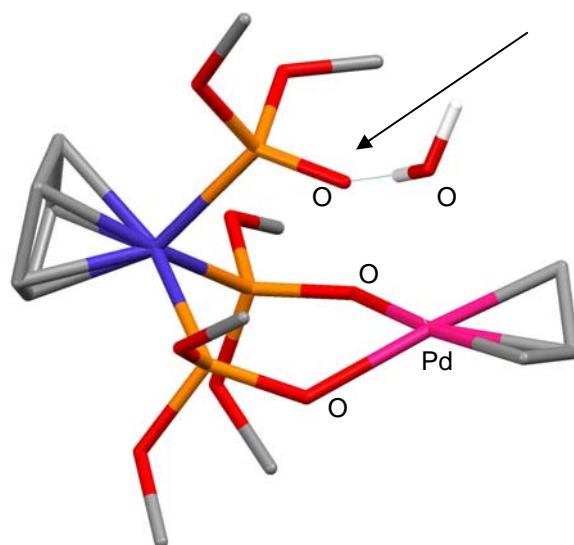
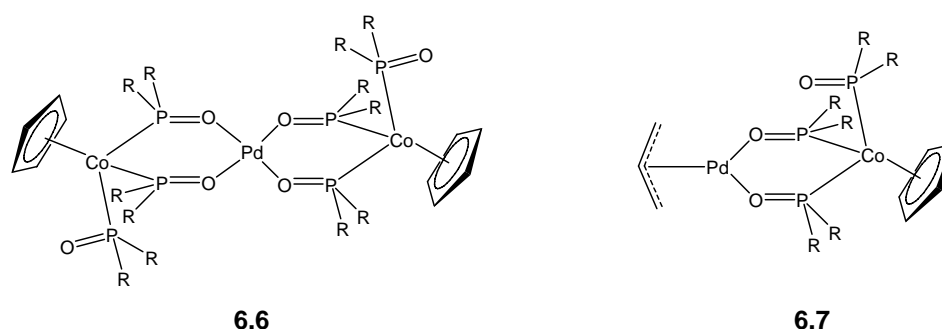


Figure 6.3 Molecular structure of the palladium Kläui complex **6.7**. Only the oxygen atoms from the P=O moieties are labelled. The non-coordinated oxygen atom can clearly be seen pointing over the palladium centre forming a hydrogen bond with a water molecule.

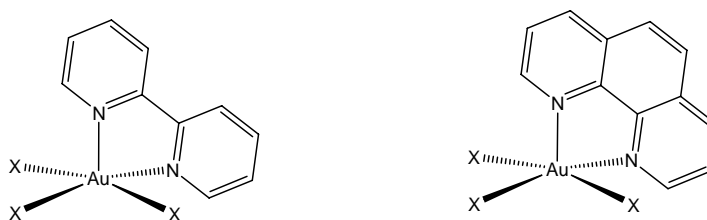


Scheme 6.4 Diagrams of the palladium Kläui complexes represented in Figure 6.2 (**6.6**) and Figure 6.3 (**6.7**).

The gold atom appears to show a distorted square pyramidal coordination geometry. The nitrogen [N(1) and carbon C(41)] atoms of the iminophosphorane ligand, along with two oxygen [O(21) and O(31)] atoms of the Kläui ligand constitute the four corners of the base of the pyramid. The ‘tip’ is provided by the third oxygen O(11), of the Kläui ligand. The gold coordination plane (*i.e.* the base of the pyramid) is slightly distorted which is expected for

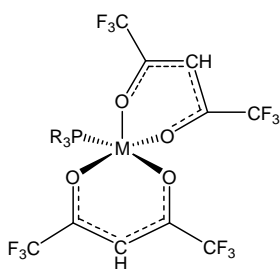
square pyramidal coordination [Au(I) sits 0.0562(13) Å above the mean plane]. In addition, the Au(1)-O(11) vector is at an angle of approximately 80° to the base of the pyramid.

Five-coordinate square pyramidal complexes of gold(III) are rare but are not entirely unknown. To date, all of the structurally characterised complexes contain rigid ligands with bipyridyl⁽¹⁰⁻¹³⁾ or phenanthroline^(14, 15) moieties which coordinate to the gold through two nitrogen atoms. In all cases, one nitrogen atom forms a corner of the base of the pyramid and because of the rigidity of the ligand the other nitrogen is placed at the apex of the pyramid, in an ideal position to interact with the gold (Scheme 6.5). The remaining ligands tend to be halides or pseudohalides, with the exception of one complex which contains PPh₃ and the bidentate dmp ligand (refer to Chapter One).⁽¹⁶⁾



Scheme 6.5 Square pyramidal five coordinate gold(III) complexes containing bipyridine or phenanthroline ligands.

In **6.5b** the interaction between Au(1) and O(11) appears to be strong enough to hold the molecule in this square pyramidal arrangement. The Au(1)-O(11) bond length [2.722(2) Å] is significantly longer than both the Au(1)-O(21) and Au(1)-O(31) bond lengths provided by the formally coordinated oxygen atoms [2.023(2) Å and 2.083(2) Å respectively]. These gold-oxygen distances are very similar to the metal-oxygen bond distances seen in the palladium(II) and platinum(II) β -diketonate complexes **6.8a** and **6.8b**. In these complexes the metal-oxygen distances of the weakly coordinated oxygen (*i.e.* the apex of the pyramid) are also approximately 0.7 Å longer than the metal oxygen distances in the base of the pyramid. However, the angle between the vertical axis of the pyramid (*i.e.* the metal-axial oxygen vector) and the base is much more acute [65.3(2)° in the palladium example **6.8a** and 66.9(3)° in the platinum analogue **6.8b**].⁽¹⁷⁾



6.8a M = Pd, R = *o*-tolyl
6.8b M = Pt, R = Cy

Scheme 6.6 Palladium(II) and platinum(II) complexes which show a distorted square pyramidal coordination.

The bite angle of the Kläui ligand in **6.5b** is $91.82(9)^\circ$, close to what is expected for square planar geometry. Because of the *trans* influence differences, the gold–oxygen bond length *trans* to the carbon [Au(1)–O(31) = 2.083 Å] is longer than the gold–oxygen bond length *trans* to the nitrogen [Au(1)–O(21) = 2.023(2) Å]. Not surprisingly, the P=O bond lengths of the coordinated oxygens [P(2)–O(21) and P(3)–O(31)] are longer than the P=O bond length of the weakly coordinated oxygen.

Substitution of the two chloride ligands of **6.4** with the Kläui ligands results in some subtle changes to the iminophosphorane moiety. The bite angle of the iminophosphorane increases from $84.86(17)^\circ$ to $85.55(11)^\circ$ in **6.5b** and this is accompanied by a shortening of the gold–carbon and gold–nitrogen bonds and lengthening of the P=N bond. In complex **6.4** the *N*-bonded phenyl ring is twisted 54° from the metallacyclic plane⁽¹⁸⁾ - in complex **6.5b** the ring is almost perpendicular (81°) to the metallacyclic plane, possibly as a result of steric constraints imposed by the bulky Kläui ligand.

6.2.3 NMR spectroscopic analysis

The ^1H and $^{31}\text{P}\{^1\text{H}\}$ NMR chemical shifts of the Kläui ligands in the complexes **6.3a,b** and **6.5a,b** are very similar to those in the sodium salts **6.2a** and **6.2b**. However, the protons arising from the Cp ring of the Kläui ligand move downfield upon coordination. The phosphorus atom in the iminophosphorane moieties of **6.5a** (δ 68.6 ppm) and **6.5b** (δ 68.2

ppm) is very similar to that seen in the dichloride **6.4** (δ 65.5 ppm) confirming the phosphorus has remained in a five-membered ring.⁽¹⁸⁾ Table 6.2 gives a comparison of these chemical shifts.

Table 6.2 ^1H and $^{31}\text{P}\{^1\text{H}\}$ NMR chemical shifts (ppm) for the Kläui ligands **6.2a** and **6.2b** (as the sodium salts) and the gold(III) complexes (CDCl_3).

	CH_3	CH_2	Cp	P
6.2a	3.59 (vq)	-	5.03 (s)	112.5 (br)
6.3a	3.67 (vq)	-	5.20 (s)	113.1
6.5a	3.54 (vq)	-	5.13 (s)	120.4
6.2b	1.20 (t)	3.95 (m)	4.97 (s)	110.1 (br)
6.3b	1.25 (t)	4.06 (m)	5.14 (s)	110.4
6.5b	1.22 (t)	3.90 (m)	5.07 (s)	117.2

Kläui complexes of square planar palladium(II) have previously shown fluxionality in solution^(6, 7) and it appeared from a first inspection of the ^1H and $^{31}\text{P}\{^1\text{H}\}$ NMR spectra that gold complexes were showing similar behaviour. In addition, the tridentate (nitrogen donor) poly(pyrazolyl)borate ligand shows fluxional behaviour when coordinated to gold(III). At room temperature it appeared all three pyrazolyl moieties were equivalent, however when cooled it was possible to distinguish two bonded pyrazolyl groups and one non-bonded.⁽¹⁹⁾ Because of these reasons we decided to carry out a variable temperature NMR study on the complexes.

$^{31}\text{P}\{^1\text{H}\}$ NMR spectroscopy

At room temperature there is a broad peak present at approximately 115 ppm in all the complexes. This is only slightly different from the sodium salts of the ligand (**6.2a** δ 112.5 ppm, **6.2b** δ 110.1 ppm).⁽²⁰⁾ For complexes **6.5a** and **6.5b**, this peak integrates 3:1 relative to the phosphorus of the iminophosphorane ligand. When the sample was cooled the behaviour of the complex is dependent on the cycloaurated ligand present (*i.e.* the iminophosphorane or 2-benzylpyridine chelating group).

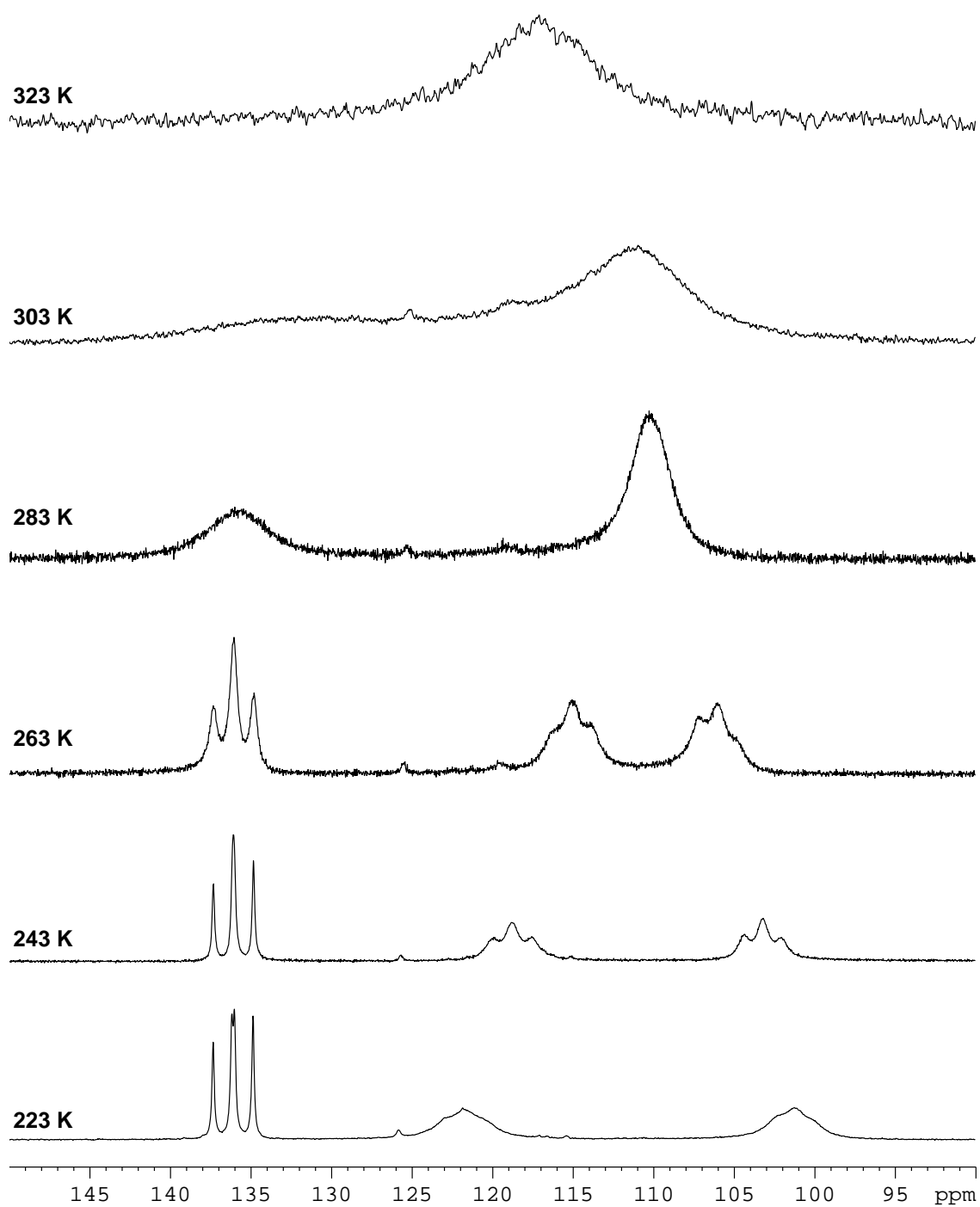


Figure 6.4 Variable temperature $^{31}\text{P}\{^1\text{H}\}$ NMR spectra of **6.3b** (CDCl_3).

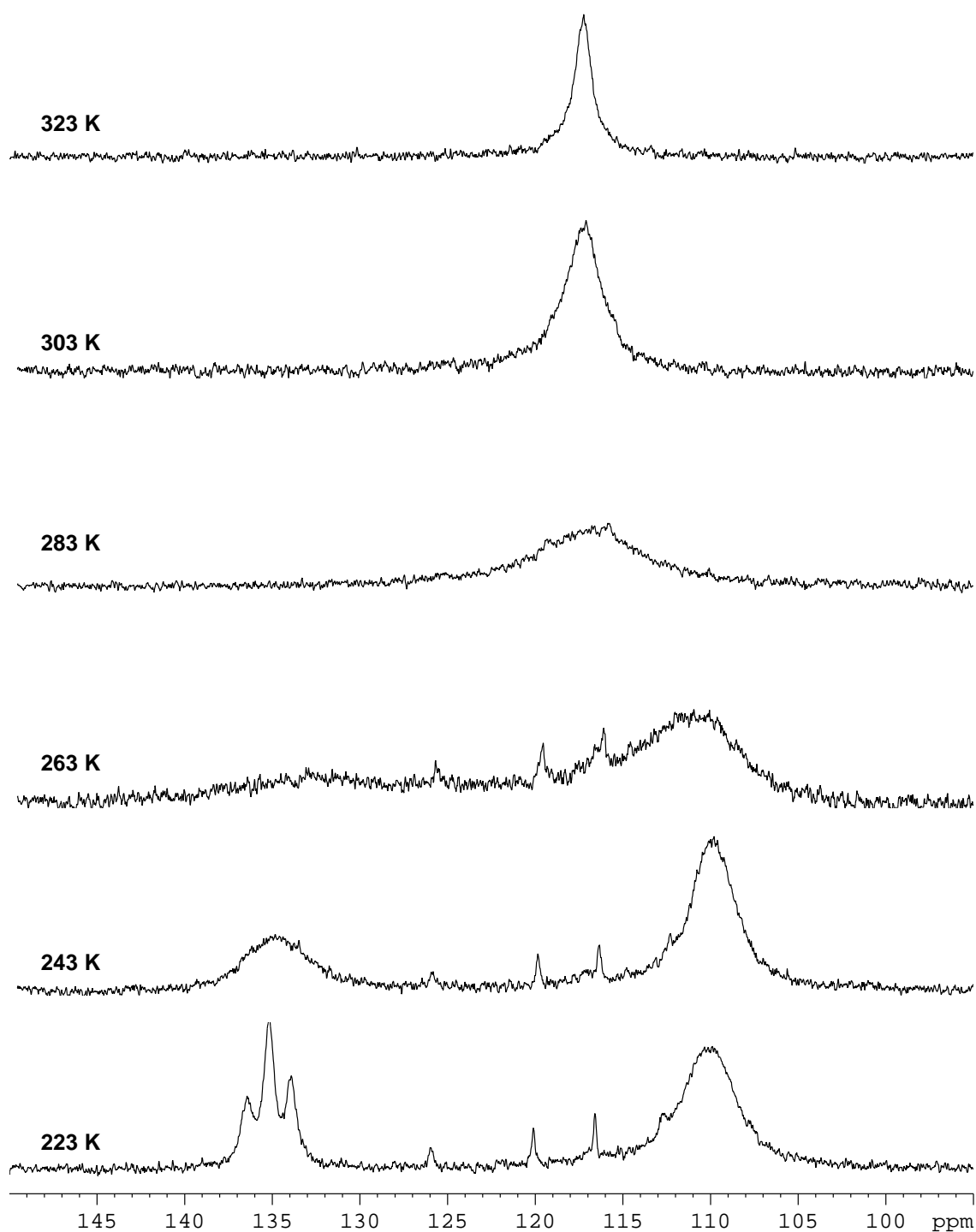


Figure 6.5 Variable temperature $^{31}\text{P}\{^1\text{H}\}$ NMR spectra of **6.5b** (CDCl_3). The phosphorus signal from the iminophosphorane ligand occurs upfield and is not included in the figures.

For the 2-benzylpyridine derived complexes **6.3a** and **6.3b** two peaks start to appear at 283 K at 135 ppm and 110 ppm in a 1:2 ratio. Presumably the peak at 135 ppm is from the non-coordinated arm of the Kläui ligand. When the solution is cooled to 263 K the second peak starts to split into two distinct triplets (at 115 ppm and 105 ppm which integrate 1:1), corresponding to the phosphorus atoms of the coordinated arms of the ligand. Because of the nonsymmetrical nature of the benzylpyridine ligand two signals appear. The signal from the non-coordinating group is also a triplet. Cooling further to 223 K results in the two peaks from the coordinated phosphorus atoms becoming broader and resolution is lost. The uncoordinated signal now appears as a distinct doublet of doublets (${}^2J_{PP} \approx 159$ Hz) because of coupling to two distinct (coordinated) phosphorus atoms. Heating the sample from room temperature to 323 K resulted in sharpening of the signal – presumably further heating would have resulted in a sharp signal but limitations of the solvent meant further heating was impossible.

The iminophosphorane complexes **6.5a** and **6.5b** showed different behaviour. At 283 K **6.5a** and **6.5b** are still fluxional and it is not until 243 K that the broad peak starts to split into two signals (at 135 ppm and 110 ppm), which again integrate 1:2. At 223 K, the limit that could be reached due to the solvent, the peak at 135 ppm (corresponding to the dangling arm of the ligand) is a definite triplet (${}^2J_{PP} \approx 153$ Hz) however the peak at 110 ppm is still broad and unresolved. Presumably, if the sample could be cooled further this peak would split into two triplets, analogous to that seen for the benzylpyridine complexes. Again, heating the sample from room temperature to 323 K results in the peak becoming sharper.

These results suggest a similar behaviour to what was observed with the poly(pyrazolylborate) ligands. At 303 K there is rapid interchange between the coordinated and the non-coordinated arms of the Kläui ligands making the three arms appear equivalent. When cooled, fluxionality is lost and three signals are observed which correspond to the three different environments that the arms occupy. The low temperature configurations reiterate what was observed crystallographically.

¹H NMR Spectroscopy

Again evidence of fluxionality can be seen in the ¹H NMR spectra. At 303 K the methyl protons of the Kläui ligand in **6.3a** appear as a virtual quartet (Figure 6.6a). This is because the molecule is fluxional at this temperature and there is rapid interchange between the two bonded arms and the one non-bonded arm of the Kläui ligand. Therefore, the virtual quartet arises from 18 equivalent protons coupled to three equivalent phosphorus atoms (*i.e.* a A₁₈X₃ spin system). A similar pattern is observed for **6.5a**.

When the complex is cooled it loses fluxionality and as a result the methyl protons (or phosphorus atoms) are no longer equivalent. The virtual quartet that is present at 303K splits into two signals which integrate with a 1:2 ratio. Again these signals show virtual coupling.

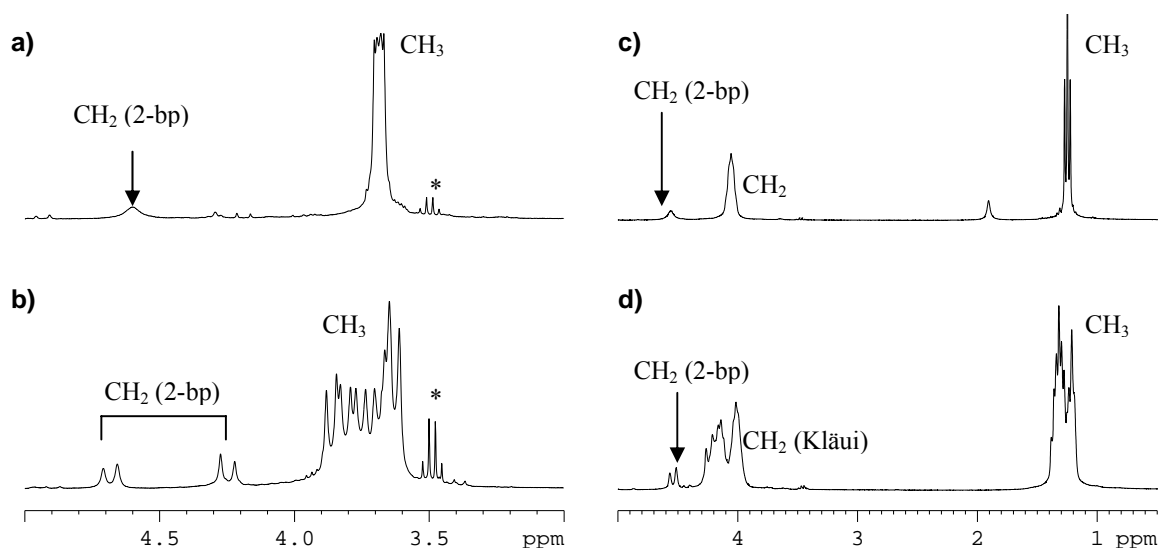


Figure 6.6 Variable temperature ¹H NMR spectra of a) **6.3a** at 303 K, b) **6.3a** at 223 K, c) **6.3b** at 303 K and d) **6.3b** at 223 K (CDCl₃, peaks marked * are from impurities in the sample).

Complexes **6.3b** and **6.5b**, which contain ethyl groups on the Kläui ligand show similar behaviour however there is complexity arising from the ethyl *versus* methyl groups. At 303 K the methyl groups only show coupling to the neighbouring protons thus appearing as a simple triplet. The signal for the methylene protons was a broad multiplet, assumed to arise because

the protons showed coupling to both the neighbouring protons and the phosphorus. Again, when the complex is cooled the signal splits into two, which integrate with a 1:2 ratio.

The benzylpyridine ring in **6.3a** and **6.3b** also shows fluxionality (because of the inversion of six-membered auracycle), and this has been discussed in detail before.⁽²¹⁾ As a result, at 303 K the CH₂ protons appear as a broad singlet. Cooling to 223 K results in the signal splitting into two doublets of doublets.

6.3 Conclusions

The reaction of cycloaurated gold(III) dichlorides with Kläui ligands results in the formation of cationic gold(III) salts. In the solid state the Kläui ligands coordinate to the gold through two of the three available oxygen atoms with the third above the gold coordination plane. This gives the gold(III) a distorted square pyramidal geometry and is the first structurally characterised example of this geometry for gold(III) with ligands other than those containing rigid bipyridine or phenanthroline backbones. In solution there is rapid interchange (on the NMR timescale) between the coordinated and non-coordinated oxygen atoms, however when cooled the ligands lose their fluxionality and three different environments can be observed.

6.4 Experimental

6.4.1 General

The gold dichloride complexes **6.1** and **6.4** were synthesised from literature procedures,^(18, 22) with both the Kläui ligands **6.2a** and **6.2b** purchased from Strem Chemicals. The NMR chemical shifts that are reported in the following experimental are those observed at 303K.

6.4.2 Syntheses

Synthesis of 6.3a

(2-bp)AuCl₂ **6.1** (1.00 g, 0.230 mmol) and the Kläui ligand **6.2a** (0.109 g, 0.230 mmol) were dissolved in dichloromethane (20 mL) with Tl[BF₄] (0.201 g, excess) and stirred in a foil-covered flask for 24 hours. After filtration and reduction in volume, slow addition of diethyl ether to the solution precipitated **6.3a** as a yellow solid (0.066 g, 32%).

Found: C 30.5, H 3.4, N 2.3; C₂₃H₃₃BNO₉F₄P₃CoAu requires C 30.6, H 3.7, N 1.6%.

NMR: ¹H: δ 3.67 (vq, 18H, CH₃), 4.58 (br s, 2H, CH₂), 5.20 (s, 5H, Cp), 7.00 (m, 1H, Ar-H), 7.17 (m, 3H, Ar-H), 7.69 (t, 1H, Ar-H), 7.88 (d, 1H, Ar-H), 8.14 (t, 1H, Ar-H), 8.96 (d, 1H, Ar-H); ¹³C{¹H}: δ 46.6 (CH₂), 52.7 (CH₃), 90.5 (Cp), 125.5, 126.9, 127.0, 128.2, 128.5 (all aryl C-H), 129.0, 130.0, 131.1 (all aryl C), 143.7, 150.6, 156.9 (all aryl C-H); ³¹P{¹H}: δ 113.1 (br s).

ESI-MS: *m/z*: 816.040 (100%, [M]⁺, calculated 816.036).

Synthesis of 6.3b

(2-bp)AuCl₂ **6.1** (0.100 g, 0.230 mmol) and the Kläui ligand **6.2b** (0.129 g, 0.230 mmol) were dissolved in dichloromethane (20 mL) and stirred in a foil-covered flask with Tl[BF₄] (0.202 g, excess) for 24 hours. The insoluble thallium salts were filtered off and the solution was reduced in volume. Addition of diethyl ether to the solution until it went cloudy and storage overnight at -20 °C gave yellow crystals (0.139 g, 61%) of **6.3b**.

Found: C 35.3, H 4.6, N 1.5; C₂₉H₄₅BNO₉F₄P₃CoAu requires C 35.3, H 4.6, N 1.4%.

NMR: ¹H: δ 1.25 (t, 18H, CH₃), 4.06 (br s, 12H, CH₂ - Kläui), 4.56 (br s, 2H, CH₂ - benzylpyridine), 5.14 (s, 5H, Cp), 6.96 (m, 1H, Ar-H), 7.14 (m, 3H, Ar-H), 7.60 (t, 1H, Ar-H), 7.93 (d, 1H, Ar-H), 8.16 (t, 1H, Ar-H), 8.86 (d, 1H, Ar-H); ³¹C{¹H}: δ 16.5 (CH₃), 46.4

($\underline{\text{C}}\text{H}_2$ – benzylpyridine), 61.4 ($\underline{\text{C}}\text{H}_2$ – Kläui), 90.7 (*Cp*), 124.9 – 157.0 (all aryl $\underline{\text{C}}$) $^{31}\text{P}\{^1\text{H}\}$: δ 110.4 (br s).

ESI-MS: *m/z*: 900.133 (100%, $[\text{M}]^+$, calculated 900.130).

Preparation of 6.5a

The gold(III) dichloride **6.4** (0.100 g, 0.162 mmol), the Kläui ligand **6.2a** (0.077 g, 0.162 mmol) and $\text{Tl}[\text{BF}_4]$ (0.142 g, excess) were dissolved in dichloromethane (20 mL). The resulting solution was stirred in a foil-covered flask for 24 hours. The insoluble salts were removed and addition of diethyl ether to the filtrate caused immediate precipitation of **6.5a** as a yellow solid (0.047 g, 27%).

Found: C 40.3, H 3.9, N 2.0; $\text{C}_{35}\text{H}_{42}\text{BNO}_9\text{F}_4\text{P}_4\text{CoAu}$ requires C 38.7, H 3.9, N 1.3%.

NMR: ^1H : δ 3.54 (vq, 18H, CH_3), 5.13 (s, 5H, *Cp*) 7.01-7.07 (m, 5H, Ar-H), 7.08 (m, 5H, Ar-H), 7.40-7.90 (m, 14H, Ar-H), $^{13}\text{C}\{^1\text{H}\}$: δ 52.3 ($\underline{\text{C}}\text{H}_3$); 90.2 (*Cp*), 123-150 (aryl C); $^{31}\text{P}\{^1\text{H}\}$: δ 68.6 (s, P=N), 120.4 (br, P Kläui), integral 1:3.

ESI-MS: *m/z*: 1000.083 (100%, M^+ , calculated 1000.080).

Preparation of 6.5b

6.4 (0.101 g, 0.163 mmol) along with the Kläui ligand **6.2b** (0.091 g, 0.163 mmol) were dissolved in dichloromethane (20 mL) with $\text{Tl}[\text{BF}_4]$ (0.142 g, excess) and stirred for 24 hours in a foil-covered flask. After filtration to remove the insoluble thallium salts slow evaporation of the dichloromethane solvent gave yellow crystals of **6.5b** (0.102 g, 54%).

Found: C 42.1, H 4.7, N 1.3; $\text{C}_{41}\text{H}_{54}\text{BNO}_9\text{F}_4\text{P}_4\text{CoAu}$ requires C 42.0, H 4.7, N 1.2%.

NMR: ^1H : δ 1.22 (t, 18H, CH_3), 3.90 (m, 12H, CH_2), 5.07 (s, 5H, Cp) 7.01-7.07 (m, 5H, Ar-H), 7.10-7.17 (m, 1H, Ar-H), 7.41-7.50 (m, 2H, Ar-H), 7.53-7.60 (m, 5H, Ar-H), 7.70-7.76 (m, 2H, Ar-H), 7.82-7.89 (m, 4H, Ar-H); $^{13}\text{C}\{^1\text{H}\}$: δ 16.7 (CH_3); 61.1 (CH_2), 90.6 (Cp), 126-150 (aryl C); $^{31}\text{P}\{^1\text{H}\}$: δ 68.2 (s, P=N), 117.2 (br, P Kläui), integral 3:1.

ESI-MS: m/z : 1084.180 (100%, M^+ , calculated 1084.174).

6.4.3 X-ray crystal structure determination of 6.5b

Yellow crystals of X-ray quality were grown by slow evaporation of a dichloromethane solution of the crude product at room temperature.

Data collection

Unit cell dimensions and reflection data were collected at the University of Canterbury on a Bruker Nonius Apex II CCD Diffractometer at 93 K. Absorption corrections to the data were made by SADABS.⁽²³⁾ Crystal and refinement data for the complex is presented in Table 6.3 – the crystallographic information file for **6.5b** is included on the supplementary CD.

Solution and refinement

The structure was solved using the Patterson methods option of SHELXS-97.⁽²⁴⁾ The gold atom was initially located, with all other non-hydrogen atoms subsequently found by a series of difference maps (SHELXL-97⁽²⁵⁾), and the hydrogen atoms in calculated positions. All non-hydrogen atoms were refined as anisotropic. Two ethyl arms of the Kläui ligand displayed slight disorder and as a result the CH_3 groups (and corresponding methylene hydrogen atoms) were refined in two positions. The BF_4^- anion was also disordered, twirling around a BF bond, however the disorder was not resolved.

Table 6.3 Crystal and refinement data for the complex **6.5b**.

Complex	6.5b
Formula	C ₄₁ H ₅₄ BNO ₉ F ₄ P ₄ CoAu
Molecular Weight	1171.44
<i>T</i> /K	93
Crystal system	Monoclinic
Space group	<i>C</i> 2/ <i>c</i>
<i>a</i> (Å)	30.7189(10)
<i>b</i> (Å)	10.1416(3)
<i>c</i> (Å)	30.0068(10)
α (°)	90
β (°)	100.490(1)
γ (°)	90
<i>V</i> (Å ³)	9192.3(5)
<i>Z</i>	8
<i>D</i> _{calc} (g cm ⁻³)	1.693
<i>T</i> _{max,min}	0.5511, 0.1530
Number of unique reflections	10525
Number of observed reflections [<i>I</i> >2σ(<i>I</i>)]	9567
R[<i>I</i> >2σ(<i>I</i>)]	0.0278
wR ₂ (all data)	0.0691
Goodness of Fit	1.049

6.5 References

1. W. Kläui, H. Neukomm, H. Werner and G. Huttner; *Chem. Ber.*, **1977**, 110, 2283.
2. W. Kläui; *Angew. Chem. Int. Ed.*, **1990**, 29, 627.
3. W.-H. Leung, Q.-F. Zhang and X.-Y. Yi; *Coord. Chem. Rev.*, **2007**, 251, 2266.
4. T. Rütther, U. Englert and U. Koelle; *Inorg. Chem.*, **1998**, 37, 4265.
5. M. Scotti, M. Valderrama, P. Campos and W. Kläui; *Inorg. Chim. Acta*, **1993**, 207, 141.
6. W. Kläui, M. Glaum, E. Hahn and T. Lügger; *Eur. J. Inorg. Chem.*, **2000**, 21.
7. B. Domhöver, H. Hamers, W. Kläui and M. Pfeffer; *J. Organomet. Chem.*, **1996**, 522, 197.
8. N. C. Lloyd, B. K. Nicholson and A. L. Wilkins; *J. Organomet. Chem.*, **2006**, 691, 2757.

9. K. A. Davidson, K. J. Kilpin, N. C. Lloyd and B. K. Nicholson; *J. Organomet. Chem.*, **2007**, 692, 1871.
10. R. J. Charlton, C. M. Harris, H. Patil and N. C. Stephenson; *Inorg. Nucl. Chem. Lett.*, **1966**, 2, 409.
11. V. Ferretti, P. Gilli, V. Bertolasi, G. Marangoni, B. Pitteri and G. Chessa; *Acta Cryst. Sect. C*, **1992**, 48, 814.
12. M. A. Cinellu, A. Zucca, S. Stoccoro, G. Minghetti, M. Manassero and M. Sansoni; *J. Chem. Soc., Dalton Trans.*, **1996**, 4217.
13. C. J. O'Connor and E. Sinn; *Inorg. Chem.*, **1978**, 17, 2067.
14. W. T. Robinson and E. Sinn; *J. Chem. Soc., Dalton Trans.*, **1975**, 726.
15. G. Marangoni, B. Pitteri, V. Bertolasi, G. Gilli and V. Ferretti; *J. Chem. Soc., Dalton Trans.*, **1986**, 1941.
16. J. Vicente, M. T. Chicote, M. D. Bermúdez, P. G. Jones, C. Fittschen and G. M. Sheldrick; *J. Chem. Soc., Dalton Trans.*, **1986**, 2361.
17. S. Okeya, T. Miyamoto, S. Ooi, Y. Nakamura and S. Kawaguchi; *Bull. Chem. Soc. Jpn.*, **1984**, 57, 395.
18. S. D. J. Brown, W. Henderson, K. J. Kilpin and B. K. Nicholson; *Inorg. Chim. Acta*, **2007**, 360, 1310.
19. N. F. Borkett, M. I. Bruce and J. D. Walsh; *Aust. J. Chem.*, **1980**, 33, 949.
20. N. C. Lloyd; *M. Sc Thesis*, **2003**, University of Waikato.
21. Y. Fuchita, H. Ieda, Y. Tsunemune, J. Kinoshita-Nagaoka and H. Kawano; *J. Chem. Soc., Dalton Trans.*, **1998**, 791.
22. M. A. Cinellu, A. Zucca, S. Stoccoro, G. Minghetti, M. Manassero and M. Sansoni; *J. Chem. Soc., Dalton Trans.*, **1995**, 2865.
23. R. H. Blessing; *Acta Cryst. Sect. A*, **1995**, 51, 33.
24. G. M. Sheldrick, SHELXS-97 - A Program for the Solution of Crystal Structures, University of Göttingen, Germany, **1997**
25. G. M. Sheldrick, SHELXL-97 - A Program for the Refinement of Crystal Structures, University of Göttingen, Germany, **1997**

CHAPTER SEVEN

A Preliminary Study of the Catalytic Activity of Gold(III) Complexes

7.1 Introduction

7.1.1 Gold(III) homogenous catalysis

Homogenous gold(III) catalysis is an area of rapidly expanding research – new reports on the topic are appearing on a weekly basis. Only recently an entire issue of *The Journal of Organometallic Chemistry* (Gold Catalysis – New Perspectives for Homogeneous Catalysis, Issue 4, Volume 694, 2009) was dedicated to homogenous gold catalysis. However, this has not always been the case and up until the late 1980's catalysis (both homogeneous and heterogeneous) by gold and its compounds was relatively unexplored. The lack of research has been attributed to a number of reasons. Hashmi proposed that the high value of gold and its corresponding compounds may have led to the thought that gold catalysts are an unviable option on economic grounds. In addition, the inertness of gold may have led to the assumption that any catalyst containing the metal would be inactive.⁽¹⁾

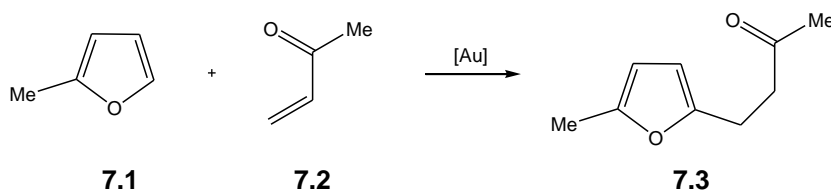
Parish proposed that the lack of homogeneous gold catalysts may be because the type of catalytic cycles that the transition metals (and their compounds) are involved in requires a delicate balance between two oxidation states *i.e.* a finely balanced oxidative addition/reductive elimination cycle. Well known examples of this type of catalysis include the rhodium(I)/(III) cycle used in the Monsanto process (manufacture of acetic acid by the carbonylation of methanol) and the Pd(0)/Pd(II) cycle in Heck reactions. Although gold(I) complexes are known to readily undergo oxidative addition the resulting gold(III) complexes are either too stable to react further or are so unstable they react immediately. Reductive elimination from gold(III) complexes is also problematic. In addition gold(III) hydrides are

uncommon, therefore oxidation of gold(I) by H₂ or the formation of alkenes by β -elimination is rare.⁽²⁾

An extensive review by Hashmi covers homogenous gold catalysis of organic reactions up until late 2006⁽¹⁾ and earlier reviews on the subject are also available.⁽³⁻⁵⁾ The early history of catalysis by gold (pre 1977) has also recently been reviewed by Bond.⁽⁶⁾ These reviews indicate that the majority of the work on homogeneous gold catalysis has been conducted using AuCl₃ which is very hygroscopic and acidic. Therefore, the development of air- and moisture-stable complexes that can act as catalysts in acid sensitive reactions is desirable.

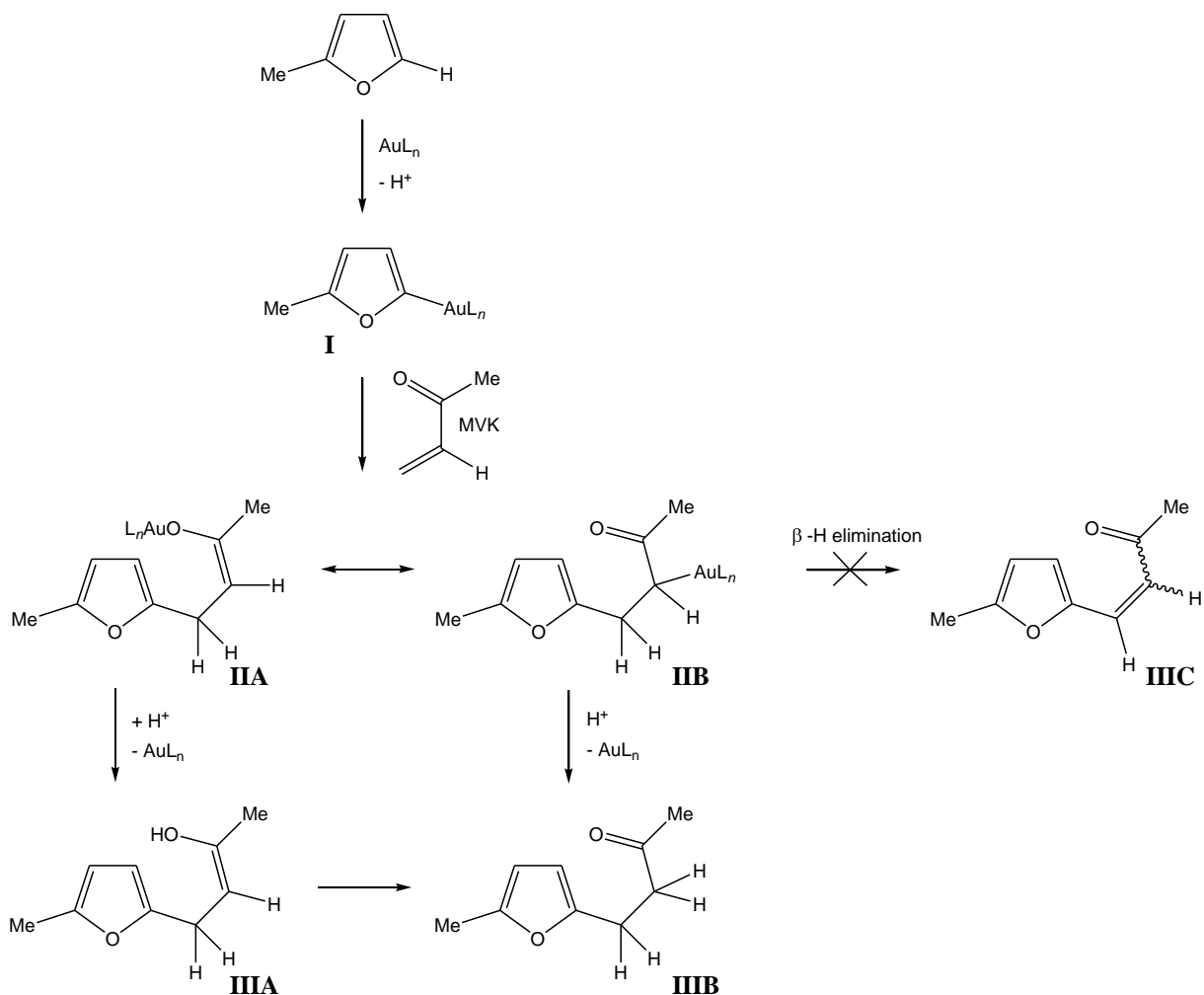
7.1.2 Catalytic addition of 2-methylfuran to methyl vinyl ketone

Gold(III) compounds have been used to catalyse the addition of 2-methylfuran **7.1** to methyl vinyl ketone (MVK) **7.2** to give 4-(5-methyl-2-furanyl)butan-2-one **7.3** (Scheme 7.1). Without a catalyst the reaction occurs under a number of different conditions including carrying out the reaction in the presence of an ethereal solution of BF₃ at low temperatures⁽⁷⁾ or by using high pressures.⁽⁸⁾ Cu(OTf)₂ has also been shown to catalyse the reaction.⁽⁹⁾



Scheme 7.1 Gold catalysed addition of 2-methylfuran **7.1** to methyl vinyl ketone (MVK) **7.2** to give 4-(5-methyl-2-furanyl)butan-2-one **7.3**.

Hashmi *et al.* have proposed a mechanism for the catalytic cycle. In separate ¹H NMR experiments AuCl₃ was added to solutions of either MVK **7.2** or 2-methylfuran **7.1** in CD₃CN. With MVK no reaction was observed. However, for 2-methylfuran the proton spectrum changed and the solution became darker. Unfortunately the NMR signals were broad and the product of this reaction was not characterised but addition of MVK to this solution afforded the addition product **7.3**.



Scheme 7.2 Proposed pathway for the reaction between 2-methylfuran and MVK catalysed by gold.

Hence it was proposed that auration of the furan occurs (to give **I**, Scheme 7.2) *via* direct electrophilic attack by the gold catalyst⁽¹⁰⁾ – this is plausible as it has been known since 1931 that AuCl_3 activates the C-H bonds of arenes such as benzene.⁽¹¹⁾ The furyl-gold species (**I**, Scheme 7.2) then acts as a nucleophile and undergoes a 1,4-Michael addition to MVK to give either a gold-enolate (**IIA**, Scheme 7.2) which may undergo the equivalent of a keto-enol tautomerism to give the gold-ketonate species (**IIB**, Scheme 7.2). Hashmi proposed that the ketonate species **IIB** is an intermediate in the catalytic pathway, and although there is probably equilibrium between **IIA** and **IIB**, we feel that the enolate species **IIA** would better represent the Michael addition product. The last step in the mechanism is protonation (by the

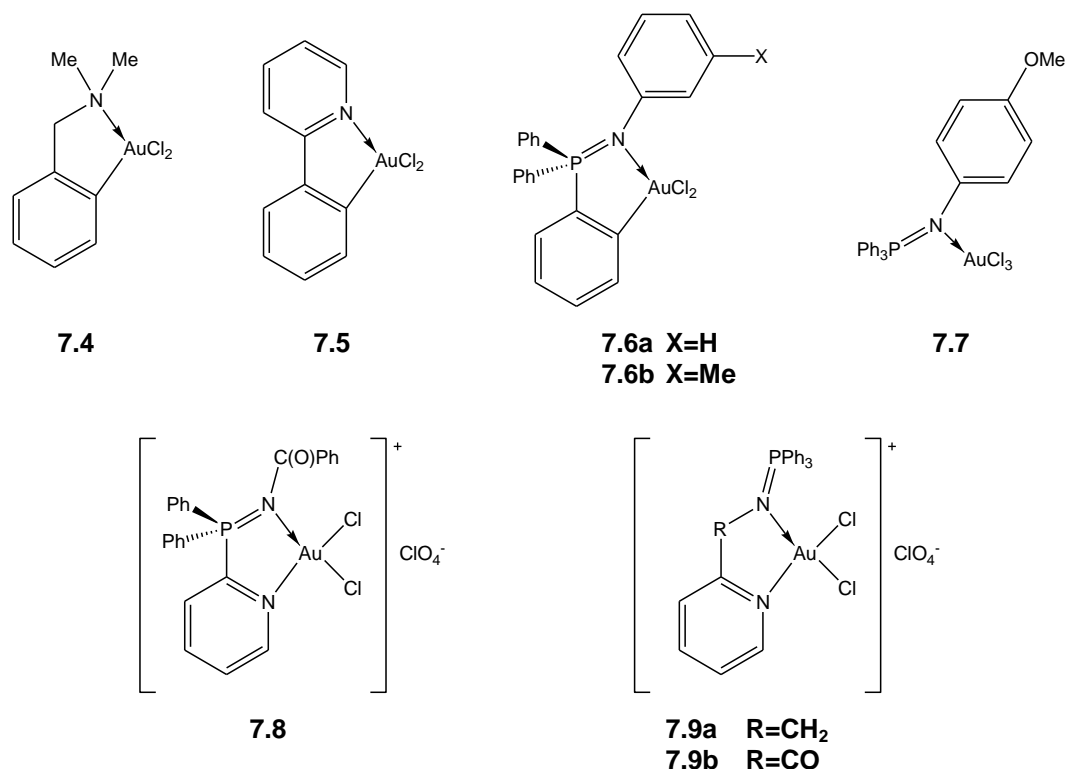
proton lost in step one) – and this is more likely to occur in the enolate species (a gold-oxygen bond would be cleaved by a weak acid (H^+) with more ease than a gold-carbon bond). Although protonation of **IIA** gives the enol **IIIA**, it would easily undergo keto-enol tautomerisation to give the ultimate product **IIIB**. In addition, Hashmi noted the β -H elimination from **IIIB** to give **IIIC** did not occur. The gold-enolate isomer **IIA** explains this observation, as there is no opportunity for β -H elimination to occur in this compound.

It was found that $AuCl_3$ catalyses the above reaction very efficiently with 80-90% yields of **7.3** after 40 minutes with 1 mol % catalyst. The Au(I) complexes PEt_3AuCl and $(THT)AuCl$ (THT = tetrahydrothiophene) also catalyse the reaction, albeit less effectively and only in the presence of $AgBF_4$ (80-90%, 1 mol % catalyst, 1 day).⁽¹²⁾ It is unclear how the $Ag[BF_4]$ enhanced the catalytic activity in this case, however oxidation of the Au(I) to Au(III) by the silver can not be excluded. It is unlikely that the catalytic activity is due to the $Ag[BF_4]$ (see later).

Because **7.3** can be formed from 2-methylfuran **7.1** and MVK **7.2** in the presence of HCl, experiments using HCl (a Brønsted acid) as a catalyst were carried out. Indeed **7.3** was obtained (50% yield) but 4-chlorobutan-2-one was also formed as a side product. Under the reaction conditions the hydrolysis products of $AuCl_3$ are $H[AuCl_3OH]$ and HCl – also Brønsted acids. Therefore both $H[AuCl_4]$ and HCl were evaluated as catalysts but they proved much less effective than $AuCl_3$, although the reaction could be forced if a large excess of MVK was present. Hence it is possible, but unlikely, that the catalytically active species may also be a Brønsted acid so interpretation of the results has to be considered carefully.⁽¹²⁾ However, catalysis of the reaction by the proton (*i.e.* a Brønsted acid) that is lost in the first step of the mechanism is unlikely as when 2-methylfuran and MVK were treated with 5% $H[ClO_4]$ only an unidentified polymeric material was formed.⁽¹⁰⁾

In light of these results Aguilar *et al.* proposed that organogold(III) complexes may also be stable catalysts in this reaction, and NMR spectroscopy may provide an insight into some of the gold intermediates.⁽¹³⁾ In addition, the cyclometallated complexes offer advantages over $AuCl_3$ – they are not as acidic as $AuCl_3$ so may be used in acid sensitive reactions and in

contrast to hygroscopic AuCl_3 , the cycloaurated complexes are air and moisture stable. Thus a selection of C,N and N,N' cyclometallated gold(III) complexes (Scheme 7.3) were evaluated as catalysts in the reaction, with the results presented in Table 7.1.^(13, 14)



Scheme 7.3 The gold(III) iminophosphorane and related cycloaurated complexes evaluated as catalysts.

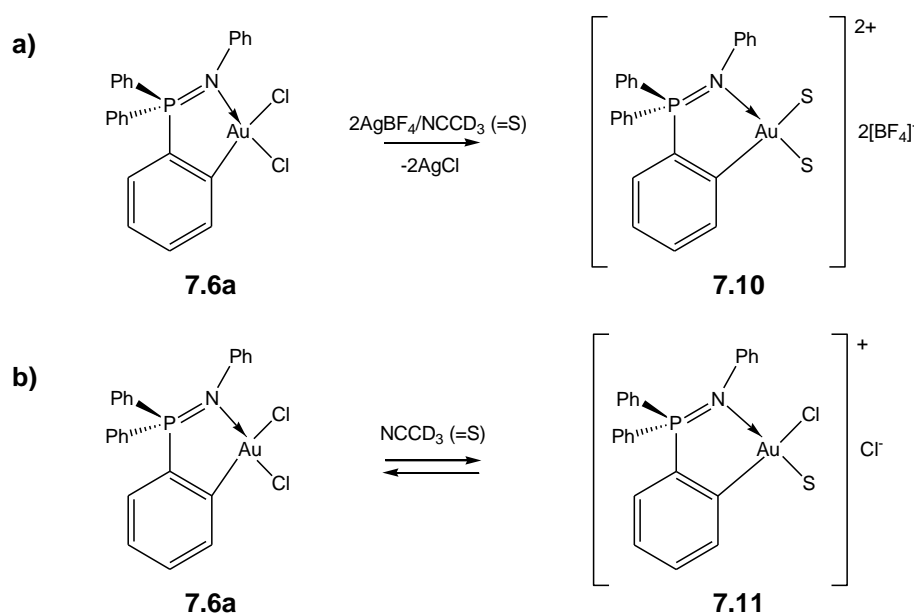
It is immediately obvious from Table 7.1 that the catalytic activity of the neutral complexes **7.4** – **7.6** is greatly enhanced by the presence of silver salts. Aguilar *et al.* proposed the catalytically active species in these cases is the cationic solvated complex **7.10**, formed by the forced removal of the chloride ligands (Scheme 7.4a). Unfortunately **7.10** could not be isolated but ^{31}P NMR spectroscopy supported the proposed cationic structure. However, addition of either 2-methylfuran or MVK to separate solutions of **7.6a** did not result in any changes to the positions or the shape of the ^{31}P or ^1H NMR signals of either 2-methylfuran, MVK or the catalyst. In the absence of silver(I) salts there is still catalytic activity and this

has been attributed to the solution equilibrium between a cationic species **7.11** (formed by *in situ* dissociation of a chloride ligand) and the neutral iminophosphorane complex (Scheme 7.4b).⁽¹³⁾

Table 7.1 Performance of cyclometallated complexes in the addition of 2-methylfuran to MVK.

Compound	% Yield of 7.3				Ref.
	1% Catalyst 6 hr, 25 °C	1% Catalyst 6 hr, 25 °C 2.2 % Ag(OTf)	1% Catalyst 18 hr, 25 °C	1% Catalyst 18 hr, 25 °C 2.2% Ag(OTf)	
7.4	N/A	50	0	83	13
7.5	N/A	65	0	80	13
7.6a	35	75	45	85	13
7.6b	38	72	N/A	80	13
7.7	N/A	N/A	N/A	65	13
7.8	N/A	70	60	79	14
7.9a	N/A	62	63	75	14
7.9b	N/A	75	76	84	14

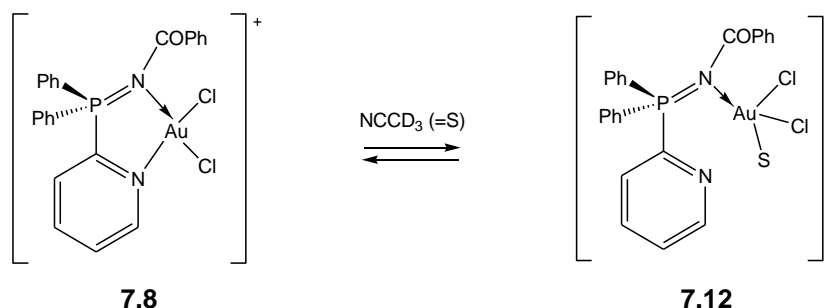
N/A Catalytic activity not reported



Scheme 7.4 Formation of the solvated cationic gold(III) species when a) silver salts are present and b) in the absence of silver salts.

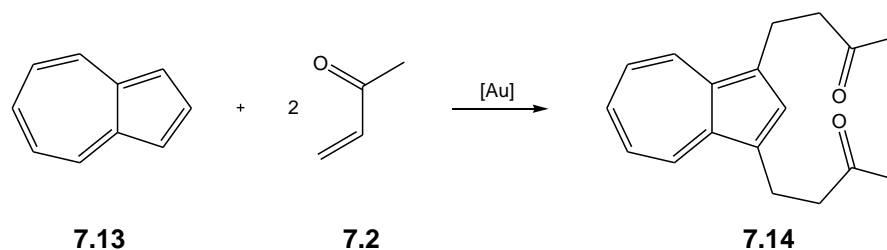
The simple coordination complex **7.7** only showed catalytic activity when silver salts were present, and even then it was not as active as the cycloaurated complexes. In addition the catalyst decomposed to metallic gold during the reaction. It therefore appears that the *C,N* cycloaurated systems are conferring stability to the gold(III) centre throughout the catalytic cycle.

In contrast, the cationic *N,N'* cycloaurated iminophosphoranes **7.8**, **7.9a** and **7.9b** showed little difference in the catalytic activity when silver cations were present. This observation was attributed to partial dissociation of the ligand effectively giving a vacant coordination site on the gold atom (Scheme 7.5). NMR spectroscopy was consistent with this observation. The ^{31}P chemical shift of the catalyst moves upfield during the catalytic process (to an intermediate value between the complex and free ligand) and in addition, the proton *ortho* to the pyridyl nitrogen also shifts upfield – both these observations point towards the formation of **7.12**. Therefore, the ligands have been described as ‘organic stabilisers’ for a reactive form of gold.⁽¹⁴⁾



Scheme 7.5 Formation of the cationic solvated gold(III) species when a nitrogen donor atom is displaced.

The complexes **7.8** and **7.9a,b** also catalyse the addition of azulene **7.13** (which is acid-sensitive) to MVK more efficiently than AuCl_3 (approximately a 90% yield in 24 hours compared with a 55% yield over three days). In both cases the double addition product **7.14** was formed with excellent selectivity (Scheme 7.6). The greater catalytic activity displayed by the cycloaurated complexes may be because they are less acidic than AuCl_3 .⁽¹⁴⁾



Scheme 7.6 Gold catalysed addition of acid-sensitive azulene **7.13** to MVK **7.2** to give the double addition product **7.14**.

In summary it appears from these results that the catalytic ability of the complexes is dependent on the presence of a vacant coordination site on the metal. This can occur *via* two possible mechanisms – the dissociation/removal of a chloride ligand or dissociation of the neutral (nitrogen) donor atom. The first method is more applicable for neutral complexes, the second for cationic complexes.

7.1.3 Scope of this work

As described in the preceding section, Aguilar *et al.* have previously shown that cyclometallated gold(III) compounds efficiently catalyse the addition of 2-methylfuran to MVK.⁽¹³⁾ We wished to evaluate the catalytic activity of the gold complexes described in this thesis and the above reaction was chosen. The method described by Aguilar seemed relatively straightforward and could easily be extended to other gold complexes and the literature results provided a useful benchmark.

The following chapter describes the results from a brief investigation into the catalytic activity of a selection of compounds which have been discussed in the preceding chapters of this thesis. Because the cycloaurated systems containing pyridine-2-thiocarboxamide ligands (Chapter Five) were not stable in solution their catalytic activity was not evaluated.

7.2 Results and Discussion

7.2.1 Development of method

The method that was used by Aguilar *et al.* was primarily gravimetric. After the appropriate time, the reaction solution was filtered through a short silica capillary, eluted with a mixture of hexane and diethyl ether and then evaporated to dryness – the weight of the residual material was used to calculate the percentage yield of the reaction product and thus the efficiency of the catalyst.⁽¹³⁾ However this method was found not to be overly effective and may overestimate the percentage yield of the reaction. When the method was followed exactly, and a ¹H NMR spectrum of the ‘product’ was recorded it showed traces of the original gold catalyst and other impurities. Therefore it was felt that GC-MS would be a more accurate method to use.

A pure sample (by NMR spectroscopy) of 4-(5-methyl-2-furanyl)butan-2-one **7.3** was acquired by chromatographic purification of the crude product (obtained by the method above) on a silica gel plate, eluting with 1:5 ethyl acetate/petroleum spirits. Three bands were obtained and band one ($R_f = 0.5$) was identified as the product. Using a standard GC-MS method (described later) the retention time of **7.3** was found to be 9.6 minutes. *o*-Xylene was chosen as the internal standard for a number of reasons – the retention time (4.6 minutes) was close to that of the product, it is inert towards any reaction and it is relatively non-volatile.

Known standard solutions of **7.3** and *o*-xylene were analysed by GC-MS. Figure 7.1 shows the response factor (calculated from the area under the two peaks) of **7.3** relative to *o*-xylene at different molar concentrations. Therefore, if a known amount of *o*-xylene (1 mmol) is added to the sample before GC analysis, the ratio of the areas under the peaks (**7.3** and *o*-xylene) can be used to determine the amount (in moles) of product in the sample using the formula (where 1.0808 is the response factor from the calibration curve) shown in Equation 7.1.

$$\text{Moles of } \mathbf{7.3} = \frac{\left(\frac{\text{Area of } \mathbf{7.3}}{\text{Area of } o\text{-xylene}} \right)}{1.08} \dots\dots\dots \text{Equation 7.1}$$

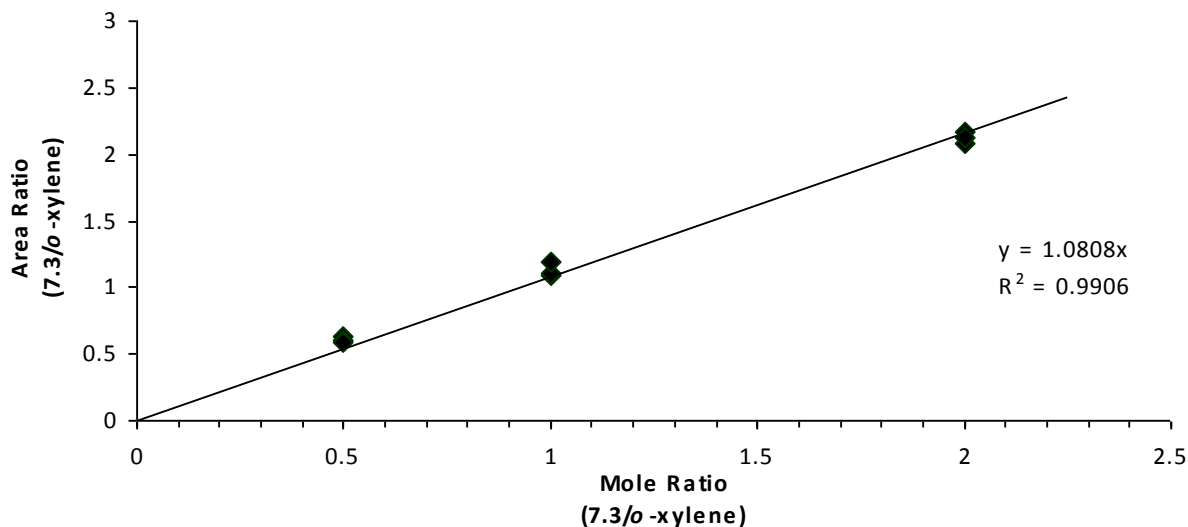


Figure 7.1 Response factor curve (determined by the area under the peaks) for **7.3** relative to *o*-xylene at different molar concentrations of **7.3** and *o*-xylene.

7.2.2 Catalytic activity of C, N cycloaurated complexes

The catalytic activity of the iminophosphorane based systems described in Chapter Two was investigated. In order to determine if substitution of the *cis* chloride ligands affects the catalytic activity a range gold(III) complexes with different ligands (*e.g.* catecholate, thiosalicylate) were evaluated (Scheme 7.7) and the results are presented in Table 7.2. In addition, the activity of **2.29a** was re-evaluated using the GC-MS method to compare with the results obtained by Aguilar *et al.*

From the results of Aguilar *et al.* it is not surprising that the addition of Ag^+ (in the form of $\text{Ag}[\text{BF}_4]$) greatly increases the catalytic activity of the neutral complexes. The chloride ligands are removed from the gold (in the form of AgCl) leaving a vacant coordination site on the metal which is presumably where catalysis occurs. When no silver is present catalysis still occurs, probably due to the dissociation of a chloride ligand (Scheme 7.4). Altering the *N*-substituent on the simple iminophosphoranes did not change the catalytic activity greatly, nor does placing the $\text{P}=\text{N}$ bond outside the metallacyclic ring (*exo* isomer **2.43**). However, the stabilised iminophosphorane **2.46** (the *endo* isomer) showed greater catalytic activity – possibly because the *N*-acyl substituent is a weaker base thus dissociates from the metal centre (to form a vacant coordination site) with more ease.

Table 7.2 Performance of C,N cyclometallated iminophosphoranes as catalysts in the addition of 2-methylfuran to MVK.

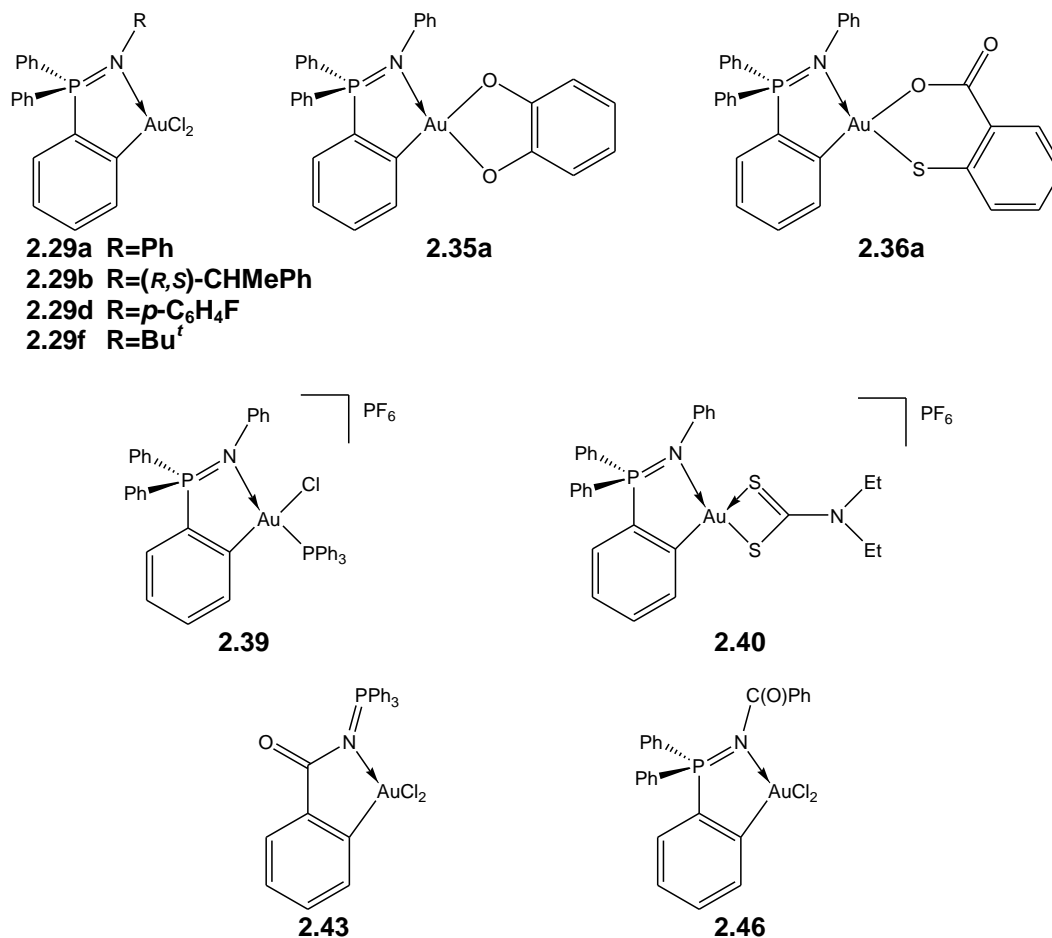
Compound	% Yield of 7.3 , determined by GC-MS	
	1% Catalyst Loading 18 hr, 25 °C	1% Catalyst Loading 18 hr, 25 °C 2.2 % AgBF ₄
2.29b	13	76
2.29d	<1	63
2.29f	0	78
2.29a	7 (45) ^a	86 (92) ^a
2.35a	0	N/A
2.36a	0	N/A
2.39	37	86
2.40	0	N/A
2.43	1	86
2.46	26	93
[Me ₄ N][AuCl ₄]	62	N/A
AgBF ₄	0	N/A

N/A Catalytic activity not determined

^a Value in brackets is the result reported by Aguilar *et al.*⁽¹³⁾

Complex **2.39**, which has a chloride ligand and a relatively labile PPh₃ ligand, showed greater activity than the dichloride complexes in the absence of silver cations. Presumably this is because the neutral phosphine dissociates from the metal with more ease than the chloride ligand, thus leaving a vacant coordination site. When silver salts are present the chloride ligand is also removed giving a ‘permanent’ vacant coordination site on the gold, which leads to an increase in catalytic activity.

The catecholate **2.35a** and thiosalicylate **2.36a** complexes were catalytically inactive. This is not surprising as the metallacyclic ring formed from the chelating catecholate and thiosalicylate dianions are held in place better than the monodentate chloride ligands. Thus dissociation of the ligand will not occur to give a vacant coordination site on the metal. The cationic dithiocarbamate complex was also catalytically inactive.



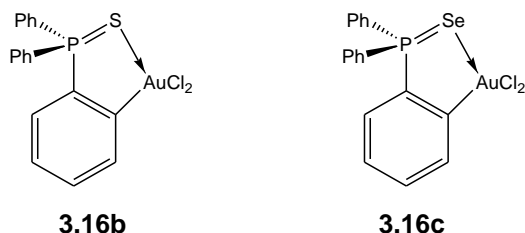
Scheme 7.7 C,N cycloaurated gold iminophosphorane complexes that were evaluated as catalysts.

It is evident from Table 7.2 that the results using the GC-MS method differ from those obtained when the gravimetric method of Aguilar is used. This is more noticeable when there are no silver salts present.

The simple Au(III) salt [Me₄N][AuCl₄] shows better activity (with no silver present) than the cycloaurated complexes. This is not surprising as H[AuCl₄] also shows catalytic activity, however with [Me₄N][AuCl₄] there is no source of protons so the activity can be attributed to the gold centre. The salt Ag[BF₄] is inactive, hence possible catalysis from BF₃ (formed by hydrolysis of [BF₄]⁻) can be excluded (refer to section 7.1.2).

7.2.3 Catalytic activity of C,E (E=S, Se) cycloaurated complexes

Because the catalytic activity of the iminophosphorane systems was promising, the activity of the isoelectronic phosphine chalcogenide (Scheme 7.8) was also evaluated. Table 7.3 shows the results that were obtained.



Scheme 7.8 C,E cycloaurated gold complexes that were evaluated as catalysts.

Table 7.3 Performance of cycloaurated triphenylphosphine sulfide and selenide as catalysts in the addition of 2-methylfuran to MVK.

Compound	% Yield of 7.3 , determined by GC-MS	
	1% Catalyst Loading 18 hr, 25 °C	1% Catalyst Loading 18 hr, 25 °C 2.2 % AgBF ₄
3.16b	8	89
3.16c	18	87

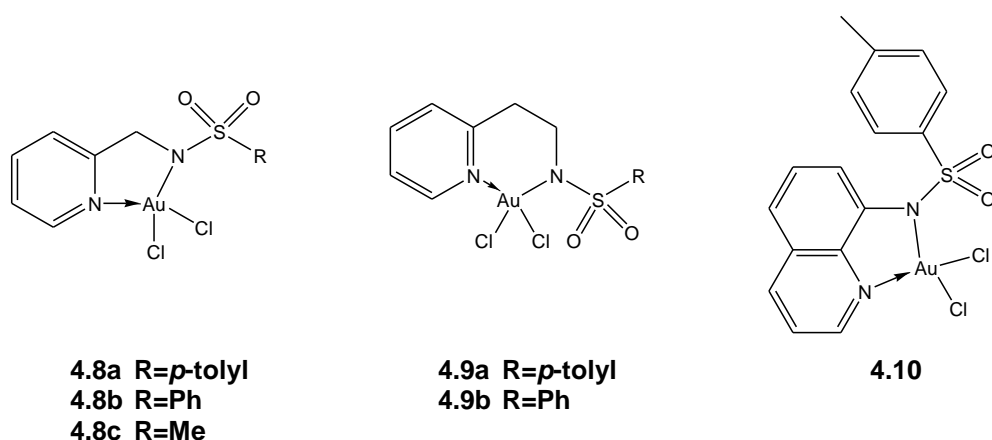
Again the presence of silver salts greatly increases the catalytic activity of the complexes, most probably due to the reasons discussed above. The selenide complex shows a higher catalytic activity than the sulfide, or indeed any of the C,N donor systems described above. This may be explained in terms of the strength of the *trans* influence of the neutral donor ligand. The selenide donor is soft thus exerts a higher *trans* influence compared with the harder sulfide or nitrogen donors. Thus, the chloride *trans* to the selenide will leave the gold coordination sphere with more ease than the chloride *trans* to either a sulfur or a nitrogen. Therefore, the chloride dissociation described in Scheme 7.4 will be more effective for the selenide, or indeed, any complexes which contain a high *trans* influence donor ligand.

From the crystallographic data presented in Chapters Two and Three (excluding **2.46**), the complexes can be ranked from those with the highest *trans* influence donor to those with the lowest – *i.e.* the complexes with the longest Au-Cl bond *trans* to the neutral donor ligand will contain the highest *trans* influence donor. Thus the series ranked from the highest *trans* influence donor to the lowest follows: **3.16c** > **3.16b** > **2.29b** > **2.29a** > **2.43**

This series roughly follows the order of the catalytic activity when no silver cations are present, however **2.46** breaks this trend. This may be because **2.46** contains a phenacyl ring, however the reasons are unclear. Conversely, the enhanced catalytic activity of **2.46** and **3.16c** may be because the NCOPh and Se group dissociate from the gold centre with more ease. More examples (including replicating the catalytic results) are needed to shed light on the trends. In addition, an investigation into the identity of the active catalyst would prove worthwhile.

7.2.4 Catalytic activity of *N,N'* cycloaurated complexes

The catalytic activity of the *N,N'* based systems described in Chapter Four (Scheme 7.9) was evaluated to determine if changing the type of ligand coordinated to the gold alters the catalytic activity. The results are presented in Table 7.4.



Scheme 7.9 *N,N'* cycloaurated gold complexes described in Chapter Four that were evaluated as catalysts.

Table 7.4 Performance of *N,N'* cycloaurated 2-pyridylsulfonamides as catalysts in the addition of 2-methylfuran to MVK.

Compound	% Yield of 7.3 , determined by GC-MS	
	1% Catalyst Loading 18 hr, 25 °C	1% Catalyst Loading 18 hr, 25 °C 2.2 % AgBF ₄
4.8a	2	68
4.8b	2	73
4.8c	2	78
4.9a	<1	93
4.9b	<1	88
4.10	68	85

With the exception of **4.10**, the *N,N'* cycloaurated sulfonamides were poor catalysts in the absence of Ag[BF₄]. The poor performance of the *N,N'* based systems is somewhat surprising. As described in Chapter Four the *N,N'* based ligands do not stabilise the gold as well as the *C,N* metallated species therefore it might be expected that the pyridyl donor could dissociate from the gold thus providing a vacant coordination site on the metal for catalysis to occur. However, it appears that for **4.8** and **4.9** the complexes are decomposing before the catalysis occurs. Complex **4.10** differs in that the system is rigid – this appears to be imparting some stability onto the complexes and decomposition does not occur as rapidly. These systems would benefit from more study including acquiring information on the catalytic profiling of other Au(III) systems containing rigid chelating ligands.

Presumably the addition of Ag[BF₄] produces the solvated cations analogous to those formed with *C,N* cyclometallated species (Scheme 7.4). These species have a greater catalytic activity than the neutral species, possibly because they are more stable in solution. Again, an investigation into the true identity of the catalyst would aid in understanding the difference in activities of the *C,N* and *N,N'* cycloaurated complexes.

7.3 Conclusions

The results that have been presented show that the Au(III) complexes described in the preceding chapters are just as efficient at catalysing the addition of 2-methylfuran to MVK as AuCl₃ and the organometallic compounds described by Aguilar *et al.* Because the complexes are air- and moisture-stable they are easily handled and stored. In addition, synthesis of the sulfonamide complexes is relatively straight-forward.

These initial results are promising however further work is needed to fully understand the results and to ascertain the catalytically active species. It appears that the gold(III) dichloride metallacycles are pre-catalysts – the active catalyst probably has a vacant coordination site on the metal centre formed by either dissociation of the neutral donor or the chloride ligand. It appears that the cationic gold(III) species are catalytically more active (*e.g.* **2.39**) hence an investigation into other cationic species with weaker donor atoms (*e.g.* replacing PPh₃ with P(OPh)₃) would be useful.

In addition it would be worthwhile to investigate other factors in the catalytic reaction. For example, replacing the Ag[BF₄] with Tl[BF₄] would determine if the oxidising Ag⁺ cation plays any role in the mechanism. Likewise, anions other than [BF₄]⁻ could be investigated, to determine if they have a role.

7.4 Experimental

7.4.1 General

2-Methylfuran and methyl vinyl ketone (Aldrich) were used as received. *o*-Xylene and acetonitrile were distilled before use. The reactions were carried out at 25° C under a nitrogen atmosphere.

7.4.2 Catalysis conditions

2-Methylfuran **7.1** (2 mmol, 0.1793 mL), methyl vinyl ketone **7.2** (2 mmol, 0.1665 mL), the gold catalyst (0.02 mmol, 1% catalyst loading) and the Ag[BF₄] (if needed) were stirred in acetonitrile (5 mL) for 18 hours. The acetonitrile and any unreacted reactants were removed under vacuum. The product was taken up into diethyl ether/hexane (20 mL, 3:1) and passed through a silica column. *o*-Xylene (1 mmol, 0.1210 mL) is added and 0.050 mL of this solution is transferred to a GC vial and made up to ~ 1.5 mL with hexanes.

7.4.3 GC-MS Conditions

GC-MS experiments were run on a HP 6890 Series GC System coupled to a HP 5973 Mass Selective Detector (operating in TIC mode). 3 µL of the sample was introduced onto a non-polar column (ZB-5, 30 m x 0.25 mm, 0.25 µm film thickness) by an autosampler. The oven was initially held at 50 °C, then the temperature was increased at 8 °C per minute until 290 °C was reached. Helium was used as the carrier gas (flow rate 1 mL/min) at a pressure of 9 psi. Manual integration of the peaks corresponding to *o*-xylene and **7.3** gave the peak areas that were to be used in the calculation. The retention times of *o*-xylene (4.6 minutes) and **7.3** (9.6 minutes) were confirmed by GC traces of the pure compounds.

7.5 References

1. A. S. K. Hashmi; *Chem. Rev.*, **2007**, 107, 3180.
2. R. V. Parish; *Gold Bull.*, **1998**, 31, 14.
3. A. S. K. Hashmi, F. Ata, J. W. Bats, C. M. Blanco, W. Frey, M. Hamzic, M. Rudolph, R. Salathé, S. Schäfer and M. Wöelfle; *Gold Bull.*, **2007**, 40, 31.
4. A. S. K. Hashmi; *Angew. Chem. Int. Ed.*, **2005**, 44, 6990.
5. A. S. K. Hashmi; *Gold Bull.*, **2004**, 37, 51.
6. G. Bond; *Gold Bull.*, **2008**, 41, 235.
7. J.-M. Poirier and G. Dujardin; *Heterocycles*, **1987**, 25, 399.
8. G. Jenner; *Tetrahedron Lett.*, **1994**, 35, 1189.
9. V. J. Bulbule, V. H. Deshpande and A. V. Bedekar; *J. Chem. Res. Synop.*, **2000**, 5, 220.

10. A. S. K. Hashmi, L. Schwarz, J.-H. Choi and T. M. Frost; *Angew. Chem. Int. Ed.*, **2000**, 39, 2285.
11. M. S. Kharasch and H. S. Isbell; *J. Am. Chem. Soc.*, **1931**, 53, 3053.
12. G. Dyker, E. Muth, A. S. K. Hashmi and L. Ding; *Adv. Synth. Catal.*, **2003**, 345, 1247.
13. D. Aguilar, M. Contel, R. Navarro and E. P. Urriolabeitia; *Organometallics*, **2007**, 26, 4604.
14. D. Aguilar, M. Contel, R. Navarro, T. Soler and E. P. Urriolabeitia; *J. Organomet. Chem.*, **2009**, 694, 486.

APPENDIX ONE

General Experimental Procedures, Instrumental Techniques and Preparation of Starting Materials

I.1 General Experimental Procedures

Unless specifically stated, chemicals were used as received from commercial sources. The majority of the gold compounds synthesised were not air or moisture sensitive but were stored in the dark as a precaution against light. With the exception of the preparative methods described in Chapters Four and Five, an oil-bath was used when refluxing solutions. For the methods described in Chapters Four and Five the round bottom flasks were mounted upon a foil dish.

Purification of solvents

Dry, degassed, deoxygenated diethyl ether, dichloromethane, hexane, THF and toluene were obtained from a Pure Solv™ solvent purification system. Prior to use, acetonitrile was distilled from CaH₂ and acetone from CaSO₄.

Air-, moisture- or light-sensitive reactions

Any reactions that were air- or moisture-sensitive were carried out under a nitrogen atmosphere using standard Schlenk techniques.⁽¹⁾ Moisture-sensitive reactions were carried out in glassware that had previously been oven dried. Light-sensitive reactions were carried out in foil-covered flasks.

I.2 Instrumental Techniques and Analysis

I.2.1 Infrared Spectroscopy

Unless otherwise stated IR spectra were recorded as KBr disks on either a Digilab Scimitar FTS 2000 series spectrometer or a Perkin-Elmer Spectrum 100 FT-IR spectrometer. In all cases the region scanned was 450 – 4500 cm^{-1} .

I.2.2 NMR Spectroscopy

NMR Spectroscopy was performed on either a Bruker DRX 300 ($^1\text{H} = 300.13 \text{ MHz}$, $^{13}\text{C} = 75.47 \text{ MHz}$, $^{31}\text{P} = 121.49 \text{ MHz}$) or 400 ($^1\text{H} = 400.13 \text{ MHz}$, $^{13}\text{C} = 100.61 \text{ MHz}$) spectrometer at 30 °C. Proton and carbon spectra were referenced to residual solvent peaks (CDCl_3 C = 77.16, H = 7.26; d_6 -DMSO C = 39.52, H = 2.50 ppm).⁽²⁾ Phosphorus spectra were referenced to H_3PO_4 (0.0 ppm). Carbon spectra were routinely acquired at a lower tip angle (30 or 45°) with an extended delay time (3-5 sec) in an attempt to optimise the conditions needed to detect the slowly relaxing quaternary carbons. In addition to these basic experiments, a number of more complex 1-D and 2-D experiments (detailed below for the assignment of complex **4.8c**) were needed to fully assign the spectra.

^1H - ^1H COSY

In a ^1H - ^1H COSY (COrrrelation SpectroscopY) spectrum the signals of a normal ^1H NMR spectrum are correlated with each other, and cross peaks appear if signals are coupled to each other. The standard ^1H - ^1H COSY that was used was optimised for $^3J_{\text{HH}}$ coupling. Figure A.1 shows the aromatic region of the ^1H - ^1H COSY of **4.8c**. The $^3J_{\text{HH}}$ coupling can clearly be seen and from this the order of the protons around the ring can be determined *e.g.* the proton at 9.04 ppm (H-1) shows a correlation (a cross peak) to the proton at 7.80 ppm (H-2), hence is next to it on the pyridyl ring.

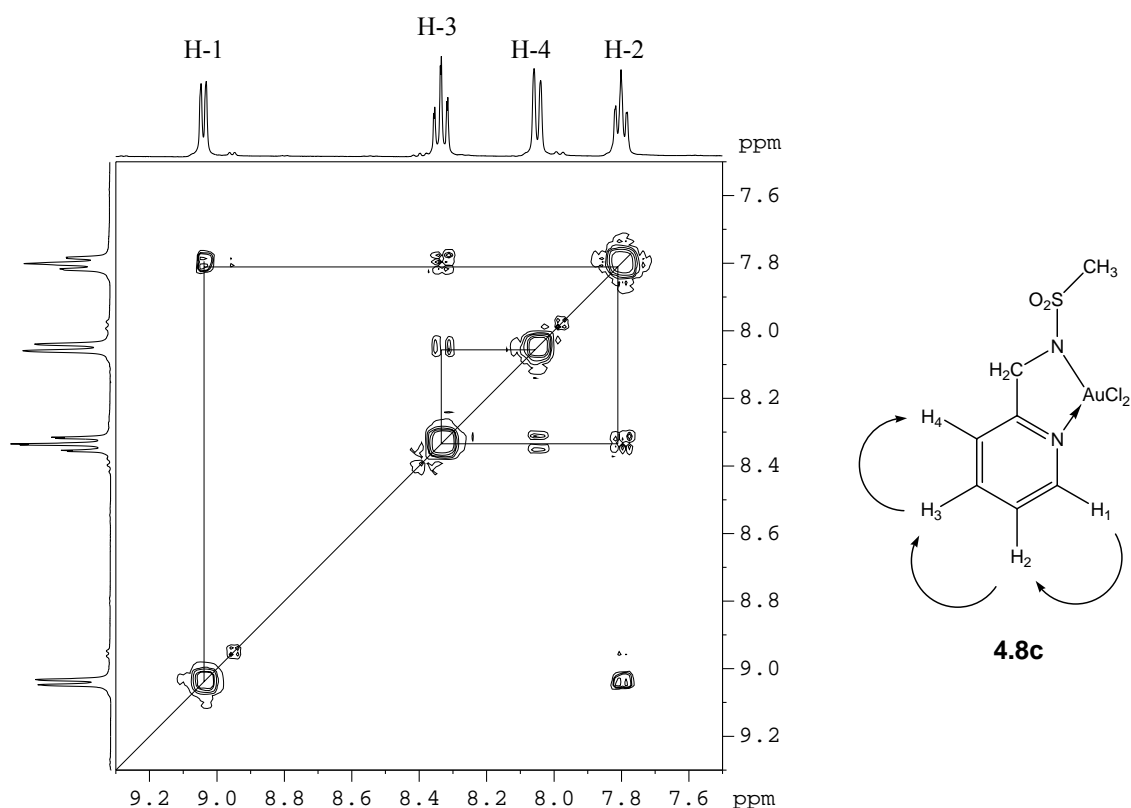


Figure A.1 ^1H - ^1H COSY spectrum (d_6 -DMSO) of **4.8c**

1-D SELTOCSY

The 1-D SELTOCSY was used in preference to the 2-D TOCSY experiment as the acquisition time was shorter, the resolution was better (therefore coupling constants can be determined) and any unwanted signals (*e.g.* solvent) were eliminated. In the experiment, one signal (*i.e.* one proton environment) is irradiated and any signals which are correlated to the irradiated peak will show up. Short TOCSY mixing times give a COSY like result (*e.g.* $^3J_{\text{HH}}$ coupling), longer mixing times give larger coupling (*e.g.* $^4J_{\text{HH}}$ and $^5J_{\text{HH}}$ coupling). An example of how the experiment was used is shown below, the proton at 8.05 ppm (H-4) is irradiated in each case. At short mixing times (15 ms), a COSY-like spectrum was obtained and coupling to H-3 was observed (Figure A.2 a). At intermediate mixing times coupling to both H-3 ($^3J_{\text{HH}}$) and H-2 ($^4J_{\text{HH}}$) was observed, at longer mixing times $^3J_{\text{HH}}$, $^4J_{\text{HH}}$ and now $^5J_{\text{HH}}$ (to H-1) can be observed.

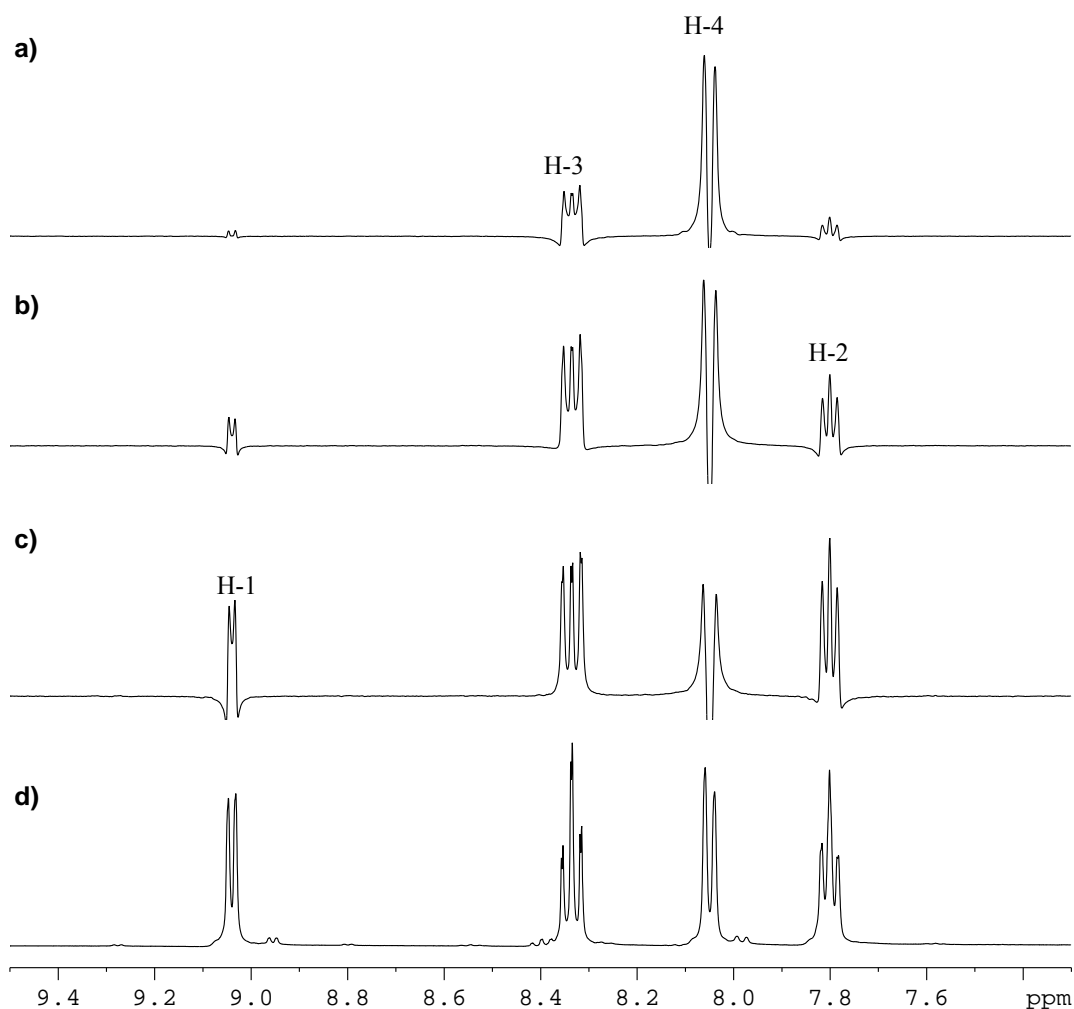


Figure A.2 1-D SELTOCSY NMR spectra of **4.8c** (d_6 -DMSO) with mixing times of **a)** 15 ms, **b)** 30 ms and **c)** 50 ms. The spectrum shown in **d)** is a standard ^1H NMR spectra of **4.8c** (see Figure A.1 for the atom labelling scheme).

1-D SELNOESY

The 1-D SELNOESY is a 1-D version of the standard NOESY experiment. Like the 1-D SELTOCSY experiment the 1-D SELNOESY has the advantages of being quicker, having better resolution and eliminating any interfering signals. Again, a proton is irradiated and any signals that show a through space interaction will appear in the spectra. The ^1H - ^1H COSY and 1-D SELTOCSY experiments described above give information about the order of the protons

around the aromatic ring, however they do not indicate the direction around the ring (*i.e.* is the doublet at 8.05 ppm H-1 or H-4). However, irradiation of the methylene protons at 4.96 ppm in a 1D-SELNOESY experiment result in a correlation to the proton at 8.05 ppm – hence 8.05 ppm must be H-4 (Figure A.3).

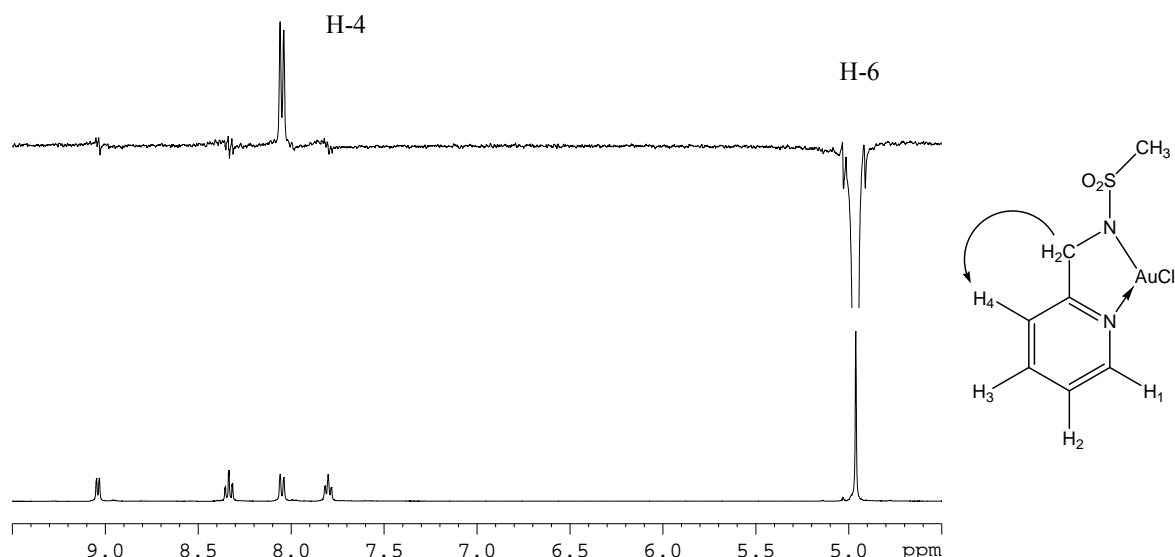


Figure A.3 **a)** 1-D SELNOESY spectrum of **4.8c** (d_6 -DMSO), with the signal at 4.96 ppm irradiated and showing a through space interaction to the proton at 8.05 ppm **b)** standard ^1H NMR spectrum of **4.8c** (see Figure A.1 for the atom labelling scheme).

^1H - ^{13}C HSQC

The ^1H - ^{13}C HSQC (Heteronuclear Single Quantum Coherence) experiment gives $^1J_{\text{CH}}$ correlations – *i.e.* it basically indicates which protons are coupled to which carbons.

^1H - ^{13}C HMBC

The ^1H - ^{13}C HMBC (Heteronuclear Multiple Bond Correlation) experiment gives larger proton-carbon correlations (*e.g.* $^2J_{\text{CH}}$ and $^3J_{\text{CH}}$) and was mainly used in the assignment of quaternary carbon signals.

I.2.3 Mass Spectrometry

Electrospray mass spectra were acquired on a Fisons Instruments VG Platform II spectrometer. Approximately 1 mg of the sample was dissolved in a drop of dichloromethane and the solution made up to approximately 1 mL with methanol.

High resolution mass spectra were acquired on a Bruker Daltonics MicrOTOF spectrometer. The samples (0.1 mg mL^{-1} , made up as above) were introduced *via* a syringe pump. The spectrometer was calibrated with a sodium formate standard prior to each use.

To aid in assignment, experimental isotope patterns were compared with theoretical patterns obtained using the *Isotope* computer program.⁽³⁾

I.2.4 X-ray Crystallography

Unit cell dimensions and intensity data was acquired at either the University of Auckland by Dr. Tania Groutso (Bruker Smart CCD Diffractometer) or at the University of Canterbury by Dr. Jan Wikaira (Bruker Nonius Apex II CCD Diffractometer). Semi-empirical absorption corrections were applied by SADABS.⁽⁴⁾

The crystal structures were solved by either the Direct Methods or Patterson (heavy atom) options of SHELXS-97.⁽⁵⁾ Refinement of the data was carried out by SHELXL-97⁽⁶⁾ with a final check on the crystallographic information file by PLATON.⁽⁷⁾ Molecular diagrams were generated using the ORTEP program.⁽⁸⁾ All programs were operating under the WinGX suite of programs (Version 1.70.01).⁽⁹⁾

I.2.5 Microelemental Analysis

Elemental analysis for carbon, hydrogen and nitrogen were undertaken on vacuum dried samples at the Campbell Microanalytical Laboratory, University of Otago.

I.2.6 Biological Assays

Biological assays to determine the *in vitro* anticancer activity against the P388 Murine Leukemia cell line were carried out by Gill Ellis of the Marine Chemistry Group at the University of Canterbury. The sample was dissolved in the solvent and incubated with P388 murine leukemia cells for 72 hours. IC₅₀ values are determined using absorbance values obtained when the dye MMT tetrazolium (yellow) is reduced to MMT formazan (purple).

I.3 Preparation of Inorganic and Organometallic Precursors

H[AuCl₄].4H₂O⁽¹⁰⁾

Gold nuggets (5 g) were dissolved in aqua regia (100 mL) with gentle stirring and heating. The resulting solution was reduced in volume (to approximately 10-15 mL) then another portion of concentrated HCl (50 mL) was added. The reduction in volume and addition of HCl was repeated twice. The yellow solution was reduced (to 10 mL) to give a red liquid which solidified on cooling to give H[AuCl₄].4H₂O quantitatively. The hygroscopic solid was stored in a tightly sealed vial.

[NMe₄][AuCl₄]⁽¹¹⁾

To an aqueous (50 mL) solution of H[AuCl₄].4H₂O (2.00 g, 4.85 mmol) excess [Me₄N]Cl (0.65 g, excess) was added. A yellow precipitate formed immediately and the resulting solution was stirred for a further 30 minutes. The solution was filtered and the bright yellow solid washed with copious amounts of water followed by ethanol and diethyl ether. Drying under vacuum gave [Me₄N][AuCl₄] in near quantitative yields.

Preparation of PhCH₂Mn(CO)₅⁽¹²⁾

In a 100 mL Schlenk flask (under a nitrogen atmosphere) a 1% sodium amalgam was prepared by carefully adding small portions of sodium metal (0.7 g) to mercury (5 mL, 70 g) and swirling until the sodium had dissolved. When cool, dry, degassed THF (60 mL) was added to

the amalgam followed by $\text{Mn}_2(\text{CO})_{10}$ (2.00 g, 5.13 mmol) and the solution was stirred vigorously for 2 hours. The resulting green solution of $\text{Na}[\text{Mn}(\text{CO})_5]$ was transferred by a nitrogen-flushed syringe to another Schlenk flask (again under nitrogen) containing benzyl bromide (1.20 mL, 10 mmol). After stirring for a further 10 minutes white NaBr precipitated out. The THF was removed under reduced pressure and the residue extracted into petroleum spirits (4×10 mL) and filtered. The solvent was removed to give a yellow solid. Sublimation of the solid onto a water-cooled cold finger gave $\text{PhCH}_2\text{Mn}(\text{CO})_5$ as a pale yellow solid (1.8 g, 70 %).

Preparation of 2-Br(C_6H_4) PPh_2 ⁽¹³⁾

Under nitrogen, *p*-dibromobenzene (5.00 g, 0.02 mol) was added to a solution of dry, degassed THF and diethyl ether (1:1, 60 mL). The solution was cooled to -110 °C in an ethanol slush bath and *n*-BuLi (10 mL, 2.0 M in cyclohexane) was added dropwise – the resulting solution was stirred at -110 °C for a further 40 minutes during which time a white solid formed. Distilled Ph_2PCl (3.57 mL, 0.02 mol) was added dropwise to the solution and stirred at low temperature for a further 15 minutes. The slush bath was removed and when the solution had warmed to room temperature NH_4Cl (sat. aq, 50 mL) was added. The aqueous layer was washed with diethyl ether (2×30 mL) and the organic layers were combined and dried with anhydrous MgSO_4 . The solvent was removed under pressure and the resulting pale yellow solid was recrystallised from hot ethanol to give 2-Br(C_6H_4) PPh_2 (4.43 g, 65%).

$^{31}\text{P}\{^1\text{H}\}$ NMR (CDCl_3): δ -4.4 ppm.

Preparation of $\text{Hg}(\text{C}_6\text{H}_4\text{PPh}_2)_2$ ^(13, 14)

2-Br(C_6H_4) PPh_2 (1.00 g, 2.93 mmol) was dissolved in dry, degassed diethyl ether (15 mL) and *n*-BuLi (1.5 mL, 2.0 M in cyclohexane) was added dropwise. After stirring for 10 minutes additional diethyl ether was added (60 mL). HgCl_2 (0.358 g, 1.32 mmol) was added in one portion and the resulting solution stirred at room temperature for 72 hours. The solvent was removed under reduced pressure and the white solid extracted into hot toluene (2×60 mL)

and filtered to give a pale yellow solution. Addition of hexanes (120 mL) resulted in the immediate precipitation of $\text{Hg}(\text{C}_6\text{H}_4\text{PPh}_2)_2$ (0.73 g, 77%).

$^{31}\text{P}\{^1\text{H}\}$ NMR (CDCl_3): δ 0.4 ($^3J_{\text{P-Hg}} = 207$ Hz) ppm.

I.4 References

1. D. F. Shriver and M. A. Drezdson; *The Manipulation of Air-Sensitive Compounds*, Wiley, New York, **1986**.
2. H. E. Gottlieb, V. Kotlyar and A. Nudelman; *J. Org. Chem.*, **1997**, 62, 7512.
3. L. J. Arnold; *J. Chem. Educ.*, **1992**, 69, 811.
4. R. H. Blessing; *Acta Cryst. Sect. A*, **1995**, 51, 33.
5. G. M. Sheldrick, SHELXS-97 - A Program for the Solution of Crystal Structures, University of Göttingen, Germany, **1997**.
6. G. M. Sheldrick, SHELXL-97 - A Program for the Refinement of Crystal Structures, University of Göttingen, Germany, **1997**.
7. A. L. Spek; *J. Appl. Cryst.*, **2003**, 36, 7.
8. L. J. Farrugia; *J. Appl. Cryst.*, **1997**, 30, 565.
9. L. J. Farrugia; *J. Appl. Cryst.*, **1999**, 32, 837.
10. Synthetic Methods of Organometallic and Inorganic Chemistry (Herrmann/Brauer), Volume 5, *Copper, Silver, Gold, Zinc, Cadmium and Mercury*, W. A. Herrmann; Thieme, Stuttgart, **1999**.
11. M. B. Dinger; *Ph.D (Chemistry) Thesis*, **1998**, University of Waikato.
12. L. Main and B. K. Nicholson; *Adv. Metal-Org. Chem.*, **1994**, 3, 1.
13. S. Harder, L. Brandsma, J. A. Kanters, A. Duisenberg and J. H. van Lenthe; *J. Organomet. Chem.*, **1991**, 420, 143.
14. M. A. Bennett, M. Contel, D. C. R. Hockless, L. L. Welling and A. C. Willis; *Inorg. Chem.*, **2002**, 41, 844.